COMPARISON OF LAYERED SURFACE VISUALIZATION THROUGH ANIMATED PARTICLES AND ROCKING

by
JAMES LANE

A dissertation submitted to the University of Cape Town
In fulfillment of the requirements for the degree of
Doctor of Philosophy in the Department of Computer Science

Cape Town
February 2010

Supervised
by
PROF JAMES GAIN

This thesis is dedicated to the Lord Jesus Christ, Who has faithfully
helped and carried me through this PhD.

"Have you not known? Have you not heard? The everlasing God, the Lord,
The Creator of the ends of the earth, neither faints nor is weary.
His understanding is unsearchable. He gives power to the weak,
And to those who have no might He increases strength."
"Fear not, for I Am with you; Be not dismayed, for I am Your God.
I will strengthen you, Yes, I will help you, I will uphold you with My righteous right hand."

"Come to Me, all you who labor and are heavy laden, and I will give you rest."
Jesus

Isaiah 40 vs. 28, 29; Isaiah 41 vs. 10; Mathew 11 vs. 28

Abstract

Visualizations that show the shape of and spatial relationships between layers of surfaces are useful to oceanographers studying water masses or oncologists planning radiation treatments. The shape of and distances between layers is effectively visualized by displaying the surfaces semi-transparently and sparsely covered with opaque markings. However, it becomes difficult to distinguish the shapes and differentiate between the markings when showing more than two surfaces. Further, finding optimal sizes and numbers of markings for the different layers, so as to best display the surfaces, requires tedious manual effort.

This dissertation firstly investigates animation of the opaque markings as a means of enhancing these visualizations. Such a Kinetic Visualization approach has several potential benefits: the perceptual grouping effect of similar motion helps distinguish between markings on separate layers, occlusions are modulated as the markings move, allowing a viewer to assemble an integrated mental image of otherwise partially obscured surfaces, and markings that follow certain trajectories such as surface curvatures, contribute to a better understanding of shape. Markings are also spread out in relation to the view point, reducing complete occlusions.

Secondly, a computational model of human perception of a single surface is extended to layered surfaces by modelling processes of perceptual grouping and surface completion, incorporating relatability criteria. This model is intended to mimic a person's perception of layered surfaces, and is used to measure the effectiveness of our visualizations, within an optimization framework, allowing optimal visualization settings to be automatically determined.

Visualization enhancements through animation were evaluated through a user experiment comparing pendulum-style rocking, static renderings and Kinetic Visualization on sets of two surfaces. This showed that rocking alone results in more accurate depth judgements, indicating that the "Kinetic Depth Effect" is not induced by Kinetic Visualization. A follow-up experiment revealed that a combination of rocking and Kinetic Visualization is more useful than rocking alone for feature identification tasks when displaying four layers.

Our perceptual model was evaluated, in an experiment, in which sets of layered surfaces were displayed using a range of different visualization settings. Respondents recreated surfaces matching their perception. Comparing our model's evaluation of the different visualizations showed a weak linear correlation to the accuracy of the participant's perception of the surfaces. This research shows that modelling perception of layered surfaces is a grand challenge and highlights the foundational problem of predicting significant variation that may arise between non-homogenous participants.

Acknowlegments

I thank Prof James Gain, my supervisor, for his patience, time, continued support, guidance and correction. His input, insight and encouragement have enabled me to complete this PhD. I am grateful for the NRF Grant-holders bursaries he organized for me, from Professor Edwin Blake, which have helped to finance this research. Further I would like to thank the University of Cape Town for the financial assistance they provided, in particular for travel costs to the USA, which was a turning point of the PhD.

I especially thank my dad, Robert Mitchell Lane and mom, Martjie Lane, who helped me so much, believed in me, supported me through their continued prayers. Their financial support has made this PhD possible. Further, my mother selflessly helped with editing. Without their help I would never have been able to complete this PhD. Thank you mom and dad.

I thank Glen Frost, who has been a project manager and true friend to me, believing in, me, calling me everyday, encouraging and inspiring me all the way.

I would like to acknowledge and thank Prof Victoria Interrante from the University of Minnesota and Prof. Russell M Taylor II from the University of North Carolina, Chapel Hill, for their comments and thoughts, which gave direction, context and encouragement that have shaped much of this dissertation, also Prof Andries Engelbrecht for his help and Prof David Levin and John Stone for their comments, and all the participants in the user experiments, who gave their time and valuable input.

I would like to thank Anton and Hanri Platzoeder and Sam and Sheralyn Cloete, who have been pillars of support through their care, friendship and prayer, Wei Chen for his encouragement and help, lending me his lap top, which made the write up possible. Further I thank, John Lane, my brother and Lona Groenendyk my sister, John and Avril Thomas, and Ashley and Rosemarie Cloete, Hagen Rode, Jonny de Villiers, Simon and Laurie Barnes and Jan Hendrik and Heidi Beetge.

Contents

List of Tables

List of Figures

Chapter 1

Introduction

The ocean and our planet being volumes are filled with a variety of three-dimensional objects, which, also being volumetric are filled with interior layers. The human body with its different layers of skin, tissue and interior organs, is also an example of this. All these objects have an outer three-dimensional surface that typically defines their form. Not surprisingly scientists, such as geologists encounter layered surfaces and are interested in their shape [Bair et al., 2006].

In many cases there is a need for scientists to understand the spatial relationships between the layered surfaces they deal with. Oceanographers, for instance, seeking to understand mixing dynamics during upwellings, study water masses and how these move and change over time.
These water masses which reside in large time varying volumetric datasets are determined by temperature and salinity. These multivariate data sets are typically, in practice examined by oceanographers through visualization techniques such as 2D slices and 2D temperature-salinity (TS) diagrams, which give only a limited understanding of the 3D shape of the water masses. Novel layered surface visualizations may make it possible to see the form of various water masses simultaneously, while maintaining spatial context and shape. Such visualizations could even be used to see temperature-salinity iso-surfaces or the same water mass at different time steps simultaneously. These more comprehensive perspectives of this data would likely lead to deeper insights into the dynamics of dissipation and interactions of water masses where mixing takes place.

Medicine also stands to benefit from layered surface visualizations, which illustrate spatial relationships between surfaces. Examples include evaluating tumour segmentation algorithms and tumour radiation treatment planning [Weigle, 2006]. Medical doctors planning a radiation treatment (chemotherapy) for malignant tumours, need to accurately determine the distance between a tumour, healthy tissue and radiation dosage volumes in order to establish how to best irradiate the cancer [Interrante, 1997]. These doctors ask the question, “Where is the dose not a good fit to the tumour or organs?” [Weigle, 2006], as they need to target the malignant tumour accurately enough so that the healthy cells are not damaged by the treatment. This requires an understanding of the shape of the different surfaces and the distances separating them. Visualization, by making use of interactive computer graphics, enables such analysis and exploration of layered surfaces. Showing a person a set of different surfaces visually provides an intuitive and comprehensive understanding of the structures of the different surfaces and the

spatial relationships between them. Other real world examples identified by Weigle [2006] that need effective layered surface displays, which facilitate spatial comparisons, include: atomic-force microscopy in Material Science and molecular docking for protein interfaces in Biochemistry. Weigle, further, performed a task analysis for layered/nested surface visualizations across these domains. His study identified the following foundational set of domain-independent spatial comparison tasks that a visualization should facilitate for exploring layered surfaces:

(1) global shape of the surfaces should be clear;
(2) local shape such as surface orientations and local features should be identifiable;
(3) distances between surfaces should be able to be accurately gauged.

While several approaches exist for displaying layered surfaces only a few techniques facilitate spatial comparisons between different surfaces. The leading class of techniques that preserve spatial relationships between layers rely on a combination of transparency augmented with opaque markings, which are dappled across the surfaces. Figure 1.1 shows one approach from this class of opaque marking-based techniques.

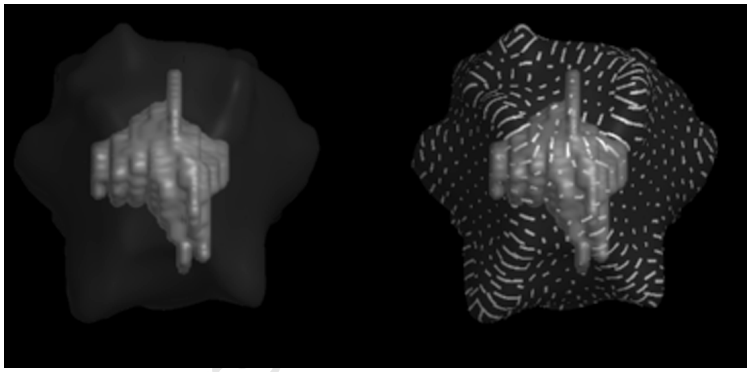

Figure 1.1 Semi-transparently rendered layers augmented with opaque markings (right) convey surface shape better than semi-transparently rendered layers alone (left) [Interrante, 97].

As illustrated in Figure 1.1, in this class of techniques the different surfaces are rendered semi-transparently and blended together. The opaque markings, which may take various forms, such as line strokes similar to hatched markings or grids, are employed to show the three-dimensional structure of the surface (Figure 1.1 right). This structure would be largely unclear, except along silhouette and contour lines, if the layers were only rendered semi-transparently (Figure 1.1 left).

While this class of layered surface techniques works well on two layered surfaces, several visualization issues arise when three or more layers are displayed. Interrante [1997] and Weigle [2006] have pointed out the need for applying layered surface visualization techniques to more than two layers. An example of this is seen in radiation treatment planning, in which it is desirable to understand the relationships between a tumour, different dosage level sets and

surrounding healthy tissue. Further, Bair et al., [2006] has shown that layered surface visualization is useful in enhancing volume visualizations. Mixing layered surface visualization with volume visualization is helpful because it creates a clearer picture and comprehension of surfaces within volume data. Volume datasets typically contain more than two nested surfaces. In summary, ways are needed to enhance current layered surface visualization techniques, so that they effectively address the visualization issues which arise when displaying more than two layered surfaces.

1.1 Visualization Issues

Layered surface visualizations attempt to simultaneously display the shape of the various surfaces as comprehensively as possible and yet facilitate comparisons between the surfaces [Weigle, 2006]. The display of layered surfaces is hence a type of optimization problem, where the challenge lies in finding the best way to show the various layers as "clearly as possible, while minimizing interference" across the layers [Bair, 2009]. In addressing this challenge, four visualization issues arise, especially in the case of displaying more than two layers:

(1) Occlusion is the first problem to be overcome when displaying layered surfaces in a way that facilitates comparisons between the different layers [Weigle, 2006]. Occlusion occurs when surfaces in the foreground obstruct or interfere with a clear view of surfaces that lie behind them relative to the line of sight. Opaque markings on multiple layers tend to obstruct the view of markings on surfaces behind them, even if individual markings are small.

(2) A second significant problem is that layers visually interact with one another [Bair et al., 2006]. This is markedly evident when using transparency in which layers are blended together. This causes a blurring of features, colours, surface lighting and shading.

(3) The third problem is that it is difficult to determine which markings belong to which layer even when they are coloured differently [Interrante, 1997]. The difficulty distinguishing markings on various layers is illustrated in Figure 1.2.

(4) The final issue for opaque marking-based techniques is finding the optimal display parameters. This requires determining: how many markings should be placed on each layer, how and where the markings should be positioned relative to each other and the viewer, and how large the markings should be?

Relating to issue (4), evaluating the effectiveness of layered surface visualizations is itself a challenging problem. Typically evaluation requires running psychophysical perceptual experiments. To perform these evaluations for multiple parameters over multiple layers would require numerous experiments, many participants and a large amount of time.

Figure 1.2 In visualizations of three layered surfaces it is difficult to make out the surface to which specific opaque markings belong. The left image is an illustration from Interrante et al. [1997], the right is from Bair et al. [2006].

Current layered surface display techniques need to be extended to more effectively address these visualization issues, especially when attempting to display more than two layers. Various ways, in which layered surface display techniques are enhanced, are through: improving usability or enhancing perception and comprehensibility of the surfaces. Some of these different supplemental approaches include using: interactive exploration, importance driven visualization, which automatically illustrates important features, and additional shape cues, e.g. displaying the surfaces in stereo, which enhances the perception of 3D shape. *Pendulum-style rocking* is another powerful means of augmenting layered surface displays through an animation of the surfaces. This rocking animation involves rotating the surfaces around different axes similar to a pendulum swinging back and forth. This induces the *kinetic depth effect*, the most powerful motion depth cue, which dramatically enhances 3D perception of the surfaces.

1.2 Thesis Statement

The purpose of this dissertation is *to develop methods to address the above visualization issues and enhance layered surface display techniques* to effectively show more than two layers. To this end, we firstly explore a novel visualization design, which relies on animating opaque markings over semi-transparent surfaces. This approach supports the foundational spatial comparison tasks identified by Weigle [2006], listed above.

Animating opaque markings over the layered surfaces is identified as a means of enhancing layered surface visualizations, because it draws on the following properties of motion, which are advantageous for addressing the aforementioned visualization issues:

(1) Motion has a strong perceptual grouping effect. Consider for example a flock of starlings flying north and slightly above them another flock of starlings flying east. The two flocks stand out perceptually as distinct groups because they move in different directions.

(2) Motion is able to produce a type of transparency effect. Opaque markings in one frame may occlude specific regions behind them but in successive frames, as the markings move to new positions, the previously occluded regions become visible.

(3) Moving the opaque markings also gives a more complete coverage of the surfaces over time than if the markings were stationary.
(4) It has been shown that points moving over a single surface enhance shape perception. This technique is called *Kinetic Visualization* [Lum et al., 2003]. *Kinetic Visualization (KV)* is an approach using animated particles which flow over a surface according to a set of motion rules to augment the standard display of a surface with additional shape and structure information.

In this work we compare the above advantages of motion against the current best practice of using rocking type animations to enhance shape perception. Based on our empirical evaluation, we posit the first thesis of this dissertation:

Rocking animation is significantly more effective than animating opaque markings on semi-transparent surfaces for displaying layered surfaces, since it contributes the depth cue of the Kinetic Depth Effect, a percept which is not apparent when simply animating the markings over the surfaces which only evokes a weak sense of motion parallax. Animating the markings over the surfaces is not more effective than displaying the markings statically. Animating the markings is however beneficial in combination with rocking for supplementing the display of four layered surfaces for exploratory feature identification tasks.

Secondly, we address the issue of finding optimal parameters (issue 4) by presenting a computational model of the way in which the Human Visual System (HVS) reconstructs layered surfaces. This model provides a means of automatically measuring the effectiveness of a layered surface visualization in terms of human perception. By quantifying the effectiveness of a layered surface visualization, we attempt to find optimal display parameters for enhancing such visualizations. Our experimental findings emphasise foundational problems with this proposal. The issues and potential benefit of the approach are expressed in our second thesis statement:

Modelling Human Visual System perception of layered surfaces for a homogenous sample of respondents has the potential of enabling automatic evaluation and optimization of layered surface visualization settings. However, modelling perception of layered surfaces is intricate and beyond the current state of theoretical modelling of the Human Visual System. A further difficulty modelling perception of such visualizations is that variation between non-homogenous participants is unpredictable.

The following research questions arise:

(1) Why use KV for Layered Surface Display when pendulum-style rocking, which provides more powerful depth cues, can be used? This question seeks to determine how KV compares to rocking in terms of its ability to facilitate specific shape tasks. It raises the sub-question: Are the shape cues induced by KV from the Kinetic Depth Effect or are the shape cues a

result of particles following contours?

The importance of this sub question is that if KV offers shape cues, which rocking does not, then using a combination of KV and rocking may well contribute more than using either alone. We therefore ask:

(2) Would a combination of KV and rocking be more useful than rocking alone for displaying multiple layered surfaces?

1.3 Approach

To address the visualization issues and answer the research questions, we develop and refine a visualization design that leverages motion for displaying layered surfaces and evaluate the design against rocking and in combination with rocking. This is done since rocking is the best alternative method for enhancing layered surface visualizations. These evaluations are achieved through controlled user experiments.

Our visualization design addresses the visualization issues by animating the opaque markings over the surfaces in the following ways:

(1) The opaque markings on different layers move in different directions or with different motion patterns. The markings on different layers are also coloured differently. Together this is proposed to help distinguish between markings on different surfaces.
(2) Static opaque markings would occlude the surfaces below them. Animating the markings causes them to move out of the way of previously obstructed markings, revealing a clear view of those parts of the surfaces that were occluded in the previous frame.
(3) Opaque markings moving over surfaces cover a greater number of samples of the different surfaces than a single set of static markings; that is, smoothly varying the set of samples of the different surfaces offers an integrated coverage of the surfaces over time.
(4) Markings flow over the surfaces according to certain motion rules help to enhance the perception of surface shape and features.

Particle systems are used to generate the animation of the markings, with each opaque marking corresponding to a particle. Different forces are applied to particles causing them to move in specific directions over the surfaces. The dynamic nature of the particles is used as a means of reducing occlusions. This is achieved by finding particles that are occluding others or very close to occluding others, and creating a force between them, which causes them to move away from one another. Potential negative effects of applying such forces are discussed in section 4.2.3.

We enhance layered surface visualizations further by developing a model of the Human Visual System for reconstructing layered surfaces. This model provides a means of quantitatively measuring the effectiveness of layered surface renderings. This in turn may be used to automatically tune display parameters. We build upon Grimson's [1981] model for reconstructing

a surface, incorporating relevant perceptual theory of surface completion, which describes how the Human Visual System recovers shape from the fragmented input typical of layered surface images. An iterative optimization process is used to optimize the visualization settings. We evaluate if our computational model correlates with human perception of layered surfaces by comparing it with user responses taken from a user experiment. We then use the model to find optimal parameters for our visualization design.

1.4 Contributions

This research advances state of the art in layered surface visualization through the following contributions:

(1) *Visualization Design Contributions*. This work primarily proposes the novel use of animating opaque markings as a means of helping to display layered surfaces. The animation of the markings is achieved through particle systems and incorporated into a framework for displaying layered surfaces. This includes modifications to Kinetic Visualization so that it may be used effectively for layered surface display. Technical modifications to KV include:

(2) *New motion strategies* for distinguishing between layers and illustrating shape.
This work is the first to take the view direction into consideration for determining how to best display layered surfaces. The framework caters for adjusting the positions of markings on different layers so as to reduce occlusions and interference through a new force rule. This rule is not only useful for animating markings over the layered surfaces and causing marking layout changes in response to changes to the viewpoint, but is also useful for static layered surface illustrations. For example, it may improve the visual layout of opaque markings by reducing occlusions in presentation images of layered surfaces.

(3) *Experimental Contributions*. Novel user experiments were performed that provide insight to researchers considering the use of animation for the display of layered surfaces. Findings from this research contribute to the theory of layered surface visualization. The experiments provide answers to our research questions and reveal additional issues, which arise when using motion to perform shape tasks. The experimental contributions include:
   (a) A novel user experiment comparing static surface markings, static markings augmented with rocking animation and markings that flow over a surface. This experiment compares these approaches for three different shape tasks.
   (b) A novel experiment, comparing a combination of rocking and KV to rocking alone for three and four layered surfaces using two different shape tasks. The experiment also compares the use of different marking types, specifically surface patches versus crosses.
   (c) A novel experiment testing for correlation between our new perceptual measure of the effectiveness of layered surface visualizations and users' performance for a shape task.

(4) *Contributions for Evaluating and Optimizing Layered Surfaces*. A novel model of HVS perception specifically for marking-based layered surface visualizations is developed and used to measure how effectively layered surfaces are being displayed. As it is not feasible to

resolve the large number of different parameters in question for a layered surface display through user experiments [Bair, 09], this is a significant step towards helping layered surface visualization researchers and designers who need to evaluate their designs or refine parameters for displaying multiple layers, without having to perform extensive user testing.

1.5 Thesis Organization

Next, Chapter 2 presents relevant theory of shape and motion perception that describe how shape is visually conveyed and perceived. Chapter 3 provides a literature study of related work in layered surface visualization. This chapter identifies the niche of our visualization design in relation to other layered surface visualization techniques. It also presents precursors to our design from multivariate visualization and particle systems.

Our novel visualization design is presented in Chapter 4. This includes modifications made to Kinetic Visualization for layered surface display. The evaluation of the approach in comparison with pendulum style rocking and in combination with rocking is presented in Chapter 5. This includes results, analysis, and a discussion of our novel visualization design and the use of KV for layered surface visualization.

Chapter 6 introduces the novel idea of using a computational model of human perception for evaluating and optimizing layered surface visualizations. It presents related work for optimizing layered surface displays and relevant theory on the perception of layered surfaces.

Chapter 7 details our model of layered surface perception and Chapter 8 presents the evaluation of this model. Chapter 9 presents recommendations, conclusions and proposals for future advancement of this research.

Chapter 2

Background on Shape Perception

Research in the perception of shape and motion, layered surface visualization and multivariate visualization provide a rich source of erudition and information that is useful for developing a layered surface visualization design. A review of related work in layered surface and multivariate visualization is addressed in chapter 3. This chapter presents a background in the perception of shape, describing how it is understood by the human visual system. This includes a review of perceptual depth cues, which play a significant role in the perception of surface shape. Kinetic depth cues resulting from objects in motion are also a key component of our proposed visualization design. Furthermore, current approaches for measuring a person's perception of shape are reviewed, since these play a crucial role in determining the effectiveness of a layered surface visualization. This background shows that these current approaches for evaluating visualizations are time consuming, and may benefit from our automatic and perceptually based measure for evaluating layered surface visualizations.

2.1 The Elements of Shape Perception

How is the shape of a surface, let alone of multiple layered surfaces, understood by a person? Upon observing a shape, a person's visual system builds a comprehension of the shape by interpreting different features and indicators of its form, such as silhouettes, that are seen. These indicators convey visible depth discontinuities [Weigle, 2006], from which an organization of depth and spatial relationships across the surface are established [Interrante, 1996]. This comprehension of shape may be accompanied by interpolation, inferences and assumptions, such as presuming that the scene is lit from above. There are several indicators that reveal the appearance of a shape. Collectively, these indicators of shape are referred to as perceptual depth cues. These are presented in section 2.2. One of these indicators of shape is shading, which refers to the way a shape appears to a viewer under various lighting conditions.

2.1.1 Shading

The variation in colour seen across a surface from a particular viewpoint is known as shading [Adelson & Pentland, 1996]. Consider for a moment the blue ball in Figure 2.1. When diffuse light is used (center), or diffuse lighting with specular highlights (right), provided there is sufficient luminance, the ball appears to have varying shades of colour across its surface, which reveal its spherical shape. However, without this shading, the ball would look like a flat disk (Figure 2.1 left). The highlights in Figure 2.1 (right) are a result of modelling specular reflections.

Figure 2.1 Illustrations of shading on a blue ball. Left: a ball without shading appears flat. Center: applying shading with diffuse lighting results in various shades of blue across the surface that convey its shape. Right: specular highlights are added to the shaded ball.

Shading gives an impression of 3D shape, curvature and depth. Shading on its own is under constrained since multiple variables affect the shading of a surface. Additional information about a scene is needed to accurately interpret the shading [Ramachandran, 1988]. People attempting to make sense of an object with only shading cues tend to assume, based on natural experience [Kersten et al., 2004], that the lighting is coming from above. Shading thus best represents shape in combination with other depth cues. The shading of a surface depends on three key variables:

(1) lighting: the direction, intensity, type of light and position of the light source(s),
(2) the surface: the position of the surface relative to the viewer and light source, the physical shape of the surface and its material properties, and
(3) the observer: the position of the observer and view direction.

2.1.2 Lighting

Visible light makes it possible for a person to see a surface. It is the light that is reflected off or transmitted through a surface, which reaches the eye that makes the surface visible. Light has both a wave nature in terms of its propagation, being an electromagnetic wave with wavelengths in the range of 400 and 700 nm (nanometres), and a particle nature, in terms of its absorptive and emission properties [Young, 1992].

The simulation of light and its interaction with surfaces, causing shading, in computer graphics is based upon on geometric optics in which light is modelled by rays, which travel in straight lines. This simplified model of light caters for the interaction of light at the interface of two materials, for example, where air and a surface meet. This interaction may result in some combination of light rays being reflected or transmitted. The Phong lighting model is most commonly used for such interactions and illustrating shape. This model conveys curvature, shape and a sense of depth [Phong, 1975]. Phong lighting empirically fits two specific physical laws of light which create a visual appearance that is similar to the way in which light is reflected off real objects. It models specular reflections and the way light is reflected from a diffuse surface by using Lambert's cosine law. This law results in varying shades (intensity) across a surface, determined by taking the cosine of the angle between the directions of incident light and the surface normal [Blinn, 1977]. When light strikes a surface it is reflected from the surface such that the angle of reflection is the same as the angle of incidence, according to Snell's law of reflection. Specular reflections and highlights are seen at points on the surface where the reflected light leaves the surface in the direction of the view point. The Phong lighting model incorporates these specular highlights. Since our work seeks to best illustrate surface shape, this is a good model to use, since even though highlights increase the visual complexity of a shaded surface, compared to diffuse lighting alone, they do seem to improve shape perception [Fleming & Adelson, 2004].

The type of light, lighting conditions and position of a light source also play an important role in the accuracy of shape perception. For instance, accurate orientation judgements have, in an experiment, been most accurate under oblique lighting (an angle of 20 to 30 degrees above the viewpoint) for smooth irregular closed shapes with cast shadows [O'Shea et al., 2008]. This is because for these conditions, lighting from this angle is assumed by the HVS.

2.1.3 The Surface

The local geometry (shape) of a surface upon which light falls also determines the direction and distribution of the light that is reflected from it.

2.1.3.1. Geometric Shape

The shape of an object is determined by the way an object's surface changes over some local

neighbourhood and the scale of this neighbourhood. A *tangent plane* is a first order approximation of a surface's orientation at a point. The tangent plane is defined by the first partial derivatives of the surface at the point and varies in two orthogonal directions. The *surface normal* is a vector, perpendicular (orthogonal) to the tangent plane at a point on the surface that represents the orientation of the surface at a point. Together the surface normal and tangent plane provide a 3D reference frame to help describe how the shape of a surface changes at a point.

As one moves over a surface, away from a point on the surface, the tangent plane changes its orientation to match the way the surface changes. Surface *curvature* is a measure of the rate at which the surface normals change and is defined by the second partial derivatives of the surface. The direction in which the steepest change occurs is known as the first principal curvature direction, also referred to as the line of transverse curvature. The direction of minimum change in the surface normals is the second principal curvature direction or radial curvature. These two directions lie orthogonal to each other in the tangent plane. Figure 2.2 illustrates a surface normal, tangent plane and curvature.

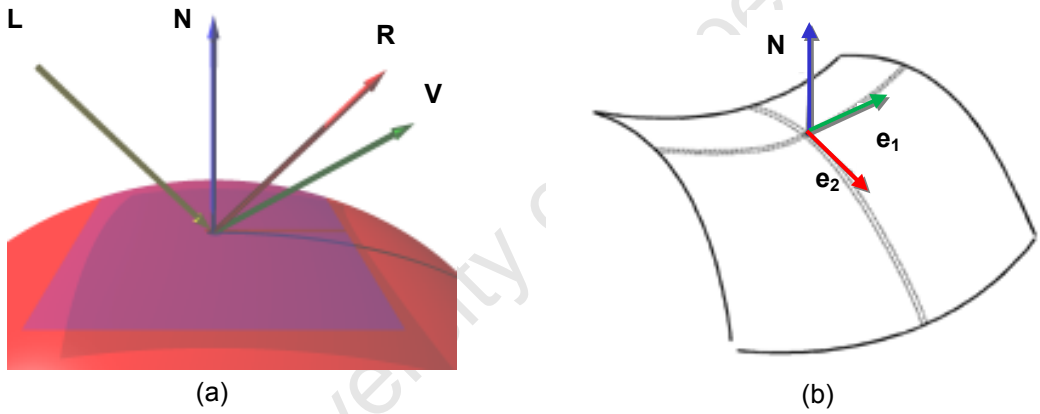

Figure 2.2 Illustration of: (a) surface normal, **N** and tangent plane, with vectors used for modelling light and surface interaction. These include **L** the angle of incident light, **R** the angle of reflection and **V** the vector to the viewer (b) curvature, $\mathbf{e}_1$ represents the first principal curvature direction-the direction in which the normals change at the fastest rate. $\mathbf{e}_2$ is the second principal curvature direction and **N** the surface normal.

Gaussian curvature is computed as the product of the maximum and minimum curvature. It indicates, when positive, that the surface is convex, when zero that the surface is flat and when negative that the surface is concave. The mean curvature, calculated as the average of the maximum and minimum curvatures, gives an indication of the average change of the surface at a point [Koenderink, 1990]. Together the surface normal and curvature influence the shading of a surface. Light that strikes a surface is reflected about the surface normal, while the curvature effects the variation of shading across the surface.

The surfaces of most real world objects are said to be two-manifold. This refers to the mathematical topology of the surface. A manifold is a space, which within a small local neighbourhood resembles the Euclidean space. Two-manifold implies that the surface has the same topology as a plane or sphere.

In perspective computer graphics, as well as the human visual system, the visible shape of an object that is seen is a projection of an object onto the view plane. This projection of a surface has several features called folds including: occlusion boundaries, contours and silhouette curves. Folds are those points (locus of points) on a smooth surface where normals are perpendicular to the view direction and where there is a discontinuity in visible depth, which arises because of the projection of objects onto the image plane. The occlusion boundary is a fold, formed by those points which are on the boundary of occluded and visible regions. Silhouettes are occlusion boundaries that separate an object from the background. These features communicate important shape structure including whether the surface is concave, convex, cylindrical, planar or saddle shaped. Silhouettes and occlusion boundaries are illustrated in Figure 2.3.

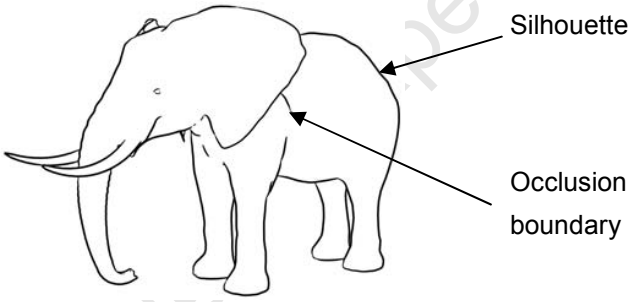

Figure 2.3 Folds, such as occlusion boundaries and silhouettes are seen at points of a surface where the surface normals are perpendicular to the view vector, and contribute significantly to the illustration of shape. Illustration from [DeCarlo et al., 2003].

2.1.3.2. Material Properties and Reflectance

When light strikes a surface some of the light is absorbed, some of it reflected and if the object is semi-transparent, some of the light is refracted through the object. The light reflected from a surface in computer graphics depends on the surface's material properties. These include:

(a) the translucence of the surface, being either opaque or semi-transparent; and
(b) the colour and the type of surface, being diffuse or specular.

Opaque objects reflect and absorb light only. The amount of light absorbed by an object depends, in physics, on the wavelength of the light reaching the object as well as the colour of the surface. Other properties of a surface that affect its appearance are the type of surface or its smoothness which determines the way light is reflected off the surface. Shininess relates to the smoothness of

a surface. Smooth or specular surfaces reflect almost all light in the direction of reflection, e.g. a mirror. Diffuse surfaces, which appear dull, typically have a rough surface that scatters light in all directions, e.g. matte surfaces. Translucent surfaces allow light to pass through the object. Light seen through a transparent surface is computationally modelled by blending colours. Figure 2.4 illustrates the interaction of light with various types of surfaces.

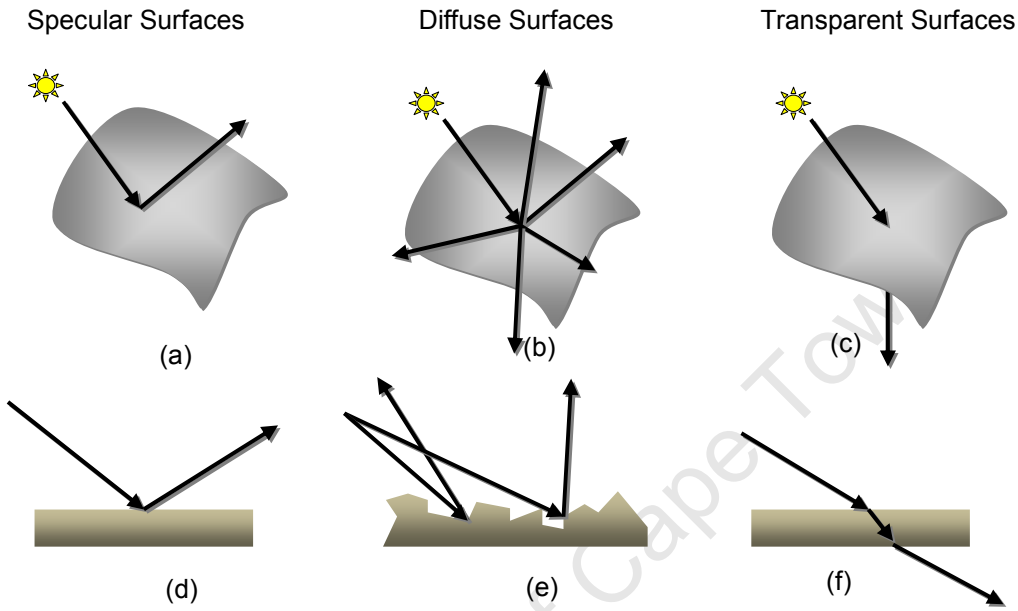

Figure 2.4 Light interacting with various types of surfaces: (a) Specular surfaces are smooth surfaces, which reflect light at the angle of reflection; (b) diffuse surfaces scatter light in multiple directions; (c) translucent surfaces allow some of the light to pass through the surface. (d) Specular surfaces are smooth surfaces (e) Shows a rough surface, which causes diffuse reflection. (f) A translucent surface causes refraction of the light that is transmitted through the surface.

2.1.4 The Viewer and the Human Visual System

The light, reflected from a surface or transmitted through a surface that finally reaches the viewer contributes to the formation of an image of that surface. The Human Visual System (HVS), which receives this light through the eyes processes and interprets the image. A person is equipped with an intricate and sophisticated visual system. Light enters this imaging system, through the eyes, which have many components that are similar to a camera. An iris like the camera's shutter controls the amount of light entering the eye. A lens and cornea focus light onto the eye's "film" or image plane (called the retina) at the back of the eye. The retina contains highly sensitive light sensors, called cones and rods which are excited by different intensities of light and frequencies in the visible spectrum. The photoreceptors of the eye vary in density and sensitivity to light. This results in a high resolution image, which is formed in the fovea or center of view. Visual acuity (resolution) depends on the sizes of the rods and cones and the properties of the lens and cornea

[Palmer, 1999][Angel, 2000]. Layers of neurons perform filtering and simple image processing of the image, in parallel, before transmitting it to the brain. Some of these parallel filters perform brightness contrasting. Optic nerves connect in a highly intricate manner to the cones and rods and convey the image to a region of the brain called the visual cortex, which performs high-level image processing such as object recognition, similar to a sophisticated signal processor.

A viewer's vantage point in relation to a surface's local geometry plays a significant role in how a shape and its features are imaged. The view direction for instance determines the visible surface features, such as silhouettes, and how effectively texture patterns on the surfaces illustrate the shape of the surface. An example of the influence the vantage point has on the perception of a surface was seen in an experiment, in which oblique views of a surface with parallel plane textures resulted in better surface orientation judgements than top down views of terrain surfaces [Sweet & Ware, 2004].

2.2 Perceptual Depth Cues

The human visual system has special processing mechanisms that are sensitive to image and object features called perceptual depth cues. These depth cues play a significant role in a person's comprehension of surface shape by establishing depth order relationships [Cutting & Vishton, 1995]. For our layered surface visualization design we desire to incorporate and combine depth cues so as to effectively convey the shape of the different surfaces. Depth cues are typically classified as being either pictoral, binocular, oculomotor or motion cues. The perception and understanding of a 3D scene from a 2D image is typically built up from a combination of these cues. Such a combination more effectively conveys shape than different cues in isolation [Ernst & Bülthoff, 2004]. For instance, texture combined with shading results in a better understanding of shape than shading alone [Todd et al., 1997].

2.2.1 Pictoral Cues

Artists faced with the challenge of illustrating 3D shape on a flat piece of paper (in 2D), use pictoral depth cues to convey a sense of depth and structure. These cues do so typically by communicating an understanding of relative arrangements and variations of size, shape or shading as a shape recedes from the viewpoint or as a shape curves. Shading is one example of a pictoral cue. The various pictoral cues displayed in Figure 2.5 are discussed below:

Occlusion or Interposition: The most effective pictoral depth cue is occlusion [Cutting & Vishton, 1995], also known as interposition. It conveys a powerful sense of relative depth order between objects or even across a single surface. Occlusion occurs where an object closer to the viewer partially eclipses an object behind it, or when part of its surface overlaps a portion of the same object further away from the viewer.

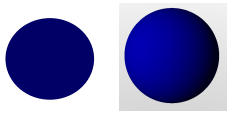

Shading

Brightness

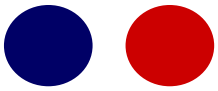

Colour

Relative Size

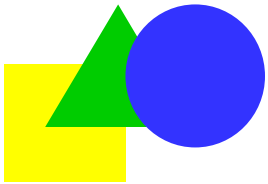

Occlusion

Lines e.g. Silhouettes

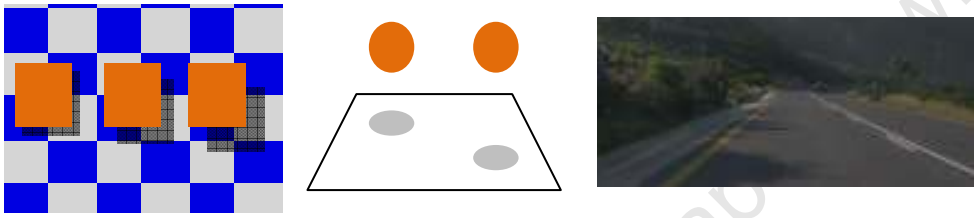

Linear Perspective and Shadows

Distance to the Horizon

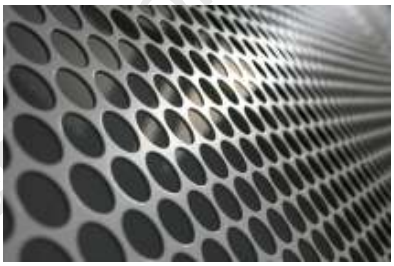

Texture Gradient

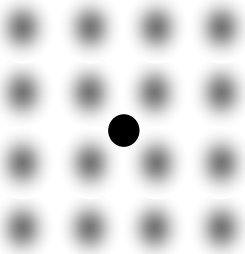

Focus

Atmospheric Attenuation

Figure 2.5 Illustrations of Pictoral cues, which create an impression of depth and shape. Adapted from [Pfautz, 2000]. Whale picture from Dragoart.com.

Perspective, Relative Familiar Size and Relative Height: Another cue arising from perspective projection is that objects appear smaller the further they are from the viewpoint. When two objects of comparable size are seen with one of them appearing larger than the other, the larger object stands out as being closer to the viewer. A person infers relative depths from differences in sizes of projected objects. For this cue to be used without error it is necessary that a person has an estimate or understanding of the sizes of the objects.

Linear Perspective: In perspective projections of 3D scenes straight parallel lines which run into the distance converge to a single vanishing point. This is illustrated in Figure 2.5 where the lines of a road running into the distance come together as they recede towards the horizon. With this cue, it is difficult to accurately judge depth for smoothly curving objects or objects with limited depth extent that are far off in the distance. This is because objects far from the viewer, or smaller objects, have less distinct differences in perspective size. However, this cue does help to infer depths for objects on the same ground plane. As a ground plane extends into the distance, objects on the level of the plane are projected to positions higher up in the image.

Atmospheric Attenuation: Atmospheric attenuation occurs when light rays are scattered by either dust or water particles in the air [Blake & Sekuler, 2002]. This causes distant objects such as the mountains in Figure 2.5 to appear "washed out", in contrast to those closer in depth. Scattered light from the sun is linearly polarized and consists mainly of blue light, since higher frequencies of the visible spectrum have shorter wavelengths (e.g. blue's wavelength is approximately 450 nanometers (nm)) and are reflected. Light with lower frequencies and longer wavelengths (e.g. red's wavelength is approximately 650nm) penetrate deeper through the haze. This is why distant mountains appear blue.

Focus and Depth of Field: Upon focusing on an object, both a camera and the human visual system cause other objects in the background or foreground to go out of focus. A difference in focus is interpreted as a difference in depth.

Shadows: Shadows arise when an object occludes light falling on another object behind it. Shadows cast onto a ground plane give a sense of relative depth and an impression of the silhouette shape of the object casting the shadow. The depth cues discussed above are effective as long as there is sufficient contrast in shading across the scene, e.g., shadows must be significantly darker than the surface on which they fall for them to be clear and effective. Uniform lighting obscures contrast, causing shadows and other cues to become vague or disappear completely. This causes depth cues to lose their effectiveness even in cases where multiple cues are combined [Mamassian et al., 1998].

Illustrative lines and markings: *e.g. boundary or occluding contours*: contribute further significant depth and shape information. These not only mark the region of occlusion and depth

change but, all along the contour, reveal the orientation of the surface. Surface normals along the points on these contours are inferred by the viewer to be perpendicular to the line of sight. This accurate knowledge of the surface normals along the contours can be interpolated across the rest of the surface, using other shape cues, such as shading. Boundary contours may cause a change in an interpretation of other perceptual cues because they are such a strong cue. Occlusion boundaries also influence the sense of continuity or global shape of the occluded objects behind them, because the human visual system performs surface interpolation across certain occluded boundaries. This surface completion is dealt with in more detail in Chapter 6.

The cues of depth of field and atmospheric attenuation reduce detail in an image. These cues often help to focus a viewer's attention more than they contribute to the sense of depth in a scene.

Lines provide strong shape cues. Examples include silhouette lines, creases, surface boundaries, ridge and valley lines, suggestive contours, reflection lines and shadow edges. Lines alone are able to convey shape in the absence of other cues, as illustrated by the picture of the whale in Figure 2.5. The human visual system infers an understanding of 3D shape from lines by considering global characteristics of an image such as context, symmetry and parallelism. While lines are useful for illustrating form, they can also have a depth collapsing effect. Silhouettes for example collapse the sense of depth for smoothly curving surfaces. This is because in real life such surfaces have a separation between the silhouette lines for the left and right eye. Drawing a single line may give an impression of a flat region or sharp edge [Koenderink, 1984].

The use of lines, curves and strokes are common to nonphotorealistic rendering (NPR) techniques for illustrating surfaces. Stippling is one NPR technique [Lu et al., 2003], which is useful for illustrating shape and depth. A sense of depth has been achieved for volume datasets by rendering fewer and smaller points for more distant surfaces, creating a type of distance-attenuation effect [Lu et al., 2002]. Interior surfaces are made visible in stippling, by using fewer points on exterior features, allowing the interior features to be seen through the points. Point rendering, like screen door transparency, has the natural ability to achieve a transparency effect. Stippling is essentially a case of opaque marking-based visualization, where the markings are points. Our work uses markings which have a larger surface area and extends these techniques through animation. Typically stippling approaches produce static images.

2.2.2 Texture

Texture is also a pictoral cue. We deal with it separately though, because of its relation to our work, in that opaque markings dappled over a surface are equivalent to a texture. A sense of surface shape, depth and structure can be significantly enhanced in perspective views through the use of texture. Figure 2.6 shows an illustration of this, from Kim et al., [2003] in which texture is used to enhance shape perception for a tooth.

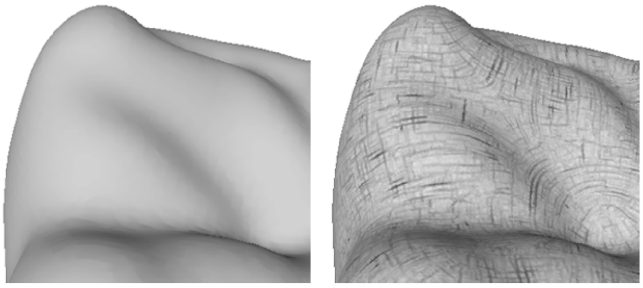

(a) (b)

Figure 2.6 Texture can be used to illustrate shape better than shading alone. (a) Shows an image of a tooth with shading; (b) Shows the same image augmented with a texture that follows principal curvature directions. The texture enhances the shape of the tooth [Kim et al., 2003].

Textures can either be homogenous or inhomogeneous and either isotropic or anisotropic. Examples of combinations of homogenous and isotropic textures are illustrated in Figure 2.7. Homogenous textures have the same pattern with constant size and repetition across the texture. Inhomogeneous textures are non-uniform in that they have larger or distorted regions of the pattern in different parts of the texture. For this reason, inhomogeneous textures are not ideal for illustrating shape, since the distortion may contradict other shape cues. The patterns of isotropic textures are the same in all directions, while patterns of anisotropic textures are not. Examples of anisotropic textures include lines or grids which are elongated only in two directions.

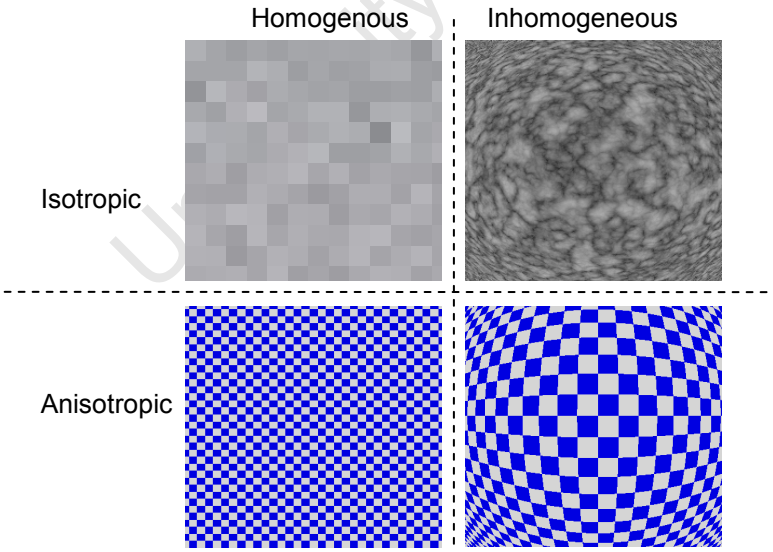

Figure 2.7 Combinations of Homogenous and Isotropic textures.

Depth cues arise from textures mapped to a surface, especially when viewed with perspective projection. This is because the per-unit surface area of a plane will appear to become decreasingly

smaller as the plane recedes from the viewer for a planar surface rendered with perspective projection. This change becomes most apparent when a uniform (homogenous) texture is placed on the surface. Textured markings appear to vary in size and frequency, depending on their depth and orientation in relation to the viewer. The cues that arise as a result of this apparent change in size of texture elements are displayed in Figure 2.8 and are described below:

Compression is the most significant of the texture cues in stereo, but is effective even in monocular displays. It shows the slant and tilt of the surface, where the slant is measured as the angle between the surface normal and the line of sight, taken perpendicular to the image plane, while the tilt is the direction of the slant in the image plane. Texture compression arises from texture gradients (variations of the projected texture pattern) [Stevens, 1981]. Texture compression is determined by the surface orientation relative to the image plane .

Perspective convergence is equivalent to perspective foreshortening. As a pattern extends into the distance, lines of the pattern converge. This is a strong textural cue and is dominant over vertical compression.

Size and gradient reveal relative depth. Gradients reveal the slant of a planar surface.

Density both that of the marks and the density gradient, depends on the distance from the viewer, "obliqueness of view" and inter-element spacing.

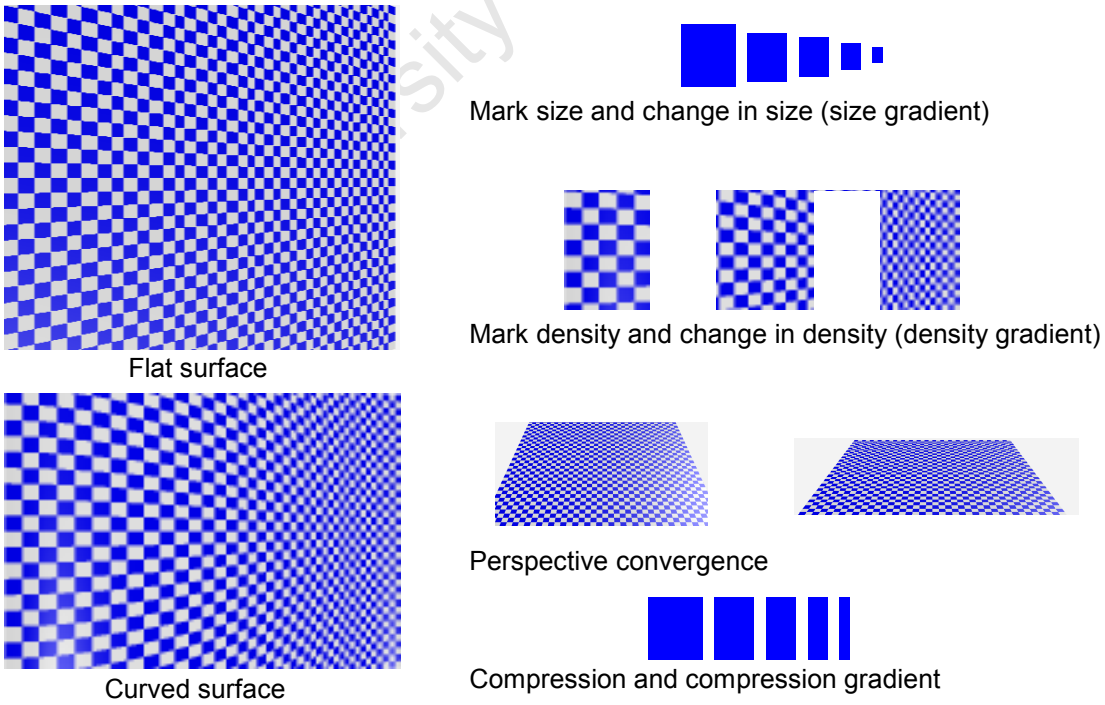

Figure 2.8. Texture cues arising from homogeneous textures. Illustration adapted from Bair, [2009] .

Finding the most effective way to render layered surfaces using opaque markings equates to trying to find the best texture patterns on these surfaces that illustrate their shape. In this regard numerous studies have been performed to determine the type of textures and viewing conditions, that most effectively convey the shape of a single surface [Interrante, 01] [Kim et al., 2003] [Sweet & Ware, 2004] and overlaid surfaces [Bair, 2009]. Sweet and Ware [2004] have shown that a grid texture with both horizontal and vertical lines is more effective than using a texture with lines in only one of these directions. Kim et al. [2003] have shown similarly for principal curvature textures that using two directions is better than using one. The use of two directions being better than one may be attributable to orientation being shown in two directions or differences in spatial frequency, contrast or higher order statistical characteristics of the textures.

Principal direction textures have been shown to be more effective than constant direction textures, such as grids with horizontal and vertical lines, for feature-finding tasks from both top down views and oblique views, without stereo [Kim et al., 2003]. However, Bair [2009] found that there is no significant difference in overall error between principal direction and projected grid textures, noting that the places on the surface where errors occurred were different for the two types of textures. Projected grid textures are inhomogeneous and therefore do not help much when viewed from the direction of projection [Bair, 2009]. However, anisotropic grid-like textures do illustrate surface contours because their shape is deformed by the shape of the surface. Variation to the texture due to perspective foreshortening and surface variation convey form. Examples of these cases, where one texture type is better than another are illustrated in Figure 2.9.

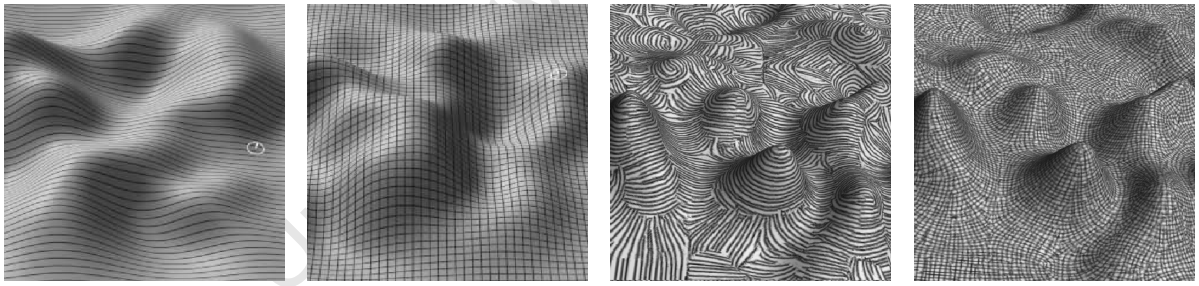

(a) (b) (c) (d)

Figure 2.9 Using textures with two directions (b) and (d), convey shape better than using a single direction (a) and (c). Principal curvature directions with two directions (d) are also more effective than projected grid textures (b). Illustrations from [Sweet & Ware, 2004], [Kim et al., 2003].

People make fewer errors in estimating surface orientation when surfaces are viewed from an oblique viewing angle rather than from above [Sweet & Ware, 2004]. This is because top down views do not capture as much of the magnitude of variation to the texture from perspective distortion as views from a 45 degree vantage point.

For layered surfaces, more so than for a single surface, texture parameters such as luminance, size and spatial frequency, significantly influence perceived shape, visibility and discrimination between the shapes of the surfaces [Bair et al., 2006] [Bair, 2009]. Brightness of textures is very important in making shading cues available. Textures with different directions and structure are useful for distinguishing between two layers [Bair et al., 2005]. Achieving success with a texture for illustrating shape also depends on the type of shape task being performed. Feature finding tasks require little help from textures while shape-dependent tasks require distinct texture cues [Bair, 2009]. Opaque texture markings placed on an outer semi-transparent surface layer, have been shown to improve 3D shape perception between two layered surfaces [Interrante, 1997].

2.2.3 Binocular and Oculomotor Cues

There are two classes of cues which arise in relation to the HVS having two eyes and the need to physically control them. The first class, binocular cues, arise as a result of the visual system fusing left and right eye images to create a 3D picture of a scene. The second class of cues, oculomotor cues relate to the control of muscles in the eyes which cause them to focus.

Binocular Disparity results in one of the strongest depth cues. Our eyes are separated by a small amount, causing the left and right eye images to be slightly different. The images from the left and right eye are fused, to form a 3D shape; the visual system matches corresponding points in these two images and uses the disparity between the images to gauge the depth of points in a scene. The further an object is from the viewer, the weaker this cue becomes, since the disparity between the images becomes increasingly small.

Vergence and accommodation are oculomotor cues that occur when the eyes focus on an object. These cues are rarely used in current computer displays, since they require eye tracking and contribute a weak sense of depth. They might become more common place in the future, especially if holographic displays become available, which engage all the depth cues.

Accomodation is a weak depth cue that arises as a result of the Ciliary muscles relaxing or contracting to change the curvature of the lens when focusing on an object. When the muscles relax, the lens flattens to focus on distant objects. The lens focuses on closer objects, when the muscles contract. Objects that are out of focus appear blurred. Inappropriate blurring of rendered 3D scenes can distort a viewer's perceived sense of the depth and shape [Watt et al., 2005].

Vergence is a depth cue which arises when a viewer focuses on an object with both eyes. The eyes turn slightly inward causing the direction of sight to converge on the object of focus. This depth cue arises as a result of the brain sending signals to the eyes to control their direction of gaze. As a cue it works best within a 6 meter range.

2.2.4 Motion Cues

Motion plays a significant role in a person's understanding of shape and depth. The perception of shape through motion has been referred to as structure-from-motion (SFM) [Wallach & O'Connell, 1953][Lum et al., 2003]. In this work, the ability of the HVS to perceive the 3-D shape of objects solely from motion cues [Andersen & Bradley, 1998] will be referred to as structure from motion perception.

The visual system deals with self motion and the motion of objects moving relative to a person. The depth cue arising from translations of objects relative to a viewer is known as motion parallax. The depth cue arising from the rotational motion of objects in relation to a stationary person is referred to as the Kinetic Depth Effect [Wallach & O'Connell, 1953].

When objects in the visual field move or when an observer moves, a sequence of images is created on the retina (optic array) of the eye. The visual system captures most motion changes in its environment in a continuous and smooth manner. The changes to the images on the optic array form a continuous gradient when motion is observed, creating a visual field of motion called the "optic flow". This optic flow is then interpreted by the brain, which infers depth by matching corresponding points in the motion patterns over time. It also provides information about an object's trajectory and speed [Sekuler et al., 2002]. The sense of depth and information about motion contributes to a person's understanding of 3D structure and layout. Optic flow is thus the mechanism used by the HVS to process motion. The optic flow, which is a velocity field, can be understood in terms of four elementary motion fields consisting of different affine transformations. Figure 2.10 illustrates these transformations, which are as follows:

- curl – a rigid rotation component;
- divergence – an isotropic or parallel expansion and compression component;
- deformation – a shear component, and
- translation

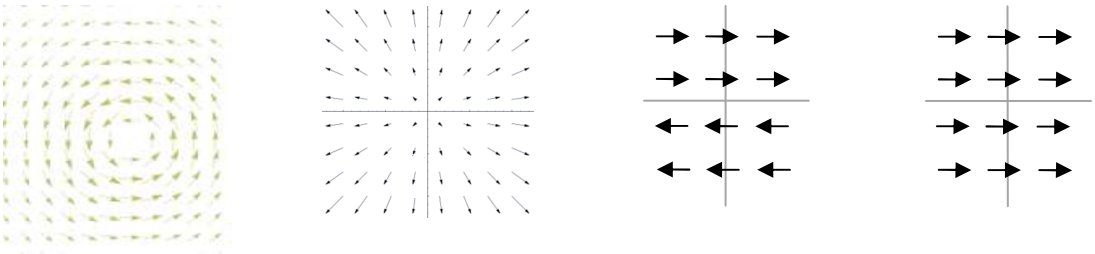

(a) (b) (c) (d)

Figure 2.10 Motion in the optic array may be reduced to combinations of atomic affine transformations. The transformations are: (a) curl, (b) divergence, (c) deformation, (d) translation.

The type of motion and the way it is observed, either actively or passively, plays a role in how

effectively the depth cues are perceived. Motion initiated by an observer (termed active viewing), provides a better understanding of a scene than passive viewing of moving objects that is not initiated or controlled by the viewer. This is because, with passive viewing, there may be uncertainty about the direction or extent of the motion.

A "building up" time is required for a person to perceive shape from motion: points need to be tracked for more than 60 milliseconds (ms) for a shape to be perceived, according to findings from a random dot SFM experiment, in which dots were rotated around a cylinder [Treue et al., 1991]. This experiment further showed that optimum perception of shape appears when points in motion are visible for at least 125ms. In such random dot experiments, the motion of markings over the surfaces is typically due to a rotation of a rigid body [Lum et al., 2003], which induces the Kinetic Depth Effect. The density of the dots on surfaces also influences how effectively the HVS interpolates a surface. Shape can be perceived in as little as two frames for a large number of dots. However, if fewer points are used, these need to appear in varying positions over the surface over time for a person to perceive three-dimensional shape. This seems to indicate that the HVS uses surface interpolation and integrates the point positions over time, to construct a representation of 3D shape [Andersen & Bradley, 1998] [Treue et al., 1995].

In addition to optic flow and depth cues, motion may also produce an effect known as motion transparency: surfaces consisting of opaque dots appear transparent when two or more sets of dots move over the surface through one another in different directions, or when the dots move with different speeds [Sekuler et al., 2002]. The various depth cues arising from motion are described next.

(1) Dynamic Occlusion

Objects that move partially in front of others create dynamic occlusions. An object in one scene may completely hide an object behind it, but a fraction of a second later move away to reveal the background object. These forms of motion reveal depth order relationships through varying occlusions. A rotating object also results in visible changes to the boundary contours and varies self occlusions and views of the object, which help to reveal shape more completely than if the object were stationary.

(2) Motion Parallax

Motion parallax is a strong depth cue that results from linear motion of objects in relation to a viewer. This motion depth cue typically arises when an observer moves in relation to objects (static) in a scene. This motion of the viewer results in a parallax effect, since multiple perspective views of the scene from different positions are seen. While stereo depth estimates are based on binocular disparity, depth is gauged in motion parallax by a disparity ensuing from perceived displacements of objects (corresponding points) over time.

Figure 2.11 illustrates motion parallax. This figure shows that the motion of the observer results in objects which lie behind a focus point seeming to move in the same direction as the viewer is moving, while objects closer than the point of focus appear to move in the opposite direction. The apparent speed at which the objects move in relation to the viewer is proportional to their distance from the point of focus. Consider driving in a car along a route parallel to a mountain. When looking at a specific point on the mountain, the clouds behind the mountain will seem to move in the same direction as the car but a tree closer than the mountain will seem to pass by in the opposite direction.

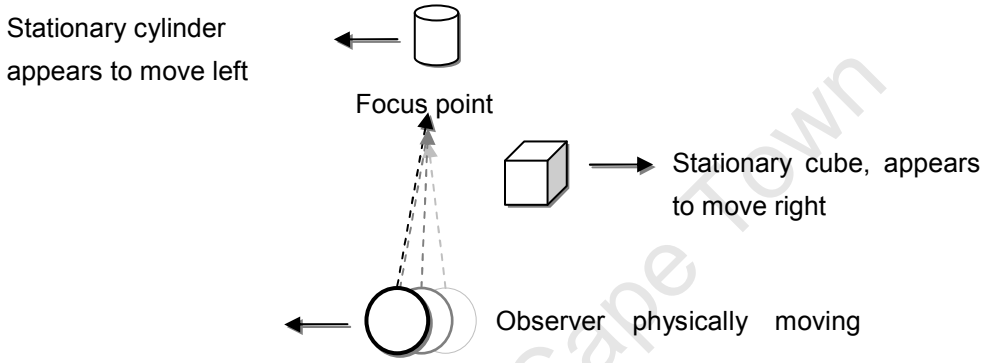

Figure 2.11 Illustration of motion parallax. As the observer moves to the left, the cylinder beyond the focus point appears to move to the left, while the box in front of the focus point moves to the right.

Motion parallax also arises when the objects move linearly relative to a stationary observer. Objects which move, transversely to an observer at different depths, but with the same velocity, cover different visual angles or distances relative to the observer. The objects further away from the viewer appear to move smaller distances across the image plane than objects closer to the viewer. Noting, that it is the objects in motion and not the observer, the apparent difference between velocities of the objects in motion reveals depth and shape information [Weigle, 2006]. This is illustrated in Figure 2.12. Motion parallax works only for perspective views of a scene as opposed to orthogonal views, since in orthogonal views translations at different distances from the viewer undergo the same relative displacement in relation to the viewer.

Objects that move relative to a viewer at the same speed in the same direction, perpendicular to the view direction result in the strongest sense of depth, since this is equivalent to a rigid body translation. However, for non transverse motions or objects moving at different speeds or in different directions, the motion parallax depth cue is less powerful. There are rare cases where people are not able to perceive depth from stereo. However, motion parallax has been shown to give a sense of depth even in these cases.

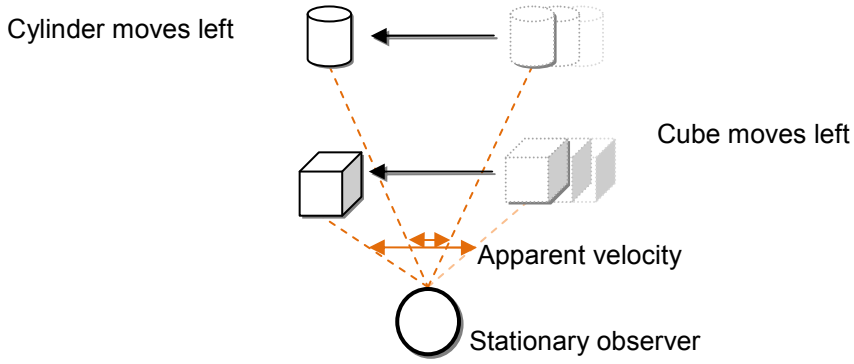

Figure 2.12 Illustration of the cue of kinetic depth. Two objects moving at the same speed, appear to be at different depths, which is revealed by their difference in apparent velocity.

The translational component of relative motion between the observer and the objects is the defining feature of the motion parallax cue. Rigid body rotations of objects, on the other hand result in the Kinetic Depth Effect [Wallach & O'Connell, 1953], which creates an impression of depth that is stronger than motion parallax and binocular disparity [Bradshaw & Rogers, 1996].

(3) The Kinetic Depth Effect

When visible points on an object rotate, a sense of depth more powerful than stereo, known as the "Kinetic Depth Effect" (KDE) is perceived. This depth cue arises for rigid body rotations. Perspective projection results in a stronger impression of depth for the KDE than orthographic projection, though a strong sense of depth and shape is nonetheless apparent under orthographic viewing conditions [Wallach & O'Connell, 1953].

Figure 2.13 illustrates the Kinetic Depth Effect, which is caused by rigid body rotations. Wallach and O'Connell [1953] performed a series of experiments to attempt to define the conditions under which observers would perceive a three-dimensional rigid object rotating. The stimulus used in the experiments consisted only of two-dimensional points changing in shape on a flat plane, displayed through a parallel shadow projection. They found that this perception seemed to depend on the property that both the lengths and orientations of the two-dimensional shadow projections changed. Thus the KDE requires the following two components:

(1) A depth order component; depth relationships between points on a surface must be seen. This helps to give definite rigid form.
(2) Depth magnitude. Orientations relative to an observer must be clear.

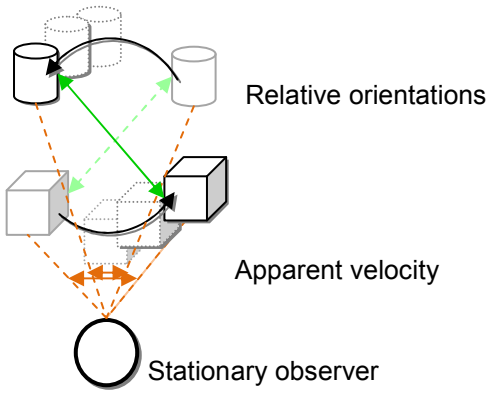

Figure 2.13 Illustration of the Kinetic Depth Effect. Rigid body rotation of two objects reveals depth through apparent velocity changes and visible changes in orientation relative to the observer.

The KDE, in addition to creating a strong depth effect, can cause isolated dots or unconnected lines to be perceived as a coherent rigid figure. This was evident in an experiment performed by Treue et al., [1995] in which random dots on a rotating cylinder, with a patch hiding the dots on a region of the surface, under orthographic projection, still appeared as a cylinder. The KDE under orthographic projection encounters the problem of reversals of apparent rotation when there are no other depth cues to help disambiguate the distances of the points from the viewer.

An experiment has also shown that coherence or apparent rigidity is better perceived for less complex rotations around axes than for tumbling motion (rotations about the three axis with non constant speeds and varying rates of change in orientation about the axes, but constant angular velocity) [Green, 1961]. Further, coherence in rotational motions depended on the axis of rotation and the orientation of the axis with respect to the view point. Rotations about a vertical axis (rotations which produce horizontal motion) were the most comprehensible.

2.2.5 Effectiveness and Combination of Depth Cues

Depth cues vary in effectiveness depending on viewing distances as shown in Figure 2.14. In terms of effectiveness of the different shape cues at a range of up to ten meters, the Kinetic Depth Effect is stronger than binocular disparity, which in turn is stronger than motion parallax [Ware & Franck, 1996]. Motion cues are more effective for coarse work than fine. These cues indicate a more absolute sense of depth. Occlusion is the strongest of the pictoral cues and represents relative depth ordering. Compression is the strongest of the texture cues.

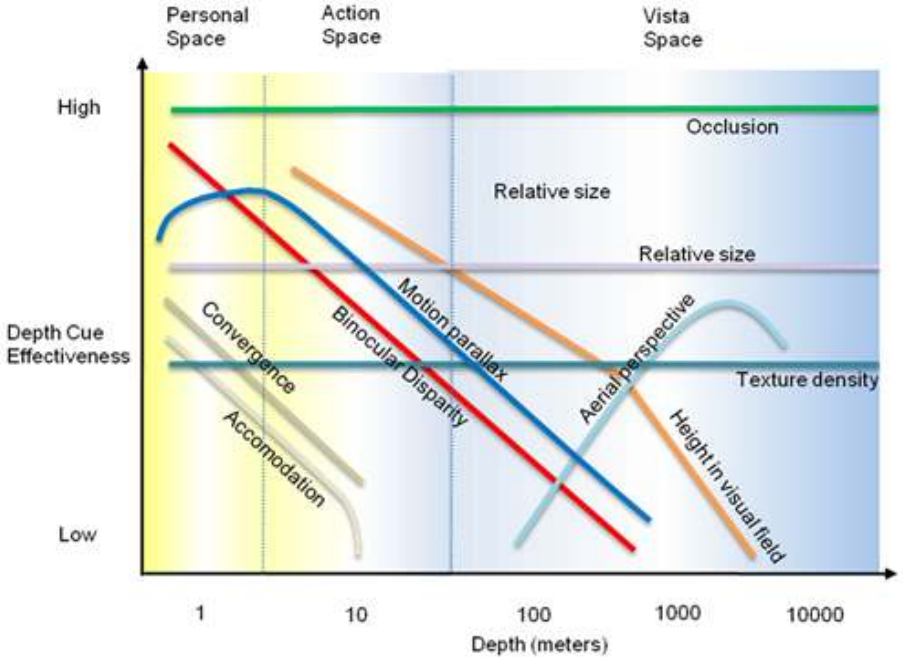

Figure 2.14 Effectiveness of depth cues at various distances, adapted from [Lyness, 2004]. The X-axis indicates distance in meters from an observer. The Y-axis represents the effectiveness in terms of visual sensitivity to the cues. Lines in the graphs indicate depth cue effectiveness at different distances.

The HVS further combines the various depth cues to resolve ambiguities and more accurately approximate depth [Ware & Franck, 1996] [Lyness, 2004]. Combinations of cues result in a more accurate understanding of shape [Bair, 2009], e.g., a combination of stereo and motion facilitates better reading of large connected graphs [Ware & Franck, 1996] also shading and texture together enable people to better perceive the shape of a surface [Sweet & Ware, 2004] [Kim et al., 2003]. Depth cues, however, may conflict and override each other. Occlusion, for instance, has been shown to overpower height in the visual field [Royden et al., 1988].

Two models of how depth cues are combined are shown in Figure 2.15. When perceptual depth cues are combined, they are weighted and summed. Model (a) is the unified model which caters for combinatorial relationships between depth cues. A single perceptual model is constructed for all types of tasks. Combining multiple cues results in more accurate depth perception, e.g. binocular disparity and motion cues together are more effective than the sum of the effect of the individual cues [Lyness, 2004].

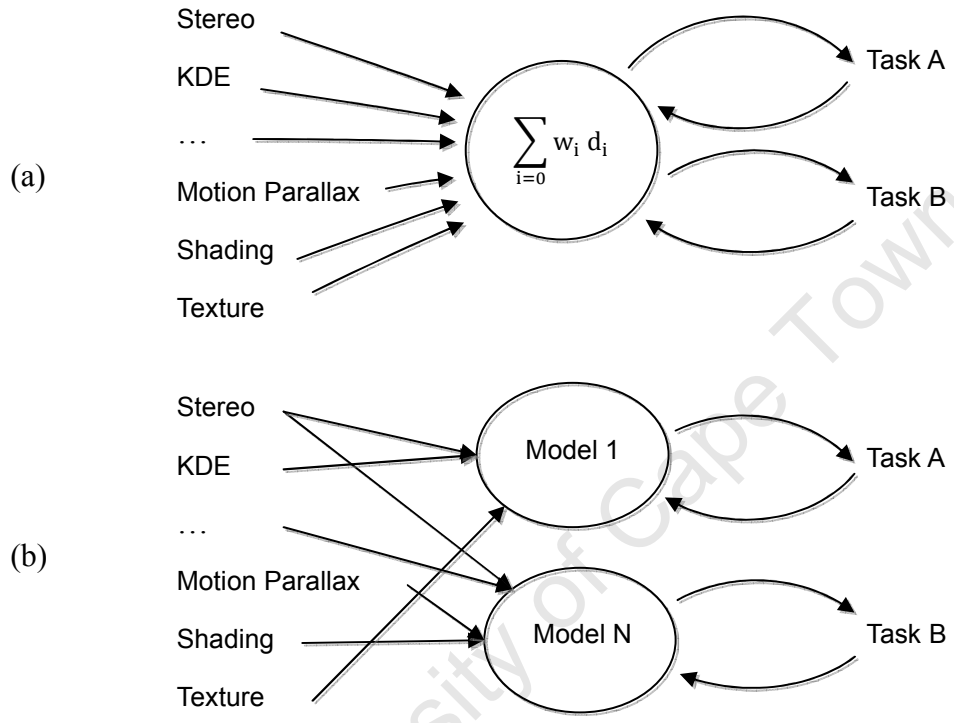

Figure 2.15 Perceptual models of how depth cues are combined. Depth approximations from the various cues and feedback from the tasks determine the viewers overall perception and depth approximation. (a) In the unified model perception is based on a weighted sum of all cues and inputs. (b) In a task based model, certain cues are combined according to the usefulness of the cue for a specific task. Different tasks use different cues and result in different perceptions [Lyness, 2004].

The adaptive model in Figure 2.15(b) caters for the optional combination of cues and various combinations and weightings for various tasks. Performing tasks such as judging surface shape and performing target surface detection depend most on the cues of shading and texture gradient, to which stereo and motion cues also strongly contribute. Pattern detection tasks in 3D point clouds rely primarily on the KDE and then stereo and relative size. On the other hand, estimating relative positions depends strongly on stereo. Once depths cues have been combined to give depth approximations from the primal sketch, they are stored in the raw 2.5D sketch.

2.3 Measuring the Perception of Surface Shape

How does one measure the effectiveness of a surface display technique? The most common approach is through perceptual user experiments, in which "naïve observers" perform a shape task during which they make shape judgements based on how they perceive a displayed surface. The accuracy of their judgements is used as a measure of how well a display technique shows the surface.

Some examples of the various shape tasks users can perform include: picking the correct local shape (ellipsoids, cylindrical, saddle, flat) of quadratic surfaces [Erens et al., 1993], feature finding tasks in which features such as peaks and valleys are identified and located [Lum et al., 2003], and by taking perceived surface orientation measurements [Sweet & Ware, 2004] [Bair, 2009]. These tasks provide a quantitative way of capturing perceived shape estimates, which serves as a means of measuring shape comprehension [Mamassian & Kersten, 1996] [Koenderink & Van Doorn, 1995].

In many shape tasks, users are asked to make a judgement either at a single point such as, "in which direction is the surface slanted at the point?", or between a pair of points, e.g. "indicate which point is furthest away.", or "at which of the two points is the surface steeper?". In many of these tasks, probes are used. Perceived orientation tasks, for instance commonly use a probe, which must be manipulated to match the perceived surface orientation at a point [Koenderink & Kappers, 1992]. Multiple readings are required to be taken across the face of a surface, in order to obtain a quantitative measure of overall surface perception, [Koenderink & Kappers, 1992]. Interrante and Kim [2001] give warning not to use multiple probes to obtain multiple orientation measurements. A methodology, in which multiple readings are taking over a scan line is experimentally more effective [Todd et al., 2004]. For layered surface displays the number of readings that must be taken is multiplied by the number of layers. Participants in these experiments find making multiple readings both fatiguing and time-consuming.

Global shape tasks ask respondents to indicate if two surfaces match. The surfaces may be displayed with different lighting, visual cues or even from different angles [Langer & Bülthoff, 2000]. When performing shape tasks, different respondents tend to make similar assumptions about shape, lighting and view conditions when inferring shape from different cues. As an observer makes eye movements to explore other parts of an image, much of the information from previous images is lost or forgotten from one glance to the next [Langer & Bülthoff, 2000].

2.4 Summary

This chapter has presented aspects regarding the display of shape including physics, mathematics and perception of surfaces. Perceptual depth cues play the significant role in a person's

comprehension of the shape of a surface. Using the correct combination of cues will determine the effectiveness of our layered surface display design. We noted differences between shape cues for objects in motion (kinetic depth cues) and specific rigid-body rotations which cause the Kinetic Depth Effect, which is the most powerful kinetic depth cue. We also describe the evaluation of surface visualizations. Such evaluations are commonly performed through Psychophysical experiments, which are fatiguing and time consuming. The next chapter presents related work in layered surface visualization.

Chapter 3

Related Work in Layered Surface Visualization

Moving on from physical and visual aspects of surface shape and how it is perceived and measured, this chapter presents a survey of related work in visualizing layered surfaces. This sets the context for our proposed visualization design, shows the need for the design, and how it is different from previous work.

This chapter then presents multivariate visualization techniques, which have achieved success in displaying multiple overlaid scalar fields in 2D. These provide insights into developing our visualization technique for displaying multiple overlaid surfaces.

The chapter concludes with precursors to our design from research in particle systems. We use particle systems as the foundational mechanism for animating opaque markings over surfaces.

3.1 Layered Surface Display Techniques

Several layered surface display techniques have been developed to address the significant problem of occlusion. Transparency, as the most obvious solution, has proven to be inadequate on its own. In response various techniques such as cut-away views [Viola et al., 2004] [Diepstraten et al., 2002] [Diepstraten et al., 2003] and exploded views [Bruckner & Groller, 2006] [Li et al., 2008] have been developed, which modify the geometry of the surfaces by distorting or removing sections of the exterior surfaces to allow a person to see the interior layers. These alternative techniques typically render the exposed sections of the surfaces opaquely. Accordingly, we classify the various layered surface display techniques into one of two major categories based on the specific approach they use to addresses the problem of occlusion. That is, techniques either:

(1) conserve the shapes and spatial relationships between the layered surfaces by using transparency to display them simultaneously, or
(2) alter the shapes by deforming them or removing sections of the surfaces and use opacity to render the visible sections of the layers clearly.

The shape and spatial relationship preserving techniques are further subdivided into:

(1.a) Techniques which use only semi-transparent renderings of surfaces, and
(1.b) Opaque marking-based techniques, which emphasize the 3D shape of the semi-transparent surfaces through the use of opaque marking textures.

The techniques which use transparency on its own blur shading and other cues when the layers are blended together. This makes it difficult to judge distances between the layers. This can be overcome by placing a sparse set of opaque markings over the transparent layers. This both emphasises the 3D shape and makes it apparent. We focus on this class of techniques because it satisfies the visualization design requirements of facilitating shape comparison tasks.

The shape altering techniques are also divided into two subgroups, based on whether or not they:

(2.a) remove geometry, or
(2.b) distort shapes and spatial relationships.

Figure 3.1 shows our categorization of the different layered surface visualization techniques.

Shape altering approaches are useful for illustrating exterior surfaces which are not so important, essentially illustrating the interior layers in the context of the exterior layer [Bair, 2009]. The techniques which distort geometry make trade-offs between deformations of the shape, spatial relationship and occlusion. Of these different techniques, Bair [2009] says “the case remains to be solved of how to visualize multiple surfaces that are both detailed and important.” There is a need for approaches which have minimal occlusions but also maintain spatial relationships. The best approach for this seems to be the shape conserving techniques, which emphasize 3D shape by transparently rendering surfaces and augmenting the transparency with opaque markings. There are additionally several ways of augmenting these techniques to better communicate the

surfaces, these are described in 3.1.3. Our visualization design uses the opaque marking-based approach and augments it with an animation technique used for enhancing surface shape. This is the first time this arrangement has been used for layered surface visualization.

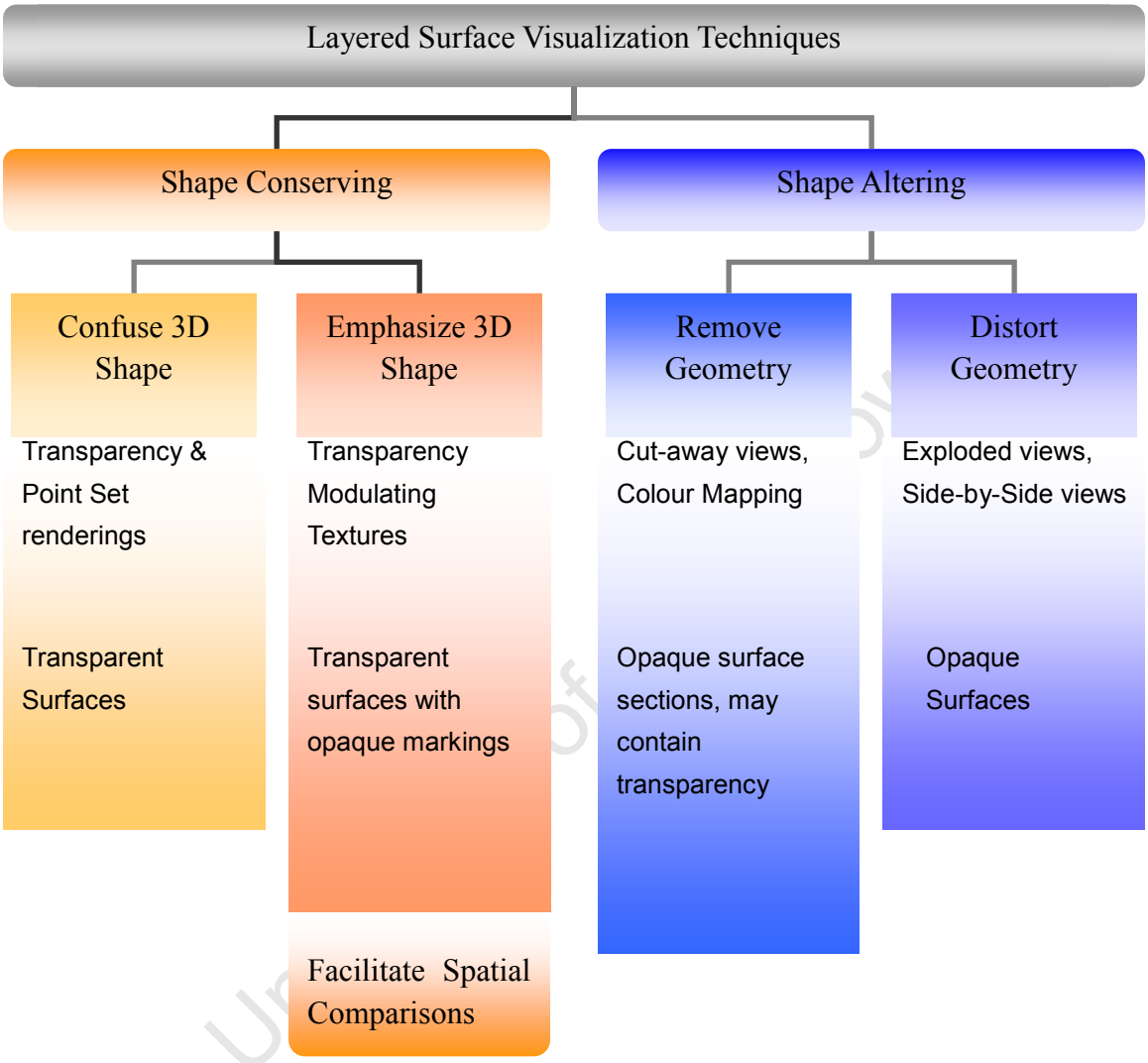

Figure 3.1 Categorization of Visualization Techniques for Layered Surfaces.

It is important to realize that spatial relationships between surfaces are not necessarily equivalent. For instance in Figure 3.2 point P_1 on the top grey surface is closest to point P_3,on the bottom surface, but the relationship is not the same for P_3 which is closer to P_2.

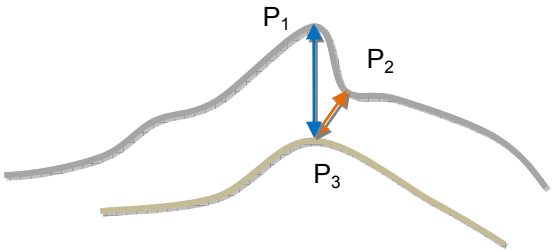

Figure 3.2 Illustration of non-equivalence between surface-to-surface relationships, adapted from [Weigle, 2006]. The closest point to P_1 on the bottom brown surface is P_3, but its closest point on the grey surface is P_2.

3.1.1 Shape and Spatial Relationship Altering Techniques

The following techniques, set out below, either distort or remove some of the geometry of the layered surfaces to allow viewers to see the interior shape.

3.1.1.1. Cut-away Views and Cross Sections

Cut-away views typically render the interior surface opaquely and remove some of the exterior surface's geometry to allow a viewer to see the interior. The opaque sections of the outer surface typically serve to provide context, with the details of the interior shape showing through the gap(s) in the exterior geometry. The removal of the geometry does not typically attempt to preserve shape. Therefore this approach is useful when illustrating interior regions in the context of outer surfaces, for which the outer surfaces are simple and not of particular significance.

A simple implementation of a cut-away view is to render a wire-frame mesh of the outer layer over an inner surface. This, however, only displays an approximation of shape rather than its surface details [Viola et al., 2004].Variations of cut-away geometry include planar contours [Levoy, 1990], ribbons [Bauer-Kirpes et al., 1987], and cross sections [Durikovic et al., 1997]. Cross sections are commonplace, frequently used in both scientific and medical imaging because of the simplicity of these approaches or lack of knowledge and availability of more powerful layered surface visualization approaches. As a result scientists are more accustomed to wade through slices of volumetric datasets rather than consider the data as a volumetric whole. While evenly spaced parallel slices of the data are useful for revealing certain patterns and allowing a person to interpolate between slices, they may lead to interpolation errors and require mental effort. High frequency details, such as fine features and higher resolution views of the surfaces, require numerous slices, which may increase occlusions. Further, understanding the global shape from slices showing contour sections is not obvious, let alone understanding relationships between different surfaces.

Figure 3.3 Illustration of ribbons [Bauer-Kirpes et al., 1987].

Certain cut-away techniques may use transparency in regions which have been cut-away. Grid textures and wireframe meshes may be thought of as a cut-away technique or at least an easy way to implement them [Weigle, 2006]. Our work categorizes grids as an approach that conserves and emphasizes the 3D shape of the surfaces, see section 3.1.2(4). Cut-away geometry is considered to be in a different class from shape conserving techniques in that extended pieces of exterior surfaces, which may have been important to understanding its shape, are removed.

3.1.1.2. Exploded and Side by Side Views

Exploded views [Bruckner & Groller, 2006] [Li et al., 2008] is an approach that renders each of the surfaces opaquely without relying on transparency. This approach shows all surfaces by deforming, peeling back or moving parts of the layers so that all pieces are visible. These deformations show the 3D structure of important components of the surfaces and how the various parts fit together, making a trade off between reducing occlusion and maintaining reasonable distance relationships. Figure 3.4 shows an example of an exploded view from [Li et al., 2008].

Figure 3.4 An exploded view illustration of a turbine engine [Li et al., 2008].

Another example of exploded views, is displaying surfaces side by side. The surfaces are rendered fully opaquely and very clearly show the structure of the individual surfaces. However, the spatial relationships between the surfaces are altered. Many of these techniques, further, lose

or hide details on either the interior layer or exterior layer. These techniques do not address the challenge of visualizing layered surfaces that have detailed exterior and interior layers, for which it is important that the layers be seen equally well in relation to each other [Bair, 2009].

3.1.1.3. Colour Mapping

A single spatial relationship may be displayed by rendering either the exterior or interior surface and then rendering a colour map on the surface of this shape to visualize the distance or some other relationship to another layer. Figure 3.5 shows an example of colour mapping, illustrating distance between two surfaces.

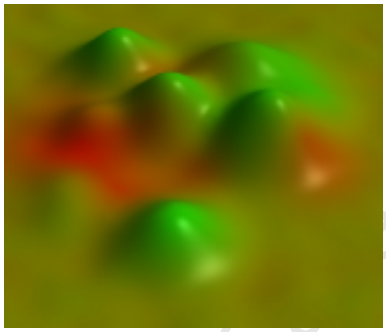

Figure 3.5 Illustration of a colour map from [Weigle, 2006] illustrating the Euclidean distance between two intersecting surfaces. The colour mapping ranges from red (indicating that the surface is on the exterior), to yellow (intersection) ,to green (the surface is on the interior).

This approach, however, has to address issues such as selection of an appropriate colour scale and how to geometrically measure the distance or relationship between the layers. A colour scale shows only an approximation of distance between surfaces and does not give a clear impression of the other surface. Colour mapping has been experimentally compared against opaque marking-based techniques. It was found that participants perform significantly worse with colour mapping for global shape tasks, distance and orientation judgements [Weigle, 2006].

3.1.2 Spatial Relationship Preserving Techniques

Approaches for displaying layered surfaces which rely on transparency to show the different surfaces simultaneously, without modifications to the shape of the surfaces, are set apart in the class of techniques which conserve shape and spatial relationships between the surfaces. Transparency techniques alone, however, do not illustrate 3D shape well and need to be augmented with opaque markings dappled over the surfaces to overcome this problem. Opaque markings are typically implemented through the use of textures. Techniques which use textures that vary opacity and transparency are referred to as transparency modulating textures [Rheingans, 1996]. Few of these opaque marking based techniques enable the display of more

than two surfaces. Challenges include difficulty distinguishing between the opaque markings on the different layers, when more than two layers are displayed, and occlusion resulting from the opaque markings on multiple outer layers. Figure 3.6 illustrates layered surface visualizations which preserve spatial relationships: (left) shows standalone transparency, (right) shows transparency augmented with opaque markings.

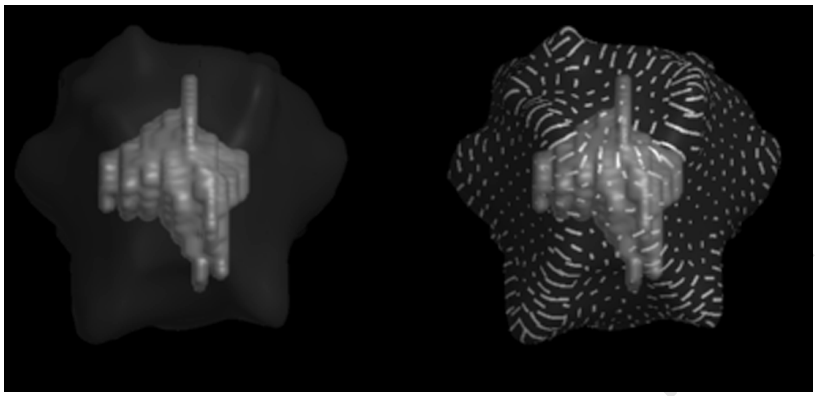

Figure 3.6 Layered surface visualization techniques which preserve spatial relationships: (a) semi-transparent surfaces; (b) transparency augmented with opaque markings(texture). Illustration from [Interrante, 1997].

(1) Point Based Renderings

Rendering surfaces in a stipple-type rendering, through sets of points is useful for illustrating intersections between implicit surfaces and provides a type of screen-door transparency [Foley et al., 1994]. These techniques give an impression of shape but do not convey the structure and surface shading clearly, since the points have limited surface area. When multiple layers are displayed together it is difficult to distinguish between points on different layers [Weigle, 2006].

(2) Standalone Transparency

Transparent surfaces or partially translucent surfaces overcome the problem of occlusion by blending the layers together. Transparency is an obvious and simple way to implement the display of layered surfaces, but on its own results in several problems. For a surface to be seen as transparent and its shape to be understood, it must have a clear difference in contrast to its background. Since transparency techniques convey shape through shading, when transparent layered surfaces are blended together, it becomes difficult to identify to which surface the shading belongs. Further, it is difficult to make 3D shape judgements between the surfaces [Interrante, 1997]. This precludes the use of transparency on its own when displaying layered surfaces for spatial shape comparison tasks.

(3) Transparency Augmented with Opaque Markings

Transparency techniques may be augmented with a texture that varies the transparency or opacity on the exterior layers. The texture causes opaque sections on the exterior surface to be visible, separating them visually from the interior surface. The markings convey shape cues, making the 3D shape of the exterior surface apparent and help overcome many of the problems with using transparency alone. The opaqueness of the markings, making them strongly visible, helps to improve shortest distance judgments between surfaces.

While several approaches exist for modulating the opacity of layered surfaces, certain problems arise when using opaque marking textures. One of the problems is that these approaches are static in that the markings or textures do not move over the surface. This means that from some vantage points, markings on the exterior layers may occlude interior layers, since the view point was not taken into account when the textures were created and mapped to the surfaces. These techniques typically only show two layers. Another problem that occurs when displaying more than two layers is that it is difficult to distinguish between the markings on the different surfaces. Using colour as a mechanism to differentiate between the markings alone is insufficient. Bair et al., [2005] have shown that hue is not a significantly effective factor in distinguishing between layered surfaces. Lastly, transparency results in a blending of markings with outer semi-transparent layers. A marking beneath three or four semi-transparent layers being blended with these layers becomes difficult to distinguish from other markings and its surface shading may also become confused. Variations to the type of markings displayed on the surfaces are described below.

(4) Grids and Repeating Patterns

The simplest approach to creating an opacity modulating texture is to use a uniform grid texture. The opaque gridlines not only make the surface apparent, but also provide texture shape cues which give a better impression of the shape of the surfaces, see Figure 3.7. Bair et al., [2006] and Bair, [2009] have shown that there are certain optimal parameters for textures for illustrating layered surfaces, namely that:

- Clearly marked grids or line textures with distinct directions are most important for illustrating shape for normal orientation type tasks.
- Bright textures indicate shading clearly and should be used.
- Opacity for the surface closest to the viewer (top surface), for two layered surfaces, could have between 30% and 60% visibility.
- Large textures on the top surface are best, but this influences visibility on the bottom surface.
- Larger openings in the grids on the top surface make it easier to see the bottom surface but have a negative impact on the perception of the top surface.

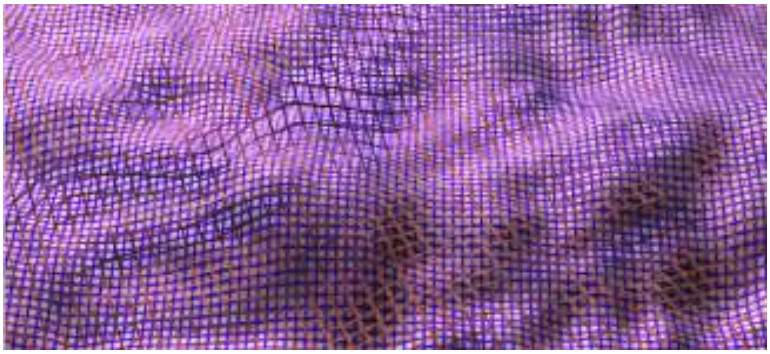

Figure 3.7 Uniform grids illustrating two layered surfaces. Illustration from [Bair, 2009].

Repetitive separable textures have been optimized through a human in the loop approach to find the best textures for illustrating two layered surfaces [Bair et al., 2005]. Bair [2009] showed that theoretically it may be possible to display up to 5 or 6 layers, extrapolating from experiments performed using one, two and three layers. Bair's work includes an illustration of 6 layered surfaces. The problem with using a uniform grid texture is that finding non-distorted texture coordinates for an arbitrary surface is not straightforward and no technique is known of that can guarantee the regularity of the texture [Weigle, 2006]. The use of applying textured grids has only been applied to layered height fields, which are 2.5D surfaces rather than true 3D surfaces, which can fold back over themselves. While it is a challenging problem to find a mapping of a grid texture onto an arbitrary 3D surface, our approach of animating markings over such surfaces is more straightforward in that the markings move and distribute themselves dynamically across such surfaces. Notable of Bair's work [2009] is that this is one of the only instances of layered surface visualizations which incorporate stereo.

(5) Principal Curvature Strokes

Line stroke textures which follow the first principal curvature directions have been shown to be useful for illustrating two layers [Interrante et al., 1997]. The strokes which follow principal curvature directions exploit the depth cue of texture compression, which gives a strong impression of shape. In many layered surface techniques the interior layer is rendered fully opaquely and the outer-layer semi-transparently. The outer-layer is dappled with opaque strokes, see Figure 3.8.

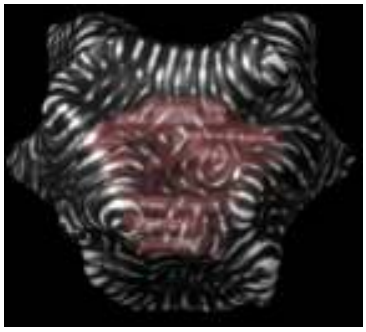

Figure 3.8 LIC Stroke Textures for a cancer treatment. Line widths determined by curvature magnitude in the stroke direction [Interrante, 1997].

This approach is susceptible to localized view dependent interference [Weigle, 2006], since the viewing direction and position is not taking into consideration when placing markings. Markings may be placed poorly, causing occlusions for instance. Principal curvature textures are created by advecting particles over a surface along the first principal curvature direction using Line Integral Convolution (LIC). Strokes which are too close to each other are removed. A Poisson distribution of the strokes results in random looking textures with a nearly uniform spread of strokes across the surface. Computing the textures is not trivial for triangle meshes. On the other hand, for volumetric datasets and isosurfaces, texture computation is straightforward and fast.

(6) Uniform Circle/Hexagon Textures

Surface textures may be used to modulate the opacity of the surfaces. This can be achieved by mapping a uniform circle or hexagon texture to the triangle vertices of a mesh. The uniform geometry of the surface causes a uniformity in the texture patterns that helps to illustrate the surface through texture cues such as compression. In this approach the interior surface is also typically rendered opaquely and the exterior layers use the transparency modulating textures. Figure 3.9 contrasts transparent layered surfaces with an opacity modulating texture. Colour and different texture patterns may be used to display multiple layers, though at most three layers have been shown [Rheingans, 1996]. Such visualization can be driven interactively due to the simplicity of the textures.

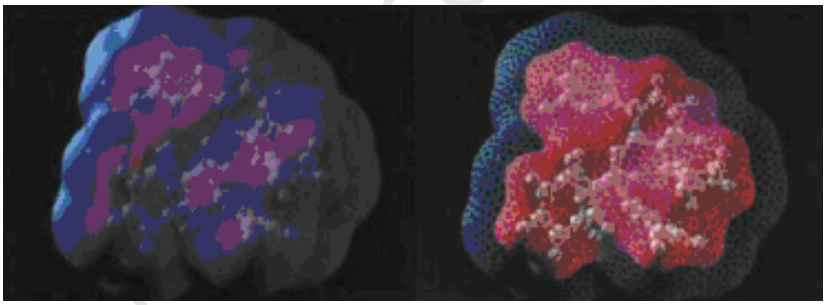

Figure 3.9 Opacity-modulating textures. A translucency-modulating texture varies the opacity of exterior surfaces to both reveal interior surfaces and illustrate exterior layers [Rheingans, 1996].

(7) Principle Curvature Crosses

A variation on the use of LIC stroke textures along the first principal curvature direction is to employ principal curvature crosses. Weigle [2006] uses this approach, which creates patches across a surface to generate a uniform texture with a Poisson distribution. Glyphs are placed at these points and aligned to the principal curvature frame. The glyphs are simple crosses with the major axes facing in the direction of the first and second principal curvatures. Disks were experimented with, but crosses were chosen for experiments after side by side comparisons. The crosses were deemed to reveal more of the interior while conveying as much surface information from side by side views of visualizations using the different glyph types [Weigle, 2006]. Table 3.1 summarizes the different approaches, listing their advantages, limitations and purpose.

Technique	Advantages	Problems/Limitations	Purpose
Opaquely rendered surfaces – approaches distort spatial relationships			
Exploded Views	Show 3D shape of important components and how they fit together	Occlusions may occur and spatial relationships are warped	Presentation, explanatory purposes
Side by Side Views	Natural & familiar, shows structure of individual shapes clearly	Do not facilitate spatial comparisons tasks or show intersection regions. No clear frame is known which facilitates such comparisons between layers	Display of individual shapes
Single opaquely rendered surface – approach represents only a single spatial relationship			
Colour Mapping	Shows a single spatial relationship	Perceptual issues - colour scale. Geometric issues measuring across the layers, shows shape of only one surface clearly	Shows single relationship between surfaces
Opaquely regions of surfaces rendered - preserve spatial context, but removes geometry			
Cut-away Views, Cross Sections	Makes interior surface visible in context of exterior, Patterns evident, viewer can interpolate across sections	Exterior surface information lost, seeing shapes as a whole difficult, higher resolution surface requires more slices, difficult to see spatial relationships	Illustrating interior surface in context of simple exterior shape
Transparently rendered surfaces with opaque markings - preserve spatial relationships			
Transparency Modulating Textures	Facilitates spatial comparison tasks	Markings on more than two layers difficult to discern, finding non distorting texture coordinates for arb shapes difficult	Illustrate spatial relationships between surfaces
Transparently rendered surfaces - preserve spatial relationships			
Standard Transparency & Point Set Renderings	Simplicity	Confuses 3D shape	Simple in place illustrations

Table 3.1. Summary of layered surface display techniques.

3.1.3 Techniques for Augmenting Layered Surface Display

The different visualization techniques for displaying layered surfaces can be extended to better convey the shapes and relationships between them through one or more supplemental approaches. These augmentation techniques may also improve usability. These different enhancements may be achieved through interaction, importance driven visualization and supplemental depth cues [Weigle, 2006] [Bair, 2009]. Two additional techniques developed for illustrating relationships between intersecting surfaces are: surface refactoring and point-correspondence glyphs.

3.1.3.1. Interaction

Giving people the ability to interactively explore their data adds significant value to layered surface display techniques, in terms of helping them understand the data. One practically meaningful interactive technique which aids perception is allowing a person to move and rotate the layered surfaces. Other useful techniques include: allowing them to switch between surfaces, allowing users to vary the opacity, and allowing them to create their own cut-away views through adjustable clipping planes. Yet, another useful interaction technique is to interactively remove the closest occluding visible layer in depth through interactive depth peeling techniques as users move around the data [Borland et al., 2006].

These techniques provide useful tools which aid in the comprehension of layered surfaces but certainly do not solve all the problems of layered surface display. Clipping planes and peeling, for instance, alter the surfaces and do not facilitate spatial comparisons, though they may provide contextual views of the interior layers.

3.1.3.2. Importance Driven Visualization

Importance driven visualization is a technique which creates cut-away views that illustrate important features. Sections of the opaque exterior layer are typically drawn semi-transparently where a surface occludes important features of the underlying surface. Figure 3.10 shows a technical illustration, which is a typical application-area for importance driven visualization. This is similar to cut-away views, except that importance driven visualizations strategically select regions to cut-away to show features.

NPR techniques, such as opaque edges, silhouettes and highlights may be used with this approach to illustrate features to add emphasis and demonstrate features. Importance driven visualizations have been created automatically: Diepstraten et al [2003] automatically produce cut-away geometry, which makes interior nested shapes visible. Silhouettes, edges and shading have also been rendered automatically [Costa Sousa & Prusinkiewicz, 2003]. Diepstraten et al. [2002] produce ‘technical illustration-like’ renderings of shapes, which is limited in that it uses only

transparency and not opaque markings. Importance driven visualization is an appropriate technique for displaying layers for which the interior object is small compared to the exterior object because this allows for a region of the exterior to be removed without destroying the context. If the exterior object were the same size as the interior object that needed to be displayed, almost the entire exterior object would need to be removed [Weigle,2006][Bair,2009].

Figure 3.10 Technical Illustrations are an example of importance driven visualization [Viola et al., 2004].

3.1.3.3. Supplemental Shape Cues

The display of layered surfaces has been significantly improved through the introduction of additional depth cues. The most simple, commonly used and powerful approaches include the following:

(1) *Pendulum style rocking*: A surface may be rotated in a manner similar to a pendulum swinging back and forth. This pendulum-style rocking is an animation of the surfaces in which the surfaces are rotated around different axes. This induces the KDE, the most significant depth cue. This dramatically enhances the 3D impression of the surfaces and understanding of the shapes. This approach has been used to significantly enhance the display of layered surfaces [Bair,2009][Weigle,2006]. Rocking an object provides coherence across different views of an object. The views of the object from different angles may reveal structure that was occluded from other angles.

(2) *Stereo*: Surfaces are viewed in stereo when two perspective views are generated from slightly different angles and separated vantage points for the left and right eye. When a scene is viewed by presenting these images to the respective eyes, it induces the powerful depth cue of binocular disparity. This enhances the 3D impression the viewer has of the surfaces, giving an additional sense of depth.

3.1.3.4. Techniques for Intersecting Surfaces

Two state of the art techniques that help to augment an understanding of distances between layers, improve the display of nested and intersecting surfaces and which illustrate intersections of surfaces, are the following:

(1) *Surface Refactoring*: Surface refactoring is useful for displaying intersecting surfaces, by determining the order of surfaces relative to the observer. A surface that intersects another surface transitions from being on the exterior to being on the interior, or vice versa. Refactoring the exterior regions of the different surfaces facilitates more effective display of the surfaces by rendering the identified interior regions opaquely and the exterior regions semi-transparently with opaque markings [Robinson & Robbins, 2005] [Weigle, 2006]. While this is useful for two layers, it is also helpful for correctly rendering three and more layers by determining depth order swap overs between the surfaces for correct back to front rendering of triangles.

(2) *Point Correspondence Glyphs*: Another visualization technique which is useful for performing shape comparison tasks and illustrating the distance relationships between surfaces is point-correspondence glyphs. These line glyphs connect a pair of points on two adjacent surfaces for which the distance is at a minimum. Weigle, [2006] solves the Laplace equations to determine heat transfer between nested surfaces to create these glyphs between two nested surfaces. This clearly shows the distance between the two surfaces. Figure 3.11 provides an illustration of point correspondence glyphs.

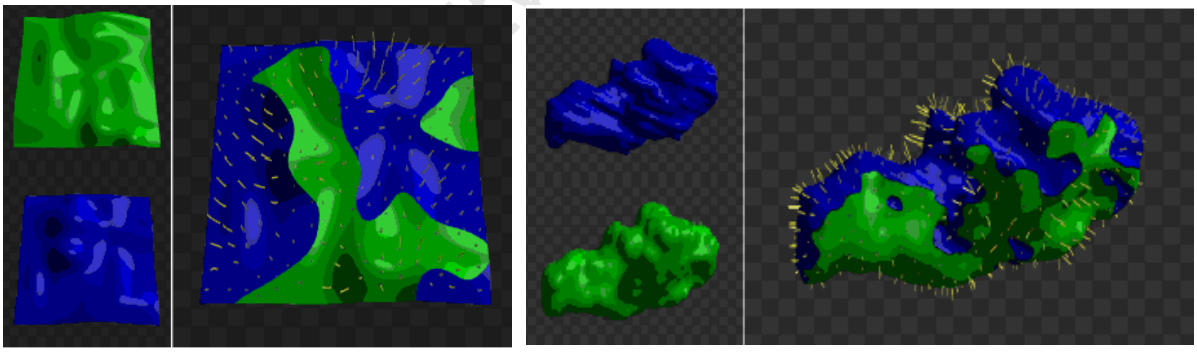

Figure 3.11 Point Correspondence Glyphs help to illustrate the distances between surfaces [Weigle, 2006].

3.2 Guidelines and Precursors from Multivariate Visualization

The visualization of multivariate 2D scalar fields, like layered surface visualization, endeavours to simultaneously show data overlaid. Both multivariate visualizations and renderings of layered surfaces strive to clearly distinguish layers, and maintain relationships between them [Hagh-Shenas et al., 2007]. Further, they share the problems of becoming cluttered and overloaded in terms of the amount of information that is displayed. Other, common visualization issues are:

- *Dimensionality,* it becomes increasingly difficult to find visual features to represent an increasing number of variables or layers distinctly, and
- *Interference;* different visual features interact with each other.

Simultaneously displaying layers has also been shown to enable the viewer to make comparisons and switches between layers, simply by shifting their focus. Layering methods are well suited for allowing a person to explore their data, that is to help them "notice the unexpected", while verifying the expected [Taylor, 2002]. The techniques from multivariate visualization of Colour Weaving [Hagh-Shenas et al., 2007], Data Driven Spots (DDS) [Bokinsky, 2003], and Oriented Slivers [Weigle et al., 2000] which bear similarities to our proposed layered surface visualization design, are described below.

3.2.1.1. Blending and Colour Weaving

A common approach for displaying multiple overlaid scalar values is to use colour to represent different scalar values or combinations of variables. Multiple layers representing different variables are overlaid by being blended together. Blending colours, however, may lead to colour combinations or patterns which are confusing and cause error prone perception of relationships amongst the variables. Blending causes misleading surface shading in the case of layered surfaces [Interrante, 1996].

Colour Weaving is an effective alternative to blending [Hagh-Shenas et al., 2007] for displaying multivariate data. It is able to clearly illustrate up to six layers and maintain the sharpness of the colours. This technique tightly interlaces strands of colour side by side without blending. The result looks like a collection of coloured speckles, each colour being represented individually [Urness et al., 2003]. The problem with using colour weaving directly for displaying layered surfaces is that as luminance values change it becomes more difficult to distinguish colours. Shading leads to variations in luminance across a surface. Colour weaving also uses pixel or small sized dots or strands. These strands having a small surface area do not convey surface shading well. Our proposed visualization design is similar to colour weaving in that it too makes

use of “small multiples” [Tufte, 2001] to represent a larger whole and that instead of blending layers together, small distinctly coloured surface patches of opaque markings depict the different layers. The problem with using colour to distinguish between overlaid markings for layered surface display also occurs in the application of Colour Weaving to multivariate flow visualization, where colour alone is insufficient to distinguish between overlapping streamlines [Urness et al., 2003].

3.2.1.2. Data Driven Spots - DDS

Data Driven Spots (DDS) bears similarities to both blending and Colour Weaving for visualizing 2D scalar functions. The approach represents multivariate data by taking random, well spaced samples of the functions, which do not occlude each other. Each sample is represented with a circular Gaussian and the Gaussians from the different layers are coloured differently and blended together to create an overlaid texture. The sampled values determine the opacity and colour saturation of the Gaussians. Data values of lower layers are visible between the spots on the upper layers. An example of this is illustrated in Figure 3.12.

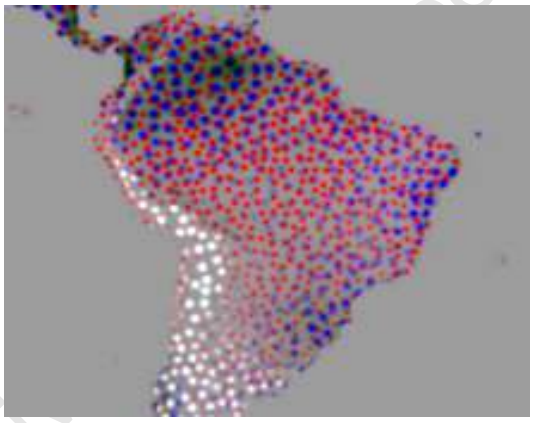

Figure 3.12 Data Driven Spots [Bokinsky, 2003], illustrating ground-frost frequency (days) in white, precipitation (millimetres/day) in blue, vapour pressure (hPA) in red and wet-day frequency (days) in green, over a region of South America.

Since DDS allows the layers to be seen simultaneously, it facilitates comparisons between different variables. Notably for spatial correlation tasks, DDS performed better than images displayed side by side [Bokinsky, 2003].

In the DDS technique, colour plays the primary role in distinguishing between layers, although motion has been shown to improve discrimination. The use of animation, moving either a single layer in a particular direction or multiple layers in different directions, dramatically increases visual salience. Animated layers required less effort to see than static layers. Further, through

moving spots multiple points are sampled, effectively increasing the spatial resolution. In DDS experiments, values not sampled or which went unnoticed because they were small in size, were highlighted and noticed when the layers were put into motion. Layers are distinguishable, with up to seven distractors. The function values between spots are also easily interpolated by the HVS.

The difference between DDS and our work is that DDS displays multiple scalar values in 2D, whereas our visualization design displays layered surfaces. The layered surface visualization design uses surface patches or opaque texture markings to illustrate local surface shape through shading, highlights and depth cues, instead of 2D spots, which represent a single scalar value. DDS results in a static texture which may be animated. Our work uses particle systems to adaptively move markings. This is equivalent to varying the texture.

3.2.1.3. Oriented Slivers

Oriented Slivers is a display technique which creates textures that combine differently oriented line markings and luminance to display multivariate data simultaneously. Sets of slivers with different orientations encode the data. Luminance of the slivers represents the scalar values, e.g. white shows the maximum value and black the minimum. The HVS response to luminance variations is logarithmic. Oriented Slivers thus scale the luminance values to correct for this. The orientation of the slivers is used to distinguish between variables (layers). In this technique images are produced separately for the different layers and composited together. For the technique to work, the slivers need to be thin and well spaced. This allows values from other fields to "show through". Oriented Slivers relates to Texton theory [Julesz, 1986] which posits that early vision detects the following three types of patterns:

(1) elongated blobs with different colour and orientation;
(2) different line endings; and
(3) different crossings of line segments.

Weigle [2000] performed psychophysical experiments in which he showed that up to 15 sliver orientations in the range of 0 deg to 180 degrees are visually distinguishable. Slivers with orientation differences of 15 degrees and more were most easily discernible. He further noted that the 0 degrees and 90 degrees cases are special, working well as background textures but are difficult to pick out as target orientations.

3.2.1.4. Lessons from Multivariate Visualization

Taylor [2002] provides several valuable guidelines from multivariate visualization, which are noteworthy for the display of multiple layered surfaces. Standard approaches for displaying multivariate data, e.g. mapping different variables to different surface properties such as colour and shape, and applying different visualization techniques to different variables, often fail when

four or more layers are displayed. Extrapolating to layered surfaces, this might indicate that marking type on its own would not be suitable for distinguishing between layers because high spatial frequencies with one type of marking would confuse shading represented with other marking types. DDS and Oriented Slivers take the approach of displaying overlapping instances of the same technique, but rely on varying attributes of glyphs, instead of different glyph types, to distinguish between layers. For layered surface displays, this would require changing texture properties of the marking types on different layers. Bair's [2009] use of grid textures, which rely on orientation and texture properties to distinguish between layers is akin to this approach, and seems promising for displaying multiple layers.

Further, it is helpful to distribute glyphs (markings, for layered surfaces) sparsely across a layer so that it is possible to see through to the other layers. Aliasing may be reduced by placing markings randomly or using a Poisson type distribution, which eliminates regularity. Contrast between the background layer and glyphs should be kept distinct.

3.3 Motion for Visualization and Particle Systems

Motion has potential to improve the display of layered surfaces, as it did for DDS. For example certain types of motion produce a perceptual grouping effect, which could be helpful associating markings from a particular layer. Motion may potentially be useful for illustrating shape [Lum et al., 2003]. Particle systems provide a mechanism for generating dynamic and adaptive motions and are useful in sampling surfaces. Uses of motion for visualization and the perception of motion are presented below.

Over and above the shape cues of motion, there are certain types of motion which stand out as perceptually distinct. In particular objects with similar motions are perceptually associated into groups and are clearly distinguishable. These motion types are useful for various visualizations, e.g. highlighting data. It is important to understand the perceptual aspects of motion when developing such visualizations.

3.3.1 Motion Perception for Highlighting and Grouping

The HVS is sensitive to motion and motion patterns [Blake & Lee, 2005]. While simple motion patterns are processed preattentively, complex motions require focus and concentration [Bartram & Ware, 2002]. Preattentive motion processing occurs at an early stage in the HVS and is performed in parallel to other perceptual processes [Woodring & Shen, 2007] and therefore only requires minimal active mental effort. Although the HVS is sensitive to motion, it is limited in the range of speeds, sizes, spatial contrasts and frequencies it can process [Watson & Eckert, 1994]. The detection of motion for instance, depending on the amplitude of the motion, needs to be fast enough to be seen.

Motion patterns that the HVS is proficient at processing are motions which result in smooth 2D transformations of points in the optic flow. Examples include motions of animals, water flowing and self motion [Langer et al., 2005]. These motions are furthermore not disruptive.
We consider that smooth motions of markings over layered surfaces are likely to result in discontinuities in the optic flow, as markings dynamically occlude one another. This would cause multiple layered motion fields to be seen.

Various motion patterns result in highlighting of objects in motion and visual grouping.
A grouping of moving objects is most likely to be detected by the HVS based on the phase of the objects in motion, which plays the significant role in "Motion coherence" [Huber & Healey, 2005] [Ware & Bobrow, 2006]. High luminance and chromatic contrasts best support the discrimination of motion. For instance, motion of differently coloured patterns [Nothdurft, 1993][Weiskopf, 2004] creates an impression of different groups. This is likely because motion is processed by separate subsystems in the HVS to colour. This is meaningful for our proposed design, indicating that motion and colour will only minimally interfere with each other and can be useful for distinguishing between markings on different layers.

(1) Highlighting

The ability of motion to catch the eye has both the advantage of being able to draw attention to something important, as well as the disadvantage of distracting a person [Bartram, 1997]. For instance, animated banners and images which have a popping effect are effective in catching and holding a person's attention, but are undesirable visual elements when one is trying to work [Bartram, 1997].

Slow linear motions strike a good balance between drawing attention and being distracting. These motions are neither irritating nor distracting and yet result in good response times and detection rates [Bartram, 1997]. In the context of the proposed visualization design, this gives a good indication that markings which move smoothly over layered surfaces are suitable to both identify and highlighting a set of markings on a particular surface, without removing a person's attention from a layer or task at hand. Travelling motions, such as markings moving in a continuous direction off the screen, involve both detection and tracking processes in the HVS, which draw attention even more than pop out motions that cause a sudden stimulus in perception [Hillstrom & Yantis, 1994]. Pop out motions are more distracting than anchored motions. Anchored motions are oscillations around a specific point. Motions anchored to a point are desirable for information display where the position of a point itself carries information [Bartram et al., 2003].

(2) Perceptual Grouping

Bobrow and Helsinger [2005] note that objects with similar motions are automatically grouped by the human visual system. An example of this is coherent oscillating motion patterns that visually stand out as groups when items oscillate at either the same frequency, phase or amplitude [Ware & Bobrow, 2006]. This grouping may occur, even if the objects are different in appearance, visually separated, or in cluttered backgrounds or even camouflaged. They refer to this, perceptual phenomenon as "Motion-induced perceptual grouping". The use of perceptual grouping through motion is of particular relevance to our design, in helping distinguish between layered surfaces and associate markings on each layer.

The literature shows that different groups of moving coloured objects may be searched individually, that is a person may be able to search for objects with a specific colour amongst a larger set of objects with similar motions. This kind of search is linear in respect to the number of objects [Nakayama & Silverman, 1986]. Perceptual grouping through motion is thus useful as a mechanism for filtering, since it can be used to cause a group of objects to stand out in visualizations [Bartram & Ware, 2002]. Up to six groups of objects that move with different frequencies may stand out as distinct [Woodring & Shen, 2007]. Objects moving out of phase to one another are most distinct when the difference in phase is 90 degrees [Bartram, 1997] [Woodring & Shen, 2007].

There are limits to how well the HVS is able to distinguish between groups using motion alone [Langer, 2005]. The HVS struggles to discriminate 2D motion gradients of speed in side by side views of motion fields [van Doorn & Koenderink, 1982]. Horizontal alternating stripes moving at different speeds require a higher speed difference for narrower stripes to be distinguishable, indicating that the HVS seems to be less sensitive to higher spatial frequencies for motion [van Doorn & Koenderink, 1982]. For sets of dots with the same colour, the HVS is reported to be limited to distinguishing at most three moving layers for dots moving at different speeds [Langer,2005]. As average speed of layers increases, the difference in speed between layers needs to be increased for a person to distinguish between the layers.

Braddick [1997] showed that the difference in orientation between moving dots and a straight line requires three times the difference when judging between a single group of moving dots and a straight line. Researchers note that motions in opposite directions may have the effect of cancelling each other out and also create a sense of depth where this may not be desirable [Andersen & Bradley, 1998] [van Doorn & Koenderink, 1982]. For oscillating objects, Huber and Healey [2005] recommended separating the direction of motion by twenty degrees to distinguish between foreground and background objects.

3.3.1.1 Related Uses of Motion in Visualization

Motion has proven to be an effective means for enhancing visualizations. It has been used for highlighting and visual grouping of items in visualization for pattern detection as well as for illustrating shape. These are the uses of motion most directly related to our work and are detailed below. Motion has also been used for brushing and flow visualization. Motion blur is often used to visually display the effect of motion in still images. The most straightforward use of motion is for the display of time varying data through a frame by frame animation over time.

Motion has been applied to multivariate visualization and used for pattern detection (for finding relationships between variables). Examples of this include mapping data values to the frequency, phase or amplitude of oscillating anchored glyphs [Ware & Bobrow, 2006]. These approaches rely on the perceptual grouping property of similar motions to reveal patterns and highlight groups of objects. Our proposed visualization design uses motion and colour to perceptually differentiate markings placed on multiple layered surfaces in 3D and to "highlight", or allow a viewer to focus on different layers.

The highlighting ability of motion has been applied to volume datasets for dataset traversal [Correa & Silver, 2005]. By locally varying the transfer function the approach emphasizes specific paths through the data or an animated traversal of the volume, highlighting features, such as vascular flow. Woodring and Shen [2007] have also incorporated animations into cluttered volume visualizations as a highlighting mechanism by adding positional motion and opacity changes for visually filtering selected data. Other examples of motion highlighting for visualization include highlighting and querying of intelligence data [Bobrow & Helsinger, 2005], alerting/signalling a human interrupt [Ware & Bobrow, 2006] and for highlighting subsets of data in large network diagrams [Ware & Bobrow, 2004]. Rocking and user interaction make use of rotations to illustrate depth and shape, by inducing the KDE. An early example of this use of motion to illustrate shape is to rotate a 3D cloud of data points around a vertical axis [Donoho et al., 1988].

3.3.1.2. Kinetic Visualization

Kinetic Visualization has been shown to enhance a sense of shape for a single well shaded opaque surface, by moving particles over the surface relative to a viewer. The shape, density, transparency and size of particles all impact the effectiveness of KV. The particles are animated according to a set of motion rules which attempt to create motions that meaningfully illustrate shape. In particular, particles follow the principal curvature directions of the shape, and flow in a consistent direction with neighbouring particles and at the same speed. An illustration of Kinetic Visualization is shown in Figure 3.13, which illustrates particles following principal curvatures, and aligning themselves to move in similar directions.

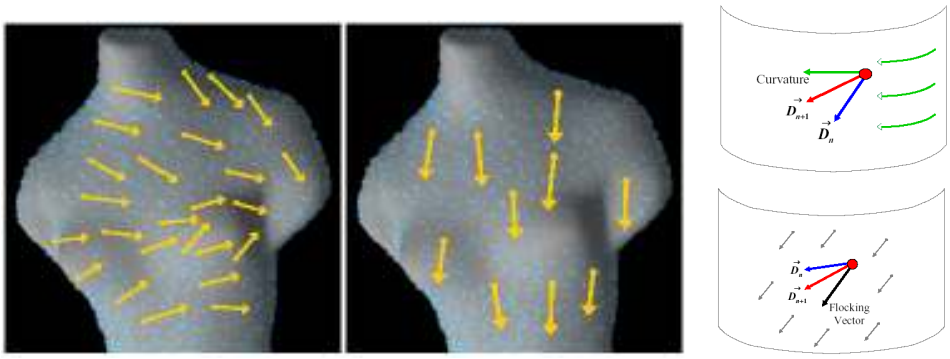

Figure 3.13 Illustration from Kinetic Visualization [Lum et al., 2003]. Particles move over a surface to illustrate shape, by moving in consistent directions, aligned to the first principal curvature direction, at the same speed.

KV effectively enhances shape perception, when the surface is covered by particles so that there are not large gaps between markings. To achieve this, the density of particles is monitored, and overcrowded particles are redistributed to regions which are sparsely covered. A separation rule, which applies a repulsion force, is also used to prevent particles from clumping together. The work in this dissertation builds upon KV, applying it to the visualization challenge of displaying multiple layered surfaces. To achieve this, modifications to KV are proposed in chapter 4. One such difference is the use of shaded patches, which convey shape better than the original unshaded particles. KV was verified to improve shape perception by a set of videos, and a user experiment in which observers viewed height field surfaces, top down [Lum et al., 2003]. Participants identified the highest and lowest peaks better with KV than for surfaces rendered with only shading.

3.3.2 Animated Particle Systems

Particle systems are used for interactive modelling of shapes [Su & Hart, 2005], physics based modelling, simulation and special visual effects such as smoke, fire and water [Reeves, 1983]. Animated particles are also used in Scientific Visualization for displaying vector fields [Kruger et al., 2005], since particles are an effective means of representing local aspects of flow [Langer, 05]. Particles have also helped to "spray paint" volume and surface datasets [Pang & Smith, 1993]. Particle systems are also useful for sampling of surfaces and simulating behaviours of animals such as the flocking of birds [Reynolds, 1987]. This work draws on these later two functions to move the opaque markings over layered surfaces smoothly and in doing so surfaces are sampled and visualized. Particle Systems consist of "collections of particles", where each particle is typically modelled as a point mass. The motions of particle systems may either be driven by differential equations or through an iterative simulation, in which forces move sets of particles in combination with various constraints [Angel, 2000].

3.3.2.1. Sampling Surfaces through Particles

Szeliski and Tonnesen [1992] used simulation style particle systems to sample and model free-form surfaces. The particles in their system each have a unique orientation. Figueiredo and Gomes [1996] modelled implicit surfaces using Delaunay Triangulation to compute neighbouring forces, while Witkin and Heckbert [1994] used particles to both show and deform implicit surface models. The particles in the latter system each have their own repulsion radius. In addition to being used for polygon models, implicit and free-form surfaces, particle systems have also been used to extract isosurfaces from volume data [Crossno & Angel, 1997]. These approaches, being concerned with only a single surface, do not need to take the view point into account, as our approach does.

3.3.2.2. Bag-of-Particles for Deformable Models

Many of the particle systems for sampling surfaces typically deal with a single surface. Stahl and Turk [2002] present a particle system which is able to model multiple surfaces. Notably their system not only allows surfaces to be sampled, but the particle systems serve as a model of the surface which can be deformed and felt through a haptic device. Both surface and volume particles are used to achieve this. Volume particles are contained by surface particles and determine the elasticity of the model through inter-particle parameters. Gradient and distance maps play a significant role in the approach, allowing the user to define objects and provide feedback reaction forces. The system can simulate multiple objects in the same scene.

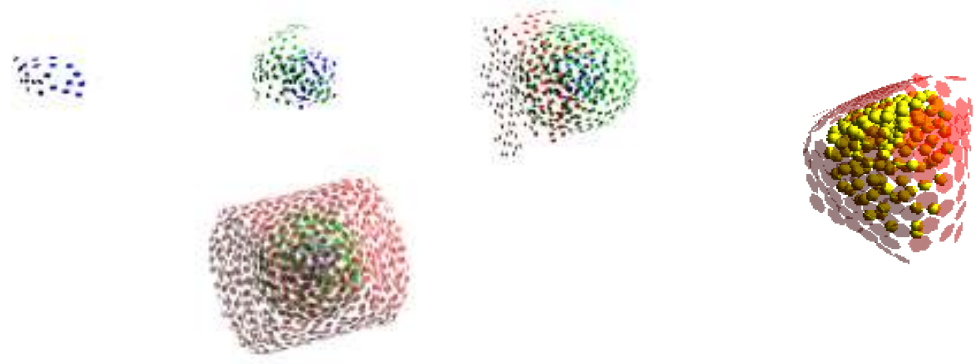

Figure 3.14 Illustrations from Bag-of-Particles [Stahl et al., 2002], *left:* a visualization of a sphere cube and cylinder; *right*: illustration of a left ventricle of a heart, the interior spherical particles that obstruct the view are not useful for layered surface visualization.

This system fortuitously offers a display of layered surfaces. Figure 3.14 above shows illustrations from their work, displaying multiple surfaces being created. In these figures layered surfaces are visible between the disks on the different surfaces.

The system, however, in support of haptic feedback fills the surfaces with volume particles to the detriment of viewing the layered surfaces. This feedback was the original purpose of their system and not the display of layered surfaces. These particles occlude the view of other layers, as can be seen in Figure 3.14 (right). Though animation plays a role in the simulation steps for sampling the surfaces and allowing interactive deformation and visual feedback, the particles eventually settle on the surface and tend to towards a state of equilibrium. This differs from the design proposed in this thesis, which relies on the particles moving over the surface in a continual animation to address the problem of occlusion. Further, Stahl and Turk's approach does not attempt to reduce occlusions as our approach does.

3.3.2.3. Flocking - Behavioural Particle Systems

Complex natural motions such as those of a flock of birds, school of fish, herd of animals etc. may be simulated in computer animation through particle systems. For this reason, some of the flocking behaviours are integrated into Kinetic Visualization and our visualization design, since the HVS is adept to these motions as mentioned in 3.3.1.

"Flocks" are typically modelled as a system of particles, with each particle representing a bird, fish etc. Each bird acts independently. The birds have steering behaviours, which determine how they adapt to and navigate through their dynamic surroundings, based on their local perception [Reynolds, 1987]. The motions are achieved through steering behaviours. Three of the classic behaviours for creating patterns similar to flocking birds or schooling fish, are:

(1) flock centering or cohesion;
(2) velocity matching or alignment and;
(3) collision avoidance or separation.

Cohesion simulates the natural way in which birds or flocks move together in a group flying near to one another. As these birds draw near to each other, they tend to fly in the same direction. They avoid collisions with neighbouring birds. This is modelled through the collision avoidance rule. Kinetic Visualization, and hence our design, makes use of the velocity matching and collision avoidance behaviours.

3.4 Summary

This chapter has reviewed the various techniques for rendering layered surfaces. These were classified as being either: shape and spatial relationship preserving, or altering. Attention was given to the former class of techniques, in particular techniques which augment transparency with opaque markings to help illustrate shape, since these address our visualization goals. Techniques such as rocking that are used to augment layered surface visualizations were also described. These techniques help significantly to make layered surface renderings comprehensible. Precursors from multivariate visualization, which have had success in layering

multiple 2D scalar fields were presented with a set of guidelines from this domain. We also reviewed various perceptual aspects of motion that may have bearing on our visualization design. Finally, precursors to our approach from work done with particle systems were presented. In particular Kinetic Visualization showed that animating markings over a single surface is useful for illustrating shape. In the next chapter, we present a design for extending this technique to augment the display of multiple layered surfaces.

Chapter 4

Visualization Design and Particle System Framework

This chapter describes a novel visualization design that uses animated particles to help display multiple layered surfaces. The design extends transparency based layered surface display techniques augmented with opaque markings. It displays multiple layered surfaces in a way that maintains the spatial relationships between the surfaces, unlike exploded or side-by-side views. The motion of the markings is useful for layered surface visualization in that the markings cover the surfaces over time and vary the visible regions of the surfaces.

Specific motion strategies, which control the way the opaque markings move over the surfaces, are an integral component of the design. These strategies are designed to be helpful for the display of layered surfaces by creating motions which vary or reduce occlusions, illustrate features and the shape of the surfaces, and help distinguish between the markings on different surfaces.

The design makes use of particle systems to achieve dynamic motions of markings over the surfaces. This particle system framework is also useful for sampling the surfaces. The appearance and type of opaque markings used, as well as the semi-transparent rendering of surfaces, are also important design considerations.

Our design builds upon and shares many similarities with the techniques of Kinetic Visualization, Data Driven Spots and Bag-of-Particles presented in the related work set forth in Chapter 3. This chapter commences with an overview of the design. It then proceeds to expound on the key aspects of the motion strategies, the particle system framework and the various rendering design choices.

4.1 Outline of the Visualization Design

Munzner [2008] defines a visualization design as a visual representation that is particularly crafted to solve a specific visualization problem in response to a task analysis and makes use of existing or novel techniques or combinations thereof. It is therefore important to consider the lower level tasks that need to be performed when exploring layered surfaces. Design requirements can be drawn up from the task analysis.

4.1.1 Task Analysis

Weigle [2006] in his study of layered surface driving problems, analyzed the questions that scientists and doctors were interested in. The analysis resulted in a reduced set of fundamental domain-independent comparison tasks. These tasks, being common to all of the problems from all the various domains, were shown to answer most of the scientists' questions. The exception being tasks that were more appropriately answered numerically [Weigle, 2006]. The spatial comparison tasks identified for exploring layered surfaces are:

- identifying global shape;
- identifying local shape such as surface orientations and local features; and
- gauging distances between surfaces.

Layered surface displays should facilitate these foundational tasks for exploratory visualization. Rather than spend time refining domain questions, which are in any event likely to lead again to these core tasks, we focus on technical issues of the visualization design that support such tasks and address the visualization issues set forth in section 1.1.

4.1.2 Visualization Design Requirements

The following design requirements are specified to support the above foundational comparison tasks for the exploration of layered surfaces. These requirements are set forth to address the visualization issues of occlusion and the difficulty of distinguishing between opaque markings without disrupting surface perception. The design is proposed to augment opaque marking-based layered surface visualization techniques to more effectively display more than two layered surfaces. The design requirements below should:

(1) show *Multiple layers*: display more than two layered surfaces;
(2) be *Shape illustrating*: show global and local features of surfaces simultaneously;
(3) be *Space preserving*: preserve spatial relationships across and between surfaces layers;
(4) aid in *Distinguishing layers*: distinguish between markings on different layers and visually group markings on the same layer; and
(5) be *Occlusion reducing*: reduce occlusion and visual interference.

A visualization design that uses motion is proposed to achieve these requirements. The design extends opaque marking based layered surface display techniques through various motion rules. The motion rules are incorporated into a particle system framework and drive the dynamic motions of the opaque markings. Each particle corresponds to an opaque marking. Further the particle system is useful for distributing the markings over the surfaces. Finally, the choices regarding the visual representation of the particles and transparent rendering of the surfaces significantly determine the effectiveness of the design. Figure 4.1 shows a visual illustration of the framework and these various design choices.

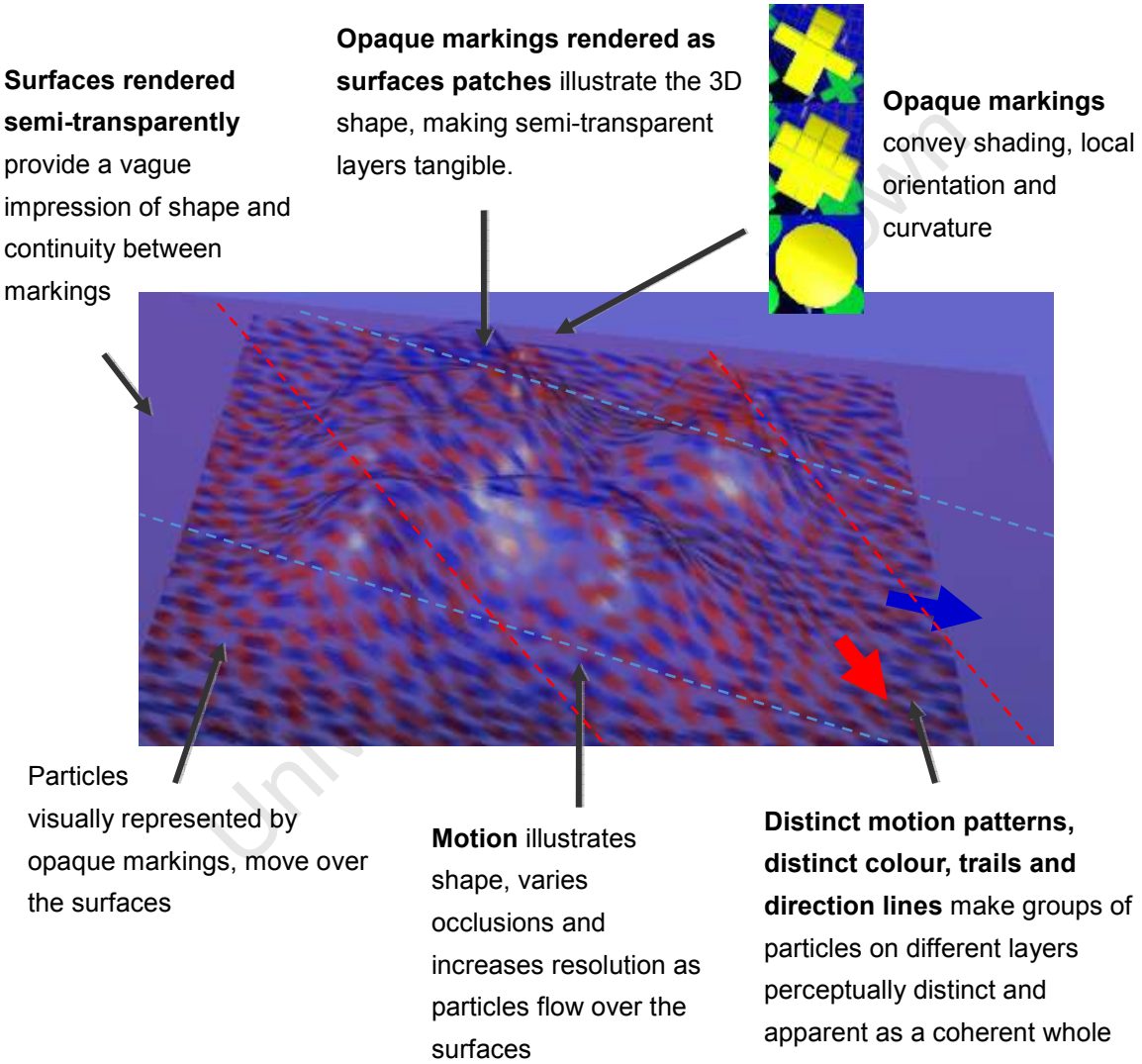

Figure 4.1 A motion blur illustration of our novel visualization design and its major components. The design, which is built on a particle system framework, relies on animation of the particles which are visually represented as opaque markings to display layered surfaces. A range of visual design choices are available to the framework including varying the type of markings, the type of motion patterns and the use of motion trails.

Motion rules are designed to cause the opaque markings to move smoothly over the surfaces. The rules are intended to:

- help better distinguish between the opaque markings on different surfaces;
- introduce additional shape cues;
- cover the surface, providing a denser sampling of the surfaces over time (increasing effective resolution); and
- vary the see-through views which reduces occlusions.

Various force calculations were designed to generate forces which, when applied to particles, move them over the surfaces in these visually meaningful ways. Opaque markings are rendered at the positions of the particles on the surfaces and reflect the local shape geometry at those positions. The surfaces themselves are rendered semi-transparently to contribute a sense of surface continuity.

The design requirements of S*hape illustration* (2) and S*pace preservation* (3) above are addressed through the use of transparency, augmented by opaque markings. These techniques are extended through motion, which has been shown perceptually to add a sense of continuity to dots in motion [Lum et al., 2003]. Motion is therefore helpful to address the *Distinguishability* (4) requirement. The visualization design uses similar motion patterns to leverage motion in combination with colour to help differentiate between markings on layered surfaces. Perceptual properties of certain motions have been shown in related work to be useful for perceptual grouping of objects [Ware & Bobrow, 2006] [Langer et al., 2005]. Distinct motion types are incorporated in an attempt to addresses the *Distinguishability* (4) requirement. The *Occlusion reducing* (5) requirement is also addressed through moving the markings. Animation of the markings on the layers varies the views of the underlying layers, seen through the outer layers. Moreover, this requirement is addressed more intentionally by taking into account the positions of markings in relation to the view point and one another. This allows forces to be computed and applied to particles which direct them away from being occluded by other markings and obstructing the view of markings behind them relative to the viewpoint. This incorporation of the view point and motion rules to determine these forces is one of the novel contributions of this work to layered surface visualization. Potential problems with applying such forces is detailed in section 4.2.3.

Motion blur trails or the use of different shapes for opaque markings are also useful for addressing requirement (4) *Distinguishability*. Motion blur leaves a temporary distinct shape reflecting the unique motions on different layers. These cues contribute to perceptual grouping, as explained by Texton theory [Julesz, 1986] and Oriented Slivers [Weigle et al., 2000]. The trade-off using such trails is that they result in a larger surface area being illustrated on each surface, which results in more occlusion. Motion blur trails are therefore not evaluated in this research. Surface patches are rendered opaquely without blending in outer transparent layers in order to reduce blurring of surface shading on the markings. Markings, which are moving over

the surfaces cause more samples of the surfaces to be seen over time than a set of static markings. Cumulatively all these design choices comprise a framework that enables the display of more than two layered surfaces, satisfying (1),the *Multiple layers* requirement.

4.2 Useful Motions for Displaying Layered Surfaces

The original Kinetic Visualization motion strategies include having markings move over a surface at the same speed, which gives a sense of depth from kinetic depth. The markings move either along a uniform direction or follow the principal curvature directions. "Flocking" type forces are used to distribute the markings over the surfaces and to cause markings to move in the same direction as neighbouring markings. These rules are illustrated in Figure 4.2 and Figure 4.3.

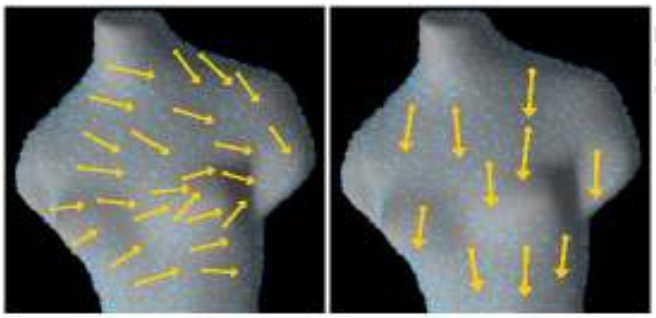

Figure 4.2 Motion rules for Kinetic Visualization [Lum et al., 2003]. *Left* markings are caused to move along principal curvature directions in locally similar directions as other neighbouring markings by using Flocking's [Reynolds, 1987] alignment rule. *Right:* Alternatively markings follow principal curvature directions which favour a specified direction.

This section describes additional rules and modifications to these classic KV motion strategies that may be useful for illustrating layered surfaces. These various rules for layered surfaces are introduced to make the opaque markings move over the surfaces in a way that helps a viewer to distinguish between markings on the different layers. These rules further produce motions of markings which enhance shape, cover the surfaces and reduce occlusions and interference.

A significant contribution and novelty of this work is that the view point is taken into consideration. Taking the view direction into account is useful for generating improved views of the markings on layered surfaces. Particles can be repositioned relative to one another and relative to the view point to reduce occlusions and interference. Furthermore, particles that move orthogonal to the view direction convey shape better than arbitrary motions since such movement evokes a stronger sense of kinetic depth than particles moving parallel to the view direction. This is because for objects moving at the same speed at different depths, orthogonal motions produce the largest visible apparent change in position relative to the viewer over time, effectively giving the largest difference in parallax. In contrast, traditional layered surface techniques do not take

the view point into consideration when placing opaque markings. To the best of our knowledge, no layered surface display techniques use motion other than rocking, to give aid to the challenge

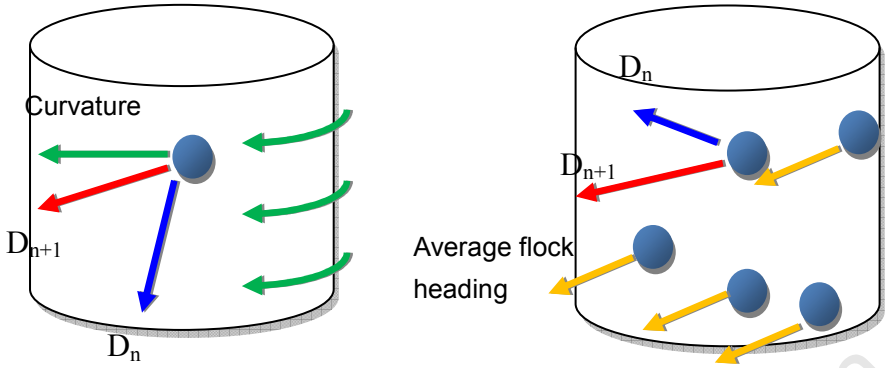

Figure 4.3 Illustrations of forces applied to markings from Kinetic Visualization [Lum et al., 2003]. *Left*: A particle adjusts its current heading, $\mathbf{D}_n$ towards the local principal curvature direction; *Right:* Particles adjust their current heading to move in the same direction as neighboring markings, according to Flocking's alignment rule [Reynolds, 1987]

of displaying the layers.

4.2.1 Motions for Distinguishing between Markings on Different Layers

Distinct motion patterns have the potential to be used in addition to colour to help visually differentiate between markings on the different layers. Perceptually, objects moving with the same motion pattern visually stand out as belonging to the same group. Static objects or a different set of objects in the same scene which are moving with a different pattern are perceived as belonging to a completely separate group [Bobrow & Helsinger, 2005]. We thus choose to animate particles over a layer with the same motion behaviour as the other particles on that layer but cause particles on different layers to move with different motion patterns. The simplest implementation of this strategy is to move particles along a uniform heading on one layer and move particles in another direction on a different layer.

Another implementation of this rule is to move particles along a uniform direction on one layer and to move particles around features on another layer or move particles along principal curvature directions on yet a third layer. The idea is that the sets of particles on the different layers each have a unique motion pattern that is clearly distinguishable from the pattern on the other layers. Different motion patterns are illustrated in Figure 4.4.

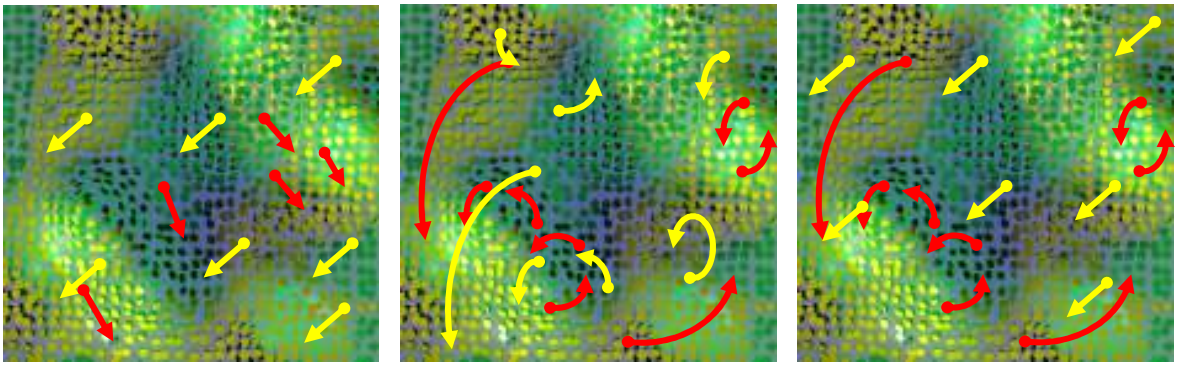

Figure 4.4 Different motion patterns: *left*: Particles may follow uniform directions, moving markings on different layers along different headings should contribute to distinguishing between the markings on different layers; *center*: Markings swirl around features. This is achieved by rotating the markings around the up vector in their local frame and re-projecting them back onto the surface; *right:* Markings on one layer move in a specific direction while markings on another layer move around features.

The first motion strategy used is to move particles along distinct uniform headings on each layer to help distinguish between markings on the different layers. The headings on different layers are separated by a minimum angle of 30 degrees. This minimum angle is based on the work by Langer et al., [2005] and Weigle et al. [2000], which indicates that for orientations to be distinguishable the variation should be at least 15 degrees for static orientations and 30 degrees for motion. To further help identify the directions in which particles are moving, line glyphs are rendered behind the scene as illustrated in Figure 4.1. These allow the viewer to line up the directions in which particles are moving with a distinct visual line. This is done because perceptual research indicates that the orientation of points moving along a particular direction is better distinguished in comparison with a line than other moving points [Braddick, 1997] [Langer et al., 2005]. Particles were not moved in orientation directions that are horizontal or vertical, though using these directions in the future may be helpful in helping observers to better distinguish between the different layers. Directions of motion in our framework are set in relation to the screen and, for simplicity, assume no interactive variation of the view direction. However, uniform directions should be relative to the view direction so that if the viewer interactively adjusts the position from which the surfaces are observed, the headings are orthogonal to the view direction.

Particles are not moved in opposite directions. Anderson and Bradley [1998] have shown that particles moving amongst each other with opposite velocities create an impression of depth. For this reason, Lum et al., [2003] do not use motions in opposite directions in their Kinetic Visualization, as this may interfere with the perception of a single surface.

Causing some layers to remain stationary while one or more other layers are in motion is also a powerful means of creating a distinction between markings, see Figure 4.5. For instance,

markings moving on the two or three layers closest to the viewer are crisply juxtaposed to the stationary markings on the furthest layer. Perceptually, the HVS seems to be limited to distinguishing up to three distinct motion patterns [Langer et al., 2005]. The use of a combination of stationary and animated markings may be useful for breaking these limits.

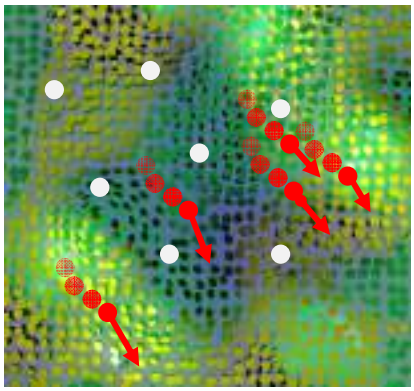

Figure 4.5 Mixing stationary markings on one layer with animated markings on other layers is an effective means of discriminating between the markings on different layers.

Though not implemented in this work, phase and frequency oscillations hold promise in helping a person distinguish between markings on different layers. Ware and Bobrow [2006] have shown that particles oscillating at different phase angles are perceptually distinct and useful for multivariate visualization. A practical implementation may quite simply entail oscillating particles at fixed positions on the surfaces at various frequencies or phases. The particles may be moved back and forth along the principal curvature directions on the different layers at these points.

Changing the motions on a layer from moving in a uniform direction to following principal curvature directions over time is more useful than employing just a single type of motion on a layer for global perception type tasks. Participants from our first experiment: "Rocking vs. KV" (see chapter 5) stated that, although uniform motion clearly showed some features, it would have been helpful to see motions along other directions. To accomplish this, motion forces are varied from one motion type (uniform heading, curvature following, rigid body motions, etc) to another motion type on each layer. The motion types on the different layers are kept separate by applying a varying phase angle to each layer which offsets the motion types for the different layers from each other. This angle is varied over time causing different motions to be in effect on each layer at different times. Over time the motions on the different layers change smoothly, illustrating different aspects of the surfaces.

Although motion bears the advantages of surface coverage, perceptual grouping, etc, it does introduce the problem of interference. Interference noticeably occurs on a local level of inspection (e.g. in estimating local surface orientation from markings). It arises when markings

move over other markings being examined or when a person is attempting to focus on a single point on a surface. Markings moving over or around the point or region of inspection were observed during this work to draw the viewer's focus away from that point.

Moving particles at different speeds on different layers is an additional way to help distinguish between the particles on different surfaces, though according to the background in perceptual research, there needs to be a significant difference between speeds to distinguish between different moving objects and such distinction is less obvious than markings moving in different directions. The faster the average motion of a set of moving points, the greater the difference in speed between the different points needs to be, for a person to distinguish between the motions [Langer et al., 2005]. Figure 4.6 illustrates how variations in speed can be used for distinguishing between markings. The effect is not as powerful as the other motion patterns.

One potentially useful variation in speed for layered surface visualization is to move particles closer to the viewer faster than particles on more distant layers. This exaggerates the sense of motion parallax between nested surfaces at different distances from the viewer. Theoretically, this may work well for helping a viewer distinguishing between nested layers, contributing an exaggerated sense of depth. This presents a trade off between accuracy in depth judgements from motion parallax and the ability to distinguish between the layers. Such distortions to depth may interfere with the other depth cues and work contrary to the shape preserving design requirement. An observation made during development was that, causing particles to move slower on layers closer to the viewer, seemed to cause less interference than having the closer particles move more quickly, especially when a viewer is focusing on an interior particle or region.

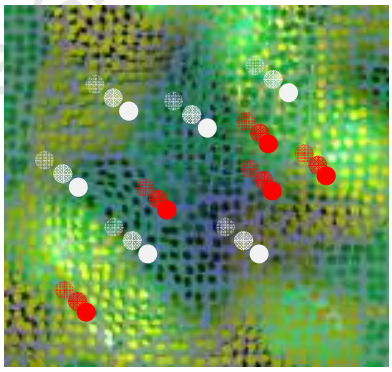

Figure 4.6 Variations in speed have to be significant to effectively discern between markings. Speed is also an overloaded visual attribute, in that it also contributes to conveying depth. The significance of depth is, however, not as strong as for Rocking animations and it may be logical to use speed for other purposes.

It is likely that the most illustrative speed settings for markings are to cause all particles on all layers to move at the same velocity (as in classic KV). This produces a kinetic depth cue.

Furthermore particles on different nested layers at different depths would naturally seem to have distinct motion speeds, which would contribute towards distinguishing between these markings, yet without distorting the depth perception.

4.2.2 Shape and Structure Enhancing Motion Strategies

The viewer's vantage point of a surface plays a role in shape perception, for instance textures following directions orthogonal to the view direction have been shown to best illustrate shape [Sweet & Ware, 2004]. Motion parallax and kinetic depth cues are strongest for motions of either the viewer or objects at different depths in a scene that are orthogonal to each other. Such motions are achieved by applying a force in the direction of the first or second principal curvature direction (either forward or backward) that is closest to the vector found by taking the cross product of the surface normal and the view-direction (see Figure 4.7).

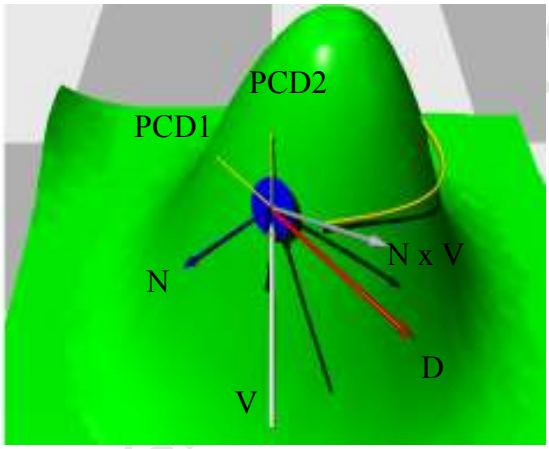

Figure 4.7 Particles moving orthogonal to the line of sight have the greatest transverse displacement relative to the viewer and thus induce a stronger sense of shape from motion parallax than markings moving parallel to the view vector. Force **D** is applied to move a marking in a direction in its local frame which is perpendicular to the view vector- **V** or along one of the principal curvature directions which is closest to this perpendicular vector in a marking's local frame, which is tangential to the surface normal **N** at the marking's position on the surface. **PCD1** and **PCD2** are the first and second principal curvature directions.

A meaningful way of illustrating features is to rotate particles around a fixed vector such as the up vector, in their local tangent plane using rigid body rotations and then re-project the particles back onto the surface. This provides a means of improving the sense of depth and structure, especially for symmetric or circular shapes and features. This is because for such shapes this rule produces motions which are identical to rigid body rotations. Such rotations induce the Kinetic Depth Effect. On terrain type surfaces these rotations are relative to a each particle's local tangent plane. This causes motions relative to the local feature each particle is on. An example of this strategy is

to rotate particles around the up vector. This causes particles on peaks or valleys to swirl around these features, locally, while particles in the plane appear to swirl around a single up vector.

4.2.3 Creating Optimal Layouts of Markings by Taking the View Point into Consideration

One of the significant contributions of this work to layered surface visualization is that it is the first to take the view direction into account to create better layered surface visualizations. Incorporating the view direction into layered surface visualizations with a particle system framework draws on the adaptive nature of particle systems to create meaningful motions and better visual layouts of markings over the surfaces. As described above, one way to create better visualizations by using the viewpoint is to cause particles to move transversely to the view direction as described above for improving the sense of motion parallax. The second proposed strategy is to cause particles to move and distribute themselves over the surfaces so as to reduce occlusions. This strategy, which causes markings to adjust their positions in relation to each other and the viewpoint, is useful for improving the visual layouts of the opaque markings over the surfaces.

Occlusion is the most significant problem encountered when rendering layered surfaces [Weigle, 2006][Bair, 09]. Opaque marking techniques typically create static textures, which may by chance result in occlusions. The particle system approach used in this dissertation is able to address this problem primarily by varying the positions of the markings over time. Simple animation of the markings is likely to haphazardly reduce or vary occlusions as the markings move past and over or under one another. Markings moving over the surfaces with different motion patterns will only occlude other particles temporarily.

However, in addition to relying on the unintentional use of motion to vary occlusions, our design explicitly addresses this issue by introducing separation forces that will steer particles away from occlusions. Particles on the exterior layers occluding markings on the interior layers are caused to move, relative to the viewer, away from markings on layers further away, which they are obscuring. Markings on the further layers also attempt to move out from being occluded beneath exterior markings. This reduces occlusions and creates more optimal use of empty space between markings. Figure 4.8 illustrates the advantage of this view separation for a particular static view compared to a Poisson distribution.

One of the problems that arise in layered surface visualizations with animations is that markings which move over other markings result in visual interference. Taking the view vector into consideration may be useful to reduce such visual interference by steering markings around other markings on lower layers rather than markings moving unwittingly over others.

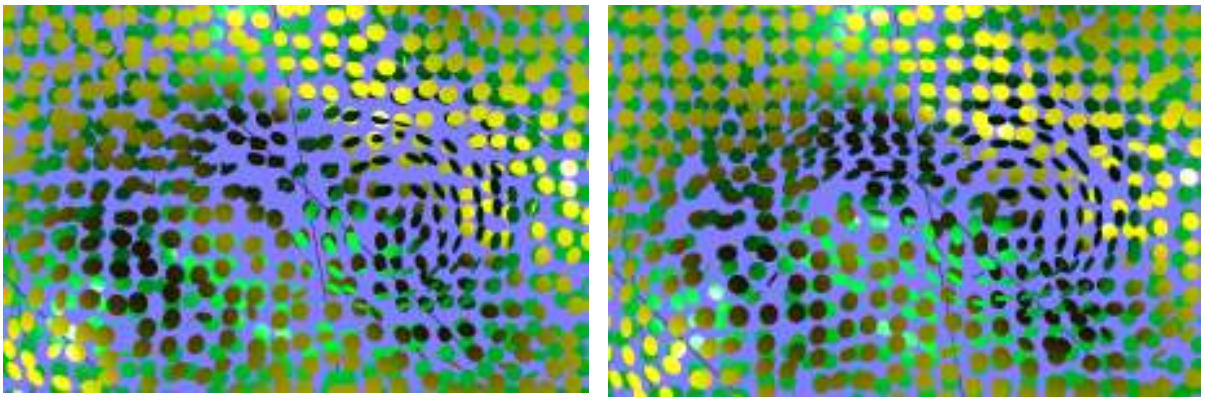

(i)

Markings distributed over layered surfaces with Poisson distribution

(ii)

Markings which have moved to avoid occlusions in relation to the view direction

Figure 4.8 Side by side illustration of the difference between placing markings over a set of layered surfaces using a Poisson distribution (left) and causing markings to spread themselves out in relation to the view direction to reduce occlusions (right).

The occlusion reducing rule is not meant not to eliminate occlusions entirely, but rather to reduce the total number of occlusions caused by particles moving over others so that interior particles are more visible. Eliminating all overlaps would be detrimental because such dynamic occlusions are the most powerful pictoral depth cue since occlusions clearly convey relative depth ordering. However, it is unlikely that the rule will eliminate all occlusions, since there are multiple particles moving over multiple overlapping surfaces and the occlusion reducing forces are typically not heavily weighted. The rule is intended to simply reduce the total number of occlusions to make markings on underlying surfaces visible. An alternative solution could be to apply forces that would steer markings to minimally occlude underlying markings without completely obscuring them, thus harnessing the occlusion depth cue and also making completely occluded markings visible. Another concern is that these forces could be misperceived as being due to variation in surface shape. This could be the case if these forces are strong, but in our implementation these forces are weak especially in relation to the shape steering forces, being a fraction of the principal curvature forces. Such weak forces create very subtle deviations to the motions along the principal curvature. Further, in the original implementation of Kinetic Visualization [Lum et al., 2003] strong “alignment” forces are applied to particles which cause them to move contrary to the shape or curvature in places yet without confounding shape perception.

Care must be taken that these forces do not cause motions that interfere with the coherence of the overall motions on different layers. Weighting the view separation force heavily, for instance, may cause jitter, as markings are repelled strongly from others to avoid occlusions, which would ruin the sense of smooth motion that the framework attempts to maintain, which is necessary to convey a sense of shape. Jitter is particularly noticeable and distracting.

Algorithm 1 Procedure for computing forces for avoiding visible occlusions

Find the projection of every particle from all layers into image space.
Find each particle's neighbours in image space.
Compute a separation force between each particle and its neighbouring particles.
Add together the separation forces for each particle.
Project these summed forces into the particle's world space.
Project each particle's resultant force vector into the particle's local tangent plane.

The procedure for computing forces between particles that will cause them to move away from occlusions is listed in algorithm 1. The final projection into the particles' tangent frame gives the force component that will cause the particle to move away from other particles near to it in image space. Figure 4.9 shows an illustration of this rule.

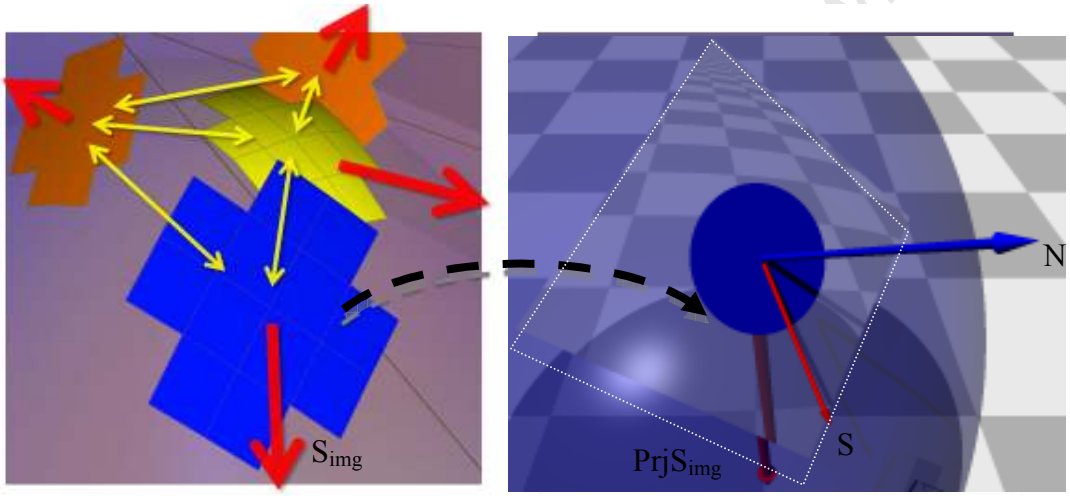

Figure 4.9 Particles in image space move to reduce occlusions. *Left:* In image space repulsive forces are determined for nearby and overlapping markings. The summed forces, $\mathbf{S}_{img}$, are projected onto a plane at the particle parallel to the image plane relative to the camera, to determine the force in world coordinates, $PrjS_{img}$. *Right:* This force is then projected into the surface's local tangent plane at the particle's position giving the final separation force **S**.

Practically neighbouring particles are found by using a grid data structure which can be constructed in linear time and which may also be queried in linear time O(N). A Grid data structure is used for finding image space neighbours rather than other spatial data structures such as kd-trees, quadtrees, binary space partitioning trees and Delaunay triangulations. Because of the dynamic nature of the problem, the data structure must typically be updated or reconstructed every time step, because the markings are continuously changing their positions and neighbours. These other data structures require no less than logarithmic reconstruction and querying time in general [Zachmann & Langetepe, 2002].

In stereo, two slightly separated views of the layered surfaces are visible. Although several points may be occluded in either the left or right eye view, it does not necessarily mean that they are occluded in both views. This raises various perceptual questions:

- How does the HVS attribute depth to a point occluded in one view but not in the other?
- Does the obstruction of one point destroy the absolute sense of depth from binocular disparity?
- Is it meaningful in stereo to have a rule which attempts to reduce occlusions?
- Which eye should occlusions be removed for?

We hypothesise that it is likely best to reduce occlusions for the view for the dominant eye as is done for selection type interaction interfaces for stereo displays [Hill & Johnson, 2008]. A solution to the stereo case is left for future work. While taking the view vector into consideration to create more optimal layouts of markings, it is useful during the animations to steer markings away from occlusions. It is likely to be useful for active interaction, where a user rotates and moves around a visualization and then stops the interaction to observe the surfaces from the new vantage point.

The view separation forces then adjust the layout of the markings so that the viewer has the best picture possible from the specific view point. This motion strategy is also useful for static presentation style visualizations, where a single image needs to illustrate a set of layered surfaces. This rule would vary the positions of the markings to be more optimal than a mere random distribution or uniform distribution of markings over the surfaces. The rule seems to function best when "flocking" repulsion and cohesion forces are used with the view separation force. The cohesion force radius must be greater than the separation radius, to draw markings towards one another, yet the markings should still maintain space between one another, which is accomplished by weighting the separation force more heavily with a smaller radius than the cohesion force. The view dependent flocking forces are then applied within these bounds to cause markings to avoid occlusions as much as possible. As with Flocking type parameters finding the right weightings and radii for the best layouts is a parameter selection problem.

4.2.4 Covering the Surface

The density and separation rules from standard Kinetic Visualization are used to maintain an even distribution of particles over the surfaces. When the density of particles moving over a surface becomes too high the particles are faded out and redistributed to regions of lower density and then smoothly faded back in. The relocation of particles which have been faded out entails translating them to either a random position or a region which is known to be less crowded.

Separation forces are also applied for the purpose of maintaining a distribution of markings across a surface. These forces also ensure a sufficiently large see-through space between markings on the surfaces. Various weights are applied to the different forces. The weighting of

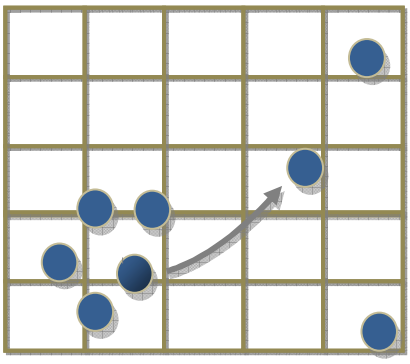

(i)

Translating markings from high density regions to low density regions. Markings are faded out and then back in

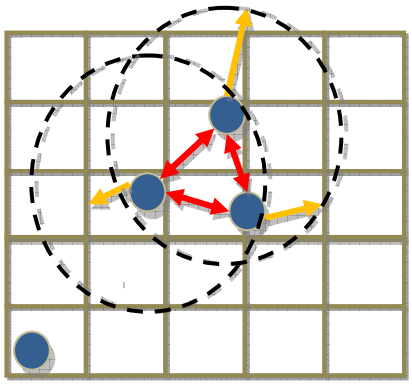

(ii)

Magnetic type repulsion is used to push nearby particles within a specified radius away from each other. This influences the density of the markings

Figure 4.10 Maintaining coverage of a surface is achieved by both redistributing markings from densely populated regions to sparsely covered regions and by applying repulsion forces between markings close to one another, causing them to spread out over the surfaces

the separation force needs to be significantly smaller than the other weights, with the exception of cohesion forces. If this force is too strongly weighted markings bounce back and forth off each other creating a jittering effect which is particularly disruptive to the viewer. Smooth motions of markings over the surfaces are best for conveying motion parallax depth cues and a sense of surface curvature.

The current implementation of the approach in this work creates near uniform, Poisson like distributions of particles over each surface. However, curvature based distributions may prove more useful for illustrating high-frequency regions of surfaces. The density redistribution rule and separation rule used to maintain coverings of the surfaces are illustrated in Figure 4.10.

4.3 Particle System Framework and Implementation

Particle systems are used in this work as the means by which markings are animated over the layered surfaces. Particle systems are particularly well suited to achieving the different motion strategies described above. The advent of modern graphics hardware makes them suitable for interactive exploratory visualization. In the context of the proposed visualization design, this is particularly useful for creating visualizations that take the view direction into account and at interactive rates adjust the visualization. The adaptive nature of particle systems helps to this end, since particles are able to dynamically adjust their motions from time-step to time-step in real-time taking into account neighbouring particles, the surfaces and view direction. Modern day particle systems on GPUs (Graphics processing units) are capable of doing this for hundreds of thousands of particles in real time-faster than 30 frames per second [Latta, 2004].

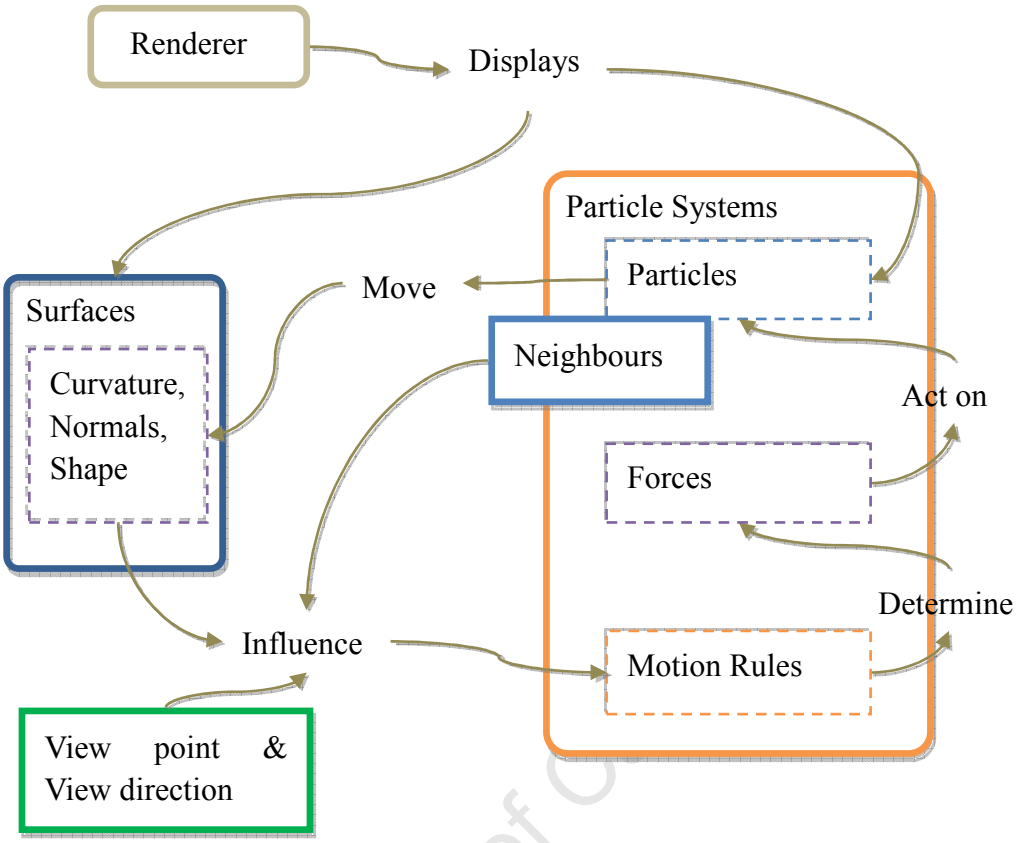

Figure 4.11 Illustration of the architecture of our particle system and visualization design. Particles move over surfaces according to motion rules which determine the forces which move the particles. The forces are influenced by surface shape, view direction and neighbouring particles. Both the particles and the surfaces are rendered to display the layered surfaces.

Particle systems are further adaptable to a diverse range of data formats used for surface representation or which may contain layered surfaces, e.g. volume data sets. In this dissertation, the particle systems developed, as in other work are able to move over (sample) implicit functions [Meyer et al., 2005], volume data sets in the form of voxel grids [Crossno & Angel, 1997] and height fields. In other work, particle systems have been animated over polygon meshes [Lum et al., 2003] and distance fields [Stahl et al., 2002] and are akin to point set surfaces [Alexa et al., 2001].

Within our framework a separate particle system is placed on every layer. The density and distribution of particles over the surfaces is a critical aspect of the design, since a sufficient coverage of the surfaces is required to provide a cohesive impression of the surfaces and spacing between neighbouring particles is necessary to allow see-through views. Determining neighbouring particles and their density for these purposes is achieved through spatial data

structures. Section 4.3.1 describes neighbour computation and determination of empty grid cels. Density, however is dynamic since it is determined by the number of particles on a surface, the surface area, the separation radius and forces between particles and redistribution. Section 4.3.2, explains how the separation forces are computed and redistribution of markings from overcrowded cels to empty ones.

Particle systems may have programmed behaviours. The different motion rules are implemented as such behaviours. These behaviours determine the forces which are applied to the particles, which in turn determine their motions over the surfaces. The force calculations, neighbour updates, velocity updates and movement of the particles are performed in an iterative simulation procedure. The algorithm for the simulation of the particle systems is presented in Algorithm 2 below.

Algorithm 2 Iterative Simulation Step for Particle System

```
Construct a grid for the image space coordinates of every particle
for each particle system
    construct a grid for the particles
    for each particle
      calculate neighbour forces
      calculate occlusion reduction forces
      calculate curvature forces and view dependent shape forces
      sum weighted forces
      update velocity
      update position
      update particle attributes (orientations, repulsion radii etc) for the new position
    end for
end for
```


In each iterative simulation step the particles move over the surfaces according to Newton's laws of motion. While the above algorithm is similar to particle systems which sample surfaces, there is, however, no check to see if the system is at a stable state. The particles simply keep flowing over the surfaces. To find an optimal static layout of markings over the layered surfaces, checks on system energy can be incorporated into the system to cause particles to tend towards equilibrium. For animated illustrations of layered surfaces, a directional following weight, and "flocking" direction following rules cause markings to continuously flow over the surfaces, without reaching a static state of equilibrium. Further, these forces are weighted more heavily than the repulsion force so as to cause the markings to move smoothly and at the same speed as other markings. A further, significant difference from standard sampling of single surfaces is that additional repulsion forces are generated between overlapping particles and particles which are too close to other particles on other layers relative to one another in image space. These forces are

proposed to give an ideal visual layout of samples over multiple layers through taking the view point into consideration. Figure 4.11 shows the various components of the framework described.

The implementation details of the neighbour determination algorithm, the force calculations, including the energy function, and motion and velocity updates are specified below. The various behaviours of the particle system were described in section 4.2, which determine how the particles move over the surfaces and interact with each other and the surface. The rendering and visualization of the particles and surfaces is covered in section 4.4.

4.3.1 Neighbour Computation

It is necessary to find the set of neighbouring particles for each particle in order to determine separation forces so as to achieve a uniform or curvature dependent distribution of markings over a surface. The bin data structure is useful for both computing neighbours and also identifying empty regions of space. Some of the particles in regions which have too many markings, packed too densely, may be translated to empty regions. The bin data structure makes such computation possible in linear time.

Figure 4.12 shows an illustration of a bin, also known as a grid data structure, which is a subdivision of space into bins or cells. Points are indexed into these cells based on their positions. To find a set of neighbouring points for a particle at a certain position, the cell to which the particle belongs is indexed and other markings which have been registered to that bin are tested to see if they are closer than a certain radius. Surrounding cells, for example in 2D, the 8 adjacent surrounding cells, are also typically searched for neighbours. Querying a grid may be accelerated

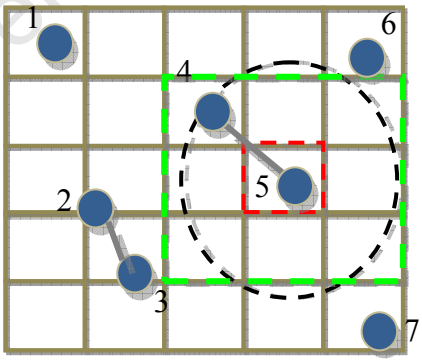

Figure 4.12 Illustration of a bin data structure. Objects are associated with bins based on their spatial position. Bins are useful for finding nearby objects within a fixed radius, without having to search through the complete set of objects which requires quadratic time. In the illustration particle 5 searches for neighbouring particles within a fixed range marked by the black circle by looking up the particles registered to the bins within that radius. Each of these bins is searched and particles within these bins and inside the radius are noted as neighbours.

for computing neighbours within a specified radius when more than the adjacent bins need to be searched through "Query Sphere Indexing" [Brodu, 07], which removes extraneous bins beyond the spherical radius from the search.

A grid may be constructed for a set of n points (particle positions) on a CPU in linear time. Alternatively, a grid can be computed on the GPU by rendering particles to a discrete texture or array. Particles search for their neighbours using shaders, which query neighbouring grid cells [Latta, 2004]. While grids are well suited for creating uniform distributions of particles, they are not ideal for curvature dependent samplings. Bins may be too large in regions of high curvature resulting in multiple particles residing in a single bin. Such cases have the disadvantage, that neighbour calculation within a bin requires quadratic time, since within a bin, the distance for all particles in the bin needs to be calculated with all the other particles in that bin. On the other extreme, low curvature areas may have bins which are too small. This requires superfluous searching and construction of empty bins. Typically bin sizes are adjusted to the largest curvature radius in the particle system [Crossno & Angel, 1997]. Delaunay Triangulation (DT), Quadtrees in 2D or Octrees in 3D are more appropriate structures for curvature based sampling. These are not typically used in dynamic scenes where all the points are in motion. This is because these structures require more time to construct or to maintain than grids and would need to be rebuilt every iteration because of the dynamic nature of the simulation. Grids on the other hand only require linear construction time and also in general require only linear query time. This is advantageous over the other data structures which typically require logarithmic time or quadratic time in the worst case to rebuild or update the data structures and then additional linear or logarithmic time to query the data structures for all the particles [Zachmann & Langetepe, 2002]. If octrees or quadtrees are used, they may be constructed for a curvature dependent sampling of the surfaces once before initialization for a specific surface shape. Since the surfaces do not change, construction needs to be performed only once. The octrees smallest size or depth would however need to be limited depending on the density of the markings. For computing the view separation forces on the other hand, calculation of a grid remains the fastest and simplest approach.

An alternative approach useful for curvature based sampling, is to use a combination of a bin data structure and a neighbour web list as proposed by Crossno and Angel [1997]. The bin data structure computes initial neighbours and in the case where there are less than three neighbours for a particle in the neighbour web, the bins are searched again to identify new neighbouring particles which have come into range. The neighbour lists are maintained for each marking and every iteration a particle's neighbours and neighbour's neighbours are searched to see if these have come into range. A re-triangulation step updates each marking's neighbour list, keeping track of the closest surrounding neighbours for each particle. The approach is useful for curvature based distributions of markings where multiple markings may fill a single bin in high curvature regions.

4.3.2 Force Calculations and Physical Simulation

The density of markings is influenced by applying a repulsion force between particles which are near to one another. The repulsion forces between neighbouring particles are determined by using the energy function proposed by Meyer [2005]. This function achieves a balance between scale invariance and compactness. It has also been shown to homogenously distribute particles across a surface without having to modify multiple parameters for each particle or insert or remove particles. Furthermore, the function is well behaved in that it results in a near hexagonal packing of particles for a broad range of shapes and varying number of particles, without the need for modification. The energy formula is shown below in equation 1.

$$E_{ij}=\cot\left(\frac{|r_{ij}|}{\sigma}\ \frac{\pi}{2}\right)+\frac{|r_{ij}|}{\sigma}\ \frac{\pi}{2}-\frac{\pi}{2} \qquad (1)$$

r_{ij} represents the distance between particle i and j. The free parameter σ defines the farthest distance at which these particles interact and thus determines the density of the particles. However, σ must be large enough that particles interact with a ring of neighbours, which is addressed in standard sampling particle systems by increasing the repulsion radius or inserting more particles. The various forces that are computed include:

(1) occlusion reduction forces (between neighbours in image space),
(2) curvature and view dependent shape forces, and
(3) forces arising between neighbouring particles.

These include the repulsion forces between particles to maintain a covering of the surface and alignment forces which cause markings to move in the same general direction.

These various forces are computed according to the behaviour rules described in section 4.2. Once the forces have been calculated they are projected into the tangent plane of each particle. The distance between particles not only influences the magnitude of the force but also whether forces are activated or not. Separation forces are engaged at close range, while alignment forces are applied at longer ranges. Separation forces are given low weights for KV purposes, since these forces must merely cause markings to drift apart. Strong repulsion forces would result in particles bouncing strongly off one another even in opposite directions to the overarching direction that most of the markings are following across the surface. This is not desirable since this will cause particles to jitter and interfere with the sense of smooth motion necessary for kinetic depth cues.

Individual separation, alignment and cohesion forces are computed between each particle and its neighbours. These forces are then projected back into the particle's local tangent plane. Each particle is steered in the direction of the final combination of these projected forces as illustrated in Figure 4.13. This is done by summing weighted contributions from the various forces in the tangent plane. The weights and radii are adjustable parameters in the system. Equation 2 shows

how **R**, the resultant force is computed.

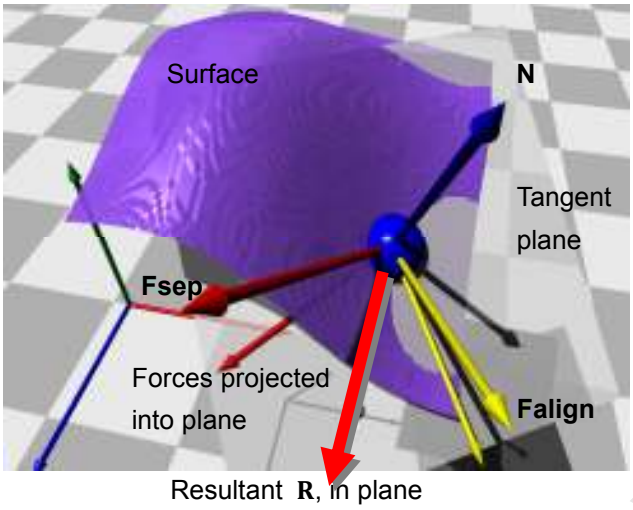

Figure 4.13 Forces are projected back into a particles local frame, tangential to the surface and summed to give **R** the final resultant force acting on the particle.

$$\begin{aligned}\mathbf{R} = {} & \text{wSeparation } \mathbf{FSeparation} + \text{wAlignment } \mathbf{FAlignment} \\ & + \text{wCohesion } \mathbf{FCohesion} + \text{wViewSeparation } \mathbf{FViewSeparation} \\ & + \text{wCurvatureFollowingWeight } \mathbf{FCurvatureDirection} \\ & + \text{wDirection } \mathbf{FDirection}\end{aligned} \tag{2}$$

Causing particles to move in the direction of the overall resultant force, may in many cases not be the best direction to best satisfy the desired motion behaviours, since the resultant force may contradict one or more of the aims of the motion strategies, as the forces work against one another. An alternative approach for computing the best direction would be to move markings in a direction, selected from a range of possible headings, that will most optimally satisfy the different motion rules. This is illustrated in Figure 4.14 below. This rule may result in smoother motions than simply causing markings to follow the resultant force.

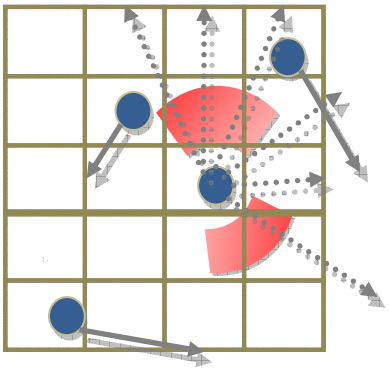

Figure 4.14 A particle chooses a heading from a range of possible directions that will minimize it breaking constraints placed on its motion by the various motion rules and neighbouring particles positions and trajectories.

Once the final force is determined for each marking, it is applied to a particle causing an acceleration of the marking in the direction of that force: a = f / m. This in turn affects the velocity of the particle and its heading: $v_{t+1} = v_t + a\,\Delta t$. The velocity update is then modified based on the behavioural rules implemented (see section 4.2.1), for instance, typically all particles move at the same speed, and therefore the velocity is normalized and multiplied by a fixed velocity magnitude.

Once computed, the velocity is applied to a particle to move it over the surface. The final velocity is used to determine the distance the particle should move and the direction. The total distance the particle has to move is broken into smaller sub-displacements, which are integrated to cause the particle to move a distance equal to the velocity magnitude. In areas of high curvature simply using a single displacement in the direction of the velocity in the tangent plane and then re-projecting the particle onto the surface may introduce inaccuracies in the distance the marking moves or cause markings to move off the surfaces. For each sub-step, the velocity is projected into the local tangent plane at that point. The total displacement is divided into ten sub-steps. A marking moves the length of a sub-displacement in the direction of the velocity projected into the tangent plane of the particle at the current sub-position. The particle is then projected back onto the surface from the new position. The re-projection step accommodates for any deviation of the particle from the surface, keeping the markings flush against the surface. Figure 4.15 shows an illustration of how markings are moved over the surface and projected back onto it.

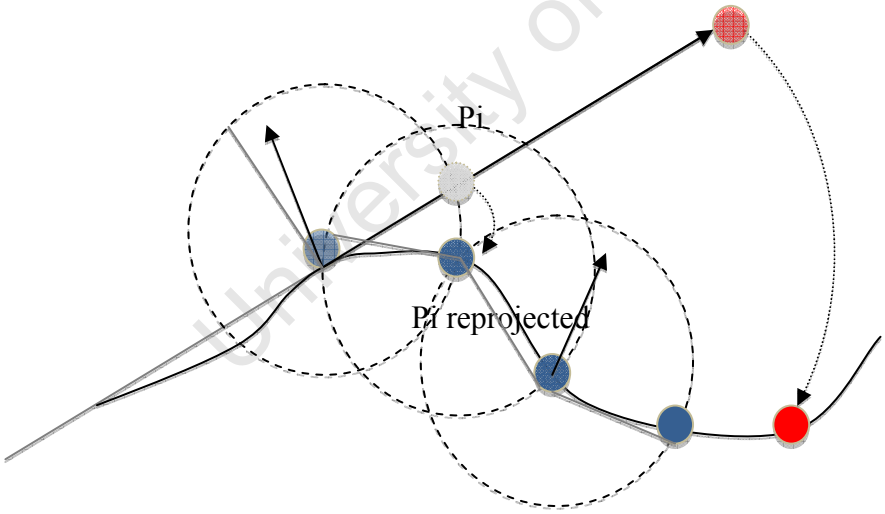

Figure 4.15 An illustration of how a particle is moved and re-projected onto a surface. The total displacement is broken into smaller sub-steps to more accurately estimate the distance travelled over a curved surface through integration rather than taking a single large step and then re-projecting the particle from that point back onto the surface.

Particles are re-projected by using an iterative Newton-Raphson method for surfaces that are defined by implicit functions. Particles are moved in the tangent plane in the direction of the

velocity and re-projected onto the surface along a circle with radius equal to the sub-step size. In this work a maximum of 10 Newton-Raphson iterations were used to keep particles close to the surfaces. If the surfaces are defined implicitly by point sets, then alternatives such as the projection methods of Alexa et al., [2001] may be used rather than the Newton-Raphson method. However, in this work height field surfaces were used for which Newton-Raphson is both appropriate and simple to use. We further experimented with using a Particle Swarm Optimization solver, in the CPU implementation, to find the surface intersection for the re-projection instead of using the Newton-Raphson approach. The PSO approach takes more operations, in terms of comparisons but does not require an implicit function or surface derivative information and is also robust against noise.

4.4 Rendering of the Surfaces and Particles

The visualization design has so far described various motion strategies which are useful for moving opaque markings, represented as particles, over a set of surfaces to illustrate those surfaces. The final component of the visualization design is the rendering module. The visualization of the layered surfaces is realized through rendering the particles and surfaces. The nested surfaces are rendered semi-transparently using blending. The markings are then rendered as opaque glyphs. Different layers are coloured distinctly to help distinguish between the layers. The particles on a surface are given the same colour as that layer to strengthen their association.

4.4.1 Surface Rendering

The surfaces are rendered semi-transparently through alpha blending using Phong illumination [Phong, 1975], i.e. with diffuse shading and specular highlights. Additive blending is used to composite the contributions from the various surfaces together, without the need for sorting them. Alternatively, the primitives (triangles) of the surfaces may be sorted and rendered from back to front [Angel, 2000]. This ensures correct blending of primitives. Such sorting does however not guarantee an artefact free rendering in all cases. Intersecting surfaces may produce pairs of triangles where certain parts of one triangle pass through the other, for which the depth ordering becomes inverted across the faces of the triangles. An alternative to sorting elements from back to front for correct rendering of transparent fragments is to use depth-peeling [Diepstraten et al., 2002]. Depth-peeling depends on the depth complexity and number of primitives in a scene.

The visualization design may rely solely on the opaque markings to visually display the surfaces. This has the advantage that the underlying surfaces do not need to be rendered thus eliminating the need to sort primitives from back to front, or in the case of depth peeling render the scene multiple times. Figure 4.16 illustrates side by side two visualizations with (left) and without (right) the underlying transparent surfaces being rendered. Having observed several visualizations, however, we find that the transparency as shown in this illustration, does

contribute a sense of wholeness and continuity to the surfaces and for oblique views of height field terrains clearly conveys regions of the surfaces, revealing silhouette edges.

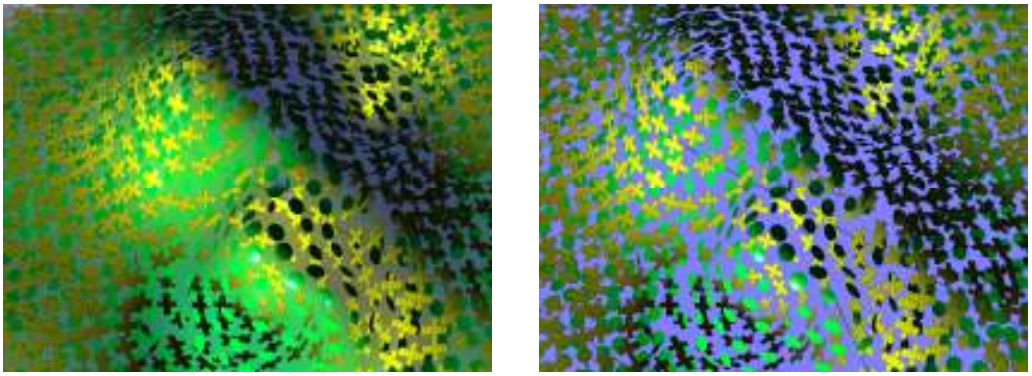

Figure 4.16 Visualizations with (left) and without (right) a semi-transparent rendering of two underlying surfaces (background in light blue). Representing surfaces with patches only and no semi-transparent rendering of the surfaces is useful for the display of intersecting surfaces as it eliminates the need for surface refactoring. It is also useful for real time rendering of layered surfaces since it does not require triangle depth sorting or depth-peeling. Such renderings, however, lose the additional shape cues and sense of continuity conveyed by the semi-transparent rendering.

In Figure 4.16, there is a significant contrast between some of the well light markings and the dark markings, upon which light doesn't fall directly. This makes it difficult to differentiate between markings on the basis of colour and obscures the variation in shading across markings, impeding the effectiveness of the shape-from-shading depth cue. In the future a more complex lighting setup may be used to improve visibility to address these issues.

The technique becomes a type of cut-away geometry in the case where the underlying surface is not rendered. This case is nonetheless effective when there are a sufficient number of markings spread over the surfaces and where the markings illustrate enough surface shading to convey the shape. Animation is useful when the underlying surface is not rendered, since it helps to vary the samples over the surfaces. This helps to overcome the problem static cut-away views incur of leaving out some of the geometry. The transparency or alpha value for each surface is set to a fraction of the number of layers, e.g. four layers, relative to the viewer, from furthest to closest are rendered with alpha values of 0.8, 0.6, 0.4, 0.2 respectively. This was done so that the surfaces further away from the viewer could be discerned through the layers closer to the viewer. Viewers are likely to assume constant opacity for the different surfaces and across surfaces. Since opacity is constant across each surface, the surfaces are interpreted as being continuous (this was the case in experiment two Alternating Rocking and KV). In the case of intersecting surfaces, when the alpha values are set differently based on depth ordering, surface refactoring is essential to apply the correct alpha value to the different regions of the surfaces. Surface refactoring was not implemented in this work, since nested surfaces were primarily used.

An advantage of the technique is that, if the surfaces are rendered with the same transparency values, the approach may be used for intersecting surfaces without requiring the additional computation needed for surface refactoring. Figure 4.14 also illustrates how nested surfaces may be displayed without the need for surface refactoring. Surface refactoring is typically computed using either image-based or geometry-based methods. Geometry based algorithms which classify regions of surfaces as being interior or exterior are typically used for non-interactive display of surfaces that require computation of spatial data structures and multiple triangle intersections. Image-based algorithms may be used for interactive scenes, for which the view dependent depth complexity is low enough and there are not too many primitives [Weigle, 2006].

Distinct hues are used to help differentiate between the surfaces and markings. The major primary colours blue, red, green and yellow are used to display up to four layers. In addition, using the colours magenta, indigo, violet and orange are useful to display and distinguish more than four surfaces. These colours have been shown to be perceptually distinct [Healey, 1996], being well separated on the HVS colour scale. However, when more than four layers are displayed lighting and shading can easily confuse the colours, e.g. shaded orange and red are easily mistaken for each other. Isoluminant colours should be used. An isoluminant colour scale has a single fixed luminance throughout the scale. Isoluminant colours are used by Weigle [2006] so that lighting in their visualizations do not interfere with the perception of surface shape. DDS is able to display up to 9 layers, using colour alone to differentiate between layers but does not use shading and lighting. The colours in DDS are distinct apart from blending and need only convey a value rather than surface orientation. Shading and lighting make it more difficult to distinguish between colours because of a reduction in contrast. Applying lighting and shading has the same effect as decreasing lightness and saturation of a colour in HSV space.

Bair and House [2007] show that texture markings and stylistic aspects of texture other than colour are more useful than colour for allowing a person to distinguish between markings on two layers. This dissertation does however, not consider the various stylistic aspects of markings for helping participants distinguish between layers, but rather the use of animation. The glyph types used for the markings on different layers, however, may be distinct. A combination of colour, stylistic aspects and animation are likely to be most useful for helping participants to distinguish between up to four layers, and is left for future work.

4.4.2 Particle Rendering

The opaque markings rendered on the surface play a critical role in conveying local surface shape and provide the additional 3D surface information which is lost due to blending. In Figure 4.17 the development of various types of illustrations of particles for displaying layered surfaces is shown. Early prototypes used non shaded points. The problems of these points not illustrating local shape were addressed by using disks. In the third figure, edge and silhouette particles were

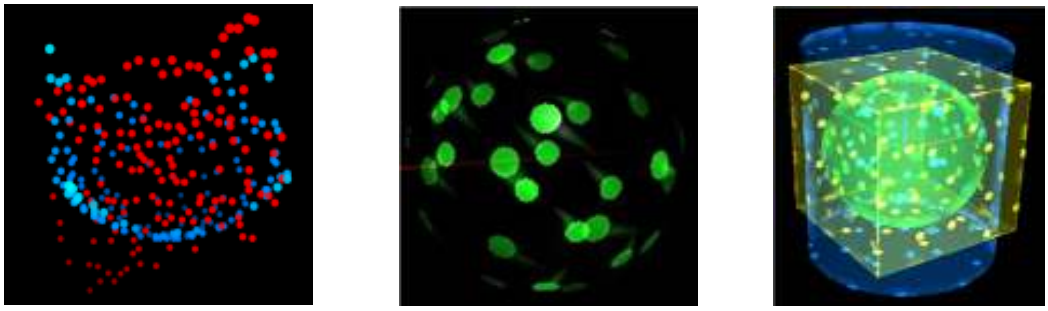

Figure 4.17 Illustrations of various types of markings which illustrate layered surfaces: *(left)* illustration of a plane and parabaloid through points; *(center)*: sphere illustrated through disks and motion blur/particle traces; *(right)* silhouette and contour particles help to illustrate the shapes.

used to help show the shape and features.

Interante [1996] points out that use of silhouette type markings are not necessarily beneficial for smooth surfaces viewed monocularly since these markings can collapse the sense of 3D depth. This is because silhouettes on smoothly curving surfaces result in two separated silhouettes that should be seen in different places for which the human visual system seeks to establish correspondences, but since these are viewed monocularly it only finds a single line. Rendering silhouette particles, may however, be effective in stereo and not collapse depth provided the 3D location of each rendered silhouette particle corresponds correctly in both the left and right eye views, since this would replicate the way people see silhouette features in real life.

As this work progressed it was realized that the markings need to be opaque or near to opaque to effectively convey 3D surface information since opaqueness provides the depth cue of occlusion. The markings need to convey local surface shape and orientation through shading and texture cues. In terms of implementation, each particle in the different particle systems is rendered as an opaque marking. Three different types of markings were used in this work to represent the particles and local surface: cross type line-glyphs [Weigle, 2006], disks and small surfaces patches. See Figure 4.18. Each particle needs to convey enough surface information to allow a viewer to perceptually combine the markings into a coherent surface in the midst of interference.

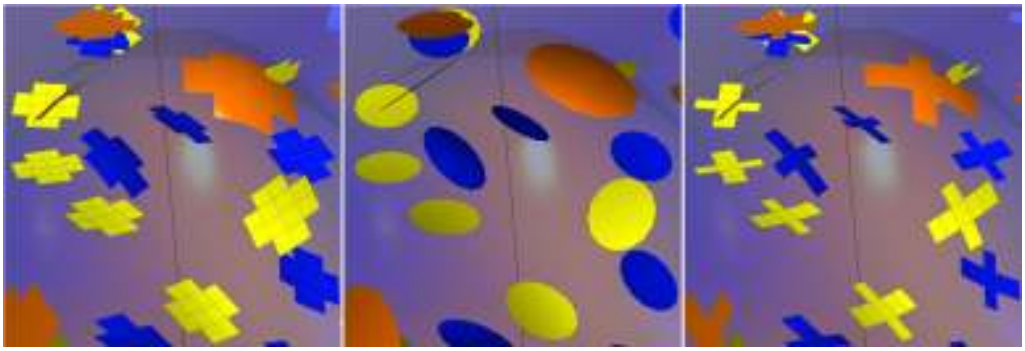

Figure 4.18 Different types of opaque markings are used to represent the surfaces, from left to right: patches, disks and crosses with their longest axis aligned with the first principal curvature direction are illustrated.

Principal curvature crosses are less occlusive compared to surface disks and patches. These crosses allow viewers to see more clearly into lower layers. However, it appears from the outcome of experiment two that the orientation of a layer is better conveyed by increasing the surface-area of markings. From user reactions to the layered surface display and experimental analysis, patches seem to illustrate the surfaces more smoothly and aesthetically.

In some of our early prototypes, Gaussian spots were experimented with and were seen to blur the shading from different layers. Completely opaque surface patches were therefore selected over Gaussians. Figure 4.19 shows a side-by-side comparison of patches compared to Gaussian spots.

The size of the markings is adjustable through the user interface. The stylistic attribute of marking size was not specifically experimented with, to find the best size of the markings. However, the size of markings certainly plays a significant role. Markings with larger surface areas occlude more of the layers behind them, while if the markings are too small, they do not convey sufficient surface shading and information and are also more easily missed or may be more easily confused as belonging to the wrong layer. The perceptual framework presented in chapter 7, presents a means of automatically estimating how large markings should be on the various layers

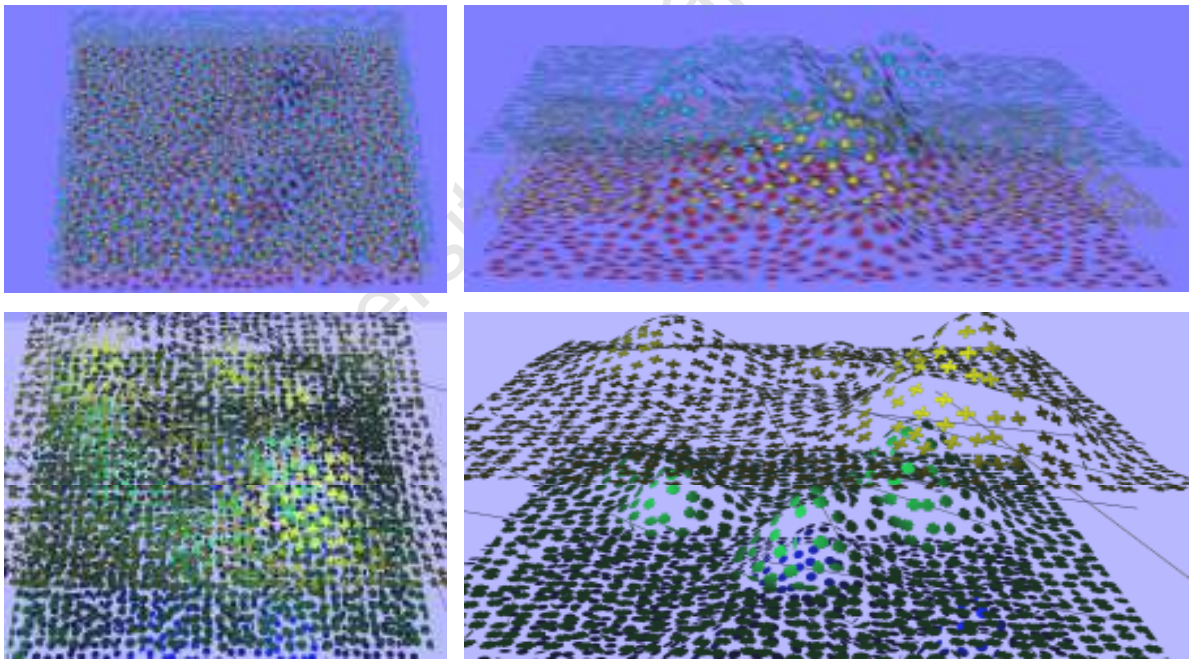

Figure 4.19 Side by side comparison of patches and Gaussian spots (DDS). Top three layered surfaces illustrated with Gaussian spots. Bottom figures illustrated with different types of markings.

.

4.4.3 Additional Visual Aids Incorporated into the Design

In addition to rendering the surface patches and the surfaces, particle traces, normal glyphs and point correspondence glyphs could be used to help convey various features of the surfaces. The current framework is only implemented for particle traces and normal glyphs.

Particle traces illustrate the surfaces giving a motion blur effect. Drawing traces is similar to Line Integral Convolution (LIC) approaches to rendering opaque markings on layered surfaces

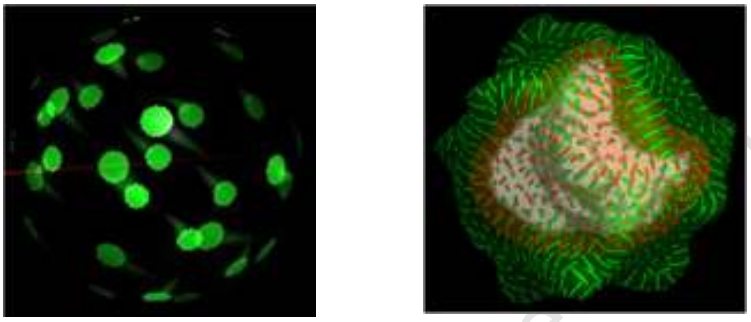

Figure 4.20 Particle traces help to illustrate a surface. *Left*: A sphere with disk particles and particle traces; *Right*: Interrante's original LIC for layered surfaces.

[Interrante, 1997]. Figure 4.20 shows particles on a sphere illustrating motion blur.

Motion blur gives the impression of moving objects and is used in this dissertation to help illustrate motion in the figures. Motion blur or particle traces have the advantage of illustrating the direction in which particles are moving, which in turn is helpful for distinguishing between the markings on different layers; the motion blur tails of markings illustrate the direction the particles are moving in. Markings moving with different motion patterns on the disparate layers result in distinct motion blur trails which like "Textons", in addition to colour and direction of motion, help a person to distinguish between the markings on different layers and group those on the same layer. The disadvantage of using Motion blur is that it extends the surface area of markings on the surfaces, thus causing them to occlude more of the interior regions.

Renderings of surface normals can also be used to illustrate surface orientation. Such renderings give the impression of surfaces covered with small blades of grass or mountains with trees. See Figure 4.21.

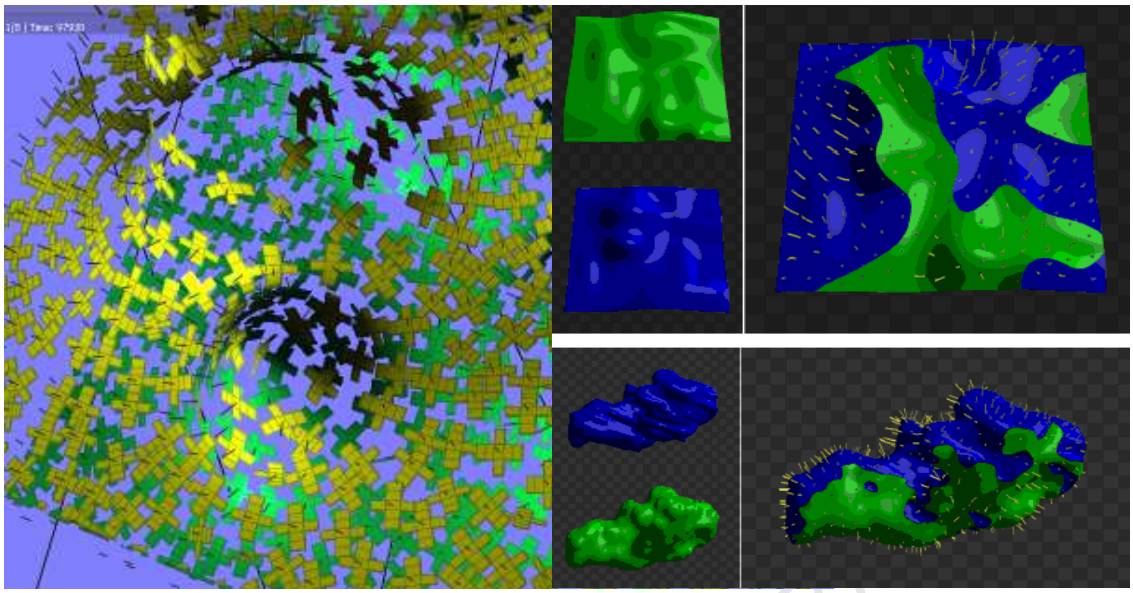

Figure 4.21 Local surface orientation illustrated with surface normals or point-correspondence glyphs [Weigle, 06].

For tasks in which visualization users are required to estimate orientations, renderings of the normals may help them to better gauge local surface orientation. Rendering only the normal glyphs without the surface patches is a means of reducing the surface area of the opaque markings, allowing a viewer to see more clearly into the interior layers. A viewer may vary the size of the patches shown, and the lengths of the normals. The length of the normals can also be automatically varied to best convey the surfaces by mapping it to the inverse surface curvature. This results in long orientation markers in regions of high curvature and smaller markings in other regions. Furthermore, curvature dependent samplings, may naturally produce a suitable sparseness of the markings. Rendering surface normals as line segments, perhaps visually more effectively as cylinders, does not convey clearly the surface orientation though. This is because the renderings have to be very small and leave much ambiguity.

Point correspondence glyphs as detailed in section 3.1.3.4 are useful for showing distances between layered surfaces as well as local surface orientation. An alternative to rendering point correspondence glyphs to increase visibility would be to animate particles between corresponding points on adjacent surfaces.

4.5 Final Implementation Details

Several prototypes of animated particles flowing over surfaces were developed during the course of this study. Iteratively the particle systems were advanced from CPU-based implementations to faster GPU-based ones and renderings improved from point rendering to shaded patches. In

experiment one, section 5.1 a CPU particle system was used to illustrate the surfaces with 1600 particles moving over a height field surface at 22 fps. This particle system was upgraded to the GPU, which is able to simulate the motion of up to 8000 particles at 30 fps over height fields. GPU particle systems, however, are extensible to simulating hundreds of thousands of particles at interactive frame rates [Latta, 2004].

The GPU particle system uses textures to store the position, velocity, force and other particle values and surface data, including curvatures, surface normals and surface heights. Each texel in the various particle textures corresponds to a single particle's data, position, velocity etc. In the implementation each particle system is assigned its own separate position, velocity and force texture. Various fragment shaders are used to update these textures. Textures are updated by rendering a quadrilateral with the same dimensions as the texture in an orthographic projection. This causes the GPU to instantiate fragment shaders for each particle. The fragment shaders perform the various force, velocity and motion updates in parallel. The GPU particle system implemented is based on the particle systems described in Mega Particle Systems [Latta, 2004].

Computing curvatures accurately is essential for obtaining both curvature dependent samplings, orienting markings on the surfaces, and moving particles along the first principal curvature directions. Working with height fields, we compute curvatures using the second fundamental form, which we derive using central differences [Interrante, 1997]. For other discrete surface representations such as meshes, curvatures may be estimated by using differential geometry or fitting a quadratic surface or higher order surface patch through the normals of a set of vertices in some neighbourhood [Goldfeather & Interrante, 2004]. Third order approximations are desirable since these are more accurate. Neighbourhoods should preferably be larger than a vertex and its adjacent vertices. Normals at vertices are computed using weighted sums of the normals on adjacent triangles. Sharp edges or irregular meshes, however may nevertheless cause significant errors.

The GPU particle system was developed on an NVIDIA GeForce 9800 GTX graphic card. The visualization design was implemented using OpenGL, C++, GLSL and Qt.

This chapter has described an approach for implementing particle systems, which, through various motion rules and rendering choices, are useful for illustrating multiple layered surfaces. The next chapter describes an evaluation of this particle system framework in comparison to pendulum-style rocking.

Chapter 5

Evaluation of the Proposed Design

The visualization design presented in Chapter 4 uses Kinetic Visualization as a means of supplementing opaque marking-based layered surface display techniques. This novel use of Kinetic Visualization to more effectively display layered surfaces needs to be evaluated in the first instance against *pendulum-style rocking*, which is the standard and most effective animation technique used for augmenting layered surface displays. Rocking enhances shape perception through rigid body rotations which induce the Kinetic Depth Effect, one of the most powerful depth cues. Further, these rotations contribute to a comprehensive understanding of surface shape by showing varying views of the surfaces from slightly different angles. Since rocking is such an effective means of supplementing layered surface display techniques, and further trivially implemented, it is necessary to prove the value of Kinetic Visualization (KV) in contrast with rocking; it must be shown that KV is either better than rocking for some tasks or that it contributes something in addition to rocking before incorporating it into a display technique.

This chapter describes two novel psychophysical experiments that were performed to ascertain if KV does make such a contribution. Experiment one, "KV vs. rocking", was performed to compare KV to pendulum-style rocking. Prior experiments performed by Lum et al. [2003] have shown that KV significantly contributes shape cues, which lead to better surface perception of shaded objects. Results from experiment one seem to give strong indication that these depth cues are likely not the same as those arising from rocking, namely the powerful Kinetic Depth Effect. This implies that KV may be useful in combination with rocking. Experiment two, "Alternating Rocking and KV", was then performed to determine if a combination of rocking and KV would be more useful than rocking on its own.

5.1 Experiment One KV vs. Rocking

An enhanced sense of 3D depth and surface shape is achieved in visualizations through pendulum-style rocking. This animation technique through simple rotations of surfaces around one or more axes contributes the powerful depth cue of the Kinetic Depth Effect (KDE). Before using animation in the form of Kinetic Visualization for the display of layered surfaces it is necessary to establish whether or not KV is comparable to rocking. The following questions arise:

(1) Why use Kinetic Visualization when rocking is simple to implement and likely more effectively enhances shape?
(2) If rocking enhances shape through the Kinetic Depth Effect and is more effective than KV, then what shape or depth cues are then induced by "Kinetic Visualization"?

Experiment one, "KV vs. Rocking", has been set up to compare KV with rocking and static renderings for various shape tasks to investigate these questions.

5.1.1 Experimental Setup

In this psychophysical experiment a sample consisting of twenty-three respondents with either normal or normal corrected vision was used, twenty postgraduates, three undergraduates, ten women – one of whom rarely uses a computer. Height field surfaces consisting of Gaussian bumps were used in these experiments, as they are representative of generic surfaces with standard shape features, e.g. saddles, valleys and peaks [Weigle, 2006]. Similar surfaces have been used by other researchers for layered surface experiments [Lum et al., 2003] [Weigle, 2006] [Bair & House, 2007]. This experiment uses similar surfaces and tasks to previous layered surface experiments since these are accepted and form a foundation upon which other layered surface techniques can build.

The independent variable in this experiment was the animation technique. Surfaces were shown to the respondents augmented with either:

(1) static renderings of disks distributed uniformly over a surface (this served as a control, against which the other techniques could be compared),
(2) moving opaque disks which flow over the surface, or
(3) a pendulum-style rocking animation of the static approach.

In this experiment, a classic implementation of Kinetic Visualization was used: disks flowed over the surface primarily in the direction of principal curvature closest to a specified heading. A flocking alignment rule was applied to cause markings to locally flow in similar directions [Reynolds, 87]. Separation and density rules were used to cause the markings to spread out over the surface. For pendulum-style rocking the surface(s) were rotated by 15 degrees around the three axes in a figure 8 motion. The motion lasted for 10 seconds. Participants were able to start and stop both the rocking and KV animation at will.

5.1.2 Surfaces, Lighting and Viewing Conditions

The surfaces used in the experiments were height fields consisting of eight random Gaussian bumps combined with surface noise on a 100x100 grid. Gaussians were allowed to overlap. The noise consisted of random Gaussians which were at most one third of the minimum size of the bumps. Figure 5.1 shows examples of surfaces used in experiment one.

Figure 5.1 Examples of the surfaces used in experiment one. Surfaces consisted of summations of eight Gaussian bumps and random noise one third the size of the smallest bump, similar to surfaces used in intersecting surface experiments performed by Weigle [2006].

Each surface was viewed using perspective projection from a 45° vantage point (rotation about the x-axis). Smooth Phong shading was used. Surfaces were lit by a directional light source from above the surface and to the right of the viewer (1, 1, -1). These lighting settings mirror settings from typical surface experiments, resulting in shading of the surfaces which illustrates the surface features [Weigle, 2006] [Sweet & Ware, 2004]. Opaque disks were uniformly distributed over the surface and provided the visibly significant surface shape information. The diffusely shaded surfaces were rendered extremely faintly (semi-transparently, alpa=0.1). This reflects the contribution of shape cues arising from renderings of semi-transparent layers in multi-layered surface displays. The semi-transparent surfaces convey minimal shape information. It is the opaque markings that play the significant role in illustrating surface shape. This is also important since it minimizes the depth and surface cues that come from the semi-transparent surfaces, allowing the results to reflect the shape information provided by the different techniques (rocking, KV, or static disks).

The surfaces were viewed monocularly at a full screen resolution of 1280 by 768 pixels with a viewport of 70cm by 27cm on a 22 inch monitor. The respondents were seated approximately 60cm from the monitor (eye distance), yielding approximately a 21 degree horizontal and 13 degree vertical visual angle subtended with the viewport. The grid units of the surface were approximately 3.5mm by 3.5mm at the center of the perspective view. The particle disks had a

diameter of approximately 3.5mm. These settings are not unlike those typically used in layered surface experiments. 1600 particles were placed on the upper surface, which seemed to show the surface clearly and still allow one to see through the space between the particles.

5.1.3 Tasks

Respondents had to complete three different shape tasks to determine if there were certain tasks for which one of the techniques performed better than the others. The tasks reflected common shape questions, and were based upon Weigle's layered surface research [Weigle, 2006]. Seven responses were gathered for each task per person for each of the three techniques, yielding 161 responses for each animation technique. Before performing a task, participants were trained on three surfaces (one surface per technique) to limit learning effects and properly introduce the tasks. The respondents were each shown a different set of 21 random surfaces (each participant saw their own set of random surfaces) for each task, 7 sets of surfaces for each visualization technique. The order of presentation was counter-balanced between the observers. At the end of the each task the participants took a break, stretched and were given a questionnaire to complete. An example of the questionnaires is provided in Appendix A. The experiment, completing the three tasks, took per participant, approximately an hour.

The orientation task required responses for only a single surface. The global shape task and the distance task required judgements to be made in the presence of two layers. This is because this experiment seeks to pioneer the use of KV for layered surface displays; an essential aspect of this exploration is that the layered surfaces need to be semi-transparent rather than opaque, to allow the interior layered surfaces to be seen. This means that the renderings of the surfaces can not be relied on to convey the shape of the surfaces. Rather the opaque markings moving over the surfaces need to illustrate the shape. Hence, this experiment is novel in that it explores the ability of KV to illustrate a surface on its own, rather than simply augment a well shaded opaque rendering of a surface. The experiment is also setup to answer questions regarding effectiveness of KV to illustrate shape in comparison to rocking, which does not necessarily require that the interior layers be illustrated with KV.

5.1.3.1. Global Shape Task

In the global shape task, participants were required to match a surface displayed using one of the three techniques to one of five different pictures of similar terrains. The height field surface was rendered semi-transparently and overlaid with opaque disks. A second random surface with valleys was rendered opaquely in gold underneath, see Figure 5.3. This bottom surface was used to make identification of the top surface more difficult. It also served as a precursor to layered surface experiments, thus helping to indicate whether or not motion helps distinguish between layers.

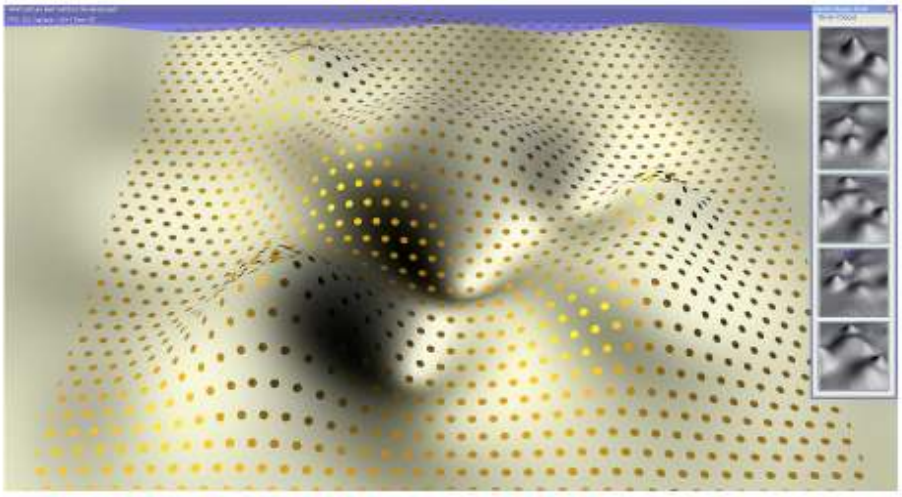

Figure 5.3 In the global shape task a surface was illustrated with opaque markings. Behind this surface, the viewer would see an opaque well-shaded surface. To the right, five pictures, one of the top surface and four variations of that surface were displayed. The task required selecting the picture that matched the surface displayed with the opaque markings, in this case the bottom of the five thumbnail images.

The top surface was rotated by 30° around the vertical axis relative to the frontal vantage point of the 5 surfaces against which it is to be compared. This is done to make the matching less obvious. Such profile to frontal view comparisons have been performed for other global shape matching tasks [Langer & Bülthoff, 2000]. Five pictures of similar surfaces were displayed next to the two overlapping surfaces. Four of the pictures showed variations of the surface to be matched. These variations were generated by modifying the height, fall-off and shifts of the Gaussians used to create the original surface. The magnitude of the variations was by 16, 33, 50 and 67 percent. In all cases the participants verified that the five pictures were distinct. The original surface and four variations thereof were displayed to the viewer to decrease the probability of observers guessing the right surface. The global shape task used by Weigle [2006] required respondents to guess if surfaces matched one of the shapes of 6 fruit. Figure 5.2 shows an example set of the variations of the surfaces.

Figure 5.2 In the global shape task, a picture of a target surface was placed amongst four variations of the original surface. The surfaces consisted of a summation of Gaussian bumps. Variations were created by distorting the height, fall-offs and centers of the Gaussians used to create the target surface.

Participants were instructed to: “Find the picture which most closely matches the shape drawn in the main window.” The dependent variable for this task was the number of correctly matched surfaces, which it was expected would be influenced by the visualization technique. Other factors of influence could include the surfaces generated and variation between the five choices and the participant.

5.1.3.2. Distance Task

A distance task similar to the forced choice distance task performed by Weigle [2006] was used to verify how well depth judgements could be made between surfaces using the different techniques. As in the global shape task, two different surfaces were rendered but with the difference that a grid was placed on the bottom surface to help make it more distinct. Two unbiased cross markers were displayed on the bottom surface at random positions but at the same orthogonal depth (z-distance) from the camera to reduce effects from perspective projection. Because of the random placement of markers we assume no bias due to placement. An example of the display is illustrated in Figure 5.4. Participants were asked to select from these two points the one where the upper surface had the smaller vertical separation: “Estimate the distance between the two surfaces at these point (the vertical distance the gold surface is above the grey surface)! Make a judgement on which vertical distance is the shortest – i.e. for which of the two points are the two surfaces closer together?” The number of incorrect responses was expected to depend on the distance between the surfaces and the approach used.

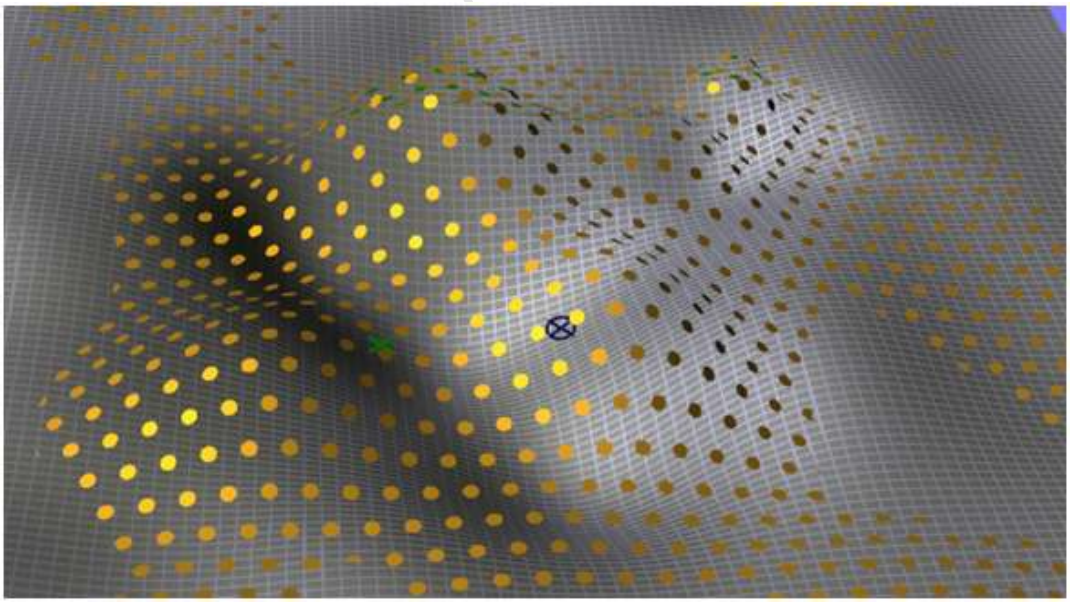

Figure 5.4 A forced choice distance task was used to obtain depth estimates to compare the effectiveness of the techniques. Two layered surfaces were displayed. The layer furthest from the viewer was rendered opaquely with a grid, the other surface was shown using opaque markings. Two unbiased cross markers were displayed on the layer farthest from the viewer. The task entailed selecting (circling) the marker with the smallest vertical separation from the layer closest to the viewer.

5.1.3.3. Orientation Task

A typical steering-wheel style orientation marker, as illustrated in Figure 5.5, was employed in a surface orientation estimation task. In this task the participants were asked to place this marker, for which the orientation was fixed, at a point on the surface where the surface has the same orientation as the marker. At such a point the pin of the marker would be aligned the surface normal and the tangent plane would be parallel to the torus of the marker. The region within which such an orientation should be searched for was bounded by a ring of dots. Respondents were instructed to: "Find the point on the surface within the ring, with the same orientation as that of the orientation marker."

This is different from typical orientation marker tasks which require participants to orient a marker to reflect the orientation at a fixed point; a task which is difficult to perform [Sweet & Ware, 2004]. To simplify and reduce effort in interacting with a marker, participants could simply point and click to place the marker. Participants would survey a surface to find a point where the orientation was most similar to the marker. To help the users focus on a particular part of the terrain, the marker was placed within a limited fixed area marked out by a ring of dots. The marker was also hidden during rocking to reduce the advantage of perspective views of the marker. Error in degrees, computed by finding the difference between the orientation at the final surface point and the orientation of the marker, was used as the dependent variable.

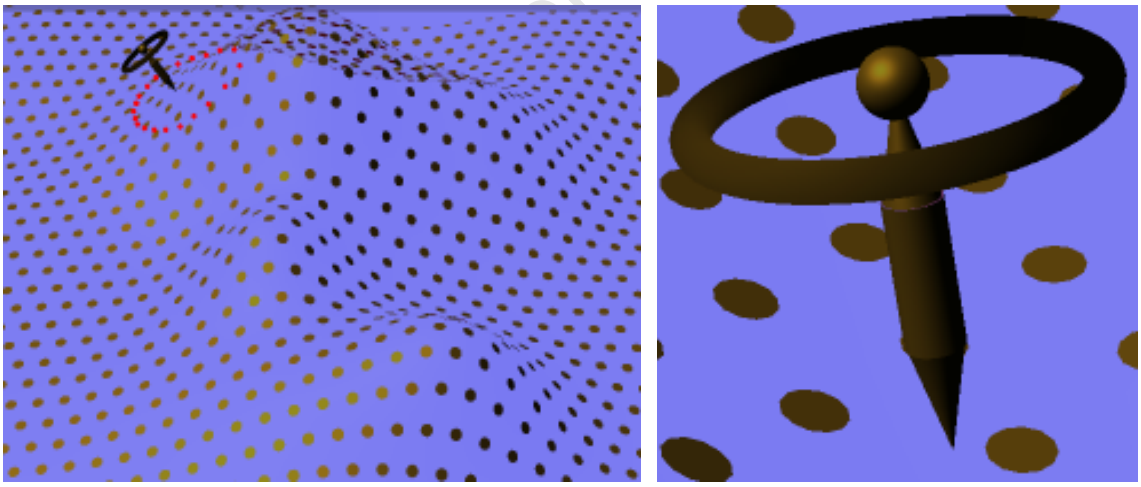

Figure 5.5 In the orientation task, a marker with a static fixed orientation was presented within a region of the surface demarcated by a ring of dots. Respondents were requested to find a point on the surface with the same orientation as the marker. An enlarged image of the marker is shown in the top right corner.

5.1.4 Results of Experiment One

5.1.4.1. Global Shape Task Results

The average errors (the number of wrongly matched surfaces) and average response times by technique for the global shape task experiment are presented in Table 5.1. Rocking on average had the lowest number of errors. Average error rates (number of surfaces incorrectly matched) between the visualization technique (still, rocking and KV), were analysed with a one-way between subject factor analysis of variance (ANOVA), measuring the effects of the visualization technique. ANOVA indicates that there was no significant difference between techniques, since $p<0.584$ with $F(2,66) = 0.548$.

	Still	Rocking	KV
Mean Error	2.39	2.0	2.43
Standard Deviation of Error	0.84	0.83	0.89
Average Time (seconds)	46.0s	43.8s	46.6s
Standard Deviation of Time	23.5s	24.5s	23.9s

Table 5.1 Global shape task, average error (number of surfaces incorrectly matched)

5.1.4.2. Orientation Task

Table 5.2 shows the results from the orientation task, including average error in degrees, standard deviations, average time participants used to complete the task and an indicator of how much concentration was required by participants for each of the techniques.

	Still	Rocking	KV
Mean Error	13.732	13.574	14.757
Standard Deviation	11.355	10.375	12.512
Average Time per Surface	42.3s	49.2s	51.5s
Standard Deviation for Time per Surface	27.5s	24.1s	27.7s
Concentration Required	2.9	3.8	3.1
Standard Deviation for Concentration	1.2	1.0	1.2

Table 5.2 Orientation task, average error (in degrees)

The results indicate that renderings with rocking produce slightly less error than the other techniques. However, a one-way between subjects analysis of variance (ANOVA) of the error in degrees for the visualization technique (still, rocking and KV) was used to measure the effects of the visualization technique. ANOVA indicates that there was no significant difference between techniques, since $p<0.7054$ with $F(2,66)=0.351$. This agrees with observations made during experiments: participants would stop rocking or KV (animation) and attempt to match the

orientation of the probe with the closest stationary disk. Table 5.2 shows mean participant concentration, which was ranked by the respondents on a Likert scale from 0 to 5, with 0 indicating least amount of concentration required and 5 indicating most concentration. Three participants noted that the moving disks were distracting.

Participants stated that it was easier to match up the marker with the static disks, commenting that hiding the marker when rocking was unhelpful and that rocking disrupted estimation of the orientation. The experimental design choice to hide the marker during rocking however had to be made to maintain the integrity and fairness of the task. In any case rocking could only have resulted in more accurate orientation estimates than KV and static renderings, but certainly no worse. The orientation task and global shape task required significant concentration and were at a saturation level in terms of number of questions asked. Respondents commented that they were losing concentration towards the end of these tasks, noting that the distance task was the least tiring.

5.1.4.3. Distance Task

Figure 5.6 shows the mean errors for the distance task with standard deviations. A one-way between subject factor analysis of variance (ANOVA) of the depth error was used to analyse the effects of the visualization technique (still, rocking, moving). This showed a statistically significant difference for the visualization technique ($p < 0.0396$). Further, Tukey's Honestly Separable Difference (HSD) test reveals that it is rocking that is statistically better than Still (<0.0204) and KV ($p<0.0291$), and that KV and Still are not separable ($p<1.0$). One-way between factor ANOVA of the visualization technique scaled by the height difference gives $p < 0.0018$. We scaled height differences to lie in the range [0;1] and used these to weight the errors. This was done in order to evaluate the mistakes in terms of distance differences. Table 5.3 shows the results for the distance task and time that participants spent on average per surface.

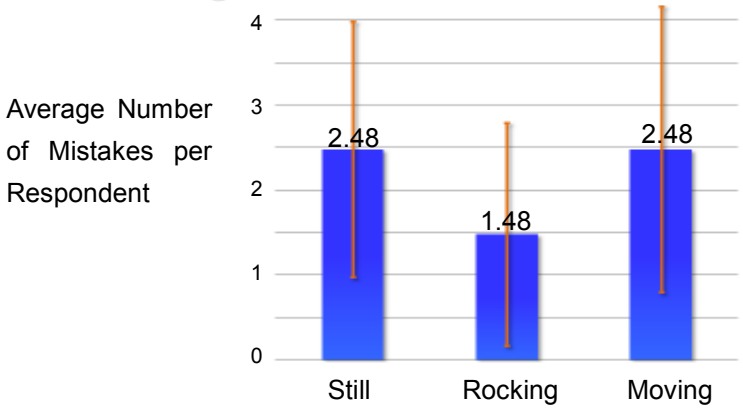

Figure 5.6 Mean errors and standard deviations for the distance task.

	Still	Rocking	KV
Mean Error	2.48	1.48	2.48
Standard Deviation for Error	1.5	1.31	1.68
Weighted Mean Error	0.16	0.09	0.18
Standard Deviation for Weighted Error	0.27	0.2	0.29
Avg Time per Surface	22.8s	23.1s	23.0s
Standard Deviation for Time	16.2s	17.0s	14.9s

Table 5.3 Distance task, average error (number of incorrect shortest distance estimates)

Even with the additional time required to rock the surfaces, respondents completed the task in the same amount of time as with static and moving points, but with greater accuracy. Further considering that each respondent encountered 7 stimuli per condition per technique, we checked to see if participants performed at chance for rocking. Of the 23 respondents only 2 of the 23 respondents performed worse than chance, the rest all made fewer errors than chance.

5.1.4.4. Depth vs. Contour Results

In the questionnaire respondents were asked to indicate "compared to rocking how much a sense of: 1. depth and 2. contour did KV provide?" The question was further explained and clarified to the participants. Participants after explanation of the question confirmed that rocking gave a better sense of the surfaces appearing 3D than KV, that is KV gave a better sense of depth. Indeed, all of the respondents indicated that rocking gave a sense of the surface jumping out into 3D. They stated that this was not the case with KV. In response to the second part of the question, they did however feel that KV better revealed the curvature of the surfaces. Table 5.4 reports these results, i.e. the sense of depth and curvature that the respondents felt was conveyed by KV in comparison to rocking.

	Depth	Contour
Mean	3.3	4.3
Standard Deviation	1.0	0.5

Table 5.4 Average participants responses as to how much a sense of depth and contour KV conveyed in comparison with rocking on a scale of [0 - none; 5 – equivalent to rocking].

Participant responses were captured on a Likert scale from 0 to 5, with 0 indicating least and 5 indicating most (in case of depth, participants were told that 5 is equivalent to rocking). A two tailed t-test of the participants' responses showed that KV gave a significantly greater impression of contour than depth ($p < 0.0001$). This agrees with the distance results in which participants made more accurate depth judgements with rocking than KV. Further, KV did not convey as great a percept of depth as did rocking.

5.1.5 Discussion

KV did not contribute to an oblique, 45° view compared to static disks. Interestingly, experiments by Lum et al [2003] show that KV does contribute to enhancing shape perception, from a top down view. Difference in view direction has been shown to significantly influence shape perception [Sweet & Ware, 2004] and it appears to be part of the reason for this discrepancy. Further significant differences between Lum et al's.[2003] experiments and this novel experiment are that in this experiment the underlying surfaces were rendered almost completely transparently. Particles were also caused to move in a dominant direction and follow principal curvatures in that direction. The difference in results between this experiment and Lum's in which observers had to identify the minimum and maximum peaks from above, could be closely linked to the particles motion for the task. Particles moving over higher sharper peaks could have exhibited conspicuous motion behaviour linked to the height of the peaks, e.g. particles could have had the longest life times on the highest peaks or smallest orbits on the sharpest peaks. Observers looking for points with distinct motions could then have identified the correct peaks. This would be consistent with our findings in experiment two in, which KV conveys shape from particles following contours.

The results for these tasks show that KV did not contribute more shape information than static renderings or renderings augmented with rocking. The goal of experiment one was to determine if KV is comparable to Rocking for a single outer semi-transparent surface with opaque markings. Results showed that it is not, and that it is better to use rocking than KV to augment such visualizations, since rocking resulted in more accurate depth judgements. The results indicate that since there is no benefit to using KV, one should rather use a static display. Future experiments may resolve if Rocking is better than KV for orientation tasks; the orientation sub-experiment shows rocking is certainly no worse, but a study of rocking is not the main line of our research.

The experiment further contributes knowledge about the shape cues arising from Kinetic Visualization, by showing which cues it is does not induce. Consider that rocking resulted in significantly more accurate depth judgements than its competitors. Compared to rocking KV perceptually gave a greater sense of contour than depth. This implies that KV does not convey shape through the "Kinetic Depth Effect" since rocking is synonymous with the KDE. Yet, experiments by Lum et al. [03] have shown that KV is able to significantly improve accuracy in feature identification tasks when viewing surfaces from a top down view and that it is able to enhance perception of shape and structure. This raises the question, what perceptual cues arise from KV?

The shape cues KV contributes arise partly from the motion cue of motion parallax (not to be confused with "the Kinetic Depth Effect", which arises from rigid body motions). Our results

seem to indicate that KV conveys shape from particles following contours. The importance of these distinctions and findings is that KV contributes different shape cues than rocking, and may therefore enhance shape perception when used in combination with rocking. Respondents commented that a combination of rocking and KV would have been helpful. Experiment two was designed to test this hypothesis.

5.2 Experiment Two: Alternating Rocking and KV

Experiment two was conducted to determine if there is an advantage to using a combination of rocking and KV compared to using rocking alone for orientation and feature identification tasks. A sample of 20 respondents consisting of 3 women and 17 men, 5 of whom had also performed the first experiment, with normal/corrected vision, was used in this experiment.

Participants were shown ten different layered surfaces, similar to those used in experiment one with the difference being that the peaks were more distinguishable, standing out as clearly separable mountains. Surfaces had from two to five distinct peaks. Figure 5.7 shows three examples of what these surfaces typically looked like.

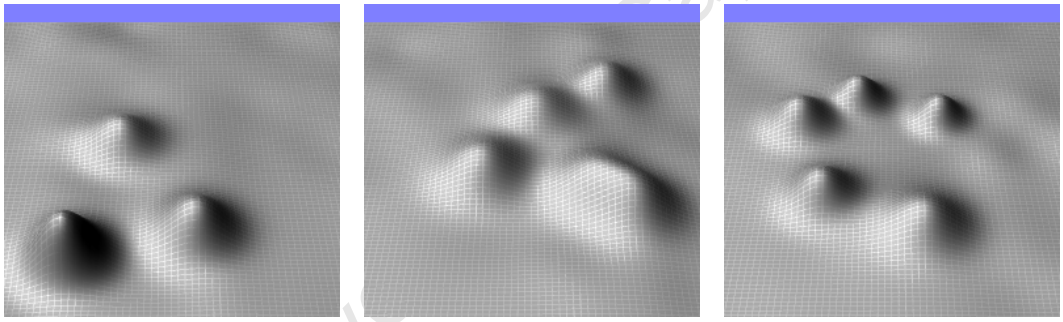

Figure 5.7 In experiment two, the surfaces consisted of between two and five clearly separated Gaussian bumps. The distinctness of the bumps was used to facilitate a peak counting task. Surfaces are illumitated here from the left of the viewer for purposes of illustration. In the experiment surfaces were lit from above.

Three or four of these surfaces were stacked above one another, with upper layers shifted slightly towards the viewer so that features were seen amidst the layers. Figure 5.8 shows an illustration of three of these layers stacked above one another with cross type opaque markings. The surfaces were sampled on a 128 by 128 grid. In the experiment, the surfaces were lit directly from above by a directional light source with lighting direction (0, -1, 0).

In the experiment three layers were illustrated using principal curvature crosses, see Figure 5.8 [left]. Patches were used in the four layer experiment, see Figure 5.8 [right]. The surfaces were

shown either statically or with a modified KV. In both cases participants could rock the surfaces. During rocking the particles were paused for KV and when rocking stopped, the particles would

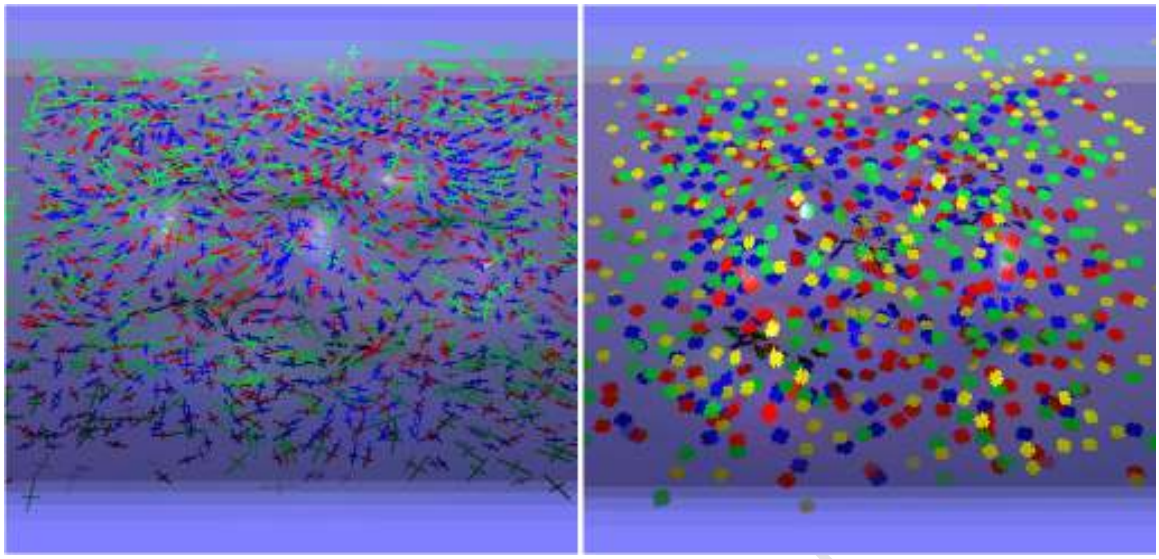

Figure 5.8 Layered surfaces were stacked on top of each other and shifted slightly towards the viewer so that features were visible amidst the interference of the other layers. [*Left*] Three layers were illustrated with curvature cross type glyphs. [*Right*] Four layered surfaces were illustrated with patch glyphs.

seamlessly resume moving over the surfaces.

5.2.1 Tasks

A forced choice orientation comparison task was used to measure how well respondents could perceive and compare the layered surfaces. During the orientation comparison task, respondents were shown fixed points on the different layers and asked to identify at which two points between adjacent layers the surface orientations were most similar. For the three layers this required comparing 3 orientations between adjacent layers at three different random points with each other, one point per surface. The closest pair of orientations, in all cases was different by less than 5 degrees. The angular difference between the alternative choices was, for the first 4 questions, between (30;35] degrees to the normals of the correct choice. For the next 4 questions the difference was (25;30] and so on to within (10;15] degrees. This narrowing of the difference between orientations was used to identify the range for which orientation errors occurred. Further it ensured that the differences were neither too obvious nor too difficult for the respondents. The points in question were oriented no more than 90 degrees away from the viewer and were more than 7 degrees from being vertical.

A feature identification task was also used, to measure each respondent's perception of the global shape of the surfaces. This task was also more similar to the original experiment performed by Lum et al [03], in which observers identified the highest and lowest peaks in a height field.

Participants performed, statistically, significantly better with KV than without it. The experiment performed in this work is significantly different from the original KV experiment, in that depth cues are significantly enhanced. Surfaces are viewed obliquely, providing silhouette cues and surfaces may be rocked. Further, in the original KV experiment by Lum et al. [03], only a single shaded surface is illustrated. This work considers the use of opaque markings for three and four layered semi-transparent surfaces. The task itself is reduced to allow respondents to merely locate the features rather than attempt to identify the highest and lowest peak.

In the feature identification task, participants counted the number of peaks (surface features) on each layer. The dependent variable, the difference between the number of peaks on each layer and the reported number of peaks per layer was used as a measure of error. It is expected that the visualization choice, rocking alone or rocking with KV, would influence the results. Additionally the minimum difference in orientation between the choices would be a factor of influence.

5.2.2 Procedure and KV Implementation

For the three-layered experiments, 10 respondents were shown a total of 20 different layered surfaces; 10 sets of surfaces were shown with rocking alone and 10 with a combination of KV and rocking. The technique was varied to prevent order effects; the first surface was shown randomly with either rocking or KV and rocking. The remaining surfaces were then shown, alternating between the techniques. This resulted in 100 responses being gathered per technique.

A separate group of 10 respondents participated in the four-layered experiments using the same procedure. These respondents were trained on three sets of surfaces. Participants were allowed to see the surface normals after answering the questions for the orientation task. During the experiments, the supervisor sat alongside the participants to assist them, observe their interaction with the system and capture their responses. Their responses were acknowledged and they were encouraged to use KV in addition to rocking, and vice versa.

A uniform distribution of 573 particles represented as crosses were placed on each layer for the three-layered tests. A random distribution of 600, 450, 375 and 300 particles represented as surface patches were placed on the bottom, second, third and upper layer, respectively, for the four-layered tests. These settings were found by an expert who adjusted the parameters until each of the layers appeared to be optimally visible. This trial and error process of finding optimal settings highlights the need for a metric to automatically and objectively determine the best parameters. Though not used for this experiment, to address this problem, we developed a model of perception of layered surfaces that enables automatic evaluation and optimization of visualization settings. This metric is presented in Chapter 7.

The change from a uniform to random distribution was made to investigate how participants

would perform with this new distribution. We note that it is not our aim to compare the three layer case to the four layer case. Each of these evaluations should be considered as an experiment on its own. The changes to the four layer case were made, since it was observed that these could well help respondents complete the experiments with less difficulty, as the respondents were experiencing fatigue and difficulty completing the experiments in the three layer case.

When the markings move over the surface, in the three layer case, the uniform distribution effectively becomes a Poisson distribution since the markings move around and repel one another, but are redistributed from high-density areas to low density regions. Effectively animating the markings continually varies the sampling distribution. This is a feature of Kinetic Visualization that may contribute to its effectiveness. A modified KV was used in which the occlusion reducing rule was implemented. Particles on different layers were also given varied motions, cycling between swirling around features to flowing in a uniform direction over the surfaces.

5.2.3 Sources of Experimental Error

During experiment two variations and potential sources of error and bias occurred. These interactions, inconsistencies, errors and variations are presented below. Did these mistakes lead to errors and bias? Reasons are set forth which argue that the differences in results for the tasks, despite this, remain ascribable to the differences between the techniques and not other factors.

Experiment two was launched using three layered surfaces and cross type glyphs. While ten users were able to complete the experiment with reasonable success (these respondents' results were analyzed and are reported), two additional participants who performed the task struggled to make sense of the visualizations. These struggling participants needed to be helped significantly beyond the other 10 observers. Their confusion about the visualization led to the decision to rather "experiment" with the visualization parameters, in an attempt to find settings that would be more helpful to them. None of their results were included in our analysis or report, but are noted, since these led to a change in the experiment.

Varying the settings seemed to allow them to better understand the visualizations, in particular, changing from cross glyphs to patches. These participants were able to complete the remainder of the experiment with far less trouble and in less time. The third observer was unable to make sense of the markings for several different variations of the parameters. It was decided then, to conclude the experiment for 3 layers. The use of patches was then tested on the more challenging problem of displaying four layers. Additionally, a random distribution of opaque markings across the surfaces was used while in the three layered case a uniform distribution of markings was used.

The experimental decision to consider four layers and change the distribution of markings does not damage the experimental aim of determining if there is an advantage to using KV compared

to rocking. This is because the changes were made between and not within groups, i.e. 10 participants used the same settings for the three layered case and 10 the four layer case for which variables were tightly controlled. The experiment in effect considers a comparison of "rocking" to "KV and Rocking" under two different sets of conditions, namely randomly distributed patches for four layers and under the case of three layers uniformly distributed crosses. The variation across experiments does, however, prevent some insight into comparing crosses to patches for various marking distributions. It would be ideal if crosses for four layers for both random and uniform distributions could be compared with patches for three layers under these various samplings. Enumerating the various visualization parameters leads to a combinatorial explosion of comparisons and variables which must be in turn varied and controlled for. This makes performing such complete evaluations infeasible. Furthermore, such extensive evaluation is beyond the scope, time-available and original intent of the experiment which aimed to merely establish if there is any advantage to using "rocking vs. rocking and KV".

Further, these experiments were extremely exhausting for the participants. The four layer experiments required, despite the use of patches, even more time and effort than the three layered experiments; surface count tasks needed to be performed on an extra layer and orientation tasks required performing an additional three cross comparison between layers. The evaluation tasks which were already simplified when expounded to four layers made evaluating layered surface experiments with conventional approaches difficult.

A potential problem with the experimental design is that of the observer-effect. To the best of our knowledge experimenter interaction with the participants did not significantly bias participants to perform better or worse for either "rocking" or "KV and rocking". This is because experimenter interaction with the participants consisted of the experimenter reminding them of and explaining the tasks, training them to correctly understand the orientations of orientation markers, capturing their responses to the peak count task and encouraging the participants to wait for and watch the various motion variations of the KV technique.

Finally, scene lighting was erroneously described as coming from the left and above the surfaces when the light was actually from directly above the surfaces, not to the left. This discrepancy would not lead to a bias towards either of the techniques. Accurate orientation judgements and identification of peaks indicates that this mistake was overlooked by the participants.

5.2.4 Results

Table 5.5 shows the average time participants spent answering both the orientation and peak count tasks and the number of times the surfaces were rocked for the three and four layered experiments, by technique.

	Rocking+Still	Rocking+KV
	3 layered surfaces with crosses	
Average Time ($p < 0.0000015$)	**134.8s**	**186.2s**
Standard Deviation Time	66.8s	76.9s
Rock Count	9.2	12.5
Standard Deviation Rock Count	4.9	6.6
	4 layered surfaces with patches	
Average Time ($p < 0.015$)	**228.4s**	**260.4s**
Standard Deviation Time	97.7s	86.1s
Rock Count	13.0	13.6
Standard Deviation Rock Count	5.3	5.3

Table 5.5 Average time in seconds and average rock counts per question for both tasks. Bold indicates which differences are statistically significant.

Participants took on average two to three minutes for three layers and approximately four minutes for four adjacent layers, to compare orientations and count the peaks on all the layers. A t-Test (paired two sample for means) for time between rocking and rocking with KV for three layers shows that users used significantly more time for rocking and KV ($p < 0.0000015$). For four layers the same occurred ($p < 0.015$).

5.2.4.1. Orientation Task Results

Table 5.6 shows the means and standard deviations for the orientation tests. The orientation errors, the number of mistakes made per surface out of 100 responses in total, for both the three-layered experiment with cross glyphs and the four-layered experiment with surface patches showed no significant advantage for using rocking alone compared to using a combination of KV and rocking; t-Tests (paired two sample for means) for the three layered case yielded $p < 0.8$, and for the four layered case $p < 1.0$.

	Rocking+Still	Rocking+KV
	3 layered surfaces with crosses	
Mean Number of Errors	2.6	2.55
Standard Deviation	1.83	1.4
	4 layered surfaces with patches	
Mean Number of Errors	1.35	1.35
Standard Deviation	1.29	1.5

Table 5.6 Average number of orientation mistakes per surface set

A t-Test of the variance for the orientation error for the three-layer case is significantly higher than for the four layer case for which patch type markings were used ($p < 0.0005$) compared to

cross glyphs for three layers; this analysis of variance does not necessarily imply that accuracy is attributable to use of patches over crosses, though it is likely the case. As the difference in angle between the possible options decreased, for the four-layer test the number of errors increased (Pearson's correlation coefficient is -0.9). This was as expected. However, for the three layer experiment this relationship was less clear, likely due to users guessing orientations or exact orientations being difficult to gauge at regions of higher curvature.

5.2.4.2. Peak Identification Task Results

Though KV did not contribute to rocking for the three layered peak identification task ($p < 0.85$), it did, however, make a significant difference in combination with rocking compared to rocking alone for the four layered test. Average total peak count errors for each surface across the 10 participants were analyzed with a two-tailed t-Test between subject factors, yielding $p < 0.044$. Average total peak counts were used, because for alternating sets of surfaces we had 6 users who completed the task using Rocking+Still, and 4 who completed it using Rocking+KV and vice versa. The averages and standard deviations are illustrated in Figure 5.9. Table 5.7 shows the average errors in peak counts for both the three layer and four layer experiments.

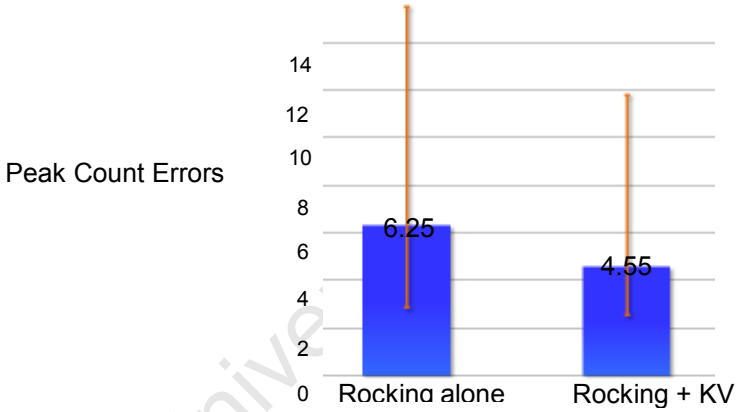

Figure 5.9 Average peak count errors with standard deviations for the feature identification task per surface set, for four layers.

	Rocking+Still	Rocking+KV
	3 layered surfaces with crosses	
Mean Error	2.95	3.05
Standard Deviation	2.86	2.67
	4 layered surfaces with patches	
Mean Error ($p < 0.003$)	**6.25**	**4.55**
Standard Deviation	2.91	2.58

Table 5.7 Average peak count errors. Statistically significant differences shown in bold.

There is an increase in the number of errors going from the three-layer case to the four-layer case, potentially due to the additional layer. There were significantly more peak count errors arising from adding a fourth layer compared to the three layered case. A two tailed t-Test result gave $p < 0.003$, indicating that either there is a significant statistical difference between using patches and crosses for peak count tasks or that a uniform distribution is better than a random distribution. However, the addition of the extra layer also likely made it much more difficult to identify surface features. Given the improvement due to patches or marking distribution, this is the likely explanation.

Table 5.8 shows the error results for each of the three layers for the feature identification task. A one-way, between subject factors, analysis of the variance (ANOVA) of the number of peak count errors on an individual layer basis shows statistically more errors in both the three-layer ($p < 0.005$) and four-layer experiments ($p < 0.03$) for the interior layers than for the bottom and top layers. The layers are numbered from closest (1) to furthest from the viewer (3 or 4). Tukey's HSD test shows that the difference lies between the middle (layer 2) and furthest (layer 3) layers ($p < 0.004$) for three layers.

	Layer 1 – closest green	Layer 2 – middle red	Layer 3 – furthest blue
Mean Error	1.55	3.5	0.95
Standard Deviation	2.14	3.43	1.54

Table 5.8 Peak count errors for three layers.

Table 5.9 shows the errors for individual layers for the four layer experiments. For four layers, a one-way between factors ANOVA, for the number of missed peaks for each layer was used to analyze which layer was the most difficult to identify. Tukey's HSD, shows the significant difference in errors between layers was between layer 3 and 4 ($p < 0.02$) and between layer 1 and 3 ($p < 0.02$). This indicates that it was most difficult to accurately identify features on the layer just before the furthest layer. This is likely due to a combination of occlusions from the layers above it and a lesser sampling than on the bottom layer.

	Layer 1 (closest) yellow	Layer 2 green	Layer 3 red	Layer 4 (furthest) blue
Mean Error	1.95	3.2	3.7	1.95
Std Dev	1.7	2.78	2.74	1.67

Table 5.9 Peak count errors for each layer in the four layer experiment

5.2.4.3. Further Observations

It was observed that, when more than four surfaces were illustrated using primary colours, it was

difficult to distinguish between red and orange, orange and yellow and purple and blue, indicating that as the separation in hue on a HSV scale becomes less, the colours are more easily confused. As saturation or value decreases the distinction between colours becomes more difficult. Applying shading and highlights has the same effect as decreasing saturation and lightness for certain regions of the surface, also making it more difficult to distinguish between the colours.

5.3 Discussion

KV contributed significantly to rocking for the feature identification task with four layers. This is a noteworthy result, since other researchers have found rocking on its own to be just as effective as rocking combined with other cues, such as shadows [Bair, 07] [Weigle, 06]. The contribution KV makes to rocking is likely due to a combination of particles illustrating contours, motion helping to distinguish between markings and animation increasing the surface area covered by markings over time. Respondents would request multiple new surface samples to help them fill in the gaps for regions with a few or no particle samples for the static approach on four layers, whereas with motion they would simply wait for a particle to move over a region. The memory load of watching particles move into new positions is less than remembering previous positions before a re-sampling, due to the smooth transition of the markings. Static rendering requires the viewer to interpolate between gaps of nearby markings. This highlights one of the reasons why a combination of KV and Rocking is more useful than KV or Rocking alone, i.e. KV provides an integrated coverage of the surfaces over time. Rocking also helps a person to distinguish between the layers through enhancing the sense of depth; depth cues have proved to induce a strong sense of perceptual grouping.

Another potential explanation for the moving points approach being better for the peak count task is that respondents spent significantly more time looking at the surfaces than for rocking alone. Respondents were indeed encouraged to watch and wait for the various motion patterns. One may argue, that during the additional time observing the surfaces, participants may possibly have noticed some of the features through the moving markings. This would then indicate that KV, nevertheless, played a role in them seeing something that was not noticed before. The participants viewing the static approach were satisfied that they had seen all there was to see and to move on to the next set of surfaces. Observation revealed that as participants watched the moving markings either vary their motion or the shading upon the markings change as they moved, would then notice a peak which had gone overlooked before. KV to some extent kept them exploring the surfaces slightly longer and appeared to draw their attention to potential features. Upon finding a potential feature, rocking was again used to confirm if the newly found features were truly peaks. This is an important finding, because it raises the question of which technique is best to locate features. The answer would seem to be Rocking, since during experiment two, I observed that rocking contributed to the rapid identification of most of the peaks. The unique KV motion

patterns of markings moving over peaks, seemed to reveal smaller less obvious peaks. This gives an indication that KV is useful for preattentive feature location.

A feature of KV is that the density of the markings on the different layers and distribution of markings varies over time. This may be a factor that led to features becoming visible on interior layers. Does KV play a role in distinguishing between markings on different layers? In experiment two, respondents were able to attentively pick out and focus on certain layers with moving points, whereas with static approaches they relied on rocking to help distinguish between the markings on the different surfaces. Many respondents were observed to associate a peak with the wrong layer, particularly when rocking stopped. After rocking, several participants were also observed to have watched moving points to help distinguish the layer to which the particles belonged, thereby helping them to reduce false positives in the peak count identification task.

Experiment two likely indicates that particle representation makes a significant difference for different shape tasks. Consider that as the number of layers increase, the number of errors per surface is likely to increase as well, primarily since visibility is reduced. However, results show that orientation accuracy improved. The variation is therefore either likely attributable to marking type or marking distribution over the surface, which was changed from uniform to random. Experiment one showed that orientation readings are typically determined by observing static local surface markings. It is therefore likely that an observer infers orientation better from patches. Patches reveal shading and surface curvature better than crosses and are therefore likely more useful for orientation tasks. Crosses on the other hand are better for seeing through to interior layers because crosses occlude a smaller surface area than patches. When using patches fewer samples should be used in order to sufficiently expose the interior layers. This results in fewer occlusions which obscure features but also more sparsely sampled surfaces.

The experiments fatigued the respondents because they required significant concentration and time to process the information overloaded displays. Perceptually making sense and processing three and four layered surfaces displayed simultaneously is extremely challenging. Further, it is likely that interference is the cause of impeding the preattentive processing ability of the visual system, which normally enables rapid detection of features. Inferring surfaces from fragmentary images requires significant concentration and mental effort. This may be a further reason respondents took so long to process the surfaces in the experiments and would explain the amount of significant concentration required. In the experiments participants would scan the surfaces repeatedly in search of features, which could also be an effect of interference from the other layers. Another potential cause for why searching took long is that multiple layers resulted in more distractors which slowed down the search. This corresponds to perceptual theory regarding preattentive target searching [Treisman, 1985].

Finally depth cues from motion are reportedly better for coarse work and a perception of overall

layout than for fine work [Lyness, 2004]. This agrees with the results of experiment two and Lum et al's [2003] results where KV showed greater success for more global impressions of the surface than for fine details e.g. orientation at a point. Several novel motion strategies were considered, which do not seem to show significant advantage over standard KV other than markings moving around features, which presents an alternative to following principal curvature directions to illustrate features.

5.4 Limitations and Recommendations

Based on these results it is recommended that rocking should be used as the primary means of supplementing layered surface display techniques. However, to address the challenge of conveying multiple layered surfaces, a combination of rocking and KV is helpful for feature identification tasks and global surface perception. Surface patches are more helpful for orientation tasks and may allow a visualization approach to convey the surfaces with fewer samples. KV is useful to this end as it reduces the number of patches required to convey a surface, since through animation, the patches ultimately cover the surfaces over time. This provides multiple samples at various locations, thus increasing the resolution of the visualization. It appears that crosses are best for feature identification tasks as these allow a viewer to see through to the interior layers.

The limitation with using KV for layered surface display is that motion can be distracting and cause interference. It is easier to make judgements between stationary samples than points in motion, and this applies to both rocking and KV. Interference occurs as a result of markings moving over a region of an interior surface while it is being examined. This breaks a person's concentration or draws attention from that region to the exterior markings moving over the region.

5.5 Conclusions

The results from experiment two show that it is worthwhile supplementing opaque marking-based layered surface display techniques with a combination of pendulum style rocking and Kinetic Visualization (KV) for feature identification tasks. While rocking best illustrates surface shape and depth, contributing the Kinetic Depth Effect (KDE), animating the particles (KV) helps a viewer to:

- distinguish between markings on different layers,
- see samples which cover the surfaces over time, and
- observe additional shape cues besides the KDE, which illustrate surface contours.

The following results were found from the experiments that were performed:

- Rocking should be used to augment layered surface displays since it results in more accurate perception of the surfaces.

- Static renderings of layered surfaces should be used instead of KV for less than four layered surfaces, since, KV is no better than a static display of a semi-transparent layered surfaces with opaque markings on top of a bottom opaque surface for various shape tasks, static renderings should be used in these cases rather than KV.
- A combination of Rocking and KV should be used for feature identification tasks when viewing four layered surfaces. KV contributes unique motion patterns (markings swirl sharply around peaks) which is useful for feature location.

Despite rocking and interactive exploration of shapes producing an accurate sense of the 3D structure of the surfaces, when the animation or interaction stops, the quality of shape perception almost immediately and drastically diminishes [Weigle, 2006]. A means of addressing this problem is to combine as many depth cues (stereo, rocking, shadows) as possible to accurately convey surface shape. Combining such cues is further considered good visualization practice. A combination of depth cues is better than a single cue on its own, especially if the cues confirm one another, working together to paint an accurate perception of depth and structure in an image. For these reasons, Weigle [2006] argues that adding cast shadows, even though this cue is masked by rocking, should nonetheless not be excluded from visualizations. This argument for inclusion should even more strongly favour Kinetic Visualization since it supplements the additional cue of kinetic depth and, more so than shadows, is significantly more effective in combination with rocking than rocking on its own. The question that should be raised when developing a layered surface visualization is: does the additional implementation costs required to apply KV outweigh the small advantage that may be gained?

This research set out to consider the potential usefulness of animating opaque markings over surfaces in the context of layered surface displays for exploratory visualization. Such visualizations should facilitate between surface comparison tasks and support a broad range of functionality, such as enabling accurate depth judgments, feature identification and orientation estimates. KV, which is marginally useful for feature identification tasks may not play a major role in enhancing displays for these purposes. However, perhaps in conjunction with interfaces that use an overview, zoom and filter, and details on demand [Schneiderman, 1996] strategy, KV may indeed be useful for layered surface visualization. KV is useful for surface overview. Further this novel research contributed empirical evidence in experiment one that seems to indicate that KV does not induce the KDE. The experiments have also revealed some of the problems such as interference effects that arise as a result of introducing KV animation into visualizations.

Finding optimal parameters for the design was identified as a challenging problem; there are a plethora of parameters including size, type, density and speed of markings etc., making it difficult to perform multiple combinations of user experiments to test the optimal configuration. Models of human perception may prove useful for automatically testing and optimizing these visualization settings.

The next chapter introduces an approach for automatically evaluating the effectiveness of marking-based visualizations, which enables automatic optimization of the parameters.

Chapter 6

Background on Optimization and Perception of Layered Surfaces

The previous chapters have presented and evaluated the use of animation as a means of enhancing opaque-marking based layered surface display techniques. Such opaque-marking based approaches have multiple parameters which must be varied for each of the different surface layers, in order to effectively display the surfaces. Some of the following questions arise: How big should the markings be on the different layers? How many markings should there be on each layer? What type of markings should be used for each layer? Visualization users such as doctors, would not spend time customizing the plethora of parameters. In this chapter relevant background is presented which underlies our novel framework for computationally modelling and measuring how effectively a visualization of layered surfaces perceptually conveys the different surfaces. This measure makes it possible to automatically optimize the parameters for the opaque marking based layered surface displays developed in this work. The framework and its evaluation are presented in Chapters 7 and 8 respectively.

This chapter commences with an introduction to the problem of computationally evaluating layered surface visualizations. Related work on measuring the effectiveness of layered surface displays is then presented in section 6.2. Theory and models of the HVS for single surface completion are covered in section 6.3. A background of relevant perceptual theory in surface completion, which forms the basis of the measure and framework developed, is set forth in section 6.4.

6.1 Introduction and Motivation

Perceptual experiments are the standard means of evaluating the effectiveness of layered surface display techniques. These user experiments allow various techniques to be compared with each other or allow the effects of varying one or two parameters to be investigated. Such experiments, however, require multiple participants and in the case of displaying layered surfaces have the drawback that they fatigue participants. In the various perceptual experiments performed during this work, we observed this; for example respondents took more than three minutes to perform a simple feature identification task and orientation comparisons between layers in the experiments. The respondents reported mental fatigue after completing experiment one and at about the half way mark in experiment two. Even single surface perceptual experiments can be exhausting [Langer & Bülthoff, 2000]. Displaying more than one layer proliferates the amount of information that is shown, the task complexity and user effort required.

In addition to layered surface experiments being strenuous on participants, it is difficult to determine the best settings for parameters for a layered surface visualization since there are many parameters for each layer. The scope of this problem is large; we identify the following 7 possible parameters and independent variables which may be varied or tested in any given experiment:

- number of layers (2,3,4,5) ×
- marking type (cross, disk, patch) ×
- marking size ×
- transparency level ×
- speed of markings ×
- density of markings ×
- distribution type (uniform, Poisson, random, curvature based, mixed).

The best settings for these parameters need to be determined for each layer so as to simultaneously reveal the shape of each of the layers as clearly as possible. This results in a trade off between minimizing occlusions and yet revealing a sufficiently large surface area of markings to clearly illustrate the shape of the surfaces. Determining the best settings for three or four layers by running psychophysical experiments becomes nearly infeasible since performing such experiments results in a combinatorial explosion of the various independent variables. Running such experiments requires significant time and would require many participants. Moreover, in these experiments typically only one or two variables can be varied at a time. This makes these experiments ill-suited for evaluating the effects of all the various visualization settings on one another, since these variables influence one another and have non-linear visual results [Bair et al., 2005].

Finding optimal parameters for a display in real world scenarios would need to be automatic; scientists and doctors would not spend time adjusting parameters to view their layered surface data, for different data sets or from different viewpoints. Making parameter adjustments manually may furthermore consume many hours, with only minimal success and uncertainty of having achieved the best display. It would be ideal if the process of setting parameters could be automatically performed by the computer.

The significant benefit of a computational means for evaluating the effectiveness of layered surface displays is thus that it enables perceptually based evaluations of layered surface visualizations without the need for running extensive user tests. It additionally serves to help find optimal parameters for a layered surface visualization. The dream is that it could essentially offer the advantage of allowing psychophysical user testing to be performed but without the need for users, i.e. automatic evaluation of layered surface visualizations. If a suitable model of HVS perception is developed it would open the door for performing evaluations of both old and new visualization techniques against one another or allowing experimentation on a particular visualization technique under various parameters and combinations of parameters. It would also provide a way of automatically optimizing the settings for a layered surface display technique for different data sets or view points. This could be accomplished by using the measure in conjunction with an optimization algorithm such as Particle Swarm Optimization (PSO), which is able to find optimal solutions for non-linear continuous problems. Developing such a measure is far from trivial though, possibly impossible. This is because the behaviour of the human visual system and an observer is uncertain and almost unpredictable. A model could only be partially representative of the way a human would interpret a visualization.

This thesis pioneers a basic approach that is meant to reflect the way people perceive layered surfaces. This entails developing a model of the human visual system that accounts for the complexities of interpreting images produced by layered surface displays. Such images consist of fragmented patches of markings. The HVS performs depth estimates on the visible fragments, clustering these together through processes of perceptual grouping and surface completion. In section 6.3 the theory of these various perceptual processes is presented, which are then incorporated into our model. The model itself is set forth in Chapter 7. Next a review of previous work that has been done on finding the optimal parameters for layered surface visualizations is covered.

6.2 Related Work

6.2.1 Measuring the Effectiveness of Layered Surface Displays

Efforts to optimize the effectiveness of visualizations of layered surfaces have to date focused on stylistic properties of layered surface textures [Bair & House, 2007] [Bair et al., 2005] [Robinson

& Robbins, 2005]. Identifying the best settings for the layered surface texture parameters have relied on performing an intensively manual process: user evaluation studies through psychophysical experiments. User experiments are used to give an indication of how effectively the settings convey the surfaces. Bair et al's work [2005] in which a human-in-the-loop approach was used to resolve a set of optimal texture settings for two layered surfaces is one example of such experiments. In their work six participants rated various layered surface visualizations under different texture settings, from which the effectiveness of various texture parameters was obtained through a qualitative user rating of the visibility of bumps on surfaces. A genetic algorithm was used to create increasingly good visualizations. The users in the loop served as the fitness function for driving the optimization process. The responses produced a large database of rated texture parameters. An extensive data analysis was then performed on this database to determine the optimal texture parameters and settings for displaying two layered surfaces. This analysis required significant manual interpretation and effort [Bair et al., 2005] [Bair et al., 2006]. Such experimental approaches are quite unlike the automatic and computationally based approach proposed in this work, in which a computer model of visual perception is used in stead of the user in the loop.

The most typical and quantitative user evaluation based approach used for determining the effectiveness of visualizations relies on participants performing some quantitative estimation task on one or more surfaces, under various conditions, which are tightly controlled. In these approaches one or two visualization parameters are varied and constitute an independent variable. Examples of such experiments included those performed by Bair et al, [2007] in which 14 participants in one experiment and 7 participants in a subsequent experiment were required to make multiple surface orientation estimations on two layered surfaces. The task performed in these experiments was one of the commonly used tasks for surface experiments; respondents estimated surface orientations at several surface positions. The accuracy at which the respondents estimate these orientations provides a quantitative measure of how well a surface is visually represented and perceived [Langer & Bülthoff, 2000] [Bair & House, 2007]. There are several other tasks, such as forced choice tasks, depth estimates etc, available for approximating how well a surface can be perceived within the context of user evaluations [Langer & Bülthoff, 2000] [Weigle, 2006].

6.2.2 Automatic Perceptual Measures

In contrast to the user dependent evaluation approaches described above, we attempt to computationally model the way the HVS perceives layered surfaces and in turn use this model as a means of quantitatively and automatically estimating the effectiveness of layered surface visualizations. To the best of our knowledge this is the first attempt to computationally and perceptually measure the effectiveness of layered surfaces through a model of the HVS.

Our work extends the computational models of various HVS processes proposed by Grimson [1980] [1981] and Marr & Poggio [1977]. These authors' original models mimic the way the HVS reconstructs single surfaces from stereo. Our work uses these models as a framework and adds perceptual processing algorithms for perceptual grouping and relatability criteria, which the HVS uses to perform surface completion on fragments of layered surfaces. An alternative set of models that simulate the formation of surface percepts from visual cues are the 3D LAMINART models of neural visual processes [Grossberg, 2003] [Grossberg & Yazdanbakhsh, 2005]. While these models may be used to simulate perceptual grouping, and 3D perception of transparency as well as the way 2D images are fused to form 3D percepts, they in terms of complexity and implementation lie beyond the scope of this work and are left for future research.

Another class of computational algorithms which may be adapted to computationally measure the effectiveness of layered surface displays include various computer vision, shape from X algorithms. These include: shape from shading (SFS), shape from motion and shape from texture (SFT) algorithms. These algorithms extract geometry and range maps from images. Such algorithms use various mathematical models to determine representations of shape. Of these, only the shape from texture algorithm of Black and Rosenholtsz [1995], which uses mixture models to compute the shape of multiple surfaces from occluded textures, stands as an application of SFX algorithms for recovering the shape of layered surfaces. This SFT approach may be incorporated into our model to improve the surface representations and approximations of the surfaces and may be beneficial for a more perceptually accurate clustering of fragments. This SFT algorithm, though, on its own does not perform surface completion in the form of interpolation, which takes relatability criteria into consideration. Multiple SFX algorithms should ultimately be built into a model of HVS perception. Our framework caters for this, though implementation and adaptation of these algorithms for layered surface displays was beyond the scope of this work. SFX algorithms make very specific assumptions which do not cater for the complexities that the HVS deals with, especially when processing fragmented input typical of layered surface displays. For instance, the HVS processes images under conditions of both diffuse and Lambertian shading in the real world whereas SFS algorithms typically only cater for Lambertian lighting [Bulthoff & Langer, 1999].

The end result of computer vision algorithms differs from human vision in that a perceived surface is not equivalent to an exact or mathematical representation of a surface. This is because from one person to the next or even for a single person, there may be many sources of variation which influence perception [Langer & Bülthoff, 2000]. A few of the factors affecting human vision include differences in spatial vision, attention, eye movements, focus, memory, concentration and learning. A mathematical representation of a surface based on various perceptual measurements e.g. a set of perceptual estimates of normals cannot be concluded to be the same surface as perceived by a person [Koenderink, 92] [Bulthoff & Langer, 1999]. Despite these differences, Bulthoff and Langer [1999] argue that insights and an understanding of human

perception can be gained through computer vision models. Further, they compare CV models for SFS under various lighting conditions with people's perception of surfaces under diffuse lighting. Their work along with that of Grimson and Marr pioneer the way for using various computational algorithms to simulate sub-processes of the human visual system.

While automatic measures of the effectiveness of layered surface display techniques have not yet been developed, various automatic objective visual quality metrics have been established for identifying perceptual image differences between a pair of images based on models of the human visual system. The two commonly used metrics for finding perceptually noticeable differences in a pair of images include the Sarnoff visual discrimination model [Lubin, 1995] and Daly's Visual Differences Predictor (VDP) [Daly, 1993]. Though the VDP has been used for comparing High-Dynamic Range (HDR) images [Mantiuk et al., 2005] and other applications, its use in Direct Volume Rendering (DVR) [Wong et al., 2006] is most akin to this work. In this application, the VDP is incorporated into a framework to compare two images rendered with different DVR algorithms or with different shading, different gradient estimations, or samplings. The VDP is used to find the algorithms and parameters which result in the least discrepancy from a good perceptual example. The VDP thus helps to steer the visualization process from a perceptual perspective. The VDP and Sarnoff visual discrimination models are metrics which focus on noticeable perceptual differences between a pair of images, giving an indication of perceptual variation between a pair of images. These measures give no indication of how well a surface within an image can be perceived, whereas we specifically establish a perceptual measure that quantifies how well layered surfaces are displayed in an image.

Considering the functioning of the VDP lends itself to developing insight into the functioning of the HVS and developing models thereof. A VDP receives a pair of images and creates a map (an image) of probability values indicating how the differences between the images will be perceived. One of the images, the mask, is a picture of an original scene. The other is the image for which visibility needs to be estimated. The VDP in its initial stages compensates for the non-linear response of the human eye to luminance and its loss of sensitivity to high and low spatial frequencies. A cortex transform and visual masking divide the image into spatial and orientational channels. This transform further predicts perceivable differences for each channel. The final stage of the VDP – error pooling, combines the probabilities of visible differences for all channels and generates a map of detection probabilities. The VDP is mentioned here for the sake of completeness but we do not use it directly. It may be incorporated at the front end of the framework proposed in this dissertation to filter the images in a manner similar to early stages of the HVS. This is left for future work. However, the Contrast Sensitivity Function (CSF) component of the VDP is integrated into and used in our model.

Understanding the way that the human visual system processes the fragmentary input seen in images of layered surfaces, will help to identify which processes should be integrated into a

framework for automatically evaluating layered surface displays. Grimson's model of the HVS is presented next.

6.3 A Computational Model of the HVS

A computational theory of the human visual system's processes by which it constructs a 3D surface from stereo images has been developed by [Marr & Poggio, 1979]. Grimson [1981] developed a computational model that extends this theory for reconstructing a single surface from stereo images. The model, based on neurophysiology and findings from psychophysical experiments, was designed to be consistent with known evidence about the visual system and is feasible for implementation in a biological system. It is however, uncertain how this model, corresponds with the state of current knowledge about the HVS. Despite this, it does form a practical point of departure in this pioneering effort to model the HVS for layered surfaces. This is because it specifically focuses on surface reconstruction and is perceptually based. For these reasons it was selected as a basis for our perceptual model. We adapt and extend the model for reconstructing layered surfaces.

Grimson's model regards the HVS as a modular information processing system that performs computations and transformations on various symbolic representations of visual information. The approach makes abstractions which help distinguish between computations, representations and their meanings. The abstractions allow stages of visual processing to be decoupled from a particular implementation (e.g. the neurological systems of the brain). This enables one to focus on the computational theory and process in a modular way [Grimson, 1981] [Ullman, 1979]. These models and assumptions allow for replicas of the HVS to be developed without having to understand or rebuild the entire HVS, e.g. the processes of structure from stereo can be studied in isolation. Making assumptions and simplifications about the complex HVS is useful to the end of both modelling and better understanding the human visual system in terms of theories and algorithms.

Figure . shows the representations and transformations used in the model through which it attempts to simulate the way the HVS reconstructs a surface by analyzing a scene. The processes and representations are as follows:

- Retinal images are transformed into representations that identify locations in the images over which there are visibly noticeable differences in some physical property of the surface, e.g. intensity or lighting. This representation, which contains various features such as edges, is known as the Primal Sketch and serves as input for later processing stages.
- Surface shape and depth information is computed next at various points in the image from the primal sketch. Various, relatively independent modules of the HVS perform these depth computations, e.g. stereo vision matches and uses corresponding points from two stereo

representations of the primal sketch. The intermediate representation created during these processes is called the “raw 2.5D sketch”.

- Explicit surface information is lastly computed over all points in a scene. Interpolation is performed over the depth points in the raw 2.5D sketch. This gives a representation of the shapes of the visible surfaces known as the “full 2.5D sketch”.

This architectural understanding of the HVS which the model follows, was developed through several perceptual studies [Marr, 1978] [Marr & Poggio, 1977] [Marr & Nishihara, 1978] [Barrow & Tenenbaum, 1981].

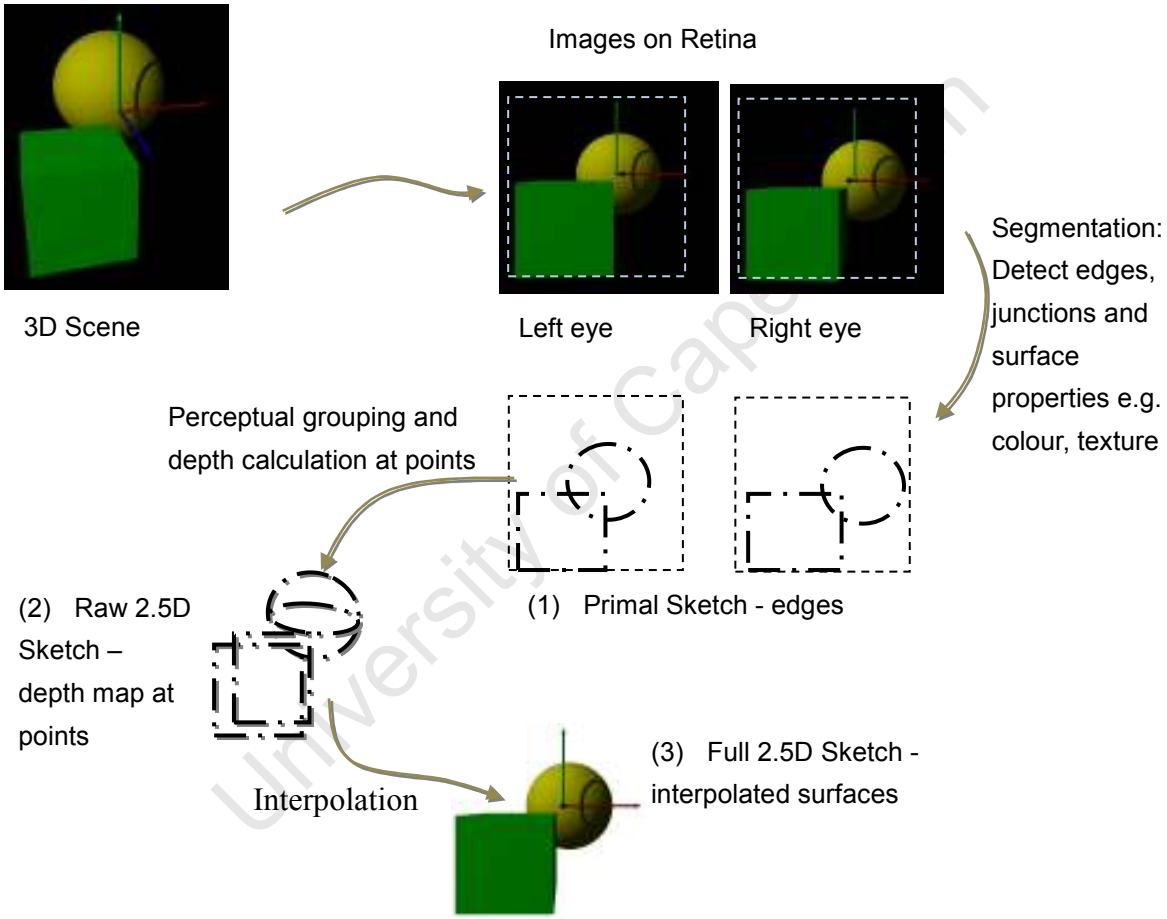

Figure .Representations and processes in the early Human Visual System [Grimson, 1981].

Various SFX algorithms in themselves may serve as computational models of the HVS which recover surface shape and depth. Sakai [1999] for instance designed a shape from texture, network model, which is based on a computational analysis of psychophysical experiments. The model correlates to the perceptual results from these experiments. SFX algorithms on their own, however, are just one of the major processes towards recovering shape from layered surfaces in the HVS. Our work proposes a framework that not only caters for use of multiple SFX algorithms

but also encompasses surface completion processes including relatability criteria and perceptual grouping required for reconstruction of layered surfaces. Each of the major processes and the representations of Grimson's model are explained in greater detail next.

6.3.1 The Primal Sketch

The Primal Sketch consists of features and edges [Marr & Hildreth, 1980]. These are acquired and used by the HVS and also various Computer Vision algorithms for later processing stages to infer shape and structure from a scene. The feature points and edges are typically found at locations in an image where there is a visibly noticeable difference in material, texture or shape [Marr & Hildreth, 1980]. Significant variations in these properties are typically marked by changes in image irradiance. Image processing functions that are useful for constructing the primal sketch include filtering, edge and contour extraction. Our implementation of the model, which is adapted to our particle system based framework, extracts feature points and fragments through rendering passes which render specific information about markings including the original particle identification numbers. This allows image statistics to be retrieved for each fragment, through simple image processing such as image moments, contrast and luminance calculation. More complicated image processing algorithms may be used in cases where per fragment information is not retrievable.

6.3.2 The Raw 2.5D Sketch - Depth and Surface Orientation Approximation

The Primal Sketch descriptions are fed as input to processing modules which determine depth and structure of the surface at various points. These processes are comparable to Shape From X (SFX) procedures from the field of Computer Vision, where X corresponds to stereo, motion, texture, shading, etc. Each SFX module computes surface information at various locations of the Primal Sketch, e.g. shape from stereo computes depth at point correspondences which are matched in a stereo image pair. The depth information from each module is combined into a single unified depth representation or depth map. The point correspondences used for many of the SFX algorithms are matches between points found in the Primal Sketch descriptions. The SFX modules effectively give zero-crossings, 3D or 2.5D points through which the surface is known to pass.

Computation of depth maps based on Primal Sketch descriptions of left and right eye images, using a theory of stereo vision similar to the way in which the HVS performs this computation, has been performed by Marr and Poggio [1979] and Grimson [1980; 1981]. Multiple depth cues have also been combined. Cryer et al., [1993] for instance merge shape from shading and stereo using a nonlinear model of the spatial characteristics of the human visual system. Other sources of important shape and depth information for the primal sketch may be calculated from focusing cues and occluding contours, e.g. silhouettes.

The various depth cues that the HVS uses to approximate depth are described in section . Depth cues establish either a relative or continuous sense of depth. Stereo and the KDE, for example, provide a sense of continuous depth or 3D position, while occlusion establishes a depth order relationship between the foreground or an occluding object and a background object. Occluding contours in particular play a significant role in helping the HVS piece together depth relationships. Depth values are also interpolated around these contours.

The HVS uses shading differently for shape recovery than computer vision algorithms [Ping-Sing et al., 1999]. It recovers perceived depth (shape), not only from shading, but also other depth cues, outlines, surface features and knowledge about objects. The final perceived image after processes of surface completion also influence how shape is perceived [Ramachandran, 1988] [Yin et al., 2000]. Computer Vision techniques on the other hand calculate depth or shape in an image using Shape from X techniques. The way in which depth is computed depends largely on the depth cue being interpreted. Shape from shading (SFS) for instance reconstructs a 3D scene from an image by performing calculations on brightness variations; changes in surface orientation across a local surface patch are inferred from changes in local intensity. Solving SFS does not give a unique solution since the problem is under-constrained [Prados & Faugeras, 2006]. SFS algorithms therefore make various assumptions based on how the image is formed. The most typical assumption is that the light source direction is known. Many algorithms also assume a Lambertian model of reflectance assuming diffuse reflectance. SFS approaches return shape as either a depth map, set of surface normals, array of surface gradients, or array of surface slant and tilt values. The depth values are either given as the relative distance to the camera or the relative height of the surface above the x-y plane.

Similar to SFS, shape from texture (SFT) is computed from variations in texture over a local surface region. Local distortion to texture gradient (the variation in texture element size) in the spatial frequency domain is modelled as a set of affine transformations. Slant, tilt and curvature shape parameters are recovered using differential methods and minimization which estimate the affine texture distortions [Black & Rosenholtz, 1995]. SFT algorithms which correlate with the HVS include Sakai's network model [1999] and Thaler et al.'s model [2007], which is not restricted to rotation or translation invariant distributions of the surface textures. While these models produce depth estimates, which correlate to observer judgements taken from psychophysical experiments, they have not been extended to cater for occluded textures encountered in images of layered surfaces.

Shape from stereo is used to compute depth values for sets of point correspondences found and matched in a pair of stereo images. Finding sets of correspondences or features which can be matched is a critical part of these methods. The recovery of depth or 3D position is accomplished

through a triangulation. It is necessary to know the stereo systems parameters to compute depth accurately [Banks et al., 1999]. Marr and Poggio [1977] present a shape from stereo algorithm that is representative of the way in which the HVS recovers depth from stereo. Similarly to shape from stereo, shape from motion algorithms also find correspondences in images, except that the images are taken over time rather than from two different vantage points. Trajectories of the feature points through triangulation give the 3D positions of the points.

The various computer vision algorithms which compute Shape from X provide a means of computing depth for the raw 2.5D sketch. Ideally perceptually based algorithms should be used for this task in the context of a perceptual measure, though even non-perceptually based approaches may suffice [Bulthoff & Langer, 1999]. However, to date, with the exception of Black and Rosenholtz [1995], SFX algorithms need to be adapted to work for layered surface cases.

6.3.3 The Full 2.5D Sketch - Interpolation

The final step in transforming an image to a surface representation is interpolation. Grimson [81], in agreement with perceptual theory of surface completion [Kellman, 03], argues that the final surface representation does not merely consist of a set of points (the raw 2.5D sketch) but a complete surface. This complete surface is obtained by interpolating a smooth surface through the points of the raw 2.5D Sketch [Grimson, 1981]. This final interpolated representation is known as the full 2.5D Sketch.

The interpolation performed by the HVS creates a smooth or complete representation of a surface that runs through the marked points in the raw 2.5D Sketch which satisfy relatability criteria. These criteria encapsulate how and when interpolation occurs between neighbouring fragments. When neighbouring fragments are relatable then human perception produces a smooth, at least once differentiable continuous surface with no inflections or torsion. Grimson's model simply interpolates between fragments and does not incorporate relatability criteria as our model does.

Grimson's model constructs a single well defined unique surface through a set of points [Grimson, 1981], referred to as the "most consistent surface". Mathematical programming and a conjugate gradient and gradient projection method are used to compute and approximate this surface, using the amount of variation in orientation over a region of the surface as a measure of surface consistency. His approach minimizes the quadratic variation passing through the known points in the raw 2.5D sketch.

Despite its simplifications our work adheres to these major stages and processes proposed in Grimson's model. While both Grimson's approach and this dissertation deal with smooth surfaces which do not have orientation discontinuities, our work extends the model for

reconstruction of fragmentary input typical of layered surface displays, incorporating more recent perceptual findings, such as 3D relatability criteria which determine how fragmentary input is interpolated. The major differences between Grimson's model and the framework developed in this dissertation include:

- Our work is specific to perceptually modelling the reconstruction of layered surfaces. Grimson model reconstructs a single surface.
- Our work extends Grimson's model, incorporating perceptual grouping.
- Interpolation processes are modified in our model, incorporating relatability criteria.
- Our work presents the novel application of the model to measure the effectiveness of layered surface renderings and to optimize these renderings and visualization parameters. The model serves a functional role in a larger process of automatically enhancing layered surface visualizations.

6.4 Perceptual Completion of Layered Surfaces

Layered surface renderings, especially for marking based visualizations, result in sets of spatially discontinuous visual fragments scattered across the displayed image. This is illustrated in Figure ., which shows a rendering of two layered surfaces. This fragmentation is a result of occlusions and spacing between markings. The question arises, how does the HVS connect these fragments and fill in the gaps to infer the underlying surfaces?

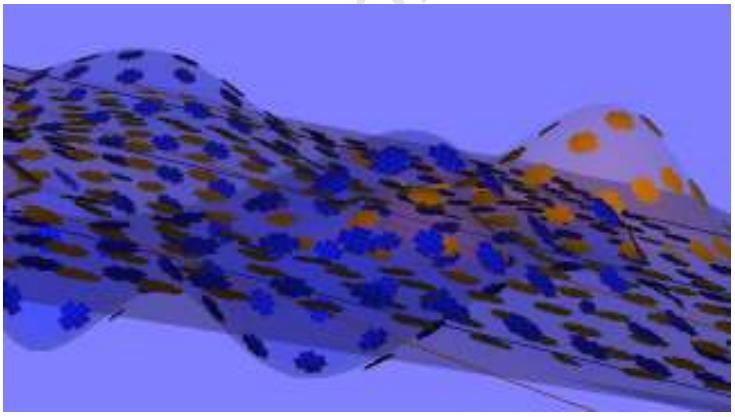

Figure . Layered surface visualizations consist of fragmented patches. The illustration shows blue and orange patches on different surfaces. The HVS performs surface completion across similar fragments to reconstruct the surfaces.

The HVS uses interpolation to connect discontinuous fragments. Interpolation processes in the HVS attempt to produce a continuous and smooth surface between the fragments [Fantoni et al., 2008]. The interpolation depends on geometric relationships between visible contour segments (e.g. edges and junctions) as well as relationships between fragments based on similar surface properties.

The HVS processes proceed as follows to perform surface completion (interpolation):

(1) Fragments are initially segmented through processes of edge and junction detection and surface property detection, which find distinct regions of colour, texture, motion luminance and depth. Segmentation processes detect fragments provided that there is sufficient contrast between them. These segmented fragments make up the primal sketch.
(2) Perceptual grouping processes then cluster sets of visible fragments that have perceptually similar visible surface properties [Treisman, 1985] [Kellman, 03]. Relatability as part of perceptual grouping, determines which neighbouring fragments in similar perceptual groups can and cannot be connected. Fragments are connected if the connection results in a smooth monotonic surface or contour.
(3) The HVS then interpolates between fragments, which satisfy relatability criteria to produce a continuous and smooth representation of a surface [Fantoni et al, 08]. Surface interpolation produces depth relationships and stores these in a shape representation - the full 2.5D Sketch.

6.4.1 Perceptual Grouping for Fragment Clustering

The HVS associates sets of similar fragments. The clustering of fragments is based upon the similarity of visible surface properties of the fragments. These surface properties include lightness, colour, texture, depth, luminance and velocity [Kellman, 03]. Even fragments which appear to be at different depths, separated by occlusions, may be perceived as belonging to a single object based on similar colour and texture. The types of similar visual patterns which the human visual system groups together are well summarized by the principles of Gestalt psychology [Wertheimer, 1923].

6.4.1.1. Gestalt Principles of Grouping

The German word Gestalt means “whole” or “form”. In the study of perception it deals with the completion of patterns of elements which are clustered by the HVS to create or infer a larger whole. Gestalt describes theoretical principles governing perceptual grouping and includes figure-ground organization and Pragnanz, which is the tendency of the HVS to favour regular, ordered, stable or balanced states [Wertheimer, 1923].

The Gestalt grouping principles, which describe the way the HVS distinguishes a whole from parts, depends on:

- Proximity: markings are grouped based on distance relationships between sets of markings, as illustrated in Figure ..

Figure . The Gestalt grouping principal of Proximity, describes perceptual grouping of objects based on distance relationships.

- Similar colour: objects with similar colours are grouped together as shown in Figure ..

Figure . Objects with similar colour are grouped together by the HVS.

- Similar size: objects with different sizes appear to be in distinct groups while those of similar size are associated with one another, this is illustrated in Figure ..

Figure . Objects with similar size are clustered together by the HVS.

- Common direction: objects moving in the same direction are perceived as a group, see Figure ..

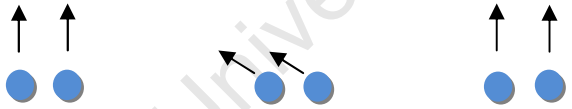

Figure . Objects moving along the same heading are seen as belonging to the same group.

- Good continuation: Figures or fragments are grouped by people when there is a *good continuation* between them. Good continuation occurs between fragments which when grouped result in a continued visual line. Under certain circumstances good continuation may leave an impression that a visual pattern continues beyond its visible end, i.e. viewers “fill in” the missing section of the pattern. Figure . illustrates this principle.

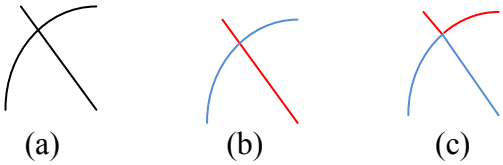

Figure . Two lines which overlap (a), are grouped as two smooth lines (b), rather than two sharp curves (c).

- Closure: objects are clustered if completion of the shapes creates an impression of an object. Closure and proximity may however be in contradiction, see Figure ..

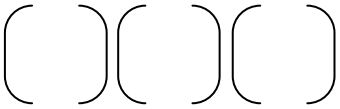

Figure . A completion of shapes or closure may cause objects to be perceptually grouped. Three sets of braces are seen rather than six disjoint curves.

- Common region: objects with a shared region of space are perceptually grouped. See Figure ..

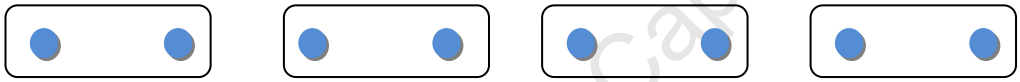

Figure . Objects in the same region are grouped.

- Element connectedness: objects that are connected with similar shapes may also be seen as belonging to a group [Rock & Palmer, 90]. See Figure ..

Figure . Element connectedness: the blue objects connected by the lines are seen as belonging to the same group.

- Similarity: Similar objects are seen as belonging to the same group. See Figure ..

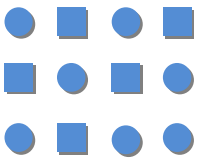

Figure . Objects with similar shapes stand out as a group. In the figure, although the objects are all similarly coloured, the squares stand out as a group distinct from the circles.

Textons are the basic elements in early (pre-attentive) visual perception which are grouped together according to the theory of Gestalt psychology. The background and distractors in an

image also affect perceptual grouping. Gestalt figure ground principles provide a theory for determining how background and foreground objects are distinguished. It is not certain how these principles combine and interact. Various factors influence the distinction between objects such as size and symmetry. Contrast is particularly important for allowing the HVS to distinguish objects.

6.4.1.2. Contrast

For a fragment or surface patch to stand out as distinct, there must be sufficient contrast locally around the fragment. Contrast in layered surface images varies significantly across an image of layered surfaces. Human contrast sensitivity in such images depends on the spatial frequency in the image [Peli, 1990]. People are more sensitive to changes with decreasing spatial frequency. Perceived contrast may thus be modelled as the ratio of the bandpass-filtered image to a low pass image filtered an octave below the local luminance mean. The final contrast at each pixel in an image is then reflected in terms of cycles per degree and luminance [Yee & Newman, 2004]. When there is low contrast sensitivity in the HVS, often more light is required to enable people to distinguish objects. Nonlinearites in the HVS are often simulated through a pyramidal image-contrast structure.

6.4.1.3. Computational Approaches and Models of Perceptual Grouping

Several computational approaches for perceptual grouping have been developed, including the Hough transform [Gillies & Khan, 1992], spectral graph theory [Sarkar, 2000] and various graph theoretical methods such as Zahn's minimum spanning tree method [Zahn, 1971]. The vision system of Lowe [1984] has a grouping component, which clusters points based on proximity and then connects gaps at various scales, increasing in size. Grouping algorithms vary based on pictoral data, type of learning and type of perceptual grouping which may be either attentive or pre-attentive. Though most algorithms are inspired by Gestalt grouping, they do not incorporate these principles and other theories of human visual perception. One approach which does mimic the HVS is FACADE, an artificial neural network "connectionist" approach to perceptual grouping that models several Gestalt phenomena [Raizada & Grossberg, 2001].

Treisman proposes that the HVS performs perceptual grouping using Feature Maps [Treisman, 1985]. The HVS places similar pictoral elements from a perceived picture into various feature maps (intermediate picture representations) based on features of the elements. Each feature map contains a set of similar features taken from the original image. The different feature maps correspond to similarity classes which preserve spatial layout of the visual fragments. Distinct classes are created based on form (shape), colour, size, brightness and orientation of objects. For instance, from an image containing a combination of red and blue squares and circles, four feature maps are generated, one with circles only, one with squares, one with red objects and one

with blue objects. An object may appear in several of these different feature maps. The spatial layout of the various objects is important since it influences how and which objects are perceptually grouped according to the proximity principal [Rome, 2001]. Feature maps are detected pre-attentively by the HVS [Treisman, 1985] and are created in parallel.

Feature maps and clusters of visually similar fragments correspond to sets of perceptual groups, which may pre-attentively stand out in the visualization. Determining which sets of objects perceptually correspond to a specific layered surface from the various feature maps may not be immediately obvious from inspection of a single feature map. Combining multiple feature maps may result in multiple potential groupings. A person looking at an image may identify several possible different target groups. An illustration of this is shown in Figure ..

Treisman's model of grouping in low-level human vision caters for this through the concept of a master map. This master map is used by the HVS to integrate multiple feature maps. A conjunction search in which a viewer searches for shapes that are both red and rectangular is an example of this integration. For such a search, elements from the colour and shape feature maps are merged through the master map. This search process requires focused attention and concentration, i.e. it is not preattentive.

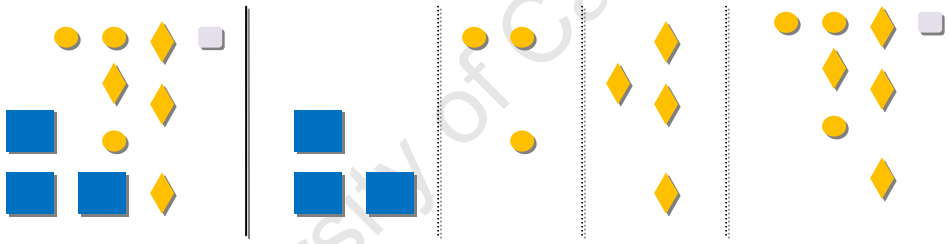

Figure . From the picture on the left (a), one may identify several groups (b) shows a grouping of blue squares, (c) a grouping of circles, (d) grouping of diamonds, (e) grouping of smaller brighter objects.

Another perceptual model is that of continuity grouping [Palmer, 83], which ensures that groupings form good continuations between neighbouring local regions in an image. Rome [01] proposes an algorithm for simulating perceptual grouping in vector graphics based on both feature maps and continuity grouping. This clustering algorithm is therefore based on more current theories of preattentive perceptual grouping processes rather than many of the aforementioned computational approaches.

Thorisson [1994] also presents an approach for simulating the pre-attentive gestalt perceptual grouping principles of proximity and similarity. The approach represents different objects as points in a multi-dimensional feature space by encoding the features of the different objects, e.g.

shape, size, colour (hue), brightness, orientation and texture. Multiple different groupings of elements can be obtained by running the algorithm. Limitations of the approach include that a fully connected graph is used to compute groupings. This causes an exponential growth in the number of graph connections with a linear increase in the number of objects. The approach is suitable for matching simple shapes. Complex shapes and those produced by layered surface visualizations however may result in significant grouping problems. Grimson's algorithm and many SFX algorithms do not deal with grouping and fragmentary processes, since they only compute shape for a single surface.

6.4.2 Relatability and Surface Interpolation

After grouping and segmentation have been performed by the HVS, it interpolates between similar clusters of neighbouring fragments to fill in the gaps between the fragments (*surface completion*). It uses geometric relationships among contours and fragments to guide segmentation and infer shape (depth relationships across the surface) [Kellman, 2003].

6.4.2.1. Surface Completion and Illusory Contours

The process of *interpolation* in the HVS by which visual fragments are connected to infer an understanding of a shape is known as v*isual completion*. There are two major forms of visual completion [Kellman, 03]:

- Modal (visual or sensed) Completion: fragments which are connected and interpolated are experienced as a physical visual stimulus. Modal completion through visual interpolation results in illusory contours - contours which are apparent, though no line is present [Saidpour et al., 1994].
- Amodal (non-visual or non-sensed) Completion: fragments are connected and interpolated but without a visual sensation of an interpolating contour or surface, e.g. occluding contours.

Figure . shows illustrations of different visual examples under which interpolation occurs:
(a) shows an example of a partial occlusion; amodal completion occurs for the occluded object.
(b) shows illusory contours; modal completion occurs for the white foreground object, amodal completion occurs for the black shapes.
(c) shows transparency.

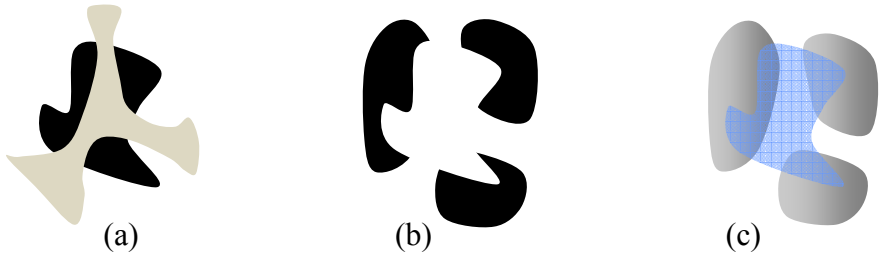

Figure . Visual Completion: (a) for occlusion – amodal completion occurs, edges are not perceived. (b) Illustrates illusory contours, the contours of the white figure though not drawn are vividly perceived. This is hence an example of modal completion. (c) Shows an example of transparency against which to contrast these forms of completion.

Modal completion is stronger than amodal completion, since an onlooker physically experiences a visual stimulus of a contour or shape. Figure . illustrates examples of visual completion:
(a) shows an example of modal (visual) completion. The edges and surfaces are visually apparent, even though they are not drawn;
(b) illustrates how illusory contours appear in the shape of a circle around the lines and at the interior, even though no physical line is drawn;
(c) shows an illustration of amodal completion, for an occluded object, for which the interpolation is nonvisual-not accompanied by a visual stimulus.

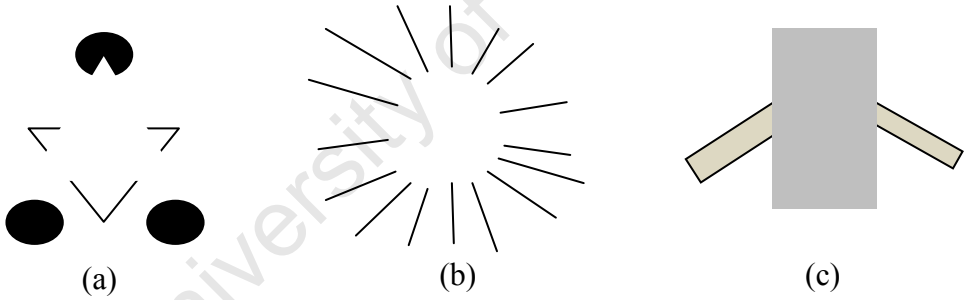

Figure . Visual Completion: (a) modal completion, for which edges of a white triangle are perceived, though not drawn (b) illustration of illusory contours in the form of an oval are seen in the center of the lines, (c) an example of amodal completion, occluded lines are not physically sensed, but can be mentally estimated [Kellman, 03].

6.4.2.2. Relatability

Surface fragments are only visually linked and interpolated by the human visual system if the fragments are *relatable*. Relatable fragments are similar neighbouring fragments which are oriented and positioned so that a smooth continuous curve or surface with no inflections can be fitted between them. The contour interpolated between relatable fragments:

- must be C^n continuous where $n \geq 1$; i.e. the interpolated surface must be at least once

differentiable and,

- the curve fitted between fragments must be monotonic (have no inflections) [Kellman, 2003].

Relatability corresponds to the Gestalt principal of good continuation. Fragments which trigger interpolation by satisfying relatability constraints are referred to as *inducing fragments*. Inducing fragments are fragments which cause the HVS to attribute object-ness or connect fragments to form a contour or surface. Non-relatable fragments do not induce an impression of object-ness, e.g. fragments offset in depth and which are not relatable are perceptually seen as two unconnected surfaces [Fantoni et al., 2008]. Inferring objects from fragmentary images requires significant concentration and mental effort [Fantoni et al., 2008], as was seen in the combined KV and Rocking experiment.

(1) 2D relatablity - Contour Interpolation

Contour interpolation occurs when inducing contours are perceptually connected through a smooth C^1 continuous monotonic path. Inducing contours may be edges or tangent discontinuities e.g. end-points and junctions [Kellman, 2003]. An additional criterion for such interpolation to occur is that the interpolated edges must not bend more than 90 degrees. When fragments are more than 90 degrees separated in particular two fragments on opposite sides of a peak a person can still imagine a peak, but this is almost a construction that requires mental effort, rather than an automatic smooth interpolation. Contour interpolation results in linear extensions in extended regions. Figure . illustrates different examples of both relatable and non relatable edges.

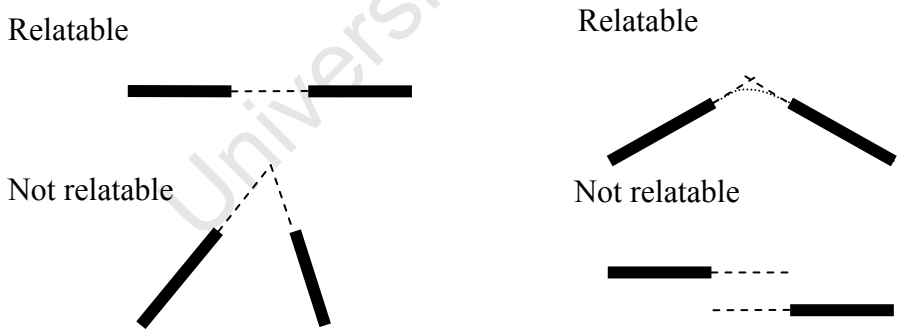

Figure . Illustration of contour relatability. Surface fragments are interpolated when the angle between the fragments is 90 degrees or more.

Relatability distinguishes between fragments which can be connected by interpolation and those which cannot [Kellman, 2003]. Interpolation strength between relatable fragments increases as the angle between the edges goes from non-zero at approximately 90 degrees to collinear. Interpolation strength decreases as misalignment between inducing parallel edges increases [Kellman, 2003]. Completion tolerates misalignments of parallel fragments with less than 15-20

minutes of arc [Hilger & Kelman, 05]. Interpolation strength between edges is proportional to $(L1 + L2)/(L1 + L2 + g)$ where $L1$ and $L2$ are the lengths of the relatable edges and g is the distance of the gap between the fragments. Both angular relationships and fragment lengths and separation distances affect the strength of interpolation [Kellman, 2003].

(2) 3D relatability – Surface Interpolation

While 2D relatability criteria define the geometric conditions under which edges are interpolated, 3D relatability constraints define when surface patches on a 3D surface are perceptually connected and interpolated [Fantoni et al., 2008]. Surface interpolation follows similar geometric constraints to 2D contour interpolation [Fantoni et al., 2008] but does not require explicit edges; in the absence of contours, interpolation is geometrically constrained by the spatial positions and orientations of the surface patches. Similar surface fragments in 3D, in proximity to one another are smoothly interpolated when the following geometric constraints hold:

- the curve between fragments has no inflections,
- there is no torsion between fragments, and
- the fragments do not bend through more than 90 degrees.

Further, a depth misalignment, or a misalignment in the image plane, or opposite inclination of fragments around the horizontal axis beyond 90 degrees, or a twist around the vertical axis will cause 3D surface relatability to break down [Fantoni et al, 2008]. When this happens, even similarly coloured patches without visible edges and significantly offset in depth, which are near to one another, may appear to belong to separate surfaces [Fantoni et al, 2008]. These constraints indicate that interpolation occurs when a smooth monotonic (no inflections) surface can be formed between fragments [Kellman, 2003].

Psychophysical research has shown that the slant, more than the tilt, of surface patches plays the significant role in surface interpolation when there is no edge information; sensitivity and speed in psychophysical experiments performed by Fantoni et al [2008] were worse for patches with horizontal tilt. The experiments showed, further, that people are able to infer the shape of a surface more accurately and quickly when patches are relatable since in the experiments 3D relatable patches yielded significantly improved performance for a classification task [Fantoni et al, 2008] than for non relatable patches.

(3) Spatiotemporal Relatability – Shape from Motion Interpolation

The above forms of relatability criteria describe conditions under which interpolation occurs between static fragments. The HVS also interpolates across gaps between surface patches which are in motion. Random dot displays, in which random dots are set in motion over some surface or are fixed to a rotating surface, have illustrated this; viewers perceive a continuous smooth surface

in 3D rather than just seeing a set of moving dots. An example of this is an experiment by Saidpour et al., [1994], in which viewers interpolated smoothly curved surfaces across and between two planes slanted at different orientations and separated by a gap. The planes were visually represented with dots. The planes (dots) were rotated about a vertical axis. The factors, which influenced interpolation of the surface in the region of the gap between the planes, depended on the slope of the planes, density of the dots and the gap size, but not on the orientation of the edge or axis of rotation between the planes. This interpolation agrees with the theory of perception of 2D interpolation proposed by Ullman, [1976] and, Kellman & Shipley [1991]. It matches Grimson's [1981] model of 3D interpolation, which fits a smooth surface through a set of dots that minimizes the quadratic variation.

Interpolation of a surface between dots also occurs between visible fragments in successive frames [Palmer et al., 1997]. For this interpolation to work, the dots should not move too fast or too slow. Further, a "building up" time is necessary for mental generation of a surface representation from moving points [Treue et al., 1991]. Point lifetimes needed to be at least 125 milliseconds (ms) to provide a precept of shape. These experiments were for rigid body motions (rotations) which cause the KDE. Other factors that influence surface interpolation and estimation for dots in motion include the projected velocity of the dots which influences the perceived depth of the dots [Saidpour et al, 92]. A temporal averaging process affects the perceived relative positions of fast moving objects visible for less than 500 milliseconds (ms) [Krekelberg & Lappe, 1999]. Spatio-temporal interpolation better explains spatial offsets in positions for slow moving objects visible for more than 500 ms [Fahle & Poggio, 1981]. The faster an object moves the more it reduces luminance of an object, which in turn increases visual latency.

6.5 Summary

This chapter has presented a background in perceptual research upon which a meaningful computational measure for determining the perceptual effectiveness of a layered surface display can be built. This review has shown that the HVS performs surface interpolation across fragmented input, typical of layered surface renderings, according to relatability criteria. The perceptual interpolation process attempts to fit a smooth monotonic surface between separated fragments, which have been perceptually grouped based on similarity of the markings and spatial position, according to Gestalt principles. The depth of the interpolated shape depends on the depth of the fragments, which is determined by interpreting and combining various depth cues. Shape from X algorithms may be used to computationally determine the perceived depth of fragments in an image. This perceptual theory of the HVS is used as the basis upon which a computational framework is developed to mimic human visual perception of layered surfaces presented in the next chapter.

Chapter 7

Framework for Simulating Perception of Layered Surfaces

Chapter six presented the difficulty in evaluating layered surface visualizations: there are a large number of visualization parameters over which the visualizations should be compared; testing visualization for various combinations of parameters would require numerous psychophysical experiments to be run; and such experiments, as seen in chapter 5, are fatiguing, and time consuming.

As a solution to this problem, this dissertation proposes a perceptual framework for automatically measuring the effectiveness of marking-based layered surface displays. Perceptually measuring the effectiveness of these visualizations is achieved through the implementation of a model of the processes and representations used by the human visual system, which infer shape from images of layered surfaces. This model incorporates the perceptual theory of surface completion and perceptual grouping, presented in chapter 6, used by the HVS to piece together fragmentary surface patches in rendered images of layered surfaces. The framework is useful for automatically optimizing the parameters of layered surface visualizations. Our framework and its use to optimize and measure the effectiveness of layered surface displays are both novel and significant contributions to layered surface visualization.

7.1 Review of the Purpose and Objectives for Optimizing Layered Surface Displays

Computers are well suited for arduous, repetitive and mundane tasks such as processing multiple images. An automatic measure of the effectiveness with which a visualization is able to "perceptually" illustrate layered surfaces would be of significant benefit to users of layered surface visualizations. It would allow perceptual experiments to be run without the need for human participants and optimizations to be performed. For instance, such a measure could be used to find and optimize the settings of layered surface displays so that they work near optimally before a person even begins to explore their data. This would be useful to medical doctors and scientists who want to immediately see their data, without having to tune their visualization by changing multiple display parameters for each of the surface layers.

Re-implementing a complete computational model of the human visual system and how it processes and completes partially occluded surfaces is a task beyond the scope of this thesis. We do, however, in this research contribute a framework, which takes into account perceptual theories and models that mirror the way the HVS performs layered surface inference. This framework is particularly focused on perception of opaque marking-based layered surface displays and takes a step towards the challenge of simulating the HVS for the purpose of measuring the effectiveness of such visualizations.

A high-level computational approach is taken and several assumptions made to make the challenge of modelling the HVS tractable. Our work builds on the computational theory of the major processes and representations of the HVS used in Grimson's [1981] model. It extends this model for processing fragmentary input, in particular for opaque markings in layered surface renderings. The model leverages our particle system visualization design presented in chapter 3. The perceptual theory set forth in chapter 6 provides a basis for our framework and serves as an abstract computational theory for solving the problem of calculating 3D surface representations from 2D projections of fragmentary patches. Grimson's model, upon which we build, being modular, caters for our own layered surface extensions and is further extensible for future advances in perceptual theory of the HVS that may both refine and extend the model to better simulate human perception of layered surfaces.

The aim of our model is to quantitatively measure how well a layered surface display visually conveys a set of layered surfaces. It aims to capture and reflect something of the contribution elements of motion, patch type and size of markings make towards an accurate perception of layered surfaces. If the measure correlates to the performance of respondents in psychophysical experiments, then it may be used to automatically optimize the settings of a visualization. An evaluation of the framework is reported in chapter 8.

7.2 Framework for Computing Perceptual Surfaces from Layered Surface Renderings

Figure . shows the major perceptual processes, representations and architecture that are incorporated into and modelled in the framework.

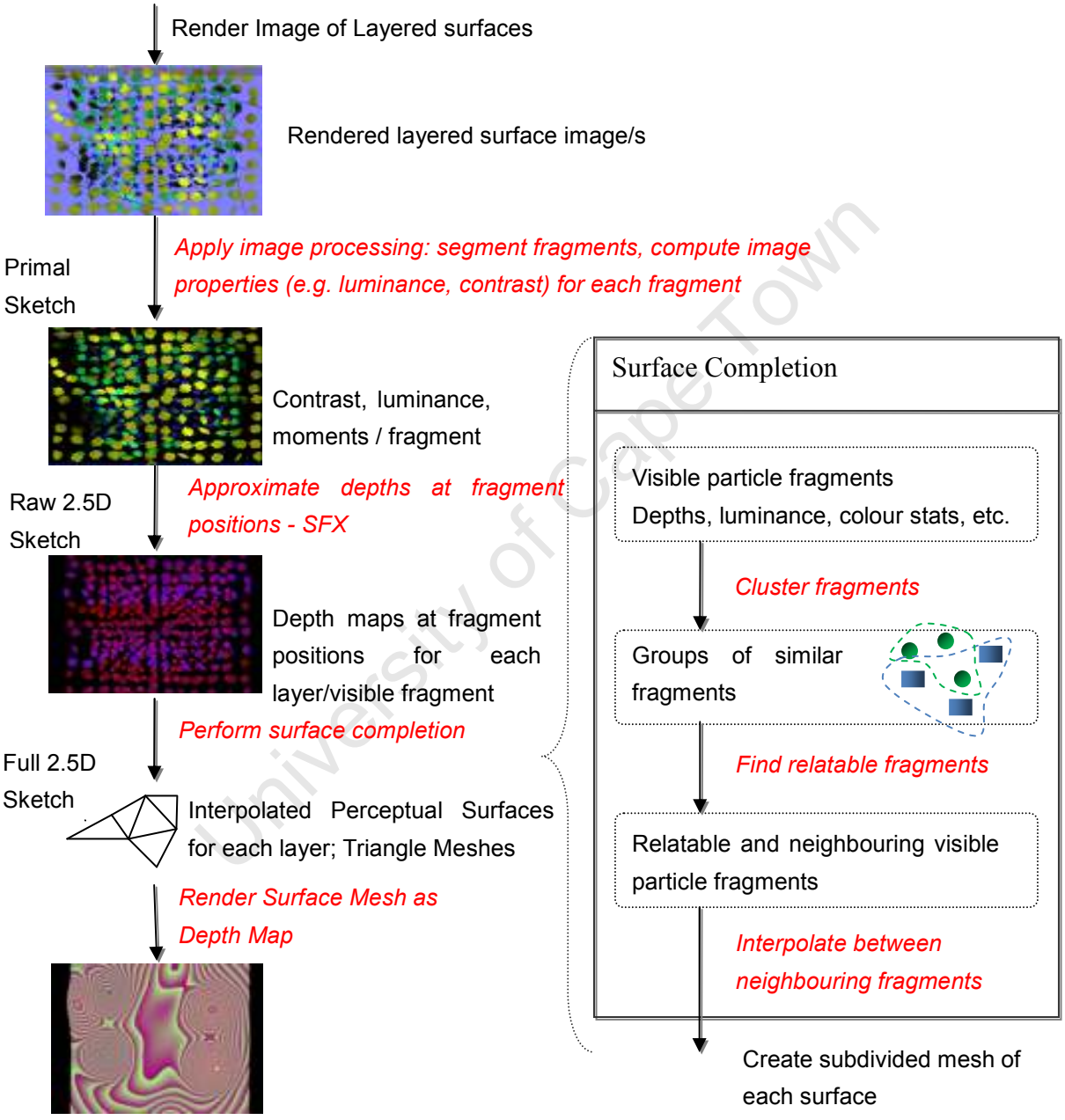

Figure . Algorithmic outline of our perceptual framework for processing layered surfaces. The model mimics the processes of the HVS for layered surface reconstruction. Transformations are shown in black, representations in orange with italics. The process produces surface meshes for each layer in an image of layered surfaces.

The framework takes as input one or more 2D images of fragmented layered surfaces rendered by a layered surface visualization. It produces a set of 2.5D surfaces and depth maps from these 2D projections of the layered surfaces in the rendered images. These 2.5D surfaces computed by the model are intended to be representative of a person's perception of the surfaces as seen in the images. The following processes and representations, illustrated in Figure . are used:

(1) Firstly, an image processing step is applied to the rendered image/s of the layered surfaces. In this stage segmentation is performed through which edges, contours and fragment patches are found that correspond to the opaque markings on the surfaces. Various image statistics such as the percentage visibility of each marking and average luminance are computed. This stage corresponds to the HVS processes which compute the Primal Sketch in Grimson's [1981] model. Normalized values of these various statistics are computed.

(2) Next, the original image and various features from the Primal Sketch are used to approximate the average depth and orientation at the position of each visible opaque marking. A relative depth map may be computed by applying a Shape from Shading algorithm or other SFX algorithms to the rendered images. Shape from Shading algorithms produce only relative depth maps rather than absolute depth values. It is the depth from stereo and motion that give more absolute depth estimates. In our model, SFX algorithms are left for future work, we instead make the assumption that stereo contributes absolute depths, which allows us to compare the reconstructed surfaces to the original surfaces. The depths from the SFX algorithms are scaled and normalized. The various scaled depth maps produced by the SFX algorithms and the various statistics for each visible fragment from the Primal Sketch are combined to stochastically approximate perceptual depth. This yields the various depth values at the visible fragment (opaque marking) positions. The depth values correspond to the raw 2.5D Sketch in Grimson's [81] model of the HVS.

(3) The final processes perform surface completion. The 2.5D Sketch and image statistics from the Primal Sketch are used to fill in the gaps between visible fragments and approximate a perceptual surface. The full 2.5D Sketch is similar to the surfaces as perceived by the HVS. This final surface completion stage consists of the following sub-processes and representations:

   (a) Fragments are clustered, based on various image statistics found in the Primal Sketch and by depth. This produces groups or clusters of similar fragments. A Delaunay Triangulation (DT) is computed for each cluster to identify neighbouring fragments.

   (b) Relatable fragments within clusters are identified by testing if a pair of connected fragments in the DT satisfies relatability criteria. Relatability modifies the way in which interpolation is performed between neighbouring fragments; for non-relatable neighbouring fragments, additional points are inserted half way between the pair of relatable fragments which serve to create an extrapolation of the surfaces from those points.

   (c) Finally, smooth continuous surfaces are interpolated through the points.

(4) The interpolation across the surface points is used to produce a discrete representation of the surfaces. The representation is a subdivided mesh with points that lie on the interpolated surface. From this mesh a depth map of the perceptual surface is rendered which can be compared to a depth map rendering of the original surface.

Step (3) above corresponds to the interpolation step in the perceptual model proposed by Grimson [1981]. The approach however, extends Grimson's model, which only interpolates between the points in the raw 2.5D sketch for a solitary unfragmented surface. The model presented in this dissertation caters for the kind of fragmentary input common to opaque marking-based layered surface visualizations. For this reason clustering and relatability criteria are incorporated into the model. In this approach, based on Grimson's model we assume that the HVS is able to interpolate a global smooth surface. This however may not be the case since people rocking and visual illustrations to help formulate a perception of a surface. From the experiments and this research I speculate that people at least develop a local impression of a surface upon which their attention is focussed.

A set of perceptual surfaces or representations of the Full 2.5D Sketch are produced by the model. These perceptual surfaces are triangulations of the surfaces interpolated across various sets of clustered points. A mesh is generated by subdividing the points of the triangulation and interpolating the value at those points. This produces a set of discrete depth maps which represent the surfaces from a given view point. Accurate depth maps of the original surfaces are also computed for comparison.

The differences between the complete perceptual surface depth maps and the depth maps of the original surfaces are computed. These differences serve as the measure for evaluating the effectiveness of the display. This measure and a global shape comparison measure are presented in section 7.3. The measure is then used to optimize the display parameters of the visualization technique. The implementation of the optimization framework and use of the novel metric is described in section 7.4. Though the framework is extensible to oblique views, the initial implementation of the framework, developed as a proof of the concept, addresses top down views of layered height field surfaces. The various stages and implementation of the perceptual model and framework are explained in greater detail below.

7.2.1 Primal Sketch Processes and Representations

The models and processes of the HVS set forth by Marr and Poggio, [1977] and Grimson [1981] identify the Primal Sketch as the first significant representation computed by the HVS. The computational model of Grimson applies image processing to an image of a single surface and extracts edges and above threshold differences in surface variations to give the Primal Sketch. Although such image processing for edge detection, feature correspondence and filtering could

be extended for processing projections of opaque markings and be incorporated into our framework, it is not necessary. This is because our layered surface visualization renders the fragments. This allows us to, in addition to rendering the layered surface image, render an image containing fragment identification numbers. These identification numbers are used to associate pixels in various images with fragments. A single pass through the images allows image properties and image statistics to be aggregated for each fragment. Applying the algorithm to images of layered surfaces without a tight coupling to the renderer would require implementation of additional image processing and segmentation algorithms, which would be beyond the scope of this dissertation.

We extract the following information from the Primal Sketch for each visible fragment (opaque marking):

- percentage visibility,
- average and standard deviation in luminance,
- average and standard deviation in colour (hue),
- image moments (image position, aspect ratio, orientation), and
- average and standard deviation in local contrast.
- edges and contours.

Building the perceptual framework on top of the visualization design presented in chapter 3 allows this information to be acquired through various rendering passes of the particles (opaque markings) with minimal image processing. This image processing includes computation of contrast and image moments for each fragment. The rendering passes and image processing are described in more detail next.

7.2.1.1. Rendering Passes

The necessary Primal Sketch information is readily available to the visualization design proposed in chapter 3, through various rendering passes. Figure . shows the various
images which are rendered in order to compute image statistics for each visible fragment. The following sets of rendering passes are performed for all the fragments on all the layers with depth ordering:

(1) The opaque markings on the layered surfaces are rendered together. This is the layered surface image rendered by the visualization technique.
(2) Luminance is computed for each pixel of the layered surface image made in step (1). These are stored in an array – a luminance map.
(3) Particle identifier numbers are rendered, which correspond to the opaque markings in the layered surface image in (1). This allows for per pixel association between the visible markings and the original particles. This association is useful for computing image statistics for visible fragments.
(4) Silhouettes and edges of the layered surfaces are rendered to an image using pixel shaders.

A distance map/image can be computed for these which stores image space distances for each pixel in an image to the nearest edge or silhouette. This distance map may be used to infer surface orientations and depth relationships at and around the silhouettes. Though implemented, this part of the framework was not necessary for the top down views, which have no silhouettes.

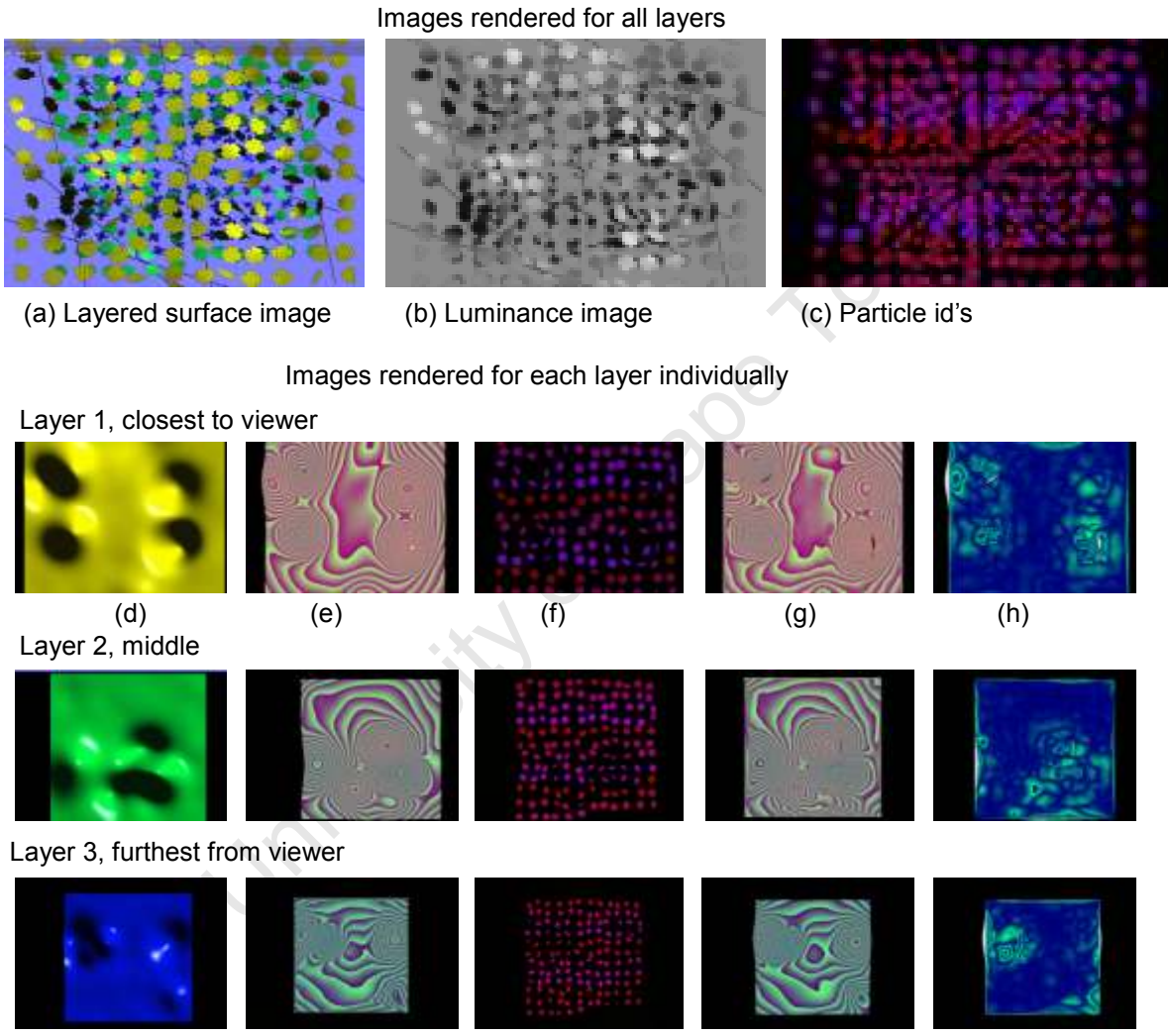

Figure . Rendering passes of the layered surfaces which contribute to the Primal Sketch. (a) shows the original layered surface image of all the layers rendered by the visualization algorithm; (b) is a luminance map of image (a); (c) is the identification map for image (a), pixels corresponding to markings store a particle id number. Images (d) to (h) are rendered for each layer individually. (d) is a rendering of the surface; (e) is a height map of the original surface; (f) is an identification map for particles on the layer, for all particles; (g) is a depth map of the perceptual surface; (h) is the difference between (e) and (g), which is used to calculate how well that layer is perceived.

The following set of rendering passes are performed for the fragments on each individual layer by itself, with depth ordering:

(1) Particle identification numbers for each fragment on each surface are rendered. These images are used to determine the maximum number of visible pixels for each fragment. These are tallied together with the number of visible pixels for each fragment in the rendered layered surface image (1). This serves to calculate the percentage of each fragment that is visible.

(2) Though not needed for the primal sketch, each ideal surface on its own is rendered as a depth map. The difference between this and the reconstructed perceptual surface from the layered surface image is used in the metric to compare the actual surface with the perceived surface.

7.2.1.2. Image Processing

Once the rendering passes have generated the various intermediate images, image processing is used to sum the visible pixels for each fragment/particle and compute image statistics for each fragment. The percentage visibility and statistics on fragment position, hue and colour are determined in this step. A list of pixel positions and luminance values are stored for each visible fragment. For animation, these statistics may be monitored over successive frames. Image moments are found for each fragment individually, by integrating over the pixels associated with each visible fragment [Freeman et al., 1998]. These pixels are gathered in the image pass that matches pixels to particles.

For oblique views which have silhouettes, a contour/silhouette image may be rendered, from which a distance map is computed. The pixel image distances from these occluding contours are computed by firstly identifying and creating a list of the pixel locations containing silhouettes. These are all given the value zero (identifying that these pixels correspond to a feature). An iterative process is then started in which all neighbouring pixels to the current features on the list are determined. These pixel positions are then added to the list, but with an incremented count (e.g. 1, for a distance of 1 pixel from the original features). The entries on the list with zeros are removed. And the process is repeated. If a neighbouring pixel already contains a value it is not placed on the list. The process is repeated until there are no more pixels to update. A figure of such a distance map is shown below in Figure ., which illustrates computation of the distances from the silhouettes.

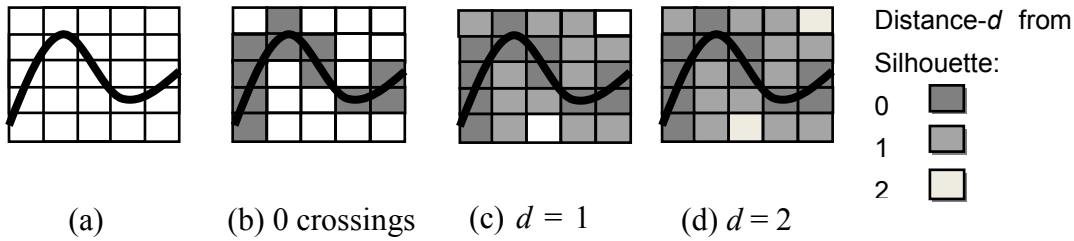

Figure . Distance map computation around silhouettes. (a) Silhouettes/edges are rendered. (b) Zero crossings marked. (c) Pixels next to zero crossings, at a distance of 1 are found and placed on a list. (d) Non-marked neighbouring pixels next to pixels at a distance of 1 are found. These are at a distance of 2 from the silhouettes. This process repeats until all pixels have been assigned a distance.

Computing the percentage visibility of each fragment and summing over all the particles gives useful statistics for the number of visible, partially occluded and fully occluded particles. These images and statistics are used in subsequent stages of visual processing and may be useful as an alternative measure of the effectiveness of the display. Contrast for each fragment is also computed. Fragments with contrast below a certain threshold are ignored from further processing, since these will be overlooked by an observer. We use a spatial frequency hierarchy to compute local image contrast using a normalized Contrast Sensitivity Function (CSF). Our framework uses Yee and Newman's [2004] approach of building a Laplacian pyramid by vertical and horizontal convolution of the luminance image with a Gaussian filter, w = [0.05, 0.25, 0.4, 0.25, 0.05]. This gives band passed frequency details, which are useful for later transformations and processing steps; for instance, transforming the image to the frequency domain is also useful for recovering shape from texture and shading.

7.2.2 Raw 2.5D Sketch and Representation

From the primal sketch and rendered image, the depths at each visible fragment (opaque marking) position are determined. This stage mimics how the HVS creates a depth map in one of its early processing stages [Grimson, 1981] [Kellman, 03]. This depth map is computed from the original rendered image. An approximate depth map may be determined computationally through any Shape from X algorithm (SFX) or combination of SFX algorithms. When using Shape from Stereo or Shape from Motion algorithms, depth positions are determined from matched corresponding points and edges found in the Primal Sketch.

The depth of the layered surfaces can only be approximated at the fragmentary visible patches in the image. This, in itself, may ill-affect standard SFX algorithms, especially in that each visible fragment patch seen in the image as a small area of pixels, corresponds to a small part of a region of each surface. Further, these patches are not continuous across a single surface in the image but are now dappled over different surfaces. Neighbouring pixels in the rendered image may

therefore belong to two different patches at varying depths. To the best of our knowledge only the mixture model approach to SFT of Black and Rosenholtz [1995] is able to reconstruct shape from occluded textures. SFX algorithms need to be adapted to process such layered surfaces. Further, the HVS out-performs current SFX algorithms, in that it is capable of distinguishing depth and establishing ownership of visibly fragmented patches belonging to various surfaces. In this framework, we assume that depth is relatively accurately estimated by observers, since rocking, stereo, shading and other depth cues are all used. Feeding depth values through the framework based on this assumption, rather than modelling these very relevant processes of the HVS for the task could well influence the validity and effectiveness of the model. However, the complexity of modelling the interactions of the various visual effects is beyond the scope of this work and is therefore left for future work. Implementations of shape from shading and shape, texture and stereo algorithms that model, specifically the way fragmentary type input of layered surface images is combined by the HVS, will likely significantly improve our model.

The HVS combines multiple depth cues to approximate the depth of objects in a scene [Lyness, 2004]. Future work should model the way the HVS combines multiple depth cues. Such a model should specifically consider visible depth cues of stereo, rocking (KDE), motion parallax, shading, texture gradient, relative size and occlusion, since these influence depth perception the most for exploratory tasks. When combining cues, it is important to realize that partial occlusions contribute to relative depth ordering of fragments, while the cues of stereo and motion provide a more absolute sense of depth. Further, the cues work together depending on how much of a fragment is visible. Particles for which depth is unclear, or which are confused as belonging to the wrong layer are ignored. Removing these from the depth computation across the face of a surface lets the neighbouring fragments, which more clearly convey depth to establish the shape of the surface.

7.2.3 Approximating the Full 2.5D Sketch through Surface Completion

The HVS infers a complete surface from the set of fragments and depth maps that make up the raw 2.5D sketch. The surface completion process which infers the complete surface firstly clusters groups of visually similar fragments according to Gestalt principles. Surface interpolation is then performed across these clusters. Smooth interpolation is performed between neighbouring fragments, which satisfy relatability criteria. Non-relatable fragments, when appearing as belonging to different surfaces (i.e. not satisfying relatability criteria) are extended to a midpoint between the fragments. These processes of surface completion are implemented in our model as illustrated below in Figure .

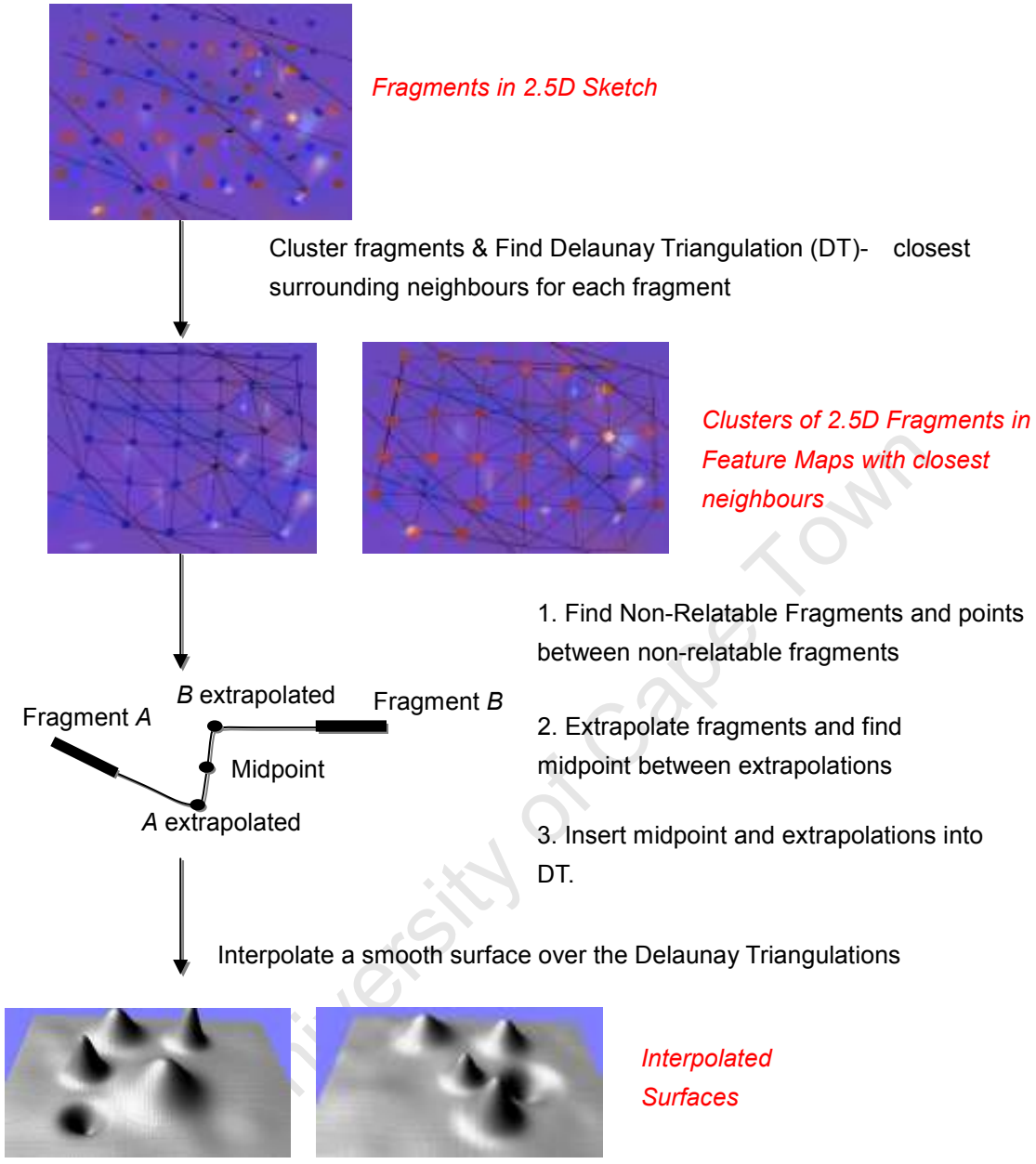

Figure . HVS Processes modelled for Surface Completion. Fragments are clustered by luminance, colour, depth etc. A Delaunay Triangulation(DT) is then found between the points in the DT for each cluster, to give the closest neighbouring fragments. Neighbouring fragments which do not satisfy relatability criteria are then identified and additional points inserted to simulate the perceived difference between surfaces. This is achieved by extrapolating the fragments towards their midpoint. Two points are inserted into the DT on either side of the midpoint and the midpoint of these extrapolations found and inserted into the DT. A smooth surface is finally interpolated across a subdivided DT for each surface.

The framework presented in this dissertation includes implementations of the processes illustrated in Figure .. For purposes of keeping the development of the framework tractable, we use simple implementations of these processes, in particular we use MacQueen's [1967]

K-means algorithm for clustering. Other models of these processes which more closely replicate the underlying processes of the HVS that are not used, such as Thorisson's [1994] and Rome's [2001] model of perceptual grouping of 2D graphic elements, may be incorporated into the model in the future. Implementations of the various surface completion processes included in this framework, used to determine the full 2.5D perceptual surface (the Full 2.5D Sketch), are described below.

7.2.3.1. Clustering Fragments

Computationally modelling the HVS processes of surface completion firstly requires that visually similar fragments are grouped together. Treisman's [1985] model of the HVS perceptual grouping processes, which perform feature integration, accessing and combining elements, of various feature maps, through a master map is modelled in this work; several visual properties of fragments are combined through a multidimensional clustering algorithm to determine a set of clusters of visually similar fragments. Treisman proposes that a master map allows a person access to the various individual feature maps or combinations of these maps. A viewer attentively merges these to determine fragment-surface ownership. This process of combining fragments from different feature maps is simulated by applying K-means to multiple pre-selected visual features.

In the layered surface visualizations produced in this thesis, viewers are directed to focus primarily on colour and motion to differentiate which fragments combine to form distinct surfaces. It is thus assumed that focused visual attention will be directed towards the feature maps of hue and motion. Shape, depth and brightness also significantly influence association of markings, since layers are at perceptually different depths and may have different marking types (crosses or patches). Depth is taken into account as a clustering dimension, because rocking is used, since it provides arguably the strongest distinction between markings on different layers. When stereo and motion parallax are used, depth should also be used as a dimension for distinguishing groups of markings, since 3D depth is a gestalt perceptual grouping property.

The visual attributes used as clustering dimensions are computed for each fragment prior to clustering as image statistics in the initial processing steps for the Primal Sketch. These values may either be standardized and scaled relative to the standard deviation and mean value for all fragments to allow for meaningful cross-variable comparisons, or weighted to model variable contributions of different visual features to perceptual clustering.

Clustering algorithms identify groupings of multidimensional data points. The groupings are based on the commonly used Euclidean distance similarity measure. This similarity measure directly correlates similarity between points to the distance between them.
In this work we use the K-means [MacQueen, 1967] clustering algorithm, to simulate perceptual

grouping of sets of visually similar fragments. K-means is an unsupervised learning algorithm. The K-means algorithm receives as input a set of *m*-dimensional points and an integer value *k* which is the number of clusters to be created. It clusters data by iteratively minimizing a squared error function, which is typically based on the sum of the distances between the data points and the cluster centers. This algorithm was selected since an implementation was readily available and the algorithm is well-established and it is also considered a good algorithm to test against. K-means does, however, have the shortcoming that *k* (the number of clusters) has to be specified. Further, it may find only a locally optimal solution. Alternative clustering algorithms overcome these flaws by dynamically finding the best number of clusters. However, many of these algorithms do not find the optimal distribution of elements in clusters. While many clustering algorithms make the trade off either to determine the optimal number of clusters or to optimally cluster the data points for a fixed number of clusters, some hybrid approaches such as PSO clustering algorithms [Omran et al, 05] are able to dynamically find the best number of clusters and also an optimal assignment of elements to clusters.

In our approach, using K-means to simulate the integration of feature maps through a master map is achieved by passing the set of all visible fragments into the clustering algorithm. Fragments are represented as multidimensional points. Each dimension of these points corresponds to a visible feature (feature map) of a fragment, such as hue, luminance and depth. If the markings are moving, motion type or direction may be added to this list. The number of clusters, K, is set equal to the number of layered surfaces because the viewers know the number of layers they are searching through and attempting to associate fragments with. This may well correspond to the way observers cluster fragments perceptually. Thorisson's [94] algorithm which uses second-order differences and proximity weighting to delineate distinct sets of clusters which correspond to perceptually significant Gestalt groups could be implemented in the future as an alternative clustering approach to more accurately cluster fragments, in terms of modelling perception.

Once fragments have been assigned to various feature maps, the visible image positions of each fragment are used to construct a Delaunay Triangulation over the set of fragments. Delaunay Triangulations are used to identify neighbouring fragments in the final clusters. Rome's [2001] model of perceptual clustering includes proximity grouping and continuity grouping. Extending the model in this way is left for future work. Good continuity can be checked by comparing neighbouring fragments and determining if they satisfy continuity criteria. Nearby neighbouring fragments in the clusters are tested for good continuation based on relatability criteria. Proximity grouping is not explicitly implemented in this version of the framework, though proximity in terms of nearby neighbours is found in each cluster through the Delaunay Triangulations. Clustering based on Gestalt perceptual spatial patterns (e.g. objects aligned in rows) is left for future work.

Perceptual clustering, in addition to being a step towards surface completion, may be useful for debugging layered surface visualizations by identifying sets of fragments, which are likely to be perceptually grouped together and which do not belong to the same surface. Tallying up fragments which have been associated as similar but belong to different surfaces, serves as an additional error metric for identifying misassociations of fragments. We do this by comparing each pair of neighbouring fragments (edges) in the Delaunay Triangulations. These edges are tagged and tallied in cases where the fragments do not belong to the same surface. This provides an indication of potentially poor clustering that may occur in the visualization. An illustration of this is shown in Figure .. The tagged edges can optionally be displayed for debugging purposes.

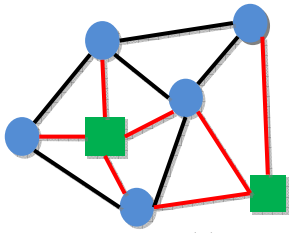

(a)

Figure . (a) A Delaunay Triangulation is constructed between fragments which have been clustered together. Fragments from one surface are indicated in blue, fragments from another in green. Counting the number of edges between fragments which are from different layers, provides a measure of the clustering errors. Red lines indicate clustering errors.

A person performs various perceptual groupings most effectively at the center of the field of view, i.e. the observer's point of focus in an image. It may be perceptually more correct to associate locally similar patches together and construct a larger interpretation of the layered surfaces from these sub-surface regions. A VDP, which takes into account spatial distortion in the visual field, may be useful to more accurately model this aspect of perception. The VDP may be used to modify an input image to represent distortion of properties as a result of position in the visual field. This work however, being a first attempt at perceptually measuring the effectiveness of layered surface displays, simply assumes that the K-means algorithm can be applied broadly across a set of fragments.

Computationally modelling clustering of markings raises the question: how are surfaces pieced together, when clusters from different layers are associated wrongly? Do the surfaces perceptually appear to vary in depth i.e. appear jagged, or does the orientation of the miss-associated marking appear adapted to its neighbours to make the most sense, or does the marking appear in the plane. There could be a depth modification, orientation modification, or discontinuity in the surface. We assume miss-associated fragments are seen as lying in the plane (ignored), while the correctly associated markings convey the shape.

7.2.3.2. Identifying Relatable Neighbouring Fragments within Clusters

Once a set of fragments has been associated with a layer, the DT of the positions of those fragments is computed. This gives the nearest surrounding neighbouring fragments for each fragment. It is necessary to identify which of these neighbouring fragments are relatable, in order to model surface completion accurately and similarly to the HVS. DT identifies points between which the surface should be constructed (interpolated).

The model proposed in this work deals with a top down perspective view of layered surfaces, represented as height fields. This removes the need for handling cases where fragments which lie on peaks on opposite sides of a valley are considered neighbours by the DT. An example of this case is illustrated in Figure .. A surface must not be interpolated between these neighbouring fragments from a side on view point. Further, the model assumes that the surfaces are without holes, which allows straightforward application of the DT. Surfaces which fold back on themselves and other difficult cases arising from convexities would need to be tested for and handled specifically. This is left for future work.

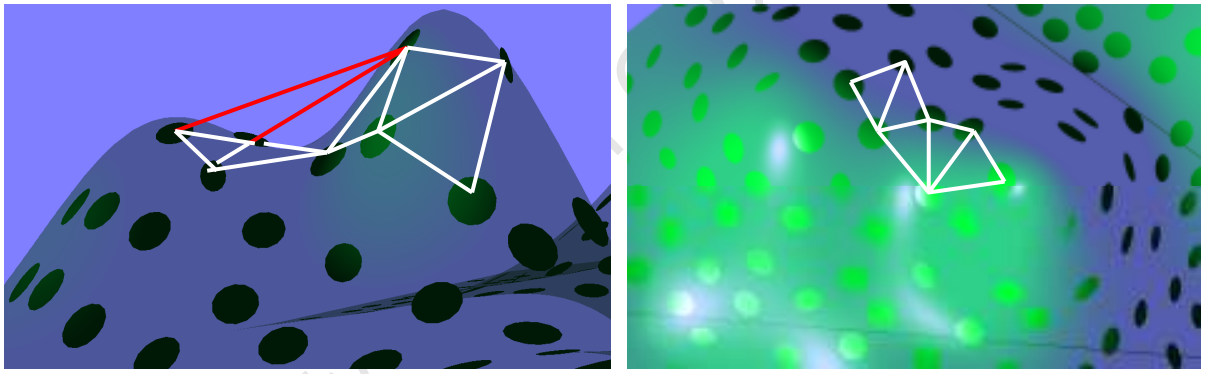

Figure . Delaunay Triangulations of frontal views of height fields may produce incorrect associations of visual points (left). In this picture red lines indicate neighbours in the DT, which should not be interpolated between. DT's of top down views provide correct neighbour relationships (right).

Before surface interpolation can be performed accurately it is necessary to determine which fragments are relatable. This is because relatability modifies the way in which interpolation occurs between neighbouring fragments; for non-relatable neighbouring fragments, additional points are inserted half way between the pair of relatable fragments. This serves to create an extrapolation of the surfaces from those points towards one another. Figure . illustrates how this extrapolation would work in the plane. The edges of neighbouring, but non relatable fragments, are extended to the point where visually one of the surfaces overlaps the other, i.e. half way between the two neighbouring points, whereas relatable points can simply be smoothly

interpolated [Fantoni et al, 08].

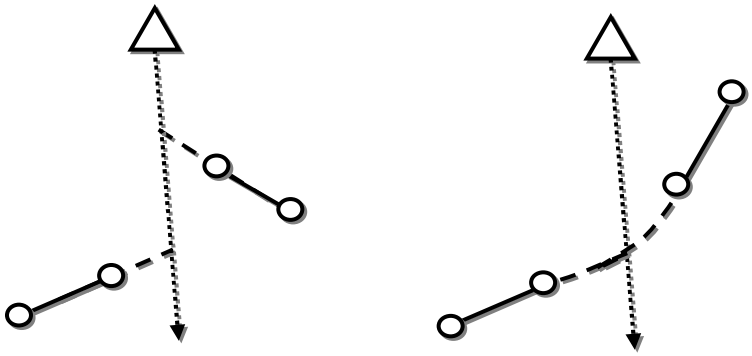

Figure . Perceptual completion between non relatable points is achieved by extrapolating surfaces at end points (left). A surface between relatable points is completed through smooth interpolation (right).

Orientation of fragments was assumed to be approximately accurate and therefore the actual orientation of fragments was used. SFX algorithms should be used in the future to simulate HVS approximations of perceived fragment orientations. Near parallel fragments are tolerated as relatable if the misalignment between the fragments is less than 15-20 minutes of arc [Hilger & Kellman, 05]. This is tested for by identifying neighbouring fragments which are oriented almost parallel to one another. If the angle between these fragments relative to their average orientation is less than 18 degrees, the fragments are considered relatable. If the fragments fail this test, then they must pass the dot product test to determine if a monotonic smooth surface may be fitted through them.

Relatable fragments within clusters are identified by testing if a pair of connected fragments in the DT satisfies realatability criteria. Two neighbouring fragments in the DT are relatable when:

- The curve between the fragments has no inflections,
- there is no torsion between fragments, and
- the fragments do not bend through more than 90 degrees.

A rough approximation of these conditions is tested by the following application of the dot product. If the dot product between the vector connecting the fragments and the normal of either fragment is less than zero (the angle between these lines is greater than 90 degrees) then the fragments are not relatable. This test is applied for reasons of simplicity and does not require testing for torsion of alignment of planes. This rule is illustrated in Figure .. In our implementation we consider fragments relatable up to 100 degrees. This grace on the angle between the normals is given, since the surfaces are rocking, and under motion orientation estimates are not as accurate as when surfaces are static. 10 degrees is used since it is less than the average orientation error of participants in the Rocking vs. KV experiment. The dot product test

in figure 7.8 could end up encountering small perturbations when fragments are very close to perpendicular. This would result in instability classifying such fragments as being relatable or not.

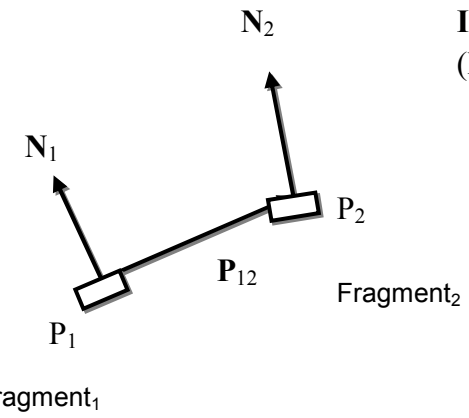

If ($\mathbf{N}_1 \cdot \mathbf{P}_{21} >= 0$) and ($\mathbf{N}_2 \cdot \mathbf{P}_{12} >= 0$) and ($\mathbf{N}_1 \cdot \mathbf{N}_2 >= 0$) **Then**

Fragment$_1$ and Fragment$_2$ are relatable

Figure . Testing if two fragments are relatable using the dot product. An epsilon may be used to provide grace identifying fragments that are very nearly perpendicular.

This is another reason why affording some grace is helpful.

Before a smooth surface is interpolated across the data points, additional points are inserted into the set of fragments for the non-relatable neighbouring fragments. These points approximate an extension of the non-relatable fragments. Insertion of these mid-points results in apparent extensions of the non-relatable patches and a sharp step at the discontinuity. Multiple points may be inserted to allow the approximation to more accurately convey the drop off after interpolation is applied, i.e. two or three points are inserted next to one another at the midpoint almost immediately on either side of the discontinuity. An illustration of inserting points to approximate non-relatable extensions is illustrated below in Figure ..

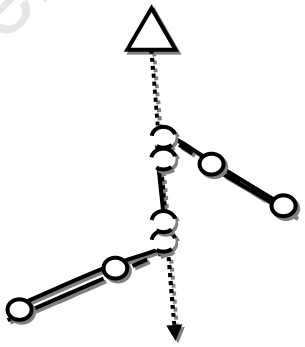

Figure . Additional points are inserted for non-relatable neighbouring fragments to generate extrapolations of the surface around those points and steep steps at the midpoint between neighbouring fragments.

7.2.3.3. Interpolation

The final step to finding a smooth surface that passes through the set of visible fragments requires fitting smooth surfaces through the points of the 2.5D sketch that have been clustered together. As with the perceptual theory of visual completion, a smooth C^1 continuous surface is fitted through the visible fragments. This interpolation corresponds to the way in which the HVS interpolates between relatable fragments [Kellman 03]. By inserting points between non-relatable neighbouring patches, smooth extrapolations beyond the points and a steep step at the insertion point are generated. In the final depth map this appears as two separate surfaces with an abrupt discontinuity between them.

A final discrete approximation to the continuous interpolating surface is computed for purposes of measuring the perceptual surface against the original surface from a specific viewpoint. This is achieved by subdividing the DT of the visible fragments and interpolating surface values across the final subdivided triangulation. This triangulation serves as a discrete mesh which is rendered to a depth map. The original surface is also rendered as a depth map, which provides a comparable discrete and meaningful representation for comparing the perceptual surface to the original. The resultant image space depth maps correspond to one another on a pixel level.

CGAL's [CGAL, 00] surface interpolation library is used to perform the surface interpolation. It uses natural neighbour coordinates in Euclidean space. The library employs Sibson's C^1 interpolation method [Sibson, 81], which uses a function gradient. This approach is used since it mirrors interpolation in the HVS sufficiently accurately and is also readily available for use through the CGAL library, working together with the natural neighbour coordinates computed by Delaunay Triangulation of the points.

7.2.4 Integration over Time

The perceptual model of the HVS proposed and implemented in this framework is further extended to capture something of the perceptual effects that occur when animating opaque markings. This extends the metric to allow for evaluating the visualization design presented in chapter 3, which harnesses the animation of the opaque markings to contribute to more effective layered surface visualizations.

What are the visual or perceptual effects, when moving the opaque markings over the surfaces and what contributions do these make towards effectively visualizing the layered surfaces and how can these effects be incorporated into the perceptual model? Theoretically, an enhanced sense of depth is contributed from motion parallax by moving the markings or fragments. These moving fragments need to be visible for more than 50 milliseconds for this cue to be effective [Lum et al, 03]. Depth approximations for moving fragments that have been visible for longer

than 50 milliseconds should therefore be more accurate.

On the negative side, particles in motion become slightly blurred, which distorts the shading, colour and texture on the fragments. Motion should therefore cause deterioration in accuracy of the Shape from Shading algorithm. Further, this blurring may negatively influence clustering of particles, since distinct perceptual grouping attributes, such as colour, become blurred.

There are several effects, which motion has on the recovery of shape. Fragments moving over a surface produce multiple samples over the surface over time, though only the samples for a brief period are retained in a person's memory and contribute to the understanding of the shape. Motion also contributes a greater sense of curvature than does a static image, especially motions along principle curvature directions. However, markings on different layers moving over one another cause interference, which negatively impacts clustering accuracy, focus and relatability, while similar motion patterns and directions improve clustering and relatability. Incorporating all of these effects accurately and balancing them against one another in a manner true to the HVS, is beyond the scope of this dissertation, since it would require in depth research including further user experimentation to determine more quantitatively how these factors influence surface perception. Nevertheless, we propose the following theoretical extensions below to our framework to cater for motion (these however, have not been tested):

7.2.4.1. Fragment Visibility Over Time

The visibility of each fragment is kept tracked over time. This is done by storing the percentage visibility of each particle, computed in each frame, for the pervious second. This is typically 30 frames. If a particle becomes completely occluded in any frame, its visibility over time is reset to 0. The distance covered by a particle is also tracked over time and gives an indication of the particle's speed. According to the perceptual literature, particles need to be visible for at least 50 milliseconds (ms) for structure from motion to take effect [Lum et al, 03]. This perceptual property is incorporated into the SFM and depth approximation calculations, according to the following heuristic rule:

If $fragment_i$ Visibility > *visibilityThreshold* for more than 50 milliseconds then
    SFM contribution for $fragment_i = 1.0$
    Decrease depth accuracy proportional to increase in speed
Else
    SFM contribution for $fragment_i = 0.0$

visibilityThreshold is a parameter that should be adjusted to the smallest visible size of markings distinguishable to a viewer.

7.2.4.2. Quantifying Interference

The variation in visibility of each particle over time presents a means of quantifying interference. One form of interference that is particularly distracting (as commented on in experiment two by the participants, and experienced by the author) is encountered when, while focusing on a particle on a bottom layer another particle on a layer closer to the viewer moves over it. This often causes the eye to unintentionally follow the occluding particle. The number of changes in occlusions per frame is used as a measure of this type of interference. This is determined by a visible particle becoming more than 90% occluded. The total of the number of particles visible in the previous frame and which have become occluded in the current frame offers a quantitative measure of this type of interference. It is the aim of the visualization and motion strategies to reduce this interference.

Popping artefacts and jiggling particles are also particularly distracting. Though not measured in this dissertation, the number of particles fading in and out, may be included in a measure of interference, as well as the number of particles leaving and entering the display. Yet another form of visual interference is engendered by fragments which lie between sets of fragments that have been clustered together. This form of interference influences surface completion and clustering. Adjusting the model for these forms of interference is left for future work.

Motion is useful for enhancing clustering. Particles with similar motion patterns, represented by direction, frequency, phase or speed may stand out from the other fragments in the display. The flow field is useful for determining similar motion patterns. A particle's direction of motion and speed should be extracted from the optical flow and used as an additional clustering dimension.

7.2.4.3. Spatio-temporal Relatability and Interpolation

Following a particle moving locally over a surface enhances a sense of the curvature of the surface and improves the accuracy of interpolation. With regard to more accurate interpolation, the particles moving over the surfaces result in more surface samples over time, which improves the sampling resolution of the surface. This sampling over time may be modelled by averaging the final perceptual surfaces/height maps over time. The averaging is, in a sense, equivalent to the motion blur effects of particles moving over the surfaces.

Langer et al., [2005] state that the human visual system's memory does not act like a buffer that maintains all surface descriptions for all time steps though, but actually, maintains a limited window of most recently seen surfaces in its memory. The above perceptual theory can be implemented by taking samples from the surfaces over a brief window of time. These could then be fed into the perceptual model to produce a surface that could be sampled at a higher rate. Perceptual experiments would need to be run to determine more accurately just how long the

window period should be. In our framework, fragment statistics are stored for each frame over the last second in a queue. The surface samples taken over the last second could be fed together into the perceptual model when generating the perceptual surface. The temporally averaged or higher sampled surfaces created could then be compared to the depth maps of the original surface in the perceptual model.

7.3 Measuring the Difference between Perceptual Surfaces and Original Surfaces

The framework and model for computing the perceptual surface and depth map provide a means of obtaining a quantitative representation of layered surfaces that reflects the surfaces as perceived by a person. Subtracting and comparing these surfaces to the original surfaces provides a quantitative measure of the effectiveness of a layered surface visualization.

Two measures are proposed in this framework for using the model output for quantitatively measuring the perceptual effectiveness of the images produced by a layered surface display. The first measure is a discrete shape difference, in which the difference between the rendered depth maps of the final perceptual meshes, as computed by the model of the HVS, are compared to depth maps of renderings of the original surfaces. The depth maps give an indication of local surface differences. This is the approach that was implemented in this work.

The second measure proposed, though not used or implemented reflects a global shape difference between the ideal surfaces and the perceptual surfaces by using Fourier shape descriptors. A comparison between the normalized Fourier shape descriptors [Zhang & Lu, 2001] of an original surface's depth map image and the perceptual depth map image provides a measure of the difference of the images in the frequency domain. This gives a measure of global shape similarity. Fourier shape descriptors provide descriptions of shape which are invariant to the affine transformations of rotation, scaling and translation. Fourier shape descriptors could be computed for the depth maps of the original surfaces and the perceptual surfaces. These depth maps would essentially equivalent to 2D intensity images. A discrete Fourier transform could then be applied to these images. This would transform the image from the spatial domain to the frequency domain. The frequency domain image could then be normalized and each component divided by the DC component or first term of the Fourier series. This division and removal of the first term would serve to make the image translation invariant. Normalization would make the frequency image invariant to scale. This final normalized 2D image would provide a shape signature – a normalized frequency domain vector, which represents the shape in the frequency domain. Different signatures could be compared, by taking the Euclidean distance between them. This would provide a measure of similarity between two shapes.

The following questions arise: Is it necessary to have two measures for comparing perceptual surfaces with original surfaces and do the measures correspond with one another? Even though the depths of the two images may be quite different the overall shape of the perceptual surfaces can still closely track the shape of the original surfaces. In such cases the global shape measure would convey a similarity in shape between the surfaces that the depth map comparison would not capture. That is, the Fourier shape descriptors are invariant to affine (translations, rotations & scaling) transformations, and therefore present a meaningful measure of global shape similarity which the depth map comparisons are unable to capture. Additionally the model produces as output the number of potential clustering mismatches and image surface areas over which the two surfaces differ. These two measures also give an indication of the effectiveness of the layered surface display.

A depth map of the ideal surface is compared to a depth map of the perceptual surface. The contour map and distance map generated in the Primal Sketch stage during the rendering passes and image processing are used to weight regions in which the visible regions of the surfaces do not overlap. For top down views the surfaces are extended to the edges of the surface for both the perceptual and original surface. This means that there are no regions of the image for which the surfaces do not overlap. The height of the surfaces is set to the base level of the plane in these regions. Future work may also include rendering feature maps of important image features e.g.

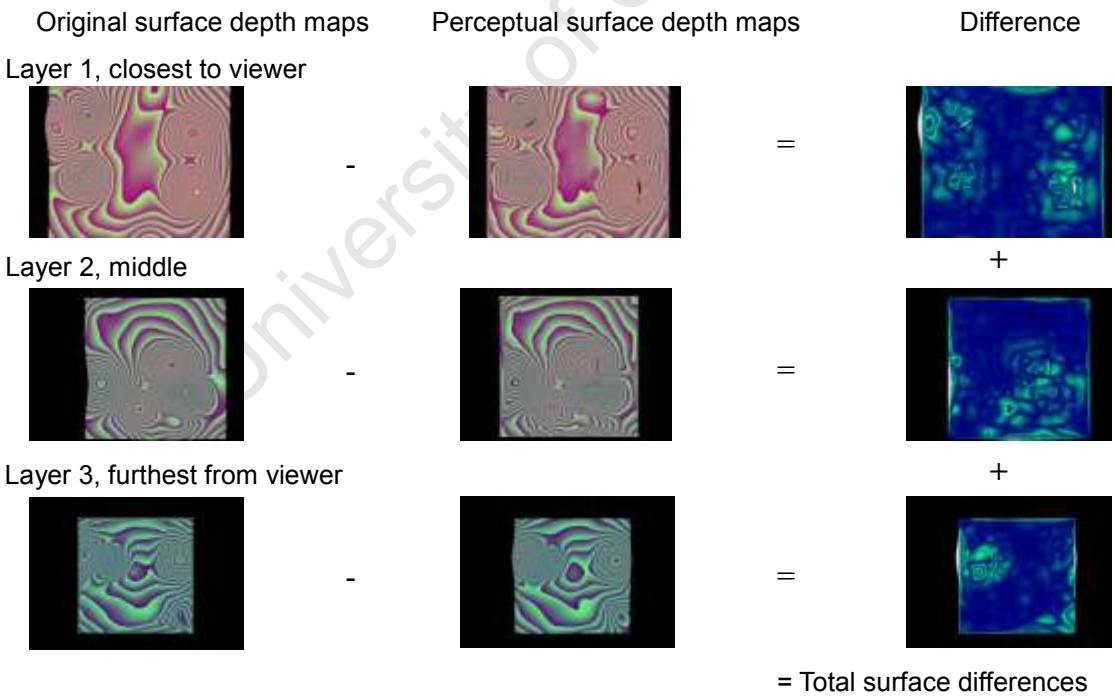

Figure . Absolute values of the depth map differences between the perceptual surfaces and the original surfaces. These are summed to give a total measure of the effectiveness of the visualization. A weighted summing may also be applied to compensate for reduced size and thus smaller contribution to the result of layers furthest from the viewer.

minima and maxima. A spatial frequency is also available from the Laplacian pyramid computed for contrast purposes. This captures regions of high frequency, e.g. regions of high curvature. These feature maps along with the silhouette maps could be used to weight the correspondences between a rendering of the ideal surface and the perceptual surface. Weighting these regions more heavily results in a measure which better reflects the effectiveness of the displayed image in conveying the surface, since such features play a significant difference in conveying shape. The process of computing the difference is illustrated in Figure .

We use the following formula as the measure of effectiveness for a layered surface visualization:

$$f = \sum_{i=1}^{n} |D_o - D_p|$$

Where D_o is the original depth map and D_p is the perceptual depth map. Extending the approach to oblique views, which use the distance map to weight regions which do not overlap or weight silhouettes and other features more heavily is left for follow up work.

7.4 Optimizing the Layered Surface Visualization

The metric described above presents a means of quantitatively measuring the perceptual effectiveness of a layered surface visualization. This opens the way for automatically generating optimal visualizations. To do this, the proposed implementation incorporates this metric into a simple yet powerful non-linear optimization algorithm, a Particle Swarm Optimization (PSO). The PSO, facilitated by the metric, is able to search for the best parameters for a layered surface visualization.

Particle Swarm Optimization (PSO) is a robust optimization algorithm that is able to find global or near optimal solutions to continuous non-linear problems. Varying the visualization parameters affects the visualization in a non-linear way [Bair et al., 2005]. This makes application of PSO to the problem of optimizing the visualization settings a suitable choice. PSO also tends not to get trapped in local extrema and is effective even in the presence of noise. The algorithm is further simple to implement.

The PSO algorithm finds an optimal solution by iteratively and stochastically flying a set of particles through a multidimensional search space. The particles converge on the best solutions among particles defined in a neighbourhood structure and compared to their own personal best solution. Our metric provides an indication of solution fitness. The dimensions over which the particles fly correspond to the possible parameter settings of the visualization.

In the implementation a star neighbourhood is used for the neighbourhood structure (topology). A ring topology, however, may be used which causes a slow transmittance of the global optimum.

The ring topology thus helps to prevent the PSO from getting trapped in local optima early on in the search. PSO is further suitable for high-dimensional search spaces with this topology. The ring neighbourhood structure requires no additional neighbourhood updates compared to other neighbourhood strategies such as using Delaunay Triangulations [Lane et al, 2008].

The particles fly through the *n* dimensional parameter space of the visualization. That is each dimension of the *n* dimensional particles corresponds to a visualization parameter, e.g. size of the particles, speed of the particles, shape of the particles, forces, etc.

The metric for measuring the effectiveness of the layered surface display, developed in this chapter is used as the fitness function. The PSO algorithm compares the fitness of the different visualizations for the PSO's individual best and neighbourhood best solutions (in the case of the star topology this is the global best). Based on these results the particles' velocities are adjusted stochastically to move around the best solutions. The velocity is damped over time to allow convergence and refinement of the parameters.

This chapter has presented a framework and implementation of a computational approach for simulating the way in which the HVS recovers surfaces from a layered surface image. The model serves as an objective means of measuring the effectiveness of a layered surface visualization technique in perceptually conveying layered surfaces. An evaluation of this framework is presented in the next chapter.

Chapter 8

Evaluation of the Perceptual Model

Chapter seven presented a computer model that simulates the way in which the human visual system reconstructs surfaces from images produced by our proposed layered surface display technique. The output of this model serves as a means for measuring how accurately renderings convey layered surfaces from a perceptual perspective. This chapter presents an evaluation of this model. The evaluation attempts to verify that there is a correlation between a person's perception of a layered surface and our model, i.e. does the measure reflect how well visualization perceptually represents a set of layered surfaces?

The evaluation entailed running a psychophysical experiment in which participants' subjective perceptions of the shapes of a set of layered surfaces were collected through a quantitative shape task. The data captured was used to reconstruct the surfaces as perceived by the participants. The visual stimuli used in the experiment consisted of a range of layered surface visualizations, produced by randomly modifying the set of visualization parameters. Our perceptual model was then, in addition to the participants' responses, applied to each of these visualizations. The model produced a set of "perceptual" approximations of the surfaces from which the metric rated the effectiveness of each of the visualizations. The model and the participants' performance were then compared for correlation. Our hypothesis is that there will be a linear correlation between these variables.

8.1 Experiment Three: Human Perception vs. Model Output

An experiment was performed to compare and test for correlation between our perceptual metric and the perceptual responses of a sample of respondents for various layered surface visualizations. The layered surface visualizations were produced by randomly varying the visualization parameters. A shape task was used to capture subjects' estimates of the height/depth, breadth and positions of Gaussian bumps. These responses of the subjects were used to generate Gaussian bump surfaces, which should be representative of their perception of the sets of layered surfaces shown to them. A correlation analysis was performed, comparing the respondents' estimates to our perceptual model's output.

8.1.1 The Sample

The sample consisted of 89 random visualizations with corresponding shape responses. This sample was taken from 24 respondents who were shown four random visualizations each. A breakdown of the sample is as follow:

Selection of Subjects: Although 42 students initially participated in the experiment, only the visualizations from 24 of them were suitable and consistent for evaluation. All 42 of the participants had not been involved in any of the prior experiments. Of the subjects 40 were undergraduates and 2 were postgraduate students, 22 were female and 20 male. These 42 participants had normal or normal corrected vision, and normal colour sensitivity. 16 of the respondents participated in an initial pilot experiment of whom 5 were shown visualizations using animation (Kinetic Visualization). Subsequently, it was decided that animation would not be tested in this experiment, for reasons explained in the pilot section 8.1.6. All the participants viewed the surfaces in stereo, except 2 participants who consistently removed their glasses during the experiment and reverted to monocular display. 18 of the respondents had to be excluded since their results were considered non-comparable. This is because 3 participants did not use rocking, 3 omitted surface sets, 2 used monocular display, 5 used motion (KV) and 5 were deemed outliers with regard to depth accuracy. These outliers were examined because their depth error estimates were beyond 1.5 times the 1st or 3rd inter-quartile range. From the final 24 respondents' visualizations there were 8 cases omitted because of incomplete tasks or for having outliers, giving the final 89 selected visualizations.

Expert Control: It became evident that there was significant variation between the responses of the participants, since the participants were inhomogeneous in terms of being meticulous and from various fields of study. A set of responses was necessary to serve as a reference point against which the participants' performance as well as the model could be judged. Consequently, the author being an expert with these visualizations performed the same tasks on the same set of surfaces as the respondents for the same visualizations. The author was aware of a stereo disparity effect in the visualizations described in section 8.1.2, which likely

helped to improve depth estimates. His responses thus serve as a "model" of perception with minimal variation and with accurate depth estimates. This more closely matches the perceptual model proposed and evaluated in this experiment. This self evaluation is not presented to be the indicator of correlation, but rather helps to reason about the model and the participants' results and correlations in relation to a controlled set of responses.

Sample Visualizations: The 89 visualizations of the sample were randomly generated by sampling the visualization parameter space. The various visualization parameters and ranges that were used in this experiment include the following:

- *particle sizes*, which, were in projected screen sizes, between 2mm and 5mm on the layer farthest from the viewer and on the front layer, closest to the onlooker, between approximately 8mm and 15mm, depending on the depth of the surface, [0.02;0.05] units in world co-ordinates.
- *number of particles per layer*, is for the middle layer set to be between 200 and 1333 (2/3 of 2000, the maximum number of particles) particles. The closest layer is set to be between 200 and the number of markings on the middle layer, and the furthest layer set to be between the number of markings on the middle layer and 2000. This was done so that the occluding layers are less densely covered so that interior layers can be seen. 2000 markings were selected for a maximum, since with this many markings the surfaces were almost completely covered with the smallest marking size, using more markings would have made no difference. In the future, it would be more meaningful to refine this measure to particle density rather than number of particles per layer.
- *particle representations* as either crosses or patches.

Particles were distributed over the surfaces using a Poisson distribution: positions were uniformly distributed and then perturbed by 1/4 of the uniform spacing between the original positions. Figure . shows that there are significant differences between visualizations created for different parameter settings.

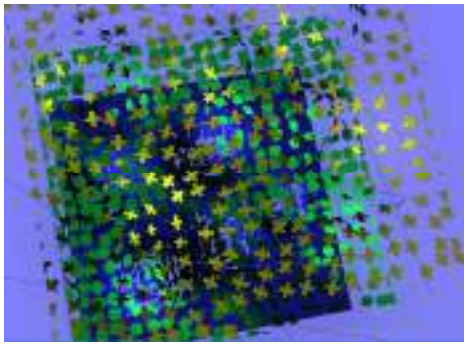

l_1 (369,0.033) l_2 (520,0.036) l_3 (1427,0.038)
f_M = 3.9, f_R = 51.6

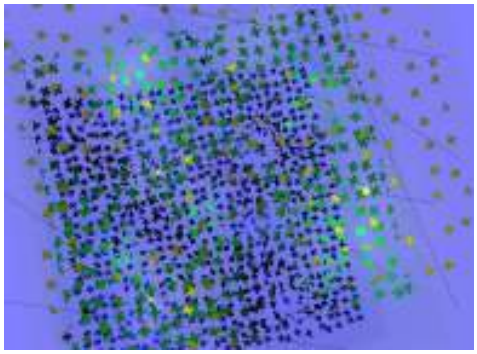

l_1 (233,0.020) l_2 (442, 0.030) l_3 (863,0.023)
f_M = 9.3, f_R = 31.3

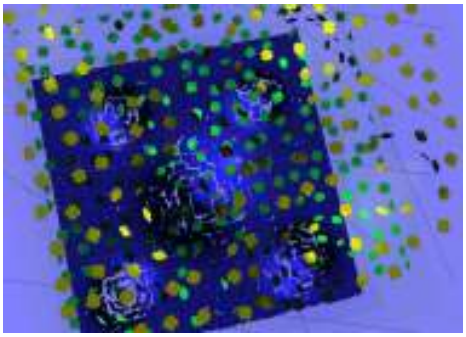

l_1 (207,0.028) l_2 (278,0.029) l_3 (1867,0.034)
f_M = 4.8, f_R = 31.5

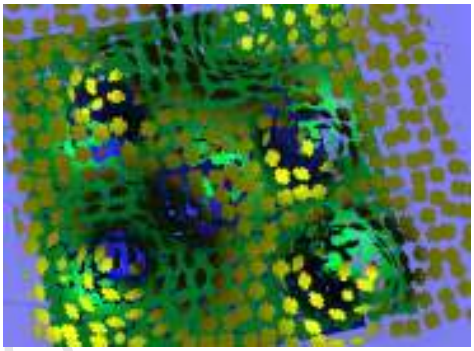

l_1 (608,0.033) l_2 (842,0.040) l_3 (1659,0.044)
f_M = 7.2, f_R = 29.1

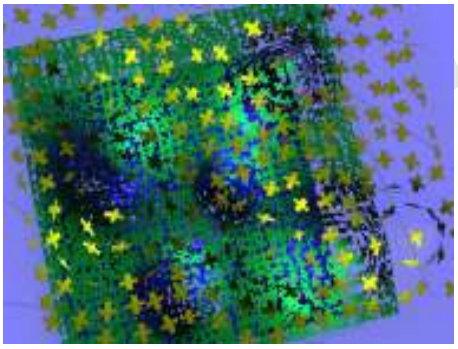

l_1 (312,0.037) l_2 (1497,0.033) l_3 (1503,0.048)
f_M = 4.5, f_R = 33.7

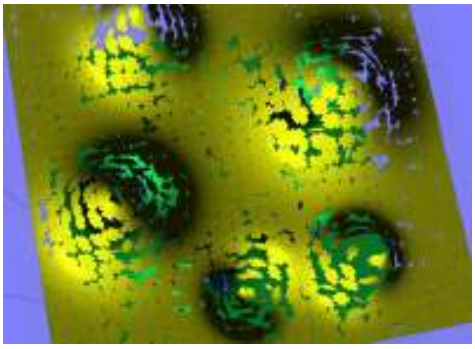

l_1 (1131,0.040) l_2 (1362,0.042) l_3 (1722,0.030)
f_M = 25.6, f_R = 40.8

Figure . Examples of sample visualizations for two layered surfaces generated by sampling the visualization parameter space. Number of particles and sizes are given as pairs (particles, size) for each layer l_1 closest to the viewer, l_2 middle layer, l_3 furthest. f_M indicates the metric score and f_R the respondents performance for the visualization. Varying particle sizes and particle densities for the different layers result in significant perceptual differences between the visualizations.

Surfaces: A set of three layered surfaces stacked vertically on top of each other was shown to each participant for each of the visualizations. Smooth height field surfaces were used in this experiment and are consistent with other layered surface experiments [Bair & House, 2007], [Weigle, 2006]. The surfaces were sampled on a 128 by 128 grid. The surfaces were generated from 5 Gaussian bumps (but importantly participants were unaware of this). Each of these was visibly distinct in that the radii of the Gaussians did not overlap. Bumps were used in this experiment to create either minima or maxima. The Gaussians had a magnitude of between [0.25 and 0.5 world units]. Their radii were in the range of [0.4; 0.7]. Random noise of 1/6 of the maximum height of the bumps was generated. Illustrations of the surfaces used are shown in Figure ..

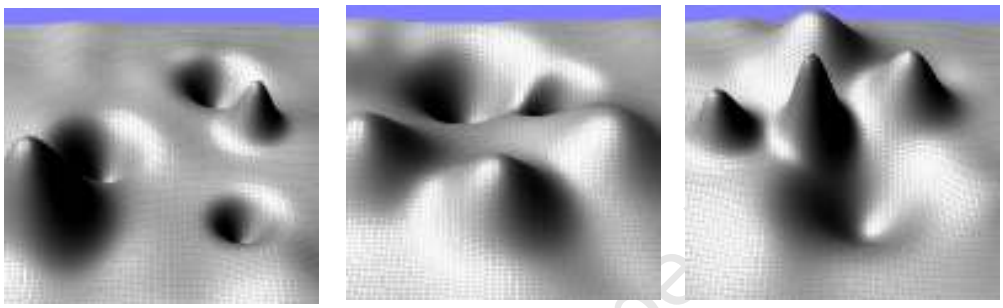

Figure . Examples of smooth height field surfaces consisting of 5 distinct Gaussian bumps, sampled on a 128x128 grid, which were used in this experiment. Both minima and maxima were used. Noise was generated which is at most 1/6th of the smallest sized bump.

8.1.2 The Shape Task

A participant's perception of each surface was quantitatively measured through a feature estimation shape task. Respondents were instructed to locate different peaks and valleys on each layer and then estimate the heights or depths of these features and the extent of the features. The experiment interface allowed participants to simply click on a feature to mark the peak's center. Participants could then, through a simple dragging operation extend a height marker and drag another marker to approximate the extent of the peak. In world space a glyph was used which indicated the extent and height of the peak, as well as the position. The extent was rendered from the top of the feature so as not to give away the extent and the height was rendered from the peak also so as not to give away the depth. When dragging the marker to a new position, this world space marker was hidden to avoid the marker giving away the surface shape. The participants' estimations of the shape features were saved with the noise of the original surface for recovery during analysis. These estimations were expected to give an indication of the perception of the surfaces as seen by the participants. Figure . shows an example of the surface markers and controls used in the surface task performed by the participants.

Participants could switch between surfaces by clicking on a coloured button to the side of the

display. This would also adjust the stereo convergence depth setting to bring the selected layer into focus. Convergence was set to the center of the line of sight and at a depth equal to the plane from which the peaks extend.

This simple shape task was chosen over other more challenging shape tasks, since these readings can be used to recreate at least roughly, the respondents' perception of the surfaces. Common shape tasks, such as estimating orientations require taking a set of readings at multiple positions over a surface [Bair, 09]. The number of readings a respondent needs to supply is compounded for layered surfaces, since such information must be captured for multiple surfaces. For these reasons the above task was designed to make the experiment tractable, without being too fatiguing for the respondents. Our task is simple and easy to perform compared to other tasks such as orienting an orientation marker. Furthermore, the proposed task requires a respondent only to make a minimum number (at most 10 estimates, 5 height and 5 breadth estimates, excluding picking the peak, which is trivial) of meaningful readings for each surface.

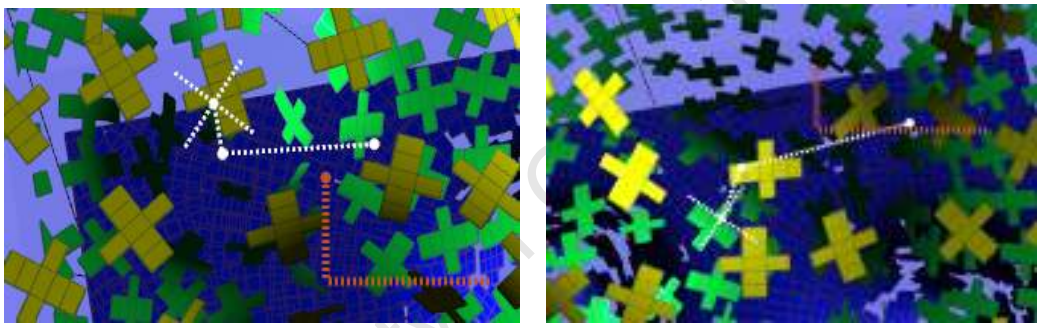

Figure . Respondents completed a task in which they would locate peaks or valleys on the different layers and estimate the height or depths of the features and the extents of the features. A red marker was rendered in image space allowing respondents to edit the feature markers even when the surfaces were rocking. The white lines show the marker in world space, helping the participants with estimating depth and extents of the peaks and valleys.

8.1.3 Experimental Setup and Design

Each of the 42 participants viewed 4 layered surface visualizations consisting of a set of 3 layered surfaces. Each set of layered surfaces was shown using our particle system with opaque markings. Participants could toggle the rocking of the surfaces. The surfaces would rock back and forth 4 times at an amplitude of 15 degrees from the center, which was then damped to 2 degrees. As mentioned, respondents completed a shape task for each layered surface. Although no time limit was set for completing the task, all respondents finished within an hour. In this experiment the independent variables were the visualization parameters which were varied between surface sets for each participant. The dependent variables included the

measures of participant accuracy, specifically: depth differences from the original surface, offset differences between peaks, the difference between radii and the difference in number of peaks. These variables were combined to recreate a surface that reflected the participants' perception of each layer. Each of these surfaces generated from the respondents responses were compared to the original surface. This was done by rendering the surfaces to depth maps and then taking the difference. The difference for each of the layers was then added to give a measure of how well in total the surfaces were visualized and perceived by the participants. This is similar to the procedure described in section 7.3, used by our perceptual metric.

Our model was trained on the controlled expert's data set, to find a best match using a Particle Swarm Optimization algorithm. The trained model was then used to estimate how well the participants could perceive the different surfaces. The model was used to produce perceptual surfaces, and the metric applied to find the total difference from the original surfaces. These results were then compared to the results obtained from the respondents.

Training of Respondents for the Task: A brief overview of the usefulness of layered surface displays was explained to participants for motivation and interest. The participants were then trained to use the feature markers, and were given a standard set of instructions, prior to performing the experiment. They were trained on four sets of surfaces. After participants completed the experiment, perceptual metric responses were generated offline for each visualization and layer. This was done by regenerating the visualization from the parameters used to create the original visualization for the participants.

The hypothesis for the experiment was that the metric would show a linear correlation to the respondents' performance for the different sets of layered surfaces across the various visualizations. It was expected that the visibility of particles on the different layers would influence the participants' accuracy on the shape tasks. The visibility would be affected by multiple factors including the density of markings and size of markings on different layers. The size of markings would also influence accuracy and the participants' ability to distinguish between markings. The measure itself should reflect and capture these effects and therefore participant accuracy is expected to relate to the metrics accuracy. The perceptual metrics' output would likely be influenced most by changes to the visualization parameters and to a lesser extent by variation from participant to participant. It was thus expected that the accuracy across the metric would vary for various participants, but that the general trend should be that the metric identifies the effectiveness of the visualizations.

8.1.4 Lighting and Viewing Conditions

Each surface was viewed stereoscopically using perspective projection from a top down view. The respondents were seated 4 world units, approximately 500mm from the origin. Before eye separation, the camera was located at (0,4,0) looking down the y-axis towards the origin. An off-axis stereo setup was used. Off-axis stereo produces a stereo rendering created by separated left and right camera's with parallel view direction vectors. Such renderings cause no vertical

parallax. For the pilot off-axis stereo settings were used with approximately 6.3cm eye separation, off-axis stereo was used for the remainder of the experiment. The variation between toe-in (the left and right cameras' view directions are oriented inwards pointing to the focal point) and off-axis stereo should not significantly affect depth estimates, but rather produces a stereo display that is less strenuous on the eyes [Grasberger, 2008]. For this reason, pilot results and final experiment results could be merged. For the off-axis stereo, the inter-ocular distance was set to a thirtieth of the focal distance, a setting that is recommended for general stereo viewing [Bourke, 99]. The focal length was set to the base depth of the selected surface plane. The layers were staggered in depth relative to the participants at approximately: 437mm y-offset = 0.5 (in front of the screen), 562mm with y-offset = -0.5 (behind the screen) and 687mm with y-offset = -1.5 (behind the screen).

Smooth Phong shading was used with a directional-light source (equivalent of a point source at infinity). The light source direction vector was set to (1, -1, 1), illuminating the scene from the bottom, left and behind the viewer. Shading was performed on a pixel scale rather than across vertices, as for standard Gourard interpolation. This better illustrates peak intensities of specularities across the surfaces and produces more realistic specular shading [Weigle, 2006].

8.1.5 The Perceptual Model used in the Experiment

In this experiment, which seeks to compare perceptual responses of people to the proposed perceptual model, it was necessary to adapt a model to closely simulate the way people perceptually performed the layered surface task. Further, this being the first time that this model would be formally evaluated, it was decided to use a simplified version of the model described in chapter 7 and to keep the experiment as simple as possible. For this reason a top-down view of the surfaces was chosen. This allowed for DT to correctly identify neighbouring fragments. The model was modified to mimic the perceptual processes respondents went through to complete the surface task on the different visualizations. The various assumptions and aspects of the model used in this evaluation are described below.

Animation: The animation processes in the model and the use of Kinetic Visualization (KV) were omitted, since during the pilot it was seen that participants who used animation used it in an interactive way to explore the surfaces, stopping and starting as required. This made it both difficult to recreate the exact images, which the respondents saw and also complicated the perceptual processes beyond what the model could cater for.

However, users were still allowed to rock the surfaces. Rocking was essential to making sense of the layers, even though stereo was used (in the results section, notice that 72% of the total time spent per surface set on average was spent rocking). However, the model itself does not account for the changes in vantage point that occur during rocking.

Fragment statistics: Contrast for each fragment was captured using the contrast sensitivity function (CSF) described in section 7.2.1.2. Fragments with below threshold contrast were

suppressed, since these fragments would not have contributed to perceived features on a surface. Average hue of a marking and shading were captured and used as clustering dimensions.

Depth approximation: In the experiment and visualizations rocking, stereo and shading were all used to give the respondents an accurate sense of depth. Accurate depth estimates were therefore assumed. True depth positions of the points were thus used. This assumption was also made since current SFX algorithms do not cater for the type of fragmentary patches present in the layered surface images. Implementing and adapting current SFX approaches to simulate depth perception for layered surfaces is far beyond the scope of this dissertation.

Clustering: The K-means algorithm was used, as described in section 7.2.3.1. Fragments, which were incorrectly associated with another layer, were suppressed, (not interpolated between). During preparation for the experiments it was noticed that rocking and depth in addition to KV, contributed to significantly clear distinctions between markings on the different layers. Since rocking, KV and depths through stereo were used, and visualizations were only static (without rocking) approximately 28% of the time, it was assumed that clustering would be very accurate across layers. To simulate the contribution of the KDE from rocking, the actual surface layer was used as one of the clustering dimensions. The depth of markings was also used as a clustering dimension. While, these simplifications were made to create a simulation that corresponds to what the users reported, we warn, that this is a simplification that is concerning, since it could well bias the clustering algorithm, leading to more accurate association of fragments than the HVS would achieve. This component of the framework, itself also needs to be further refined.

Relatablility: In the model used, relatability criteria were relaxed, to lie within a range of 10 degrees of the strict criteria. This was done since rocking was used significantly during experiments and in experiment one and two, orientation errors were under rocking on average 13 degrees out. Catering for a range of degrees compensates for observer's misjudgements of fragment orientations which may cause them to see fragments as relatable.

It was noticed that respondents clustered nearby sets of fragments and interpolated a smooth surface across these fragments even when relatability criteria were not strictly met. Semi-transparency of the layers may have contributed to this. Further, the task itself does not capture the finer perceptual differences caused by relatability criteria. Fragments significantly close to one another are related even if they do not satisfy the geometric relatability constraints. This is possibly because the shape task involved identifying and estimating peaks over the surfaces, which did not require finer detail readings but a smooth and interpolated surface over sets of fragments.

The various assumptions made about the model may significantly influence the correlation results. The assumption of accurate depth, if wrong is likely to be a significant cause of deviation from the respondents' results. Suppressing incorrectly clustered fragments may also

cause differences in shape from the respondents' perception of the surfaces. The extent of this error is uncertain. Relatability assumptions may result in slight depth deviations, but should not alter the overall shape significantly.

Model Parameters and Training: The parameters of the model included thresholds for the sizes of the markings to be noticed on each of the layers and whether or not relatability should be used. A contrast threshold was also used. Markings which had a contrast below this threshold were suppressed. Relatability criteria could also be switched on and off. The best settings for the parameters were found through the use of a Particle Swarm Optimization algorithm. The overall correlation between the model for different parameter settings and the observers' responses was used as the fitness function in the PSO algorithm. Each particle in the PSO corresponds to a set of parameters (minimum visibility thresholds for particles on each layer, a contrast threshold and whether or not relatability is turned on or off). The PSO searches for the parameters that result in an optimal correlation. It does this by flying the particles through the parameter space and keeping track of the best particles. In this way it minimizes the error between the model's output and the respondents' responses.

We found the optimal parameters by finding a best fit with the PSO. This was done using the expert data as a training set. This model was compared to the respondents' data, (the test data). Additionally, for comparison reasons, we also found the best parameters that fit the 24 respondents' data.

8.1.6 Pilot

Before finalizing the experimental design, a pilot was run using 16 participants (9 male, 7 female). During the pilot 5 participants used animation. The pilot led to the following observations and changes to the experimental design presented above.

Performing the shape task for four surfaces in the final experiment took the respondents less than an hour, after which they were not significantly fatigued. The pilot which originally required participants to complete the tasks for 5 sets of surfaces showed that respondents needed in some cases more than an hour to complete the task. Consequently, only the first four responses for participants from the pilot were merged with the participants' responses from the final experiment, to avoid learning and fatigue effects which may have influenced the responses for the 5^{th} set of surfaces.

Toe-in stereo was used in the pilot experiment, and for one of the participants we explored using monocular display. There were advantages and disadvantages to both. From observation of training, it seemed more difficult for subjects to approximate the heights of the peaks with a monocular display. The monocular display was, however, more crisp – the surfaces were displayed at a higher resolution than for the interlaced stereo display. Stereo left and right eye pairs also created more noise; the out of focus or blurred markings would occlude more of the

bottom layer than the single monocular view. Rather than observers gaining advantage from having a view from the two perspectives, this seemed to interfere more with a clear view of the interior layers. Rocking helped to overcome this problem by varying the vantage point. However, the monocular display was also observed to cause more confusion for the viewers as it was more difficult to distinguish between the markings on different layers from shading alone. Stereo made it easier for the participants to distinguish between the layers, partly because of the additional depth cues, but also because the other layers not selected were slightly out of focus. It was decided to use off-axis stereo in the final experiment. The difference between these stereo setups was motivated by comfort and does not influence depth accuracy.

During the pilot the constraints on the number of markings on each layer were more relaxed than in the final experiment. In particular, the number of markings on the middle layer was set randomly. The top layer was given fewer (or at most the same amount of markings) and the layer beneath it more markings. This, however, still resulted in a majority of the visualizations in which the bottom layer could not be seen at all. In the main experiment, the number of markings on the middle layer was set to be 2/3 of the maximum number of markings, which in general reduced the number of markings on the middle and closest layer, allowing the bottom layer to be seen more clearly.

The participants who used KV (markings moving over the surfaces) during the pilot used the animation to redistribute the markings over the surfaces. They would then pause the animation, rock the surfaces and then use the new distribution to explore the surfaces or find and complete the task for each different feature with a distribution that was more helpful. This interactive exploration of the layered surfaces through animation was difficult to track and re-create and is something which the model does not currently cater for. It is equivalent to changing the visualization parameters, and although this is one of the potential advantages of animating the markings, it complicates our evaluation. Combining views from multiple redistributions is not catered for by the current model, since the metric considers only the averaging of fragment samples from motion over time.

During the pilot we attempted to make modifications to the animation so that it could still be used in the experiment. In order to prevent respondents from interactively gaining different distribution snapshots of the visualization through animation, when an animation was paused or rocked, the markings were reset to their original distribution and the amount of time for which the animation was active was measured. Respondents commented that this was not helpful, since the animation was useful for varying the distribution, allowing them to see through to the interior. Rocking would then be used to help estimate the depths. Respondents simply stopped using motion because of this. After observing these complications for motion, it was decided to remove Kinetic Visualization from the final experiment. Because of these variations, the responses for motion were not mixed with other results in our final analysis.

8.2 Observations

An observer was present during training, and only offered help with interface problems. The following observations were made during both the pilot and final run of the experiment. Similar to the first experiments the participants commented that rocking helped to gauge depth and height and helped distinguish between markings on the different layers. They reported that it also helped them to pick out peaks or valleys on occluded layers by providing variation in the vantage point. This helped them see behind markings which occluded the bottom layer from a purely top-down view. One respondent, however, considering the application of the display in real life, asked, "Who's going to sit and rock this the whole time?" A display that constantly rocked would also not have been helpful since respondents needed to stop rocking to accurately place the marker at the center of the bumps and estimate the breadth of the bumps. In real world tasks, when an observer wishes to focus on a particular point, or consider data from a particular vantage point, or if the visualization user has to place or mark a position on a surface, or make an orientation judgment, it is likely that rocking will be stopped. Two other participants commented that user interaction would likely be more useful than rocking alone. Observers also commented that the amplitude of rocking should be adjustable. Three respondents reported dizziness due to the rocking of the surfaces, though stereo has been known to cause dizziness effects [Hale & Stanney, 2006] and they may have indirectly attributed the cause to rocking.

The respondents in the pilot would animate the markings and occasionally pause them. They would effectively move the particles to find a better distribution over the surface and then freeze the motion and use rocking to help perform the surface task. One person commented on their use of motion, saying that the blue layer furthest away was too thickly marked and that they could not make out the surface well until the markings moved. Blue, being the furthest layer, makes this a counter intuitive observation in that a fully covered layer should best represent the surface. However, in this particular case the observer found it more helpful to have a less dense distribution of markings. This could be because the markings themselves act as a surface enhancing texture, conveying the principal curvatures. A completely covered surface does not show the surface texture markings as strongly because of reduced contrast across the surface. The participants did not require motion for certain visualizations as rocking was sufficient to see the different peaks and valleys and identify these. Respondents commented that as the particles moved over the surfaces the dense packing of the markings broke up, which improved visibility of the underlying blue layer. In one case motion did not help the viewer to see the blue layer under the dense layers obscuring it; visualizations for which two of the layers were strongly illustrated by large and numerous markings overwhelmed a single layer for which there were small or few markings. Attention seemed to naturally settle on the strongest layer. In this regard, stereo had the advantage of giving focus to a particular selected layer with other layers appearing slightly out of focus.

During this experiment it was realized that respondents could have approximated the depths of the peaks by observing how in focus or out of focus the depth marker was. However, none of

the respondents seemed to have noticed or used this cue during training or the experiment and they tried to estimate the depth properly.

8.3 Results

This section reports on the various data that was gathered from the experiment. Table . shows means and standard deviations of the time it took the 24 respondents to complete the surface tasks and the rocking usage statistics per surface set. From this table it can be seen that respondents took on average 9 minutes per set, of which 6 minutes was spent rocking the surfaces. The standard deviations are approximately half this duration, indicating a large variation between responses per visualization or person. Notably, during the task participants were observed to use rocking to help estimate depths, but located the center of the peaks and estimated their extents, while the visualizations were stationary. This indicates that rocking played a significant role in helping them to estimate depths and find features but interfered with the task of placing markers.

	Time per surface set	Rock count	Time Rocking	% of time spent rocking
Average	9 min + 4.786 s	35.490	6 min + 34.99 s	70.9%
Std Dev	4 min + 11.398s	25.520	3 min + 35.29 s	13.5%

Table . Average time spent per surface set, average number of times rocking was used, average amount of time spent rocking and percentage time spent rocking per surface set

Correlations were investigated between participant performance (in terms of error) and the different potential factors that may have influenced performance such as rocking, the percentage of the total time respondents spent rocking the surfaces and the number of times the visualization was rocked. Table . shows the correlation values for these comparisons. Marked in red, are the r values for which there is no linear correlation. These values show that the amount of time rocking the surfaces and the time used did not influence respondents' accuracy. Rock count, however does correlate to respondents performance, likely those people who rocked the surfaces more, picked up on missing peaks or were able to estimate depths more accurately. Depth error is strongly correlated to performance. This indicates that poor depth accuracy strongly influences a respondents' performance in a negative way. Poor depth accuracy is also attributable to the visualization. If respondents could not see a surface clearly then they may well have misjudged depths for those surfaces.

Factor	r	r^2
Percentage of total time spent rocking	0.0255	0.001
Time spent rocking	-0.09	0.008
Rock count	-0.3817	0.146
Time	-0.11	0.012
Task accuracy		

Depth error	0.7062	0.498
Misplacement error (distance)	0.25	0.063
Misplacement error (12 outliers removed)	0.45	0.203
Missed bumps	0.407	0.166
Radius estimation error	0.338	0.114

Table . Correlations between participant performance and different potential influences for the different visualizations.

Misplacement error did not correlate to participant performance, but when outliers were removed (12 outliers removed from the 89 visualizations) this showed indication of correlation. In 12 case respondents likely misplaced the peaks, which may be because of poor visibility. Missed peaks and estimation of the peak radii were indeed correlated to performance.

A result not shown in the table above is a comparison between the number of bumps that were missed and the rock count. A negative linear correlation, $r = -0.48713$ was found, likely indicating that the more times the surfaces were rocked the more peaks were found, which resulted in less error.

The respondents' estimates were compared to the expert's estimates. A paired two sample for means with 80 degrees of freedom, (two tailed) t-test with $\alpha = 0.05$, showed significant difference $\rho << 0.05$, for the metric, the missed bumps, depth error, radius error, and misplacement error between the expert's and the respondents' results. The averages and standard deviations are listed in Table .. In this table mean metric scores, which are computed as the sum of differences for each layer divided by the volume of the surface (the summed absolute height and depth values of the original surface) are reported. These indicate that the expert more accurately, for the same set of visualizations, approximated the surfaces than the participants. This is highly likely due to the expert's skewed depth accuracy. The expert in general also missed fewer bumps, had less error in depth, less error estimating radii and more accurately identified the bump centers.

	Expert		Participants	
	Avg	StdDev	Avg	StdDev
Metric (Summed surface error)	27.193	7.915	34.725	8.044
Missed bumps	2.333	2.706	4.111	2.945
Total depth error	1.389	0.898	2.654	1.189
Total misplacement error	0.132	0.122	0.235	0.272
Total radius error	0.458	0.263	0.682	0.319

Table . Comparison of averages and standard deviations between the expert and respondents. The expert's results for all measures are statistically significantly different from the participants' results.

A discrete difference between the surfaces generated by the model and the original surfaces was calculated, as well as the difference between the original surfaces and the respondents' surfaces. These served as an indication of error for each surface. This error was divided by the total volume (discretely summed height magnitudes) of the surface, above or below its base plane. This was done to normalize for variation between surfaces. The error for each of the 3 layers was determined and summed to give a measure of surface error for a set of surfaces (each visualization), i.e. the performance. The respondents' performance was compared to our model's metric scores for each surface set and visualization. Figure ., shows a scatter plot of the metric results for the model compared to the results for the respondents' performance. This is for a model trained on the respondents' data, i.e. a best model fit to the respondents' data. A point in the graph corresponds to a particular respondent's performance on the x-axis, and the model's performance on the y-axis for each of the visualizations.

A numerical evaluation of the correlation between the metric applied to the respondents' surfaces and the model's surfaces using Pearson's correlation coefficient gives r = 0.276 and r^2 (the coefficient of determination - the proportion of explained variance) = 0.0762, indicating that only 7% of the total variation between the model and respondents' responses is explained by a linear relationship. For a 95% confidence interval with df (degrees of freedom) = 87 the lower and upper confidence interval is between [0.072; 0.458].

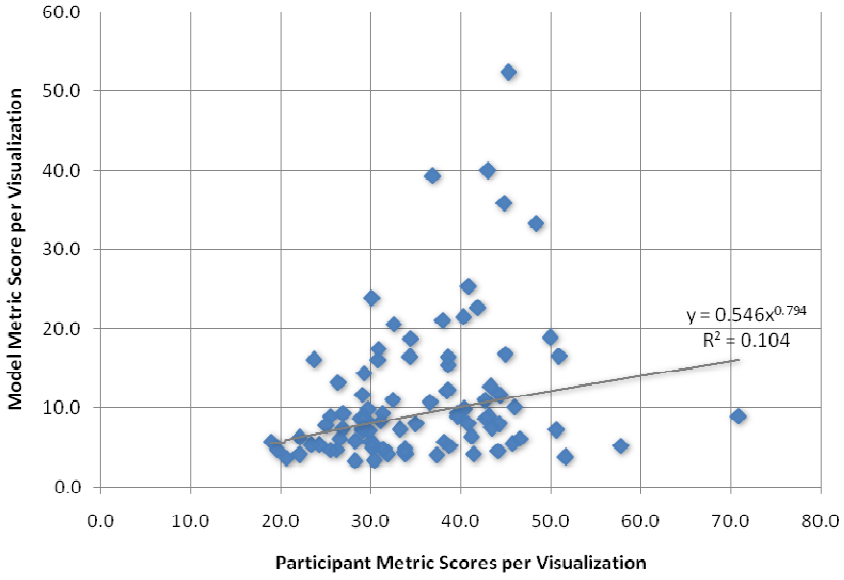

Figure . Scatter-plot showing the correlation between the metric applied to the perceptual surfaces created by the model and the metric applied to the surfaces created from the participants responses. Each scatter point corresponds to one of the 89 visualizations. A trend-line is fitted to the data. The r^2 value for this line indicates that 10.4% of the total variance is explained by the model. Pearson's correlation coefficient is 0.322 for the trend-line, this trend-line shows only marginal linear correlation. The linear correlation before transformation is 0.276. Lower values on the axes indicate less error.

To determine whether there is a correlation between this model and the respondents' responses, the statistical inference below was used:
Let the null hypothesis and alternative hypothesis be:
H_0: $\rho = 0$, is that there is no linear correlation, while the alternative is:
H_a: $\rho \neq 0$, that there is some linear correlation.
A population with r = 0, no correlation, would mean that the correlations of samples follow a Student's t distribution, for which we find, for a two-tailed t-test, with $\alpha = 0.05$ (95% confidence), n = 89 and r = 0.276 that:
t = 2.678, giving, for an assumed normal distribution
$\rho = 0.0088$, which is less than 0.05, for which we reject the null hypothesis. Thus it can be concluded that the sample correlation is not by chance and that there is indeed some linear correlation. However, the strength of this linear correlation is weak, since r^2 is closer to 0 than 1 (an indicator of a strong linear correlation is $|r| \geq 0.7$ [Steyn et al., 1994]). This and Figure 8.4 indicate that despite this correlation, the model itself is not a good fit to the data, even when outliers are removed, indicating that there are many potential sources of variation that are not accounted for by the model

These results reflect the best correlation for our model after fitting the model parameters to the participants' data with a PSO. Model settings for minimum identifiable marking size for the layers as they recede from the observer require at least 17 pixels, 75 pixels and 45 pixels to distinguish markings on each layer. Relatability is incorporated in this fit and the minimum contrast threshold requires a minimum contrast difference of 0.2 units.

The correlation between the respondents' performance and the model's performance for each layer separately, was also analyzed. These results are displayed in Table .. The correlations are weak across these various measures indicating that the model did not correlate with the participant's results.

Layer	Metric Results for Participants	Total Bumps Missed	Total Depth Error	Total Error for Distance to Bump Center	Total Radius Error
Closest, 1	r = 0.281, $r^2 = 0.079$	r = 0.191, $r^2 = 0.036$	r = 0.039, $r^2 = 0.002$	r = 0.209, $r^2 = 0.044$	r = 0.095, $r^2 = 0.009$
Middle, 2	r = 0.249, $r^2 = 0.062$	r = 0.391, $r^2 = 0.153$	r = 0.3, $r^2 = 0.09$	r = 0.163, $r^2 = 0.026$	r = 0.383, $r^2 = 0.147$
Furthest, 3	r = 0.374, $r^2 = 0.14$	r = 0.161, $r^2 = 0.026$	r = 0.053, $r^2 = 0.003$	r = 0.23, $r^2 = 0.053$	r = 0.231, $r^2 = 0.053$

Table . Correlation results per layer.

An exposition of the data with outliers removed is presented below. However, because of the weak correlation in the data a crisp statistical procedure for identifying outliers was unclear, and outliers were removed by visual inspection of the graph. This analysis of outliers should

thus not be considered statistically rigorous but is included for completeness. It was expected that outliers influenced correlation significantly. Ten outliers from the 89 visualizations, that is 11% of the most extreme values were removed. The correlation results with outliers removed are presented in Figure ..

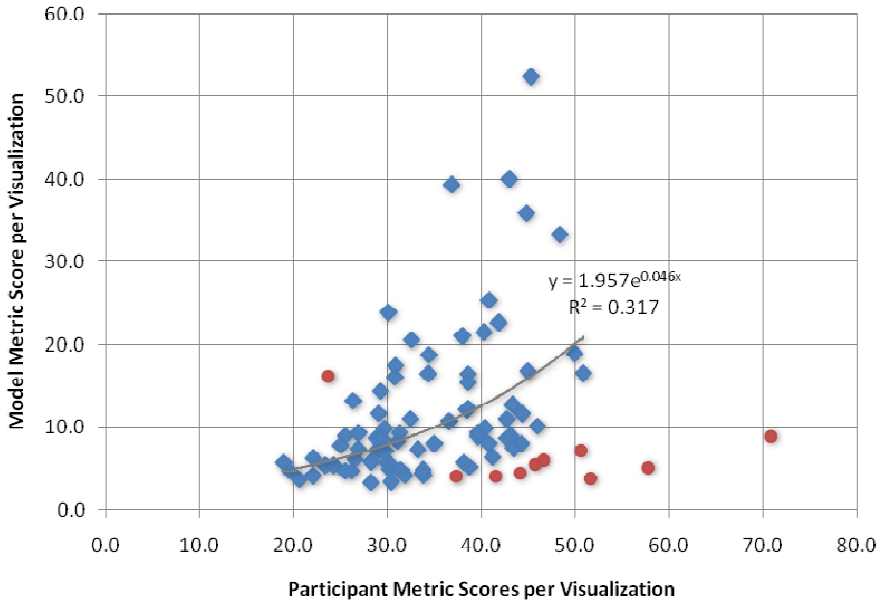

Figure . Scatter-plot with outliers removed showing the correlation between the metric applied to the perceptual surfaces created by the model and the metric applied to the surfaces created from the respondents' responses with 10 of the 89 values removed. The r^2 value now indicates that 31.7% of the total variation can be explained by the model for which Pearson's correlation coefficient is 0.563 (for the trend-line). Pearson's correlation coefficient is 0.5 for a linear correspondence between the measures, $r^2 = 0.25$. Outliers which were removed are marked in red.

Pearson's correlation coefficient for a linear correlation between the results improves to 0.5 with $r^2 = 0.25$. A transformation of the data, yields slightly greater correlation $r = 0.563$ with $r^2 = 0.317$. The 95% confidence interval for the transformed fit is between [0.402; 0.69] for df = 87, z = 0.637. For a two-tailed t-test, testing to see if there is linear correlation, we find for r = 0.506 and n = 79, df = 77, that t = 5.06 and that, $\rho = 0.000003$, indicating that there is a linear relationship, though it is still not strong.

Similarly, comparisons were made between the best model (fit to the expert's results) and the respondents' performance. The respondent' performance was also compared to the expert's performance. Further, the best model that could be fit to the expert's data was also considered. Figure . shows scatter plots for all these various models and comparisons that were made, both including and excluding outliers and Table 8.5 summarizes the numerical correlation for these comparisons. The settings for the model trained on the respondents' data and on the expert's data are [17, 75, 45, 1, 0.2127] and [51, 64, 61, 1, 0.636], respectively. The first three entries indicate the minimum number of pixels required for a fragment to be detected. The fourth entry

indicates whether relatability should be used in the model (1) or not (0) and the final entry indicates the minimum contrast threshold.

The values in Table 8.5 show Pearsons correlation coefficient computed between the best fit models compared to the expert's and respondents' performance. Also included is a comparison between the expert's performance and the respondents' performance, $\alpha = 0.05$. This table shows correlations for the full sample of visualizations, $n = 89$, as well as for the sample with transformations applied. Also listed are the correlations for the sample with outliers removed, for which both linear correlation results are shown and results after applying a transformation (fitting a curve to the data). The results indicate in the first column that the expert's performance also only weakly correlates with the respondents' performance. The curves were fitted to the data for the purpose of illustrating that with some transformation of the data or model output, the model could better predict the participants understanding of the visualizations.

In the second column our perceptual model, trained on the expert's results (training was used to determine the parameters for the model, which best fit the training data) is compared with the respondents' performance. For the trained settings statistical correlation is found between this model and the respondents' performance. Applying a transformation improves correlation, to a weak $r = 0.297$. ρ values less than 0.05 indicate that the correlation is not by chance. When outliers are removed the correlation improves, and when a transformation is applied the correlation is strengthened even more. The correlation, however, does not become a "strong" correlation.

The third column in Table 8.5 shows an optimal correlation of the model, trained on the expert data, with the expert data itself. The fourth column lists the best possible correlations for a model trained on the respondents' data compared with the respondents' performance. In this case correlation is found for the complete set and is improved by transformations, or removal of outliers, or both. However, it does not become a strong correlation in any case, as in the case of the expert trained model, which indicates that there is variation due to having multiple differing subjects, which makes it more difficult to obtain strong correlation.

Figure . shows scatter plots of the results from Table 8.5. The graphs on the left show the scatter plots for the full sample of visualizations, while those on the right, indicate outliers in red and show a trend-line for the data without outliers.

	Expert's performance vs. Respondents	Expert Trained Model vs. Respondents	Expert Trained Model vs. Expert	Respondents Trained Model vs. Respondents
Complete sample, n=89, linear correlation				
r	0.543	0.257	0.612	0.276
r^2	0.295	0.066	0.375	0.076
df = 87, t, two-tailed ρ	t=6.038, ρ=0.0	t=2.484, ρ=0.015	t=7.225, ρ=0.0	t=2.678, ρ=0.009
Correlation interval	[0.378;0.675]	[0.052;0.442]	[0.463;0.728]	[0.072;0.458]
Complete sample, n=89, with transformations				
type of transformation	log	power	log	power
r	0.562	0.297	0.643	0.322
r^2	0.316	0.088	0.413	0.104
df=87, t, two-tailed ρ	t = 6.340, ρ=0.0	t = 2.897, ρ=0.0047	t = 7.824, ρ=0.0	t = 3.178, ρ=0.002
correlation interval	[0.401;0.690]	[0.094;0.476]	[0.502;0.75]	[0.122;0.497]
Outliers removed - linear correlation				
	n=82	n=78	n=81	n=79
r	0.748	0.515	0.646	0.500
r^2	0.560	0.265	0.418	0.250
df, t, two-tailed ρ	df=80,t=6.046, ρ=0.0	df=76,t=5.239, ρ=0.0	df=79,t=7.530, ρ=0.0	df=77,t=5.068, ρ=0.0
correlation interval	[0.39;0.693]	[0.33;0.662]	[0.498;0.758]	[0.314;0.649]
Outliers removed, with transformations				
	n=82	n=78	n=81	n=79
type of transformation	quadratic	log	log	exponential
r	0.760	0.577	0.719	0.563
r^2	0.578	0.333	0.517	0.317
df, t, two-tailed ρ	df=80,t=10.47, ρ=0.0	df=77,t=6.160, ρ=0.0	df=79,t=9.196, ρ=0.0	df=77,t=5.978, ρ=0.0
correlation interval	[0.651;0.839]	[0.407;0.709]	[0.594;0.810]	[0.391;0.697]

Table . Correlations between the best fit models compared to the expert's and respondents' performance, including a comparison between the expert's performance and the respondents' performance, α = 0.05.

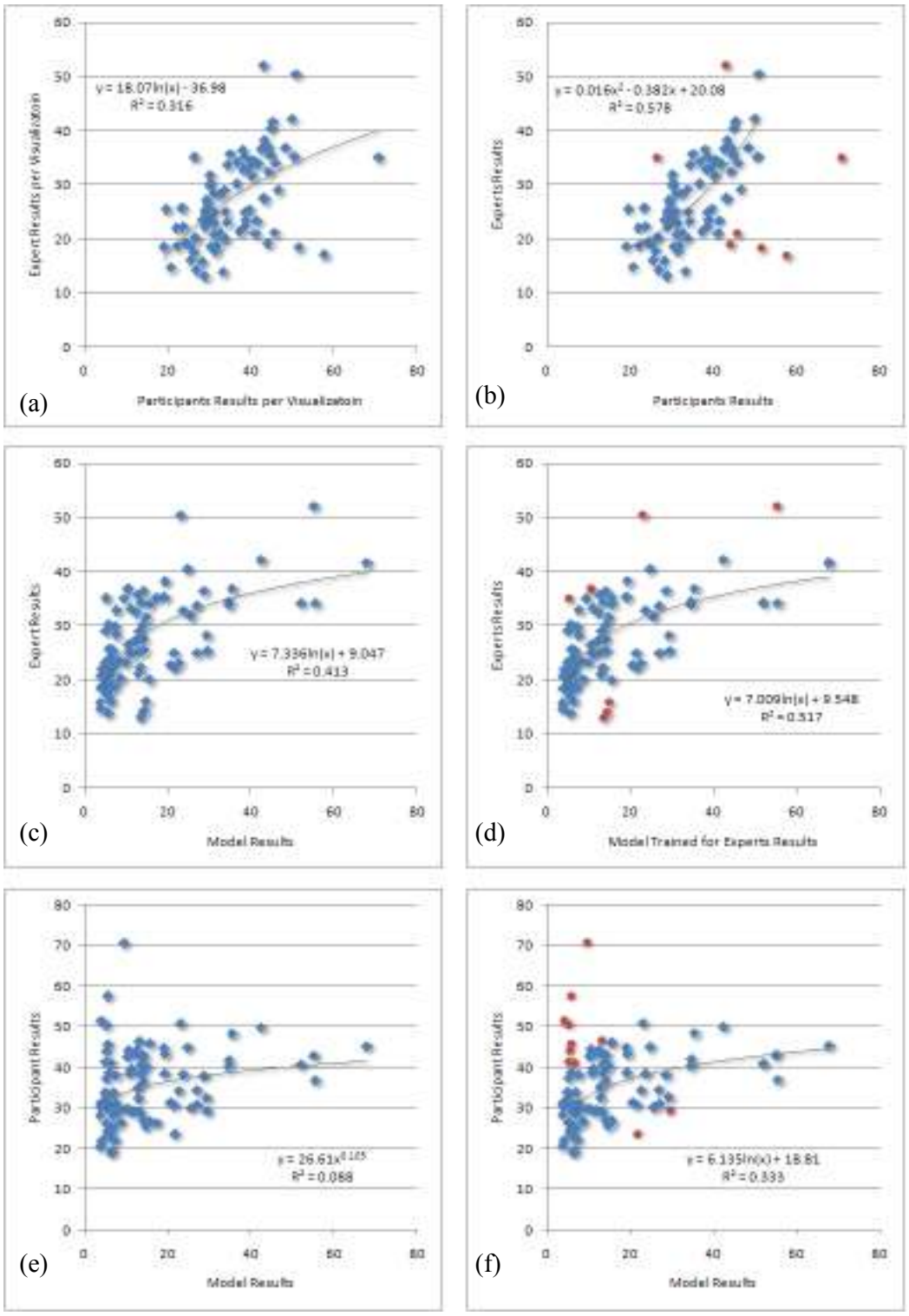

Figure . Scatter-plots of the correlations between: (a),(b) the expert and participants performance;(c),(d) the expert and the model trained on the expert's data; and (e),(f) the respondents' results and the model trained on the expert's data. (a),(c),(e) on the left show the plots for the full sample n = 89, while on the right (b),(d),(f) show the correlation with outliers (marked in red) removed.

A paired t-test was performed on the 89 corresponding fitness value results for each of the visualizations between the respondents and the expert to analyse the variance in perception between these different human users. The test reports $t = 9.73$ and $p < 0.0001$ for 88 degrees of freedom. This indicates that there is a significant difference between the expert user's responses and those of the respondents. The means and variances are shown below in Table ..

	Participants	Expert
Mean	36.0	27.0
Variance	17.0	17.2

Table . Mean fitness and variances between fitness values for the 89 results for the participants and the expert user on the same visualizations.

8.4 Discussion

The aim of our model was to find a way to closely predict participants' ability to understand layered surfaces from a visualization. The results in Table 8.5, in particular the respondents' performance compared to the model, gives an indication of a weak linear correlation between the perceptual model and the participants' performance, indicating that the extent to which the model achieved its goal was minimal. Yet, even though only a weak correlation was found it gives some hope that perhaps in the future a better model could be developed, though from this research it was learnt that modelling HVS perception of layered surfaces is an extremely challenging task for vision research.

Human visual perception is subjective and may vary widely from one person to another [Langer et al., 2005]. Therefore, the fundamental problem of creating a model for predicting user perception of layered surfaces is that two different users may well give very different responses. This would mean that no model could be created that would have low variance, i.e. an oversimplified model could not be created that would fit the data. Our results show signs of this problem since large variation between different human respondents is evident: Figure . (a) shows the relationship between an expert user's responses and those of "off the street" participants. The results are largely scattered across the graph indicating that there is little correlation. The t-test with corresponding variances reported in Table . indicate the significant difference between the expert and the user. This cause of variation is not only evident between an expert and the respondents but also within the group of "off the streat" respondents. A sample of 42 "off the street" respondents were recruited, but only 24 of these respondents' data could be used, because the other respondents had incomplete or extreme outlying responses. The set of respondents was evidently "non-homogenous" in terms of their perception. It is therefore likely difficult to model the significant variation in perception of layered surfaces between a group of non-homogenous respondents.

It is difficult to be certain of the causes for variation since the visualizations themselves had to be varied from surface to surface, in order to test the model across a range of the visualization parameters. Some, further reasons for the variation between the respondents within the smaller

reduced sample include the following:

- The standard deviations were significantly large for measures of time spent on surfaces between respondents, the rock counts, the time spent rocking, the participants' depth error, missed bumps error and radius error.
- The standard deviations for the respondents' missed bumps and radius error results for the 89 visualizations are larger than for the expert user. This might seem an obvious result since multiple different people completed the task, which means that there would be more variation between these multiple participants than for a single person completing the task. This is an indication that there is variation between the respondents.
- Removing approximately 10% of the outliers from the participant set improved the correlation by more than 20% between the respondents' and the expert's results, as well as the respondents and the models.

During observations it was noticed that some respondents were not meticulous about finding and picking out features on layers that were partly or completely obscured. If they could not see the layer clearly they simply moved on. Our instructions to the respondents were that if they were unable to see a layer clearly they should move on and simply report what they could see. However, various respondents were more meticulous, rocking the surfaces over and over again to help them pick out or seek features obscured below other layers. A subset of the data taken from participants with the best responses could, perhaps have been used to obtain more meticulous responses and also address outliers. This however would have reduced the sample size too significantly.

Another potential source of variation between the respondents' performance and the model is that the respondents were able to rock the surfaces, which would have allowed the respondents to gain slight oblique views. The model, on the other hand, catered for only a static top-down view. We investigated this by examining if there was any correlation between each respondent's performance and the percentage of time that each respondent spent rocking the surfaces. The results in Table . indicate no correlation for an entire set of surfaces. During the experiment respondents identified all the markings on a single layer and then moved to the next layer, however, time was not recorded on a per layer basis but rather for completing the task for a set of layers. Correlation may well have been found at a per-layer level though, for cases where the middle and lower surfaces could not be clearly seen, since it was in these situations that some of the participants used rocking to gain a view of the features, which would have otherwise remained hidden from the simple top-down view. Future experiments should take note of time on a per layer basis to provide a more thorough analysis.

The surfaces were processed monocularly by the model, whereas respondents observed the layers in stereo. This too may have contributed to the discrepancies between performance and metric results. Other sources of variation may be attributed to the model itself; discrepancies in the model which do not replicate the perceptual processes the HVS goes through to complete a particular task, would result in a lack of correlation. One component which shows variation

from subject responses is the depth component. Depth estimates significantly influence the model and respondent's performance as shown in Table .. But the respondents' depth estimates are significantly worse than the model's, since the model assumes and simulates accurate depth approximations. Further, the expert's depth estimates are more accurate than the respondents and less variable. This partly explains why the model more closely correlates with the expert's performance, and why the correlation is weaker between the model and respondents' performance. The model's correlation would likely be improved in relation to the respondents' performance by using a more accurate model of the respondents' perceptual depth estimates.

The significant accuracy with which the expert estimated the depth, in comparison to the respondents' depth estimates is likely due to a combination of the expert using the stereo convergence of the depth marker to help better approximate depths as well as experience with these visualizations. This raises the issue of the validity of the self experimentation used in this evaluation. Self experimentation has been used in perceptual experiments for layered surfaces before [Bair, 2009] in order to provide a comparative perspective with regard to other participants. Koenderink has also used himself as a subject in his own experiments involving low level vision, for cases where tasks are wearisome. His results are still considered valid. Self experimentation, in our research was not used to reflect linear correlation between the model and HVS perception; the correlation between the model and the participants' performance indicates this. The expert's results provide useful results though, in other respects. The expert's results are known to both have less variation than the participants' results and also more accurate depth estimates. This helps us to reason about the model and the participants' results, providing, in a sense, a more constant point of reference for comparisons. For instance, it helps to confirm that variation is significantly based on inter-respondent differences, since removing outliers improves the correlation between the expert and respondents', making it stronger than that between the expert's performance and the expert trained model, which indicates that the outliers themselves are a cause for significant variation from the model. From these models we learn that rocking and stereo do not provide a precise absolute sense of depth.

8.5 Finding the Best Visualizations

We used the models to automatically determine the best set of parameters for the visualizations and compared these to the visualizations on which the participants performed the best. The parameter space consisted of the parameters used in the user study, namely number of markings per layer, size of markings per layer and type of markings used on each layer. We found a set of the best visualizations from our user study by identifying the visualizations which resulted in the best performance for both the respondents and the expert and those that were common to both. This was done by first finding the top 7 visualizations for both the expert and the respondents. Visualizations which were common to both were then found. Then in each group of 7, the settings with the least squares difference in the normalized parameter space were found. Distance in this space was determined by normalizing and combining the performance scores. Parallel coordinate graphs are used to illustrate these visualizations from their successive pools in Figure .. The x-axis indicates the layers 1, 2, or 3. The line colour

indicates if there were mixed marking types on the layers (blue lines), or if the marking types were all the same (orange lines). The y-axis corresponding to the layer indicates a rough measure of visibility for each layer (the size of the markings multiplied by the number of markings).

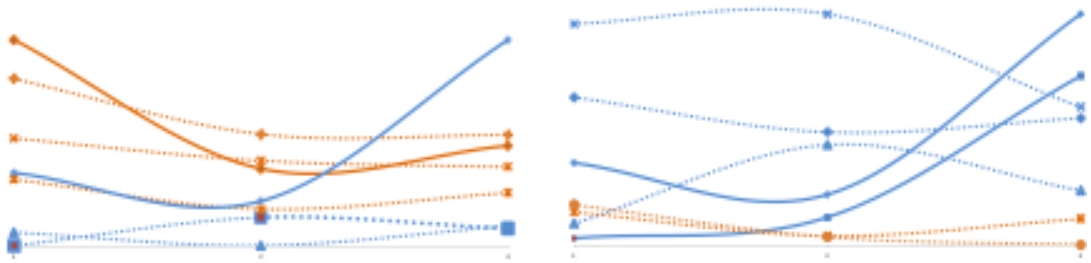

Expert bests Respondent bests

Figure . The top visualizations from the expert and the respondents. The top visualization, which minimized the least squares difference from a visualization common to the bests from the expert's and respondents' results are indicated by the thick solid lines. The X-axes indicate the layer, the Y-axes indicate a normalized numerical value corresponding to the number of markings multiplied by the size of the markings. Orange lines indicate markings were the same type, blue lines indicate visualizations for which markings on different layers were different.

In addition to finding the best visualizations, we also used our model with a PSO to automatically find a set of optimal parameters, GM_R. These parameters and visualizations are similar to the best found by the expert and respondents indicating that our model is able to find good visualization settings. These settings for the best visualizations from the datasets are presented in Table . and the visualizations are illustrated side by side in Figure . with the best visualizations which could be created automatically using our model: M_e refers to the parameters and settings for the expert model and M_p refers to the participant model.

	Closest Layer – l_1			Middle Layer – l_2			Farthest Layer – l_3		
	Particles	Size	Type	Particles	Size	Type	Particles	Size	Type
C	371	0.0274	cross	431	0.045	cross	1966	0.0485	patch
E	369	0.0329	cross	520	0.0358	patch	1427	0.0384	patch
R	594	0.0242	patch	860	0.037	cross	1427	0.038	cross
M_E	371	0.0274	cross	431	0.045	cross	1966	0.0485	patch
M_R	488	0.0349	cross	1154	0.029	cross	1358	0.0408	cross
GM_R	350	0.02	patch	360	0.04	patch	1356	0.039	patch

Table . Settings for the best similar visualizations. Settings for the different responses and models are for: M_E: the expert's best model; M_R: the respondents' best model. C: best common visualization for respondents and expert; E: the expert; R: respondents, The best expert model found the same best as the best visualization common to the expert and respondents. General optimal parameters found for

the respondents' data, GM_R.

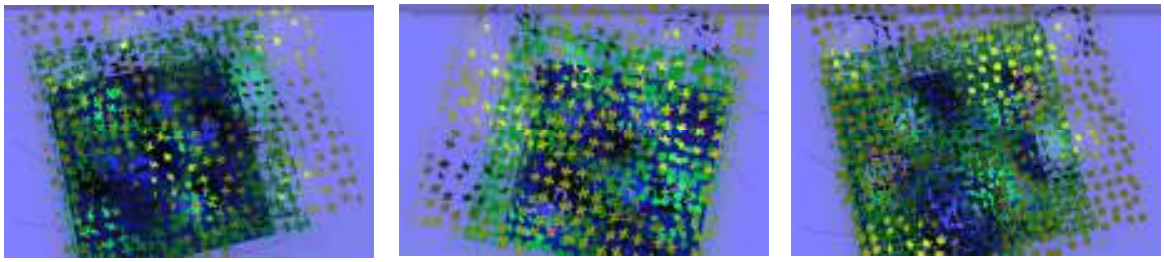

Common - C
f_M = 3.811,f_R = 20.614, f_E = 14.626

Respondents Best - R
f_M = 4.646, f_R = 19.576

Experts Best - E
f_M = 4.109, f_E = 18.421

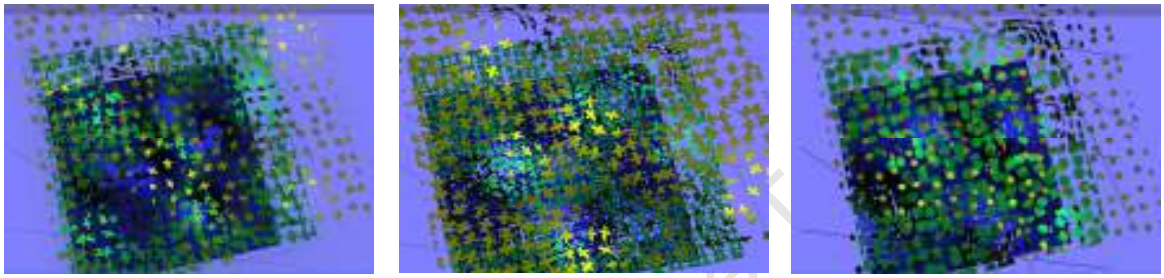

Expert Model Best - M_E
f_M = 3.811, f_E = 14.626

Respondents Model Best - M_R
f_M = 3.41525, f_R = 28.212

Optimized settings - GM_R

Figure . The best visualizations corresponding to the visualization parameters (number of markings, size and type of markings) in Table .. M_E and M_R correspond to the best visualizations automatically found for the models, trained on the expert's data and the respondents data respectively. GM_R is a visualization with an optimized set of parameters. The settings for these visualizations are listed above in table 8.6. Our measure of fitness for the model - f_M and the respondents - f_R and the expert - f_E respondents - f_R are listed.

The values in Table . indicate the settings that resulted in the best results for various layered surface visualizations, specifically for the number of particles, size of particles and type of particles on each layer for a three-layered surface visualization. Variability in the table reflects the weak correlation. It also indicates that the problem is hard, since different settings can result in seemingly good visualizations. From the table it can be seen that the expert and respondents best understood the layered surfaces from the visualizations where, as the surfaces got further from the observer, the number of markings and size of the markings increased. Values for the models seem to reflect this trend. The preference for markings on the furthest surface seems to be for patches. On the middle and closest layer crosses are preferred though. There is a large difference between the number of markings for the model trained on the respondents' data and other settings, on the middle layer. This could likely be because the model used many small markings, rather than fewer larger markings.

8.6 Limitations and Recommendations

The model is currently limited to smooth surfaces and visualizations that do not cater for sharp corners or surfaces with varying levels of detail. The model integrates well with the particle

-based layered surface display framework presented in this dissertation. However, interpreting images of layered surfaces without meta-knowledge about the layers to which the fragments belong, would require lower level image processing and computer vision techniques that could isolate and determine the fragments belonging to disparate layers. Texture-based display techniques for grids would need to be adapted to work within the framework of our model. Grids do not consist of known standalone fragments and would require more complicated image processing.

In order to reduce variation it is recommended that in future experiments fewer participants be used and that they capture a larger sample of the data; or that a more homogenous group of participants be used, in particular a population of domain experts. The proposed model provides an indication of how clearly layered surfaces can be distinguished. A non-perceptual visibility based measure could be established, which would be a simpler and faster way to determine the effectiveness of layered surface images. It was, however, our aim to model HVS processes for layered surfaces, since this not only serves to help reason about and understand the HVS, but would be a more accurate measure. A simple visibility model would overlook regions without markings in images, whereas the HVS uses surface completion to infer shape across such regions.

Visualizations that illustrate where the difference between the model and participants' perception would be helpful in gaining insight into how well the model is making its predictions and which aspects are determining a good or poor match. Since many factors influence the accuracy of the model, including density of markings, proximity to peaks on surfaces, occlusions from other layers, such a display would be helpful in refining HVS models. This is however left for future work.

8.7 Conclusion

The aim of the second part of this research was to introduce an effort to predict a person's ability to comprehend layered surface visualizations. We learnt, from this study, that modelling the numerous and complex mechanisms of the human visual system for complicated images produced by these visualizations is an almost insurmountable challenge. So much so, that numerous simplifications and reductions to potential models of the HVS had to be made in order to construct our model. Nevertheless, this model serves as an initial contribution towards the initiative of leveraging knowledge of the HVS to automatically quantify the effectiveness of layered surface visualizations.

This chapter set out to verify the hypothesis that our proposed model is correlated with a person's perception of a layered surface visualization, i.e. the measure reflects how well a visualization perceptually represents a set of layered surfaces. This hypothesis is weakly supported by the results obtained through this evaluation, since only a weak linear correlation is evident between a visualization user's performance and the metric's score. This correlation being weak highlights that there are many potential sources of variation not accounted for by

the model since the model is not a good fit to the data. The indications of correlation are nonetheless an encouraging result, since this is a first attempt at developing a computational model for quantifying the perceptual effectiveness of layered surface visualizations. We recommend that a homogenous population of respondents, be used to reduce variation.

This evaluation has highlighted various sources of potential variation that may have influenced the results, including differences between respondents, outliers, and in particular depth estimation deviation from user to user that were not catered for in the evaluated model. From the results we learnt that rocking and stereo did not provide an accurate absolute sense of depth. This means that our assumption about depth being accurate is flawed making the depth computation in the model incorrect. This is another cause of discrepancy between our model and the HVS. A perceptually more accurate simulation of depth perception needs to be implemented to correct the model. However, since, the model correlates broadly to perceptual performance for visualizations of a set of layered surfaces the model presents an approach that may be useful for automatically finding optimal or promising settings for such visualizations. Visualizations were found by the metric that are similar to the visualizations on which participants performed the best.

To achieve a better correlation the model should be improved. Future work could therefore follow two major directions. The first thrust should focus on improving the computational model to simulate the different HVS processes. For instance, the clustering component implemented in this work, makes use of a simple k-means clustering algorithm and may likely misclassify fragments, causing them to be suppressed. Perceptually based clustering algorithms need to be adapted to more accurately reflect the way layered surface fragments are pieced together in the presence of multiple interfering fragments. In particular, influences of fragment size and nearness to other markings and shading need to be considered more carefully.

The second major direction for future work would be to better understand the HVS processes in the context of layered surface displays. Correct models of the HVS, serve as computational simulators of the HVS which can be tuned and varied to help understand processes and thresholds of the HVS. Effects of interference (fragments from multiple layers which visually interact with one another or reduce contrast) that cause markings to go unnoticed need to be better understood, since participants were observed to focus their attention on interpolating a surface across small, camouflaged or sparse sets of markings.

Various aspects of surface completion also need to be refined in the model. The role and contribution of relatability and clustering, which seem to depend on the task being performed, need to be better understood for layered surface images. It may be that relatability criteria were unnecessary for the perceptual task respondents were faced with in the experiment, since in the tasks respondents estimated smooth surface features. Requesting orientation judgments between non-relatable fragments in a future perceptual experiment may shed light on whether or not relatability should be included in the model, and for what type of tasks. There may

indeed be processes in the HVS for layered surfaces which are task dependent, similar to the way different depth cues are integrated for depth perception across different tasks.

The role of transparency was not considered in this evaluation, but it is likely that it could help participants to interpolate and complete the surfaces. How transparency influences surface completion and relatability criteria is uncertain. Again, perceptual research is needed to gain insight into these complicated cases for surface completion.

The model itself needs further testing. The various components of the model should be tested in isolation (e.g. validate that the clustering components are functioning in the same way that respondents would cluster the markings on different layers). The depth estimation components need to be extended to use a combination of various SFX techniques. Our framework and an approach for integrating these techniques are presented in chapter 7. Current SFX techniques need to be refined to deal with layered surface input. The model needs to be tested and refined for oblique vantage points in which edges and silhouettes contribute to depth and shape perception. Many challenges may need to be overcome. For example, if a surface has folds, the computer vision algorithms could miscalculate the depths at various points around silhouettes, and the clustering algorithms may incorrectly connect fragments on the same surface but at different depths.

The model further needs to be extended to cater for rocking and stereo and these animation components of the model need to be experimentally evaluated. Hindsight from the experiment shows that there is more to modelling animation than simply integrating the views over time. This is particularly the case in interactive settings where animation may be incorporated with rocking and an observer's perception of surfaces varies as the observer investigates the surfaces using these techniques. This has implications for the main argument of this research, since it indicates that animation is beneficial for exploratory visualization of layered surfaces.

Finally, finding optimal parameters through use of a perceptual model should be extended to use a larger parameter space. In this study the parameter space explored included a subset of the larger number of possible parameters, namely number of particles, size of markings and type of markings for each layer. The optimization should be performed for the larger parameter space and should be evaluated by an expert to establish if the visualization looks good. Once the model has been extended and improved it should be used to create an optimal visualization. This optimal visualization having model-selected parameters should be evaluated against a visualization created by an expert with human selected parameters, to see if the model can truly produce comparative visualizations to an expert.

Chapter 9

Conclusions

9.1 Review

In this dissertation we have explored two novel ways of enhancing visualization techniques for displaying layered surfaces through opaque markings. The first method of enhancing these displays is by animating the opaque markings. The second way is through an optimization process that uses a model of the way in which the human visual system perceives layered surfaces to set visualization parameters. These novel approaches were evaluated and outcomes reflected in the two thesis statements below.

9.1.1 Enhancing Layered Surface Visualizations through Animation of Opaque Markings

We developed a particle system framework through which we could explore the novel use of animation of opaque markings on semi-transparent surfaces, i.e. Kinetic Visualization. Our work extends existing opaque marking approaches by animating the markings to modulate the see-through views, which allows the viewer to see the underlying layers more clearly. Various motion strategies are used to achieve this. The animation of the markings relies on similar motion patterns to help differentiate between markings on the various layers and motion depth cues to enhance the sense of shape perception. Markings that follow principal curvatures help to illustrate the shape and curvature of the surfaces. Markings following different uniform directions on the different layers help distinguish between markings on different layers. Moving markings at the same speed provides a weak motion parallax depth cue, but not the Kinetic Depth Effect. The opaque markings may be rendered using different glyph types to help differentiate between the markings on different layers.

The framework further includes a novel approach to creating layouts of markings which take the view point into consideration for distributing markings over the surface in a way that reduces occlusions. This is achieved by introducing repulsion forces between markings which would otherwise occlude one another with respect to the view point. It may be better though to introduce forces that encourage only partial occlusions, i.e. a particle should only be partially

occluded, since lack of occlusions means that the effective depth cue of occlusion would be omitted. These layout strategies need to be evaluated formally to determine their effectiveness and impact on layered surface visualizations. This is left though for future work.

Two novel user experiments were performed to answer various research questions regarding the effectiveness of using Kinetic Visualization for enhancing layered surface display techniques. Since pendulum style rocking is, to date, the most effective animation technique for enhancing layered surface visualizations, the first experiment compared Kinetic Visualization to pendulum-style rocking on a global shape task, an orientation estimation task and a depth comparison task. The second experiment evaluated using a combination of Kinetic Visualization and rocking.

A major result of the first experiment was that Rocking was superior to Kinetic Visualization, since it helped respondents to better estimate depth than when they used either Kinetic Visualization or static visualizations of layered surfaces. This indicates that one should use Rocking to enhance two layer semi-transparent surface visualizations with opaque markings rather than KV and if Rocking is not available a simple static visualization should suffice instead of KV, since Kinetic Visualization, did not significantly enhance the performance of respondents for any of the tasks. Results from experiment two, however, showed that when viewing four layered surfaces a combination of Kinetic Visualization and rocking is more advantageous than using rocking on its own for feature-finding tasks. The contribution that Kinetic Visualization makes for the feature identification task, when used in combination with rocking, is likely due to unique motion patterns and the modulation of the see-through views over time, which causes an integrated coverage of the surfaces and further helps respondents to distinguish between markings on the different layers.

Noting that rocking, which causes the "Kinetic Depth Effect", produces significantly better depth perception than Kinetic Visualization, we reason that Kinetic Visualization does not enhance shape perception from the "Kinetic Depth Effect" but rather from a weak motion parallax depth cue or from markings following contours. Reorganization of markings generated by KV may also be useful since participants used KV to see markings in different positions. A mechanism for creating new distributions of markings upon request may be useful to users, since this would allow them to see the layered surfaces almost from a different view. Such redistribution is left for future work. The results from the experiments lead to our first thesis statement:

Rocking animation is significantly more effective than animating opaque markings on semi-transparent surfaces for displaying layered surfaces, since it contributes the depth cue of the Kinetic Depth Effect, a percept which is not apparent when simply animating the markings over the surfaces, which only evokes a weak sense of motion parallax. Animating the markings over the surfaces is not more effective than displaying the markings statically. Animating the markings is however beneficial in combination with rocking for supplementing the display of four layered surfaces for exploratory feature identification tasks.

9.1.2 Enhancements through Modelling Perception of Layered Surfaces

We also developed a novel approach for enhancing layered surface visualizations through automated optimization. As the major part of this automation, we make the contribution of extending current models of human perception of surfaces to layered surfaces by modelling perceptual processes of perceptual grouping and surface completion incorporating relatability criteria. The model is intended to mimic a person's perception of layered surface displays.
This model of layered surface perception makes it possible to automatically measure the effectiveness of a layered surface visualization. Measuring the effectiveness of such a visualization is incorporated into a Particle Swarm Optimization (PSO) algorithm to serve as the fitness function. Through this PSO algorithm, an optimization process is performed to automatically determine the best settings for a particular layered surface visualization. In order to evaluate this model of human perception and the optimization process, it was necessary to run a further experiment, in which respondents' perception of layered surfaces was compared to the surfaces produced by our model.

Results from this experiment showed that this initial model has only marginal correlation with human visual perception. Large fluctuations in responses for different people, is one of the likely causes of variation which results in weak correlation. Significant variance between our model and human perception of layered surfaces indicates that the model needs to be refined, in particular in its prediction of perceptual depth. Despite this, optimization of the visualization settings through this model seemed to produce good visualizations to an expert. The evaluation strongly indicates that modelling Human Visual System perception of layered surfaces to automatically evaluate and optimize layered surface visualization settings is a grand challenge. From our results, our second thesis statement is that:

Modelling Human Visual System perception of layered surfaces for a homogenous sample of respondents has the potential of enabling automatic evaluation and optimization of layered surface visualization settings. However, modelling perception of layered surfaces is intricate and beyond the current state of theoretical modelling of the Human Visual System. A further difficulty modelling perception of such visualizations is that variation between non-homogenous participants is unpredictable.

Our evaluation indicates that a fundamental problem modelling such perception is the variation between random "off the street" participants. It may however be possible to predict perception of a homogenous group of respondents.

9.2 Recommendations

This research set out to find ways to effectively show layered surfaces. Based on the observations, results and conclusions of the above experiments, we recommend the following when rendering three or more layered surfaces:

(1) *Rocking and interaction should be used to convey 3D shape and distinguish between the layers* since the experiments showed that rocking significantly helped the respondents.

(2) *For exploratory feature-finding tasks of four layered surfaces, Kinetic Visualization should be used when the surfaces are not rocking*. The viewer should be able to switch this animation on and off. This recommendation is made because moving markings improved performance in combination with rocking, but not simultaneously with it. Rocking and KV were not evaluated or explored in concert because the combined motions together appeared overwhelming and distracting, e.g. when rocking caused the surface to move in the same direction as the markings, the markings appeared to move twice as fast, but when rocking was in the opposite direction, the markings appeared to be almost stationary.

(3) *For distance estimation tasks point correspondence glyphs should be used, together with principal curvature markings, rocking, stereo and other depth cues*. These glyphs provide a visual marker, indicating maximum local distance between surfaces [Weigle, 2006].

(5) *Animation of the opaque markings on different layers should follow different motion patterns on the different layers*. The motion strategies should also vary from flowing over the surfaces in uniform directions to swirling around features to following principal curvature directions. Varying these motions will help an observer to distinguish between the layers and also contribute to feature identification and detection. Markings should move at the same speed to achieve motion parallax, as in classic KV.

(6) *Markings on the different layers should be rendered using different glyph types to help distinguish the markings*. The distinct shapes help to distinguish between markings on different layers. In our optimized solutions, only the respondent's model generated surfaces where the same marking types are used on all layers. All the other best solutions used a combination of the two possible marking types.

(7) *The interior layer should not only be rendered opaquely but also make use of textured markings* to help illustrate its shape more distinctly.

(8) *Fair parameters for visualizations can be automatically found using our proposed perceptual model*, an improved model should be developed and used for these purposes.

9.3 Future Work

This work has explored ways of improving opaque marking-based layered surface display techniques. The ideas of using animation and perceptually modelling the HVS for such displays are at an early stage of development and need to be expanded upon and refined. In particular, the view dependent marking layout method should be refined and evaluated more formally. The various motion strategies need to be further developed and evaluated, i.e. animating just a single layer to help it stand out may be a useful focus and interaction tool.

Adaptive sampling, in particular curvature-based sampling, which best illustrates high frequency regions of surfaces, should be used and the various motion strategies adapted and evaluated for such sampling.

The techniques developed in this dissertation were initially intended for an oceanographic model output data set to help oceanographers better understand the factors influencing changes in water masses. Layered surface display techniques are likely to contribute insights into such phenomena over commonly used slice based techniques. Many of the current state-of-the art layered surface display techniques are rarely applied in modern science. Application of these techniques should be explored, in comparison to current practices in various fields of science and medicine. Current layered surface techniques also need to be extended for non-smooth surfaces.

Layered surface techniques, which facilitate spatial comparisons, may use a multi-view approach to offload the requirements for exploring global and local shape to a set of side by side views. State of the art layered surface display techniques should be used with this multi-view approach to help illustrate orientation and distance judgements.

A problem that may well arise when using stereo for comparing multiple stacked surfaces, is that it becomes difficult to focus on two layers at the same time. Stereo convergence is set to one of the layers, causing other layers to go out of focus as a result of the binocular disparity between left and right eye images at different focal depths. This was observed during our perceptual experiment. It is particularly an issue in making comparisons between layers, e.g. depth or orientation estimates between multiple layers. These issues for stereo display need to be resolved.

Active exploration and interaction with a set of surfaces is arguably the most powerful means of analyzing and understanding a set of layered surfaces. No known research has considered the advantages of interaction with layered surfaces and how it may best be utilized to provide an optimal understanding of a set of layered surfaces. For instance, better depth estimates may be made between surfaces at particular points by allowing a user to rotate the model to a side on view, in which depth can be more accurately compared.

The view dependency rule for optimal marking layouts has not been explored to its full potential. The view point could be taken into account in addition to view dependent surface features, i.e. high frequency regions. Using such knowledge of both the surface landscape and the view point, may allow for visualizations which more effectively reveal important regions of the different layers and sparsely cover low detail regions with markings. A curvature dependent sampling of the surfaces may well best illustrate features and yet help to sparsely cover low frequency regions. Such a distribution used in combination with the view dependent layout strategy may well result in layouts that best illustrate high frequency features on multiple layers and therefore best illustrate the layered surfaces the best. This is left for future research.

Further research needs to be done to extend the perceptual model. This research indicates that this is a significant challenge and we believe that with greater expert knowledge and as more is learnt about how the HVS functions, a better model can be developed. A model should be developed and tested for a more homogenous group of users though, to eliminate variation from respondent to respondent. Each of the components of the model should be carefully crafted to mimic systems of the HVS for which specific viewing parameters should be empirically found. This should be done to remove the training stage of our approach, i.e. the model should be usable without requiring users to wade through a set of layered surface visualizations. We also suggest that non-perceptual approaches to quantify the effectiveness of layered surface visualizations be explored.

A suitable model should also be adapted to process other layered surface display techniques. This may well pave the way for comparing and testing various layered surface techniques automatically. By so doing layered surface visualizations, which optimally display more than three layers simultaneously, may be obtained. Perceptually accurate shape from X algorithms, which are specifically adapted for images of layered surfaces, also need to be developed.

Appendix A

Questionnaires

1 Experiment 1

Distance Task: *start time:* *end time:*
Ratings/Scale:
0 – unclear, bad, none | 1 – poor/little | 2 – average | 3 – good/well | 4 – very well | 5 – Excellently, best/the most

How clearly did the techniques convey the information necessary for the task?

Rocking:	0	1	2	3	4	5
Moving:	0	1	2	3	4	5
Still:	0	1	2	3	4	5

How clearly did the techniques allow you to distinguish between the bottom and top surfaces?

Rocking:	0	1	2	3	4	5
Moving:	0	1	2	3	4	5
Still:	0	1	2	3	4	5

Order the techniques in terms of your preference for use.

1st: 2nd: 3rd:

Rank the techniques in terms of concentration required. (0 – least amount of concentration, 5 most)

Rocking:	0	1	2	3	4	5
Moving:	0	1	2	3	4	5
Still:	0	1	2	3	4	5

Comments/observations about the different techniques:

Orientation Task: *start time:* *end time:*

Ratings/Scale:

0 – unclear, bad, none | 1 – poor/little | 2 – average | 3 – good/well | 4 – very well | 5 – Excellently, best/the most

How clearly did the techniques convey the information necessary for the task?

Rocking:	0	1	2	3	4	5
Moving:	0	1	2	3	4	5
Still:	0	1	2	3	4	5

Order the techniques in terms of your preference for use.

1st: 2nd: 3rd:

Rank the techniques in terms of concentration required. (0 – least amount of concentration, 5 most)

Rocking:	0	1	2	3	4	5
Moving:	0	1	2	3	4	5
Still:	0	1	2	3	4	5

Comments/observations about the different techniques:

Was it easy to use the orientation marker? Yes | No

How clearly did the orientation marker represent an orientation?

0 | 1 | 2 | 3 | 4 | 5

Global Shape Task: *start time:* *end time:*

Ratings/Scale:

0 – unclear, bad, none | 1 – poor | 2 – average | 3 – good/well | 4 – very well | 5 – Excellently, best

Were the five choices (pictures) of the surfaces discernibly different in all cases? Yes | No

How clearly did the techniques convey the information necessary for the task?

Rocking:	0	1	2	3	4	5
Moving:	0	1	2	3	4	5
Still:	0	1	2	3	4	5

How clearly did the techniques allow you to distinguish between the bottom and top surfaces?

Rocking:	0	1	2	3	4	5
Moving:	0	1	2	3	4	5
Still:	0	1	2	3	4	5

Order the techniques in terms of your preference for use.

1st: 2nd: 3rd:

Rank the techniques in terms of concentration required. (0 – least amount of concentration, 5 most)

Rocking:	0	1	2	3	4	5
Moving:	0	1	2	3	4	5
Still:	0	1	2	3	4	5

Comments/observations about the different techniques:

2 Experiment 2

Scale:
0 – unclear, bad, none | 1 – poor/little | 2 – average | 3 – good/well | 4 – very well | 5 – Excellently,best/most

How clearly did the techniques convey the information necessary for the task?
Rocking and still: 0 | 1 | 2 | 3 | 4 | 5
Rocking and moving: 0 | 1 | 2 | 3 | 4 | 5

Rank the techniques in terms of concentration required. (0 – least amount of conentration, 5 most)
Rocking and still: 0 | 1 | 2 | 3 | 4 | 5
Rocking and moving: 0 | 1 | 2 | 3 | 4 | 5

How clearly did the techniques allow you to distinguish between crosses on different layers and help associate crosses on the same layer?
Rocking and still: 0 | 1 | 2 | 3 | 4 | 5
Rocking and moving: 0 | 1 | 2 | 3 | 4 | 5

Rate the following:
the moving points flowing over the surface compared to when the surface was still:

Gave a better coverage of the surface:

0 | 1 | 2 | 3 | 4 | 5

Varied the see-through views to allow markings on lower surfaces to be seen:

0 | 1 | 2 | 3 | 4 | 5

Was distracting/confusing interfering with my ability to focus on the marks on the bottom surface:

0 | 1 | 2 | 3 | 4 | 5

Which was the most difficult layer to distinguish?
Comments/observations about the different techniques:

Bibliography

Adelson, E.H. & Pentland, A.P., 1996. The perception of shading and reflectance. pp.409-23.

Alexa, M. et al., 2001. Point set surfaces: Proceedings of the conference on Visualization '01. Washington, DC, USA, 2001. IEEE Computer Society.

Alexa, M. et al., 2001. Point set surfaces: Proceedings of the conference on Visualization '01. Washington, DC, USA, 2001. IEEE Computer Society.

Andersen, R.A. & Bradley, D.C., 1998. Perception of three-dimensional structure from motion., 1998.

Angel, E., 2000. *Interactive Computer Graphics with OpenGL*. Addison-Wesley.

Bair, A.S., 2009. *Optimization of Single and Layered Surface Texturing*. PhD Thesis, Texas A and M University.

Bair, A. & House, D., 2007. Grid With a View: Optimal Texturing for Perception of Layered Surface Shape. pp.1656-63.

Bair, A., House, D. & Ware, C., 2005. Perceptually optimizing textures for layered surfaces: Proceedings of the 2nd symposium on Applied perception in graphics and visualization. New York, NY, USA, 2005. ACM.

Bair, A., House, D.H. & Ware, C., 2006. Texturing of Layered Surfaces for Optimal Viewing. pp.1125-32.

Bajcsy, R. & Lieberman, L., 1976. Texture gradient as a depth cue. pp.52-67.

Banks, J., Bennamoun, M., Kubik, K. & Corke, P., 1999. An accurate and reliable stereo matching algorithm incorporating the rank constraint. pp.23-32.

Barrow, H.G. & Tenenbaum, J.M., 1981. Interpreting line drawings as three0dimensional surfaces. pp.75-116.

Bartram, L., 1997. Perceptual and interpretative properties of motion for information visualization. In *NPIV '97: Proceedings of the 1997 workshop on New paradigms in information visualization and manipulation*. New York, NY, USA, 1997. ACM.

Bartram, L. & Ware, C., 2002. Filtering and brushing with motion. pp.66-79.

Bartram, L., Ware, C. & Calvert, T., 2003. Moticons: detection, distraction and task. pp.515-45.

Bauer-Kirpes, B., Schlegel, W., Boesecke, R. & Lorenz, W.J., 1987. Display of organs and isodoses as shaded 3-d objects for 3-d therapy planning. pp.135-40.

Black, M.J. & Rosenholtz, R., 1995. Robust estimation of multiple surface shapes from occluded textures. In *ISCV '95: Proceedings of the International Symposium on Computer Vision*. Washington, DC, USA, 1995. IEEE Computer Society.

Blake, R. & Lee, S., 2005. The role of temporal structure in human vision.

Blake, R. & Sekuler, R., 2002. *Perception*. McGraw-Hill.

Blinn, J.F., 1977. Models of light reflection for computer synthesized pictures. pp.192-98.

Bobrow, R. & Helsinger, A., 2005. Kinetic Visualizations: A New Class of Tools for Intelligence Analysis., 2005.

Bokinsky, A., 2003. *Multivariate Data Visualization with Data-Driven Spots*. PhD Thesis, University of North Carolina at Chapel Hill.

Borland, D., Clarke, J., Fielding, J. & Taylor, R., 2006. Volumetric depth peeling for medical image display.

Braddick, O., 1997. Local and global representations of velocity: Transparency, opponency and global direction perception. pp.995-1010.

Bradshaw, M.F. & Rogers, B.J., 1996. The interaction of binocular disparity and motion parallax in the computation of depth. Nov. pp.3457-68.

Bruckner, S. & Groller, M.E., 2006. Exploded Views for Volume Data. pp.1077-84.

Bulthoff, H.H. & Langer, M.S., 1999. Perception of Shape From Shading on a Cloudy Day. pp.467-78.

Burns, M. et al., 2005. Line drawings from volume data. pp.512-18.

Busking, S., Vilanova, A. & Wijk, J.J., 2007. VolumeFlies: Illustrative Volume Visualization using Particles., June 2007.

Correa, C.D. & Silver, D., 2005. Dataset Traversal with Motion-Controlled Transfer Functions., Oct 2005.

Costa Sousa, M. & Prusinkiewicz, P., 2003. pp.381-90.

Crossno, P. & Angel, E., 1997. Isosurface extraction using particle systems: Proceedings of the 8th conference on Visualization '97. Los Alamitos, CA, USA, 1997. IEEE Computer Society Press.

Cryer, J., Tsai, P. & Shah, M., 1993. Integration of shape from x modules: Combining stereo and shading. June. pp.720-21.

Cutting, J.E. & Vishton, P.M., 1995. Perceiving layout and knowing distance: The integration, relative potency and contextual use of different information about depth. pp.69-117.

Daly, S., 1993. The visible differences predictor: an algorithm for the assessment of image fidelity. pp.179-206.

DeCarlo, D., Finkelstein, A., Rusinkiewicz, S. & Santela, A., 2003. Suggestive Contours. pp.848-55.

Diepstraten, J., Weiskopf, D. & Ertl, T., 2002. Transparency in interactive technical illustrations. p.2002.

Diepstraten, J., Weiskopf, D. & Ertl, T., 2003. Proceedings of Eurographics Conference '03 (to appear in Computer Graphics Forum)., 2003.

Donoho, A.W., D.L., D. & Gasko, M., 1988. MacSpin: Dynamic Graphics on a Desktop Computer. *IEEE*, pp.51-58.

Durikovic, R., Yauchi, T., Kaneda, K. & Yamashita, H., 1997. Shape-based calculation and visualisation of general cross-sections through biological data.

Erens, R.G., Kappers, A.M. & Koenderink, J.J., 1993. Perception of local shape from shading. pp.145-56.

Ernst, M.O. & Bülthoff, H.H., 2004. Merging the Senses into a Robust Percept. pp.162-69.
Fahle, M. & Poggio, T., 1981. Visual Hyperacuity: Spatiotemporal Interpolation in Human Vision. pp.451-77.
Fantoni, C., Hilger, J.D., Gerbino, W. & Kellman, P.J., 2008. Surface interpolation and 3D relatability. pp.1-19.
Figueiredo, L.H. & Gomes, J., 1996. Sampling implicit objects with physically-based particle systems. pp.365-75.
Fleming, R.W. & Adelson, E.H., 2004. Specular reflections and the perception of shape. pp.798-820.
Foley, J.D., van Dam, A., Feiner, S.K. & Hughes, J.F., 1994. *Computer Graphics: Principles and Practice*. Addison-Wesley.
Freeman, W.T. et al., 1998. Computer Vision for Interactive Computer GRaphics. pp.42-53.
Gillies, D.F. & Khan, G.N., 1992. Perceptual Grouping and the Hough Transform. pp.188-96.
Goldfeather, J. & Interrante, V., 2004. A novel cubic-order algorithm for approximating principal direction vectors. pp.45-63.
Green, B.F., 1961. Figure Coherence in the Kinetic Depth Effect. pp.272-82.
Grimson, W.E., 1980. Computing Shape Using a Theory of Human Stereo Vision. June.
Grimson, W.E., 1981. From Images to Surfaces: A computational study of the human early visual system.
Grimson, W.E., 1982. A Computational Theory of Visual Surface Interpolation. pp.395-427.
Grimson, W.E., 1983. An implementation of a computational theory of visual surface interpolation. pp.39-69.
Grossberg, S., 2003. Laminar cortical dynamics of visual form perception. pp.925-31.
Grossberg, S. & Yazdanbakhsh, A., 2005. Laminar cortical dynamics of 3D surface perception: stratification, transparency, and neon color spreading. pp.1725-43.
Hagh-Shenas, H., Kim, S., Victoria, I. & Christopher, H., 2007. Weaving Versus Blending: a quantitative assessment of the information carrying capacities of two alternative methods for conveying multivariate data with color. pp.1270-77.
Hale, K.S. & Stanney, K.M., 2006. Effects of low stereo acuity on performance, presence and sickness within a virtual environment. pp.329-39.
Healey, C.G., 1996. Choosing effective colours for data visualization. In *VIS '96: Proceedings of the 7th conference on Visualization '96*. Los Alamitos, CA, USA, 1996. IEEE Computer Society Press.
Healey, C.G., 2009. Perception in Visualization.
Hertzmann, A. & Zorin, D., 2000. Illustrating smooth surfaces: Proceedings of the 27th annual conference on Computer graphics and interactive techniques. New York, NY, USA, 2000. ACM Press/Addison-Wesley Publishing Co.
Hill, A. & Johnson, A., 2008. Withindows: A Framework for Transitional Desktop and Immersive User Interfaces. In *3DUI '08: Proceedings of the 2008 IEEE Symposium on 3D User Interfaces*. Washington, DC, USA, 2008. IEEE Computer Society.
Hillstrom, A. & Yantis, S., 1994. Visual attention and motion capture. pp.399-411.

Huber, D.E. & Healey, C.H., 2005. Visualizing data with motion. pp.527-34.

Interrante, V., 1996. *Illustrating Transparency: Communicating the 3D Shape of Layered Transparent Surfaces via Texture*. USA: University of North Carolina at Chapel Hill.

Interrante, V., 1997. Illustrating Surface Shape in Volume Data via Principal Direction-Driven 3D Line Integral Convolution. apr. pp.200-300.

Interrante, V., 1997. Illustrating surface shape in volume data via principal direction-driven 3D line integral convolution. In *SIGGRAPH '97: Proceedings of the 24th annual conference on Computer graphics and interactive techniques*. New York, NY, USA, 1997. ACM Press/Addison-Wesley Publishing Co.

Interrante, V., Fuchs, H. & Pizer, S., 1997. Conveying the 3D Shape of Transparent Surfaces via Texture., 1997.

Interrante, V., Fuchs, H., Pizer, S.M. & Member, S., 1997. Conveying the 3D Shape of Smoothly Curving Transparent Surfaces via Texture. pp.98-117.

Interrante, V. & Grosch, C., 1997. Strategies for effectively visualizing 3D flow with volume LIC. p.421.

Interrante, V. & Grosch, C., 1997. Strategies for effectively visualizing 3D flow with volume LIC. p.421.

Interrante, V. & Kim, S., 2001. Investigating the effect of texture orientation on the perception of 3D shape. pp.330-39.

Jo, Y. et al., 2007. Stochastic visualization of intersection curves of implicit surfaces. apr. pp.230-42.

Julesz, X.Y., 1986. Texton gradients: The texton theory revisited. pp.245-51.

Kellman, P.J., 03. Interpolation processes in the visual perception of objects.

Kellman, P.J. & Shipley, T.F., 1991. A theory of visual interpolation in object perception. pp.141-221.

Kersten, D., Mamassian, P. & A, Y., 2004. Object Perception as Bayesian Inference. pp.271-304.

Kim, S., Hagh-Shenas, H. & Interrante, V., 2003. Conveying Shape with Texture: an experimental investigation of the impact of texture type on shape categorization judgments. p.21.

Kim, S., Hagh-Shenas, H. & Interrante, V., 2003. Showing shape with texture - two directions are better than one. pp.332-39.

Koenderink, J.J., 1984. What does the occluding contour tell us about solid shape? pp.321-?330.

Koenderink, J.J., 1990. *Solid Shape*. MIT Press, Cambridge, Massachusetts.

Koenderink, J.J. & Kappers, A.M., 1992. Surface perception in pictures. Percept Psychophys. pp.487-96.

Koenderink, J.J. & Van Doorn, A.J., 1995. Relief: pictorial and otherwise. pp.321-34.

Krekelberg, B. & Lappe, M., 1999. Temporal recruitment along the trajectory of moving objects and the perception of position. pp.2669-79.

Kruger, J., Kipfer, P., Kondratieva, P. & Westermann, R., 2005. A Particle System for Interactive Visualization of 3D Flows.

Langer, M.S. & Bülthoff, H.H., 2000. Measuring Visual Shape using Computer Graphics Psychophysics. London, UK, 2000. Springer-Verlag.

Langer, M.S., Rekhi, D., Pereira, J. & Bhatia, A., 2005. Layered motion field visualization: perceptual issues. New York, NY, USA, 2005. ACM.

Latta, L., 2004. Building a Million Particle System., 2004.

Levoy, M.F., 1990. Volume Rendering in Radiation Treatment Planning. May. pp.4-10.

Li, W., Agrawala, M., Curless, B. & Salesin, D., 2008. Automated generation of interactive 3D exploded view diagrams. pp.1-7.

Lowe, D.G., 1984. *Perceptual Organization and Visual Recognition*. PhD thesis, Stanford University,Stanford, (CA).

Lubin, J., 1995. A visual discrimination model for imaging system design and evaluation. pp.245-83.

Lu, A. et al., 2002. Non-photorealistic volume rendering using stippling techniques. pp.211-18.

Lu, A. et al., 2003. Illustrative Interactive Stipple Rendering. pp.127-38.

Lum, E.B., Stompel, A. & Ma, K.-L., 2003. Using Motion to Illustrate Static 3D Shape- Kinetic Visualization. pp.115-26.

Lyness, C.A., 2004. Perceptual depth cues in support of medical data visualisation.

MacQueen, J.B., 1967. Some Methods for classification and Analysis of Multivariate Observations.

Mamassian, P. & Kersten, D., 1996. Illumination, shading and the perception of local orientation. pp.2351-?2367.

Mamassian, P., Knill, D.C. & Kersten, D., 1998. The perception of cast shadows. pp.288-95.

Mantiuk, R., Daly, S., Myszkowski, K. & Seidel, H., 2005. Predicting Visible Differences in High Dynamic Range Images - Model and its Calibration.

Markosian, L. et al., 1997. Real-time nonphotorealistic rendering., 1997.

Marr, D., 1978. Representing visual information. pp.101-80.

Marr, D., 1982. *Vision*. Freeman and Company, San Francisco.

Marr, D. & Hildreth, E., 1980. Theory of edge detection., 1980.

Marr, D. & Nishihara, H.K., 1978. Representation and recognition of the spatial organization of three-dimensional shapes., 1978.

Marr, D. & Poggio, T., 1977. *A Theory of Human Stereo Vision*. Cambridge, MA, USA: Massachusetts Institute of Technology.

Marr, D. & Poggio, T., 1979. A theory of human stereo vision., 1979.

Massot, C. & Hérault, J., 2008. Model of Frequency Analysis in the Visual Cortex and the Shape from Texture Problem. pp.165-82.

Meyer, M.D., Georgel, P. & Whitaker, R.T., 2005. Robust Particle Systems for Curvature Dependent Sampling of Implicit Surfaces: Proceedings of the International Conference on Shape Modeling and Applications 2005. Washington, DC, USA, 2005. IEEE Computer Society.

Munzner, T., 2008. Process and Pitfalls in Writing Information Visualization Research Papers. pp.134-53.

Nahum, D.G., 1992. Visualization of fuzzy data using generalized animation. pp.268-73.

Nakayama, K. & Silverman, G.H., 1986. Serial and parallel processing of visual feature conjunctions. March. pp.264-65.

Nishihara, H.K. & Larson, N.G., 1981. Towards a Real Time Implementation of the Marr and Poggio Stereo Matcher. May. pp.114-20.

Nothdurft, H.C., 1993. The role of features in preattentive vision: comparison of orientation, motion and color cues. Sep. pp.1937-58.

O'Shea, J.P., Banks, M.S. & Agrawala, M., 2008. The Assumed Light Direction for Perceiving Shape from Shading.

Palmer, S.E., 1999. *Vision science : photons to phenomenology*. Cambridge, Mass.: MIT Press.

Palmer, E.M., Kellman, P.J. & Shipley, T.F., 1997. Spatiotemporal relatability in dynamic object completion.

Pang, A. & Smith, K., 1993. Spray rendering: visualization using smart particles., 1993.

Peli, E., 1990. Contrast in Complex Images.

Pfautz, J.D., 2000. *Depth Perception in Computer Graphics*.

Phong, B.T., 1975. Illumination for computer generated pictures. pp.311-17.

Ping-Sing, R.Z. et al., 1999. Shape from Shading: A Survey. pp.690-706.

Prados, E. & Faugeras, O., 2006. Shape From Shading. pp.375-88.

Raizada, R. & Grossberg, S., 2001. Context-sensitive bindings by the laminar circuits of v1 and v2: A unified model of perceptual grouping, attention, and orientation contrast.

Ramachandran, V.S., 1988. Perceiving shape from shading. pp.23-32.

Ramasubramanian, M., Pattanaik, S.N. & Greenberg, D.P., 1999. A perceptually based physical error metric for realistic image synthesis. In *SIGGRAPH '99: Proceedings of the 26th annual conference on Computer graphics and interactive techniques*. New York, NY, USA, 1999. ACM Press/Addison-Wesley Publishing Co.

Reeves, W.T., 1983. Particle Systems - A Technique for Modeling a Class of Fuzzy Objects. pp.359-76.

Reynolds, C.W., 1987. Flocks, herds and schools: A distributed behavioral model. pp.25-34.

Rheingans, P., 1996. Opacity-modulating Triangular Textures for Irregular Surfaces., 1996.

Robinson, M.A. & Robbins, K.A., 2005. Towards perceptual enhancement of multiple intersecting surfaces. pp.339-49.

Robinson, M.A. & Robbins, K.A., 2008. Towards perceptual enhancement of multiple intersecting surfaces.

Rogers, B. & Graham, M., 1979. Motion parallax as an independent cue for depth perception. pp.125-34.

Rome, E., 2001. Simulating Perceptual Clustering by Gestalt Principles. In *Proc. of the 25th Workshop of the Austrian Association for Pattern Recognition ((AGM/AAPR) (AGM 2001)), Scherer, S. (ed), Oesterreichische Computer Gesellschaft, Vienna, ISBN*., 2001.

Ropinski, T. & Preim, B., 2008. Taxonomy and Usage Guidelines for Glyph-based Medical Visualization. In *Proceedings of the 19th Conference on Simulation and Visualization (SimVis08)*., 2008.

Royden, C.S., Baker, J.F. & J, A., 1988. Perceptions of depth elicited by occluded and shearing

motions of random dots. pp.289-?296.
Saidpour, A., Braunstein, M.L. & Hoffman, D.D., 1992. Interpolation in structure from motion.
Saidpour, A., Braunstein, M.L. & Hoffman, D.D., 1994. Interpolation across surface discontinuities in structure from motion.
Sakai, K., 1999. Network algorithm for shape-from-texture based on human visual psychophysics and computational analysis. pp.9-17.
Sarkar, S., 2000. Supervised learning of large perceptual organization: Graph spectral partitioning and learning automata. pp.504-?525.
Schneiderman, B., 1996. The eyes have it: a task by data type taxonomy for information visualizations. Washington, DC, USA, 1996. IEEE Computer Society.
Sekuler, R., Watamaniuk, S.N. & Blake, R., 2002. *Perception of Visual Motion*. J. Wiley Publishers, New York.
Shreiner, D., Woo, M., Neider, J. & Davis, T., 2005. *OpenGL(R) Programming Guide : The Official Guide to Learning OpenGL(R), Version 2 (5th Edition)*. Addison-Wesley Professional.
Stahl, D., Ezquerra, N. & Turk, G., 2002. Bag-of-particles as a deformable model: Proceedings of the symposium on Data Visualisation 2002. Aire-la-Ville, Switzerland, Switzerland, 2002. Eurographics Association.
Stevens, K.A., 1981. The information content of texture gradients. pp.95-105.
Steyn, A.G., Smit, C.F., Du Toit, S.H. & Strasheim, C., 1994. *Modern Statistics in Practice*. JL van Schaik Publishers.
Su, W.Y. & Hart, J.C., 2005. A Programmable Particle System Framework for Shape Modeling: Proceedings of the International Conference on Shape Modeling and Applications 2005. Washington, DC, USA, 2005. IEEE Computer Society.
Sweet, G. & Ware, C., 2004. View direction, surface orientation and texture orientation for perception of surface shape: Proceedings of Graphics Interface 2004. School of Computer Science, University of Waterloo, Waterloo, Ontario, Canada, 2004. Canadian Human-Computer Communications Society.
Szeliski, R. & Tonnesen, D., 1992. Surface modeling with oriented particle systems. pp.185-94.
Taylor, R., 2002. Visualizing Multiple Fields on the Same Surface. pp.6-10.
Thaler, L., Todd, T.J. & Dijkstra, T.M., 2007. The effects of phase on perception of 3D shape from texture: Psychophysics and modeling. pp.411-27.
Thorisson, K.R., 1994. Simulated Perceptual Grouping: An Application to Human-Computer Interaction. In *CONFERENCE OF THE COGNITIVE SCIENCE SOCIETY*., 1994.
Todd, J.T., F., N.J., J., K.J. & L., K.A., 1997. Effects of texture, illumination, and surface reflectance on stereoscopic shape perception. pp.807-?822.
Todd, J.T., Oomes, A.H. & Koenderink, J.J., 2004. The Perception of Doubly Curved Surfaces From Anisotropic Textures. pp.40-46.
Treisman, A., 1985. Preattentive processing in vision. pp.156-77.
Treue, S., Andersen, R.A., Ando, H. & Hildreth, E.C., 1995. Structure-from-motion: Perceptual

Evidence for Surface Interpolation. pp.139-48.
Treue, S., Husain, M. & Andersen, R.A., 1991. Human perception of structure from motion. pp.59-75.
Tufte, E.R., 2001. *The Visual Display of Quantitative Information*. 2nd ed. Cheshire, CT: Graphics Press.
Ullman, S., 1976. Filling-in the gaps: The shape of subjective contours and a model for their generation. pp.1-6.
Ullman, S., 1979. Relaxation and constrained optimization by local processes. pp.115-25.
Ullman, S., 1979. The interpretation of visual motion.
Urness, T., Interrante, V., Longmire, I.M. & Ganapathisubramani, B., 2003. Effectively visualizing multivalued flow data using color and texture. pp.151-21.
van Doorn, A.J. & Koenderink, J.J., 1982. Spatial properties of the visual detectability of moving spatial white noise. pp.189-?195.
van Doorn, A.J. & Koenderink, J.J., 1982. Temporal properties of the visual detectability of moving spatial white noise. pp.179-?188.
Viola, I., Kanitsar, A. & Groller, M.E., 2004. Importance-Driven Volume Rendering. In *VIS '04: Proceedings of the conference on Visualization '04*. Washington, DC, USA, 2004. IEEE Computer Society.
Wallach, H. & O'Connell, D.N., 1953. The kinetic depth effect., 1953.
Wanger, L.R., Ferwerda, J.A. & Greenberg, D.P., 1992. Perceiving spatial relationships in computer-generated images., 1992.
Ware, C., 1988. Color sequences for univariate maps: Theory, experiments and principles., September 1988.
Ware, C. & Bobrow, R., 2004. Motion to support rapid interactive queries on node–link diagrams. pp.3-18.
Ware, C. & Bobrow, R., 2006. Motion coding for pattern detection: Proceedings of the 3rd symposium on Applied perception in graphics and visualization. New York, NY, USA, 2006. ACM.
Ware, C. & Franck, G., 1996. Evaluating Stereo and Motion Cues for Visualizing Information Nets in Three Dimensions.
Watson, A.B. & Eckert, M.P., 1994. Motion-contrast sensitivity: Visibility of motion gradients of various spatial frequencies. pp.496-?505.
Watt, S.J., Akeley, K., Ernst, M.O. & Banks, M., 2005. Focus Cues Affect Perceived Depth. pp.834-62.
Weigle, C.C., 2006. *Displays for exploration and comparison of nested or intersecting surfaces*. Chapel Hill, NC, USA.
Weigle, C. et al., 2000. Oriented Sliver Textures: A Technique for Local Value Estimation of Multiple Scalar Fields., 2000.
Weinstein, D., 2000. Scanline surfacing: building separating surfaces from planar contours.
Weiskopf, D., 2004. On the Role of Color in the Perception of Motion in Animated Visualizations:

Proceedings of the conference on Visualization ’04. Washington, DC, USA, 2004. IEEE Computer Society.

Wertheimer, M., 1923. Laws of Organization in Perceptual Forms. pp.301-50.

Witkin, A.P. & Heckbert, P.S., 1994. Using particles to sample and control implicit surfaces. In *SIGGRAPH ’94: Proceedings of the 21st annual conference on Computer graphics and interactive techniques*. New York, NY, USA, 1994. ACM.

Wong, H.-C. et al., 2006. A Perceptual Framework for Comparisons of Direct Volume Rendered Images.

Woodring, J. & Shen, H.W., 2007. Incorporating highlighting animations into static visualizations.

Yee, Y.H. & Newman, A., 2004. A perceptual metric for production testing. In *SIGGRAPH ’04: ACM SIGGRAPH 2004 Sketches*. New York, NY, USA, 2004. ACM.

Yin, C., Kellman, P.J. & Shipley, T.F., 2000. Surface integartion influences depth discrimination.

Young, H.D., 1992. *Univeristy Physics, 8th Edition*. Addison-Wesley.

Zachmann, G. & Langetepe, E., 2002. Geometric Data Structures for Computer Graphics., sep 2002. The Eurographics Association.

Zachmann, G. & Langetepe, E., 2002. Geometric Data Structures for Computer Graphics., sep 2002. The Eurographics Association.

Zahn, C.T., 1971. Graph-theoretical methods for detecting and describing Gestalt clusters. pp.68-?86.

Zhang, D. & Lu, G., 2001. A Comparitive Study on Shape Retrieval Using Fourier Descriptors with Different Shape Signatures. pp.1-9.

Zhang, R., Tsai, P.S., Cryer, J.E. & Shah, M., 1999. Shape from Shading: A Survey. August. pp.690-706.